METABOLIC CONSEQUENCES OF CELLULAR EXPOSURE TO DECANOIC ACID

AZIZA KHABBUSH

UCL GREAT ORMOND STREET INSTITUTE OF CHILD HEALTH

Thesis submitted for the degree of Doctor of Philosophy (PhD)
Awarded by University College London

Funded by Vitaflo International Ltd

JANUARY 2018

I, Aziza Khabbush, confirm that the work presented in this thesis is my own. Where information has been derived from other sources, I confirm that this has been indicated in the thesis.

Signed .....

Date .....

This thesis is dedicated to my parents.

For their endless support, love and guidance.

For their patience and for their sacrifices.

And for instilling in me from the youngest of ages the burning desire to learn and succeed.

ABSTRACT

The medium-chain triglyceride ketogenic diet (MCT KD) is an effective treatment for drug-resistant epilepsy. However, its complexity and associated side effects necessitate the need for improved therapeutic strategies. Although the exact mechanisms for its efficacy remain unknown, there is a growing interest in the potential roles of medium-chain fatty acids octanoic (C8) and decanoic (C10) acids, present in MCT oil administered in the diet and found to be elevated in patient plasma. Moreover, it is emerging that C10, but not C8, elicits anti-seizure effects, inhibits AMPA receptor, and enhances neuronal catalase activity and mitochondrial biogenesis via peroxisome proliferator-activated receptor-γ (PPARγ). In this thesis, the biochemical and mitochondrial effects of C8 and C10 were further characterised in neuronal cell line SH-SY5Y, in addition to the effects of a C10-enriched MCT product in drug-resistant epilepsy patients. In cells treated for 6 days with 250μM of either fatty acid, C10, but not C8, was found to regulate mitochondrial content, as measured by mitochondrial enzyme marker citrate synthase (CS). The effect of C10 was observed to be dependent on control CS activity, increasing mitochondrial content in cells with low control levels and decreasing it in cells with high control activities. Furthermore, C10, but not C8, was found to raise mitochondrial membrane potential in cells, whilst neither of the two fatty acids were seen to affect cellular energy charge. The evidence suggests C10 may potentially optimise mitochondrial enrichment, generating mitochondria with increased function. For these effects to occur in the brain, however, significant concentrations are likely to be required. The neuronal β-oxidation rates of C8 and C10 were investigated and C10 β-oxidation was found to be significantly lower than that of C8. C10 β-oxidation was also found carnitine-dependent, whilst C8 was only partially dependent. In the presence of C8, C10 β-oxidation was further decreased. Consequently, C10 may be relatively spared from β-oxidation, permitting accumulation for it to exert its effects. In view of the evidence presented, the effects of a C10-enriched MCT product was examined in a feasibility study with drug-resistant epilepsy patients. Plasma levels of C8 and C10 were raised in participants. However, a lack of ketosis and no effects on blood lipid and acylcarnitine profiles were observed. Participants were found to have high baseline white blood cell CS activities, which decreased with treatment with the product. How these effects relate to seizure control remains to be determined, but the findings presented in this thesis suggest that a shift towards greater C10 enrichment in the MCT KD may be potentially beneficial.

IMPACT STATEMENT

Epilepsy is a chronic neurological disorder that affects approximately 50 million people worldwide, the majority young children and older adults. However, approximately 1 in 3 patients suffer from drug-resistant epilepsy, meaning that seizures are uncontrolled by medication. In these patients, the medium-chain triglyceride (MCT) ketogenic diet is often used to control their seizures. A high-fat, low-carbohydrate diet, the MCT ketogenic diet is highly effective against seizures. However, the diet is difficult to maintain and not without its complications, including unpleasant gastrointestinal side effects. As a result, very few patients adhere to the diet, necessitating the need for new and improved therapies.

The fatty acids decanoic and octanoic acids, which are provided in the MCT ketogenic diet, are thought to play a role against seizures. Decanoic acid, particularly, has been previously reported to block seizures, increase antioxidant levels and increase the function of mitochondria in neurons, the key energy producers of cells. Building on this research, the studies in this thesis explored the metabolic effects of decanoic and octanoic acids in neuronal cells, uncovering several findings that provide further insight into the mechanism of the diet and lay the foundations for new treatments to be developed.

Decanoic acid, but not octanoic acid, was found to increase the function and regulate the number of mitochondria in cells to potentially optimum levels. With mitochondria underpinning cell function, ensuring optimal numbers of enhanced mitochondria may be vital in protecting the brain against seizures. The studies here also shattered common misconceptions about how cells metabolise these two fatty acids. Despite their similarities, decanoic acid is metabolised more slowly by neurons than octanoic acid, allowing it to accumulate. In the presence of octanoic acid, decanoic acid metabolism was further slowed down, suggesting the benefit of having both fatty acids in dietary treatments. The findings, which reveal how decanoic acid might build up in the brain during the diet to exert its potent antiepileptic effects, are published in the journal *Epilepsia*.

This discovery enabled the development of a new nutritional product, Betashot, for drug-resistant epilepsy patients in the management of their seizures. Currently on trial with adults and children at the National Hospital for Neurology & Neurosurgery and Great Ormond Street Hospital, Betashot contains a mixture of decanoic and octanoic

acids. Available as a drink or powder, Betashot offers an innovative approach to treating epilepsy, with patients able to consume it with their normal diets. Whilst the trial remains ongoing, Betashot has already been found to influence patients, including altering their mitochondrial levels, but how Betashot affects seizures has yet to be established. If successful, the trial may pave the way to providing simpler treatments for drug-resistant epilepsy patients, improving their quality of life without the caveats of the MCT ketogenic diet, making treatment accessible to a wider group of patients. With the effects of decanoic acid on antioxidants and mitochondria in the brain, Betashot also offers a novel therapy in the treatment of a huge range of neurological and metabolic diseases, including Alzheimer's disease and cancer.

TABLE OF CONTENTS

LIST OF FIGURES

LIST OF TABLES

LIST OF EQUATIONS

LIST OF ABBREVIATIONS

ADP	Adenosine diphosphate
AMP	Adenosine monophosphate
AMPA	α-amino-3-hydroxy-5-methyl-4-isoxazolepropionic acid
ANOVA	Analysis of Variance
ATP	Adenosine triphosphate
BMI	Body Mass Index
BSA	Bovine serum albumin
C10	Decanoic acid
C12	Dodecanoic acid
C16	Palmitic acid
C8	Octanoic acid
CAA	Chloroacetaldehyde
CAT	Carnitine acyl carnitine translocase
CI	Chemical ionisation
CoA	Coenzyme A
CoQ	Ubiquinone
$CoQH_2$	Ubiquinol
CPT1	Carnitine palmitoyltransferase I
CPT2	Carnitine palmitoyltransferase II
CS	Citrate synthase
CV	Coefficient of variation
DMEM	Dulbecco's Modified Eagle's Medium
DMSO	Dimethyl sulfoxide

DNA	Deoxyribonucleic acid
DPBS	Dulbecco's Phosphate Buffered Saline
DTNB	5,5-dithiobis-(2-nitrobenzoic acid
EAR	Estimated Average Requirements
EDTA	Ethylenediaminetetraacetic acid
EI	Electron impact
FAD	Flavin adenine dinucleotide
FAMEs	Fatty acid methyl ester
FBS	Foetal bovine serum
FCCP	Carbonyl cyanide-4-(trifluoromethoxy)phenylhydrazone
FSC	Forward scatter
FSMP	Food for special medical purposes
GABA	γ-Aminobutyric acid
GC-IRMS	Gas chromatography isotope-ratio mass spectrometry
GCMS	Gas chromatography mass spectrometry
GTP	Guanosine triphosphate
HBSS	Hank's Balanced Salt Solution
HPLC	High-performance liquid chromatography
KD	Ketogenic diet
LCFA	Long-chain fatty acid
LCT	Long-chain triglyceride
LPS	Lipopolysaccharide
m/z	Mass-to-charge ratio
MCAD(D)	Medium-chain acyl-CoA dehydrogenase (deficiency)
MCFA	Medium-chain fatty acid

MCT	Medium chain triglyceride
MCT KD	Medium-chain triglyceride ketogenic diet
MELAS	Mitochondrial encephalomyopathy, lactic acidosis, and stroke-like episodes
MERFF	Myoclonic epilepsy with ragged-red fibers
MEST	Maximal electroshock seizure threshold
mtDNA	Mitochondrial DNA
NADH	Nicotinamide adenine dinucleotide
NCI	Negative chemical ionisation
NEFA	Non-esterified fatty acids
PFBBr	Pentafluorobenzyl bromide
PMT	Photomultiplier tube
PPARγ	Peroxisome proliferator-activated receptor gamma
PTZ	Pentylenetetrazol
PUFA	Polyunsaturated fatty acids
RNA	Ribonucleic acid
ROS	Reactive oxygen species
rRNA	Ribosomal ribonucleic acid
SD	Standard deviation
SEM	Standard error of the mean
SIM	Selective ion monitoring
SSC	Side scatter
TCA	Tricarboxylic acid
TEA	Triethylamine
TG	Triglyceride

TMRE	Tetramethylrhodamine, ethyl ester
TNB	5-Thio-2-nitrobenzoate
tRNA	Transfer ribonucleic acid
UCP	Uncoupling protein
VNS	Vagal nerve stimulation
WBC	White blood cell
ΔΨm	Mitochondrial membrane potential

ACKNOWLEDGEMENTS

These past few years have been a tremendous journey for me, academically, intellectually and personally. However, this growth could not have been achieved alone.

Firstly, I'd like to thank my supervisors, Prof Simon Heales and Dr Simon Eaton. Simon H. for his unwavering guidance and gentle understanding. Firm but fair, and always with a dose of humour (sprinkled with a dash of politics). His expertise and professionalism have been invaluable to my growth, and his passion for the field is infectious. Simon E. for his exceptional knowledge (a biochemistry guru in fact), fantastic sense of humour and enthusiasm when teaching. He teaches with genuine passion and kindness, and I'm grateful for all the time that he's spent supporting me. I'd also like to thank him for his support with developing the assays in this thesis, and particularly, for his development of the GC-IRMS method. Science aside, though, I've been incredibly fortunate to have both as my supervisors. The dynamic, the banter and team spirit has been fantastic.

I'd also like to thank Dr Michael Orford, "The Method Man", and the very definition of a mad scientist if there ever was one, for all the work he's put into the Betashot assays and the HPLC assay. His support in and out of the lab has been endless, and I've thoroughly enjoyed every moment working with him. His kindness (and banter) is endless. And his enthusiasm for science and limitless creativity is inspiring.

This PhD has also been a journey of friendships. I'd like to thank my PhD comrades, Carmen and Mesfer, without whom I wouldn't have enjoyed this degree so much.

Carmen for her beautiful personality and friendship, for sharing the tears and the laughter (and the thesis suffering!). I'm going to miss her terribly. And Mesfer for his generosity like no other, his humour and his admirable commitment to not just his work, but our team and our friendships. With Michael, the four of us make the dream team.

I'd also like to thank Dr Derek Burke, for his endless supply of patient plasma and humour! It's been a pleasure working with you over the years. And Dr Iain Hargreaves, for kindly teaching me the first assay I ever got to do during this PhD and which now forms the basis of my work!

There are also those outside of the lab, without whom I could not have made it this far. My family, for being annoying but loving and supporting. My parents, Samira and Khaled, especially, who've bent over backwards to make this journey as smooth as possible, for being incredibly patient with me and for always cheering me on.

And my friends, who've fed me an endless supply of brownies, cakes and cookies to cushion the stress during the PhD. I'd like to especially thank Q (who let me drag her to the lab on weekends), Christina and Alaa, who pored over my thesis at strange hours of the night and cheered me endless, and Foofy, for being the crutch who always keeps me standing.

Finally, I'd like to thank Vitaflo, for sponsoring this fantastic project, and particularly Tricia and Maura. Your dedication to the cause is inspiring, and your warmth and kindness is always appreciated. I would not have had the opportunities to have experienced so much without your support.

CHAPTER 1

Introduction

1.1 EPILEPSY

Epilepsy is a common chronic neurological disorder, affecting approximately 50 million people worldwide (Megiddo et al., 2016; World Health Organization, 2005). Accounting for 1% of the global burden of disease, epilepsy occurs at an incidence of 4-10 in 1000 people (Fisher et al., 2005; Wallace, Shorvon, & Tallis, 1998) and although ubiquitous across all age groups, its prevalence is bimodal, primarily affecting children and the elderly (World Health Organization, 2005). Epilepsy is characterised by seizures, defined as atypical synchronous or excessive neuronal electrical activity in the brain, as well as alterations in the brain that increase predisposition to seizure generation (Fisher et al., 2005). These seizures lead to transient uncontrollable changes in behaviour, altered awareness and/or motor movements, detrimentally impacting neurological function, cognition and mental health.

Underlying seizure aetiology varies greatly amongst patients, and whilst aetiology often remains unclear, seizures are known to be caused by a number of factors, including genetic defects, structural brain abnormalities, infection, trauma, autoimmune responses and metabolic disorders. In some cases, epilepsy may also be cryptogenic, with no apparent genetic, structural or metabolic defects. Table 1.1 summarises a range of common aetiologies, causes and the typical conditions associated with the causes.

TABLE 1.1 General aetiology and causes of epilepsy, and typical examples of associated conditions. Adapted from the ILAE online Diagnostic Manual (www.EpilepsyDiagnosis.org).

Aetiology	Examples of Causes	Examples of Conditions
Genetic	Single gene defects	West syndrome; juvenile myoclonic epilepsy; Lennox-Gastaut; familial lobe epilepsy; Rett syndrome; Angelman syndrome; Dravet syndrome
	Chromosomal defects	Down syndrome; Fragile X syndrome; 4p-syndrome; isodicentric chromosome 15; ring chromosome 20
Structural	Acquired	Traumatic brain injury; stroke; hypoxic-ischaemic injury; neurosurgery
	Developmental malformation	Tuberous sclerosis; focal cortical dysplasia; lissencephaly; schizencephaly; hypothalamic hamartoma
	Vascular malformation	Cerebral angioma; Sturge Weber syndrome; arteriovenous malformation
	Tumours	Hypothalamic hamartoma; ganglioglioma; Dysembryoplastic neuroepithelial tumour (DNET)
Metabolic	Mitochondrial disorders	Myoclonic epilepsy with ragged-red fibers (MERRF); Mitochondrial encephalomyopathy, lactic acidosis, and stroke-like episodes (MELAS); Alpers' syndrome; Leigh syndrome
	Creatine disorders	Guanidinoacetate methyltransferase (GAMT) deficiency; creatine transporter (CT1) deficiency
	Peroxisomal disorders	Zellweger syndrome; neonatal adrenoleukodystrophy (NALD); infantile Refsum disease (IRD)
	Other	Glucose transporter type 1 (GLUT1) deficiency; Pyridoxine dependent epilepsy/pyridoxine 5' phosphate oxidase (PNPO) deficiency
Immune	--	Rasmussen syndrome; Systemic Lupus Erythematosus (SLE)
Cryptogenic	--	Febrile infection related epilepsy syndrome

Of particular interest to this thesis is the role that mitochondria play in epilepsy. Mitochondrial disorders are a common group of metabolic diseases, with epilepsy reported in approximately 35-60% of patients (Rahman, 2012). Whilst mitochondrial disorders, such as myoclonic epilepsy with red ragged fibres (MERRF) and

mitochondrial encephalomyopathy, lactic acidosis, and stroke-like episodes (MELAS), often present epileptic seizures as a primary manifestation, mitochondrial defects have also been associated with a range of symptomatic and acquired epilepsies (Chang & Yu, 2010; Kudin et al., 2009; Lee et al., 2008; Sabbagh et al., 2010). Experimental studies also reveal a relationship between mitochondrial dysfunction and seizures, although it remains unclear if alterations in mitochondrial function are primary or secondary to seizure generation (Cock et al., 2002; Kovac et al., 2012; Kovacs et al., 2005; Kudin et al., 2002; Rowley et al., 2015).

1.2 EPILEPSY AND ENERGY

Defects in mitochondrial energy metabolism have long been considered to underlie the pathology of neurodegenerative diseases (Beal, Hyman, & Koroshetz, 1993). Whilst epilepsy has historically been considered a disease of neuronal excitability and transmission, substantial advances in research place dysfunctions of mitochondria and energy metabolism as a primary cause of epilepsy, raising the need for broader perspectives of the disease (Scharfman, 2015; Zsurka & Kunz, 2015). However, prior to considering the role of mitochondria in epilepsy, an appreciation for how neurons are excited and how these mechanisms are impacted during seizures is necessary.

1.2.1 Neuronal Excitability

Neuronal electrical activity is regulated by a complex series of tightly knit processes. At the most fundamental level though, neuronal excitability is dependent on the homeostasis of ions that govern the electrical basis of nerve cell function. Disruption of these mechanisms can perturb the delicate balance of excitation and inhibition within this system. Thus, seizures are essentially a manifestation of this imbalance.

Action potentials are the basic mechanism underlying neuronal excitability, and the means through which electrical information is transferred within the brain. Propagated by waves of depolarisation and repolarisation of neuronal membranes, action potentials culminate in synaptic transmission at axon terminals, where neurotransmitters are released. They occur in an all-or-none fashion, induced by local changes in membrane potential, caused by neurotransmitter binding or intracellular ion compartmentalisation (Bromfield, Cavazos, & Sirven, 2006). Local stimulation causes an influx of Na^+ ions into neurons through Na^+ channels, resulting in depolarisation of the membrane that triggers a positive feedback loop at a threshold potential. This induces the opening of additional Na^+ channels, further depolarising the membrane. At peak depolarisation, Na^+ channels begin to close whilst voltage-gated K^+ channels open, causing an efflux of K^+ from the cell. This net positive outward flux of ions repolarises the membrane, with the voltage-gated K^+ channels closing once the membrane is hyperpolarised. Resting membrane potential is then restored by the action of transmembrane Na^+/K^+-ATPase pumps, which re-establish the Na^+ and K^+ gradients across the cell membrane, by exporting Na^+ and importing K^+ into the cell (Holm & Lykke-Hartmann, 2016; Purves et al., 2004). Na^+/K^+-ATPase pumps rely on energy from adenosine triphosphate (ATP) to power its activity. The self-generating nature of action potentials ensures that they are propagated along axons, with the initial depolarisation stimulating the opening of adjacent Na^+ channels farther along the axon, triggering further action potentials that lead to synaptic transmission. Glutamate and γ-aminobutyric acid (GABA), the major excitatory and inhibitory neurotransmitters, respectively, are released for neurotransmission according to neuronal cell type, before active reuptake from the synaptic cleft by transporters (Scharfman, 2007).

1.2.2 The Metabolic Cost of Neuronal Signalling

Despite the brain only making up ~2% of total body weight, it is thought to utilise more than 20% of resting whole-body metabolism (Schönfeld & Reiser, 2013). The neuronal signalling processes described above represent a significant energy demand on the brain, with approximately 75% of total energy expenditure in neuron-rich grey matter estimated to be involved in neuronal excitatory signalling (Attwell & Laughlin, 2001). Action potentials and postsynaptic transmission make up the bulk of this expenditure, with the majority of ATP consumption utilised by numerous ion pumps to restore ion gradients and maintain membrane potential (Attwell & Laughlin, 2001; Liotta et al., 2012), whilst presynaptic energy consumption is mostly devoted to vesicle cycling for neurotransmission (Rangaraju, Calloway, & Ryan, 2014). Mitochondria are the main producers of ATP within the brain (Schönfeld & Reiser, 2013), with mitochondria found highly distributed in areas of significant need within neurons (Zsurka & Kunz, 2015). Therefore, ATP supplied by mitochondria is crucial to meeting the energy demands of the brain.

1.2.3 The Neuronal Energy Crisis of Seizures

The rate of action potentials also strongly affects metabolic demand, with increased frequency of discharges significantly increasing ATP utilisation (Attwell & Laughlin, 2001). During seizures, action potentials fire in excess in an abnormally synchronised manner, soliciting hyperexcitability in populations of neurons either locally or across the whole brain. This observed hyperexcitability of neurons may arise from a combination of factors that shift the balance of inhibition and excitation, including increased excitatory synaptic transmission, reduced inhibitory synaptic transmission, changes in voltage-gated ion channels and alterations in local ion concentrations (Bromfield et al., 2006; Scharfman, 2007).

Regardless of their cause, however, seizures impose an excessive energy burden on the brain. Increased neuronal discharges and the necessary restoration of the changes induced by excitation present a substantial bioenergetic challenge in cells, leading to an energy crisis. Furthermore, seizure activity has been associated with decreased levels of ATP and metabolic substrates in the brain (King et al., 1967; Kovac et al., 2012; Sanders et al., 1970). This depletion of ATP is thought to affect the function of ion-pumping ATPases, particularly Na^+/K^+-ATPase which is estimated to utilise up to 50% of total energy production in the brain (Ames III, 2000; Astrup, Møller Sørensen, & Rahbek Sørensen, 1981). In addition to maintaining the Na^+/K^+ electrochemical gradients necessary for regulating action potentials, the ion gradients generated by Na^+/K^+-ATPase are also essential for neurotransmitter reuptake (Albers, Siegel, & Xie, 2012; Holm & Lykke-Hartmann, 2016). Thus, disruption of ATPase activity can have severe consequences on neuronal excitability and neurotransmission. Increased extracellular K^+ concentrations from reduced Na^+/K^+-ATPase activity can trigger depolarisation, leading to hyperexcitability, with defects in pump function also reported in experimental models of epilepsy (Clapcote et al., 2009; Du et al., 2016; Fernandes, Naffah-Mazzacorati, & Cavalheiro, 1996; Grisar, Guillaume, & Delgado-Escueta, 1992; Haglund & Schwartzkroin, 1990; Somjen, 2002).

Conversely, decreased neurotransmission as a result of depressed ATPase activity and loss of ionic homeostasis can also occur, leading to seizures. This is particularly salient when considering the role of synaptic transmission in the balance between inhibition and excitation. Depleted energy supply may depress the activity of inhibitory interneurons, local-circuit cells pivotal in the regulation of excitatory neurons, resulting in the increased neuronal network excitation observed during seizures (Haglund & Schwartzkroin, 1990; Kann et al., 2011; Kudin et al., 2009; Vaillend et al.,

2002). Thus, with the dependence of these processes on an adequate energy supply, mitochondrial function and ATP production are of critical importance.

1.3 MITOCHONDRIA IN EPILEPSY

Often described as the powerhouses of cells, mitochondria play a pivotal role in cellular homeostasis and function, and are involved in a range of processes that influence neuronal excitability, including energy metabolism, calcium signalling, neurotransmitter biosynthesis and cell death. Mitochondria are also a primary site of reactive oxygen species (ROS) production, leaving them vulnerable to oxidative damage (Lenaz, 2001; Marchi et al., 2012; Popa-Wagner et al., 2013; Turrens, 2003). Consequently, alterations in mitochondrial function frequently underpin a range of disease conditions, particularly epilepsy. Thus, understanding mitochondrial function, and dysfunction thereof, is imperative in the quest towards understanding the pathogenesis of epilepsy.

1.3.1 Mitochondrial Structure

Double-membrane bound organelles, mitochondria present an inner and outer phospholipid membrane, separating the intermembrane space between the inner and outer membranes, and the mitochondrial matrix, bounded by the inner membrane. The inner mitochondrial membrane is further compartmentalised into folds called cristae and is highly impermeable to ions and solutes, containing specific ion channels and transport systems, including those for ATP and fatty acid translocation. The inner mitochondrial membrane is also home to the electron transport chain, involved in oxidative phosphorylation and ATP synthesis. In contrast, the outer mitochondrial membrane is more permeable, containing porins for the regulated flux of small molecules and metabolites (Rich & Maréchal, 2010).

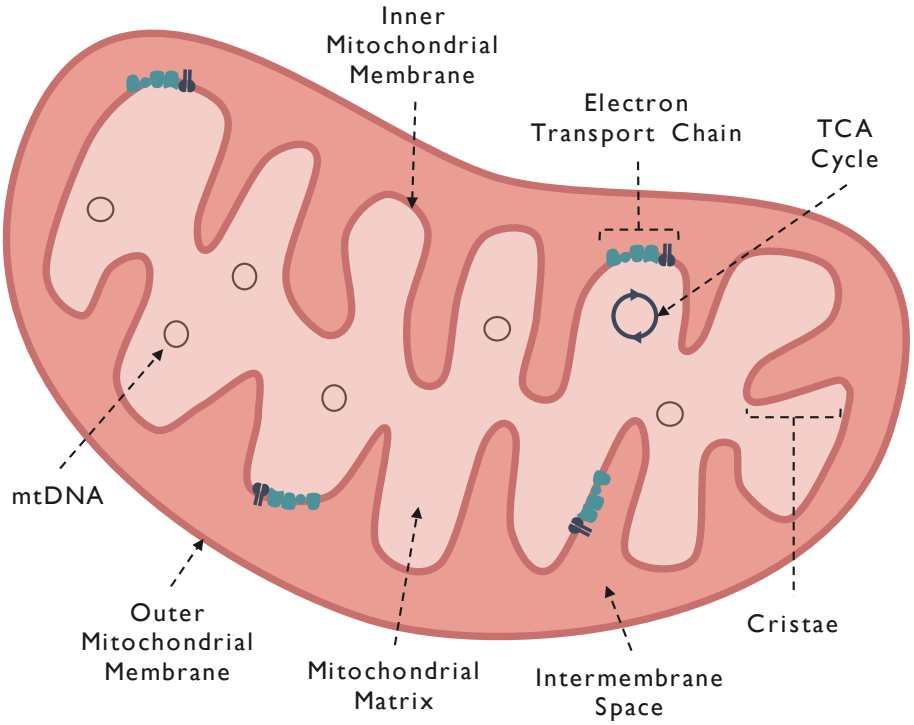

FIGURE 1.1 Structure of a mitochondrion.

Mitochondria also contain their own unique and independent genome which is critical for cellular function. Circular and double-stranded in structure, mitochondrial DNA (mtDNA) is composed of 16,569 base pairs and encodes for 37 genes, 13 of which encode for polypeptide subunits of the electron transport chain complexes, and the remainder for the essential machinery involved in their translation (22 transfer RNAs (tRNAs) and 2 ribosomal RNAs (rRNAs)) (Duchen, 2004; Taylor & Turnbull, 2005). However, mitochondria are under dual genetic control of both nuclear and mitochondrial DNA, with most mitochondrial gene products encoded by nuclear DNA and specifically imported into mitochondria. Maternally inherited, mtDNA is also highly prone to heteroplasmy, with frequent replication giving rise to numerous heterogeneous copies of mtDNA in individual mitochondria (Taylor & Turnbull, 2005).

1.3.2 The TCA Cycle

The primary function of mitochondria is the generation of ATP, the energy currency utilised by cells to fuel cellular processes. Free energy is captured into ATP during the oxidation of fuels, with ATP acting as a free-energy donor, through hydrolysis, to drive a range of processes. The tricarboxylic acid (TCA) cycle, otherwise known as the Krebs or citric acid cycle, constitutes the first step in cellular respiration, before leading to the electron transport chain, from which energy is harvested to synthesise ATP. Consisting of a series of eight catalytic reactions, the TCA cycle converts acetyl coenzyme A (acetyl CoA), derived from the oxidation of carbohydrates, amino acids and fatty acids, into CO_2, with the energy conserved into NADH, $FADH_2$, and GTP (Berg, Tymoczko, & Stryer, 2012). Taking place in the mitochondrial matrix, the pathway acts as the final central hub for the catabolism of all metabolic fuels and can oxidise an unlimited amount of acetyl CoA due to its cyclical nature.

The TCA cycle is initiated by the condensation of two-carbon acetyl CoA with four-carbon oxaloacetate to produce the six-carbon compound citrate, a process catalysed by the enzyme citrate synthase. The enzyme aconitase then catalyses the reversible isomerisation of citrate into isocitrate. The third step of the TCA cycle is the oxidative decarboxylation of isocitrate into five-carbon α-ketoglutarate, via the enzyme isocitrate dehydrogenase. The oxidation of isocitrate results in the reduction of the cofactor nicotinamide adenine dinucleotide (NAD^+) to form NADH, with the resultant intermediate decarboxylated to release CO_2. This step generates the first NADH electron carrier and CO_2 of the cycle. The enzyme α-ketoglutarate dehydrogenase catalyses the oxidative decarboxylation of α-ketoglutarate into succinyl CoA, also releasing NADH and CO_2. It is of note that the CO_2 formed in these steps of the cycle are not derived from the acetyl CoA that initially entered the cycle, but from the TCA

cycle substrates. CO_2 generated from acetyl CoA is released in subsequent rounds of the cycle. Upon formation of succinyl CoA, the enzyme succinyl CoA synthetase cleaves the high-energy thioester bond in succinyl CoA to form succinate, and utilises the free energy released to drive substrate-level phosphorylation that generates either guanosine triphosphate (GTP) or ATP (Berg et al., 2012; Pratt & Cornley, 2014). Succinate subsequently undergoes a series of reactions to regenerate oxaloacetate and complete the cycle. Succinate dehydrogenase oxidises succinate into fumarate, reducing flavin adenine dinucleotide (FAD) to $FADH_2$. Located in the inner mitochondrial membrane, succinate dehydrogenase is also known as complex II and participates in the electron transport chain, providing a direct link to the TCA cycle. $FADH_2$ requires re-oxidation prior to the next cycle, and thus transfers electrons to succinate dehydrogenase, which subsequently passes them to the lipid-soluble electron carrier Coenzyme Q (CoQ, Q or ubiquinone), a key component of the electron transport chain (see Section 1.3.3). Fumarate is then catalysed by fumarase in a hydration reaction to form malate. Finally, malate dehydrogenase oxidises the conversion of malate into oxaloacetate via reduction of NAD^+ to NADH, and thus drawing the TCA cycle back to the beginning to repeat the process once more.

For every turn of the TCA cycle, electrons are recovered in a total of three NADH and one $FADH_2$ molecules, with one GTP or ATP also produced. Electrons gained from the TCA cycle can be transferred to the electron transport chain from NADH and $FADH_2$, and ultimately lead to the generation of ATP through oxidative phosphorylation. An overview of all the reactions and products described are presented in Figure 1.2.

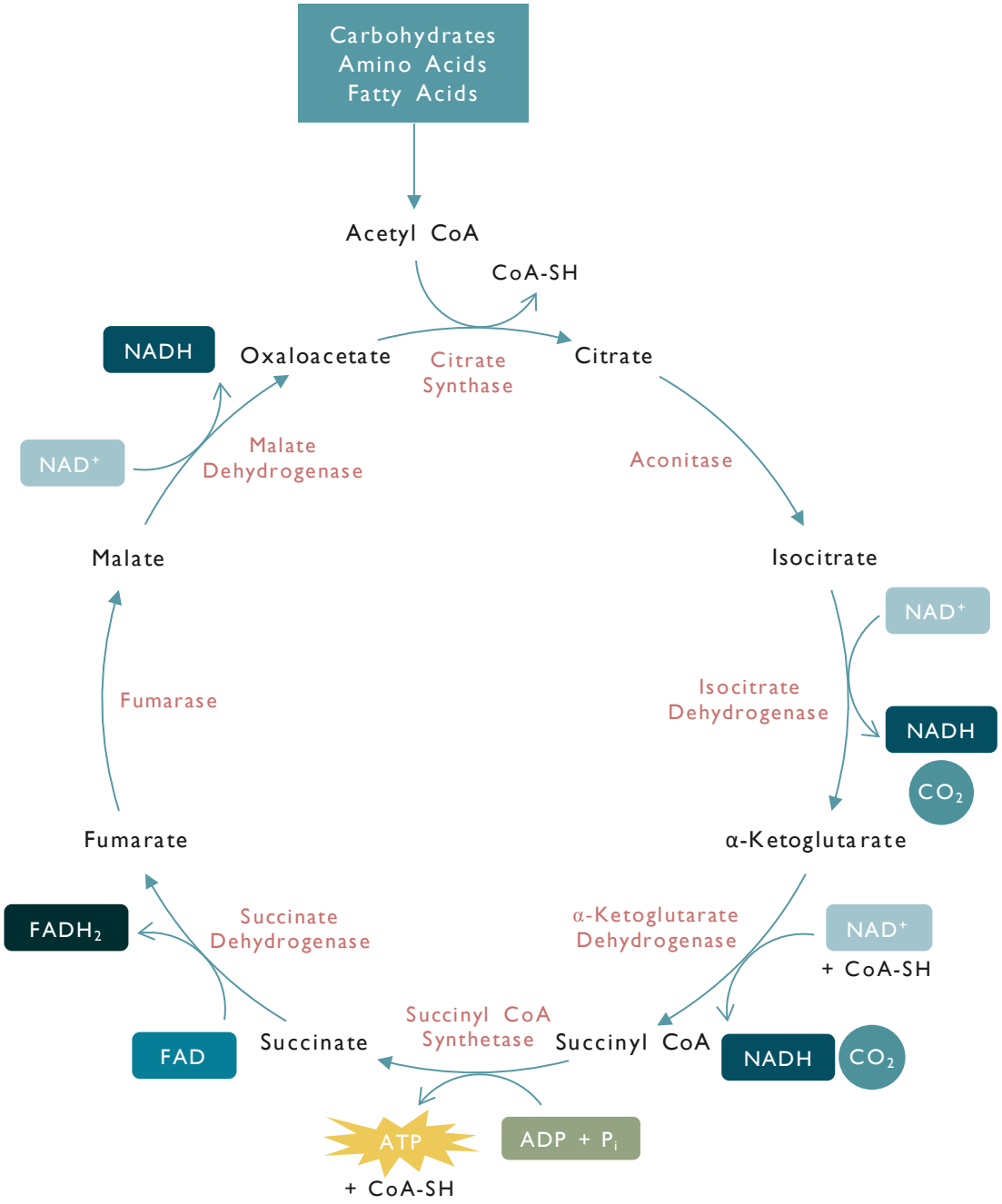

FIGURE 1.2 Reactions of the TCA cycle. Acetyl CoA, derived from the oxidation of various substrates, is converted into CO_2, with the energy conserved into NADH, $FADH_2$, and GTP or ATP (substrates in black; enzymes in pink; coenzymes in blue).

1.3.3 The Electron Transport Chain and Oxidative Phosphorylation

As previously described, the electron transport chain is located in the inner mitochondrial matrix, where electrons derived from the TCA cycle are shuttled to reduce O_2 to H_2O and the energy from electron transport conserved in the production of ATP in a process known as oxidative phosphorylation (Figure 1.3). This transfer of electrons occurs through a chain of four protein complexes embedded within the inner mitochondrial membrane, three of which also function as redox-driven proton pumps to generate a proton gradient across the membrane (Rich & Maréchal, 2010).

Complex I, also known as NADH:ubiquinone oxidoreductase or NADH dehydrogenase, begins the chain by accepting two electrons from NADH and transferring them via prosthetic group flavin mononucleotide (FMN) and a series of iron-sulphur clusters to the electron carrier CoQ. As CoQ is reduced to $CoQH_2$ (QH_2 or ubiquinol), complex I transfers four protons from the mitochondrial matrix to the intermembrane space. Coupling of electron transfer with proton translocation greatly increases the efficiency of NADH oxidation and consequential ATP generation (Rich & Maréchal, 2010).However, electron leak at complex I can also occur, with electrons reacting with oxygen to generate superoxide (Jastroch et al., 2010). Alterations in complex I function are implicated in a wide range of pathologies, including epilepsy, with defects affecting respiratory chain capacity and producing a significant source of ROS (Jastroch et al., 2010; Kunz et al., 2000; Rahman, 2012; Sipos, Tretter, & Adam-Vizi, 2003).

$CoQH_2$, having taken up two protons from the matrix, leaves complex I to join a pool of CoQ in the lipid bilayer, already reduced by complex II. Complex II (succinate CoQ oxidoreductase; succinate dehydrogenase), as previously mentioned, is integral to the

TCA cycle, with $FADH_2$ forming a component of the complex. As a consequence of this coupling to the TCA cycle, electrons from $FADH_2$ are transferred to iron-sulphur clusters within complex II before reducing CoQ to $CoQH_2$. Unlike complex I, complex II does not pump protons between the mitochondrial matrix and intermembrane space.

$CoQH_2$ is then oxidised by complex III (CoQ-cytochrome c oxidoreductase; cytochrome bc_1) to reduce cytochrome c in a two-cycle process, commonly known as the Q cycle (Pratt & Cornley, 2014; Rich & Maréchal, 2010; Voet, Voet, & Pratt, 2013). Much like in complex I, electron transfer through complex III is coupled to proton translocation. Cytochrome c is an electron-transferring protein that contains a haem prosthetic group. As cytochrome c can only carry one electron at a time, the two electrons from $CoQH_2$ must follow two paths. Complex III contains three cytochromes b_H, b_L and c_1, as well as an iron-sulphur protein (the Rieske centre), and two binding sites: Q_0 for $CoQH_2$ and Q_i for CoQ. In the first cycle, $CoQH_2$ binds to Q_0, donating one electron to the iron-sulphur protein which is then transferred to cytochrome c_1 before finally reducing cytochrome c, which is free to diffuse to the next component of the electron transport chain. Two protons are released and pumped into the intermembrane space, and a stable semiquinone radical $CoQ^{\cdot-}$ is yielded. The second electron is transferred from $CoQ^{\cdot-}$ to cytochrome b_L and then to cytochrome b_H, to form CoQ. CoQ binds to Qi, where it accepts the electron from cytochrome b_H to form $CoQ^{\cdot-}$ once more. In the second cycle, an additional $CoQH_2$ joins the Q cycle, transferring one electron to reduce cytochrome c, releasing two protons as described before, with the other electron going to cytochrome b, where it reduces the $CoQ^{\cdot-}$ waiting at Q_i into $CoQH_2$ using protons from the mitochondrial matrix. Overall, this process yields the pumping of four protons into the intermembrane space and the removal of two protons

from the matrix, contributing to the proton gradient. The nature of these processes also places complex III as a major site of ROS production. Inhibition of complex III, such as with antimycin A which blocks Q_i, results in superoxide generation (Lenaz, 2001; Sipos et al., 2003). In is also thought that in conditions of high energy demand, such as during seizures, complex III contributes to the ROS production associated with seizures (Malinska et al., 2010).

Finally, the reduced cytochrome c generated from complex III shuttles electrons to complex IV (cytochrome c oxidase). Complex IV catalyses the transfer of four electrons from cytochrome c to reduce O_2 into H_2O. This process occurs within the redox centre of complex IV, which contains two haem groups (haem a and haem a_3), a pair of copper ions (Cu_A) and an individual copper ion (Cu_B). Two cytochrome c molecules sequentially transfer electrons into complex IV, via Cu_A and haem a, to reduce haem a_3 and Cu_B. O_2 binds to the reduced Cu_B and iron in haem a_3, forming a peroxide bridge between the two groups. This is cleaved upon the addition of two electrons from two cytochrome c molecules, and two protons from the matrix, resulting in hydroxyl groups being formed on haem a_3 and Cu_B. The addition of two further protons from the matrix then results in the final product of H_2O, formed from the hydroxyl groups. Overall, this process contributes to a total of four protons being removed from the mitochondrial matrix, with four protons pumped into the intermembrane space. With its vital role in the electron transport chain, changes in complex IV function are critical. Complex IV deficiency is a common cause of mitochondrial disease, such as Leigh syndrome or MERRF, with seizures frequently presenting in patients (Patel, 2004; Rahman, 2012).
The resultant proton gradient from the translocation of protons across the inner mitochondrial membrane during electron transfer is key to ATP synthesis. The increased concentration of protons in the intermembrane space and the decreased

proton concentration in the mitochondrial matrix results in an imbalance in electrical charge, also known as an electrochemical gradient, or more specifically, a proton-motive force (Zorova et al., 2017). This difference in charge also results in the polarisation of the inner mitochondrial membrane, called the mitochondrial membrane potential. Coupled with this proton motive force is an associated free energy, which is utilised by ATP synthase to produce ATP (Rich & Maréchal, 2010).

ATP synthase (also known as Complex V) is a transmembrane proton pump that catalyses the phosphorylation of ADP with orthophosphate (P_i) to form ATP. ATP synthase is composed of two units: F_0, which forms a transmembrane channel for proton flow into the matrix, and F_1, which comprises the catalytic unit of the protein, found in the matrix. Passage of protons through F_0 is coupled to ATP synthesis. As protons flow through F_0, conformational changes are induced that cause a mechanical rotation in structure, affecting F_1 affinity for ADP and P_i, and allowing ATP synthesis and release. In the absence of a proton gradient, ATP synthesis is unable occur. When mitochondrial respiration is compromised and membrane potential drops, ATP synthase can reverse, hydrolysing ATP to pump protons across the membrane and into the intermembrane space to generate a proton gradient (Popa-Wagner et al., 2013). Prolonged reversal of this reaction, however, leads to ATP depletion and can precipitate cell death.

The effective coupling of the oxidative phosphorylation processes described is essential to ATP production and mitochondrial function. Defects in any of the components of the electron transport chain can present in a variety of clinical abnormalities, including inborn errors of metabolism, epilepsy and other neurodegenerative disorders (Onyango et al., 2010; Rahman, 2012). These deficiencies have a deleterious impact on

ATP supply, ROS generation and energy demand, potentially leading to cell death, neurodegeneration and seizures (Folbergrová & Kunz, 2012).

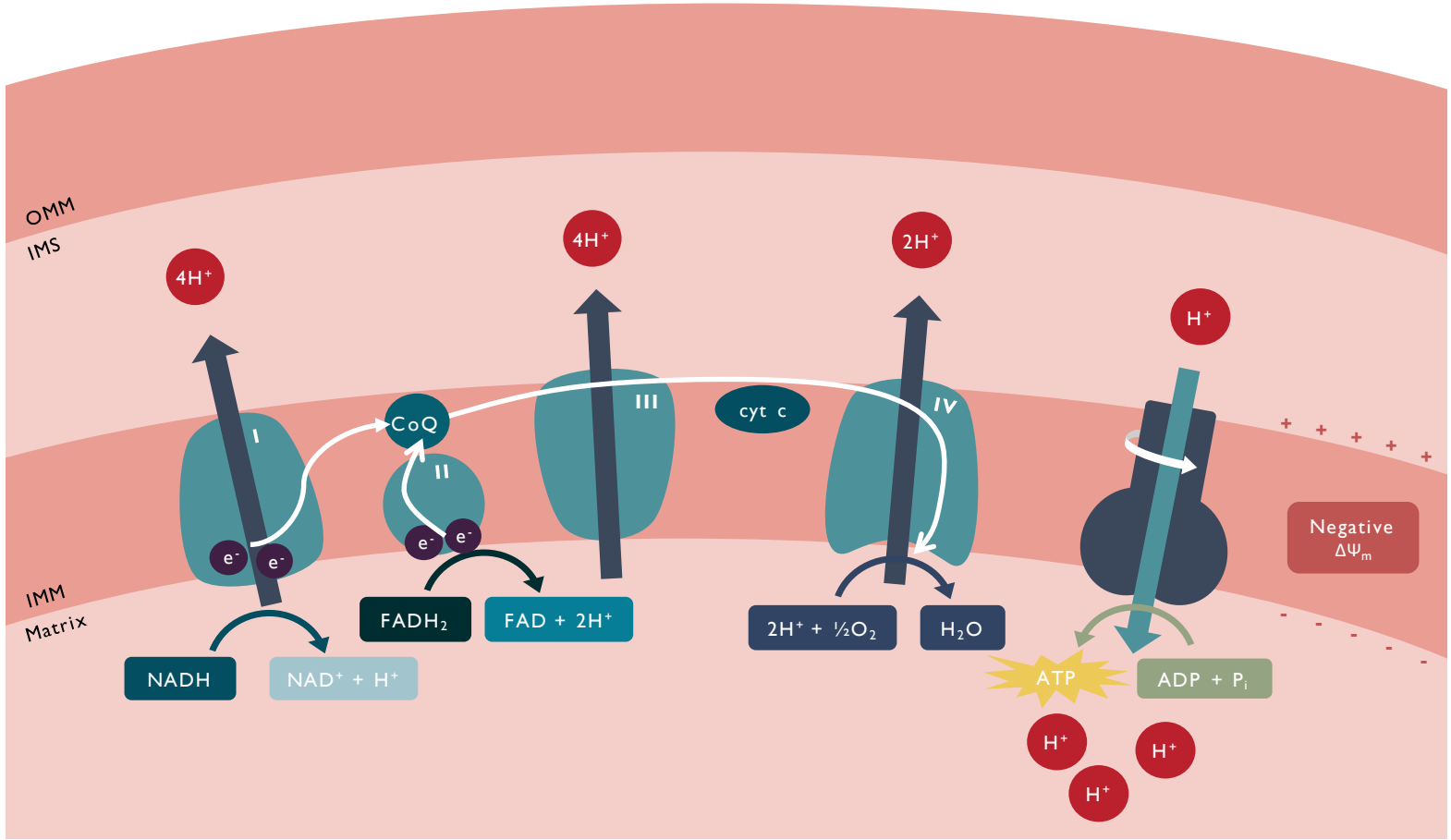

FIGURE 1.3 Overview of the electron transport chain. (Abbreviations: OMM, outer mitochondrial membrane; IMS, intermembrane space; IMM, inner mitochondrial membrane; cyt c, cytochrome c; $\Delta\Psi_m$, mitochondrial membrane potential.)

1.3.4 Mitochondrial Dysfunction in Epilepsy

In neuronal cells, a substantial proportion of ATP produced by mitochondria is used to maintain cellular plasma membrane potential and neuronal excitability, as described in Section 1.2. Thus, defects in the electron transport chain or oxidative phosphorylation can have severe consequences on neuronal excitability and lead to seizures. Loss of mitochondrial electron transport chain function, particularly complex I, has been reported in the brains of both animal seizure models and samples derived from epilepsy patients (Cock et al., 2002; Kudin et al., 2002; Kunz et al., 2000), whilst peripheral defects in electron transport chain function are frequently reported in mitochondrial epilepsies and other symptomatic/non-symptomatic epilepsies (i.e. epilepsy that presents with features typical of syndromes or idiopathic epilepsies that occur alone) (Khurana et al., 2008; Lee et al., 2008; Rahman, 2012; Sabbagh et al., 2010). Dysfunctions in complex I have also been found to inhibit synaptic vesicle cycling, with neuronal vesicle cycling thought to be highly dependent on mitochondrially-derived ATP, potentially affecting neurotransmission and excitability (Pathak et al., 2015). In an experimental model of epilepsy, decreased expression mitochondrial proteins involved in energy metabolism was also observed following seizure insult, further implicating the bioenergetic importance of mitochondria in epilepsy (Araujo et al., 2014). Mutations in mtDNA are also associated as a genetic cause of epilepsy (Lightowlers, Taylor, & Turnbull, 2015; Wallace et al., 1994; Zsurka & Kunz, 2015).

The role of mitochondria in ATP synthesis and oxidative phosphorylation also results in mitochondria generating the primary source of ROS in cells. Electron leak from the electron transport chain leads to the formation of superoxide radicals ($O_2^{\bullet -}$), particularly at complexes I and III, and hydroxyl radicals ($OH^{\bullet -}$) from H_2O_2 (Jastroch et

al., 2010; Turrens, 2003). Whilst this ROS generation is a normal process of electron transport chain activity, it leaves mitochondria susceptible to oxidative damage. Aberrant ROS generation can lead to damage of surrounding mitochondrial components, such as the electron transport chain and mtDNA, as well as damage to other cellular components. Increased evidence suggests a role for mitochondrial oxidative stress in epilepsy and epileptogenesis, with experimental studies revealing increased ROS generation in various models of epilepsy (Erakovic et al., 2003; Liang & Patel, 2006; Malinska et al., 2010; Rowley et al., 2015), decreased seizure threshold and hippocampal cell loss in antioxidant deficient ($Sod2^{-/+}$) mice (Liang et al., 2012; Liang & Patel, 2004), and indications of oxidative damage in acquired epilepsies such as temporal lobe epilepsy (Rowley et al., 2015). Furthermore, the involvement of mitochondrial oxidative stress in epilepsy is further implicated with the observation that increased age increases seizure vulnerability (Brodie & Kwan, 2005). Increased mitochondrial oxidative stress is a hallmark of ageing and strongly associated with age-related neurodegenerative disorders (Mariani et al., 2005).

1.4 EPILEPSY TREATMENT

Typically, in high-income countries, the first line of treatment for patients is through antiepileptic drugs (AEDs), which provide symptomatic treatment of the condition, suppressing seizures rather than treating disease origin. Prognosis for most patients is good with AEDs, but for approximately 20-40% of epilepsy patients, pharmacological treatment is clinically ineffective (French, 2007; Kwan & Brodie, 2000). These patients are rendered as drug-resistant (i.e. refractory), pronounced upon the failure of two or more appropriate and tolerated drug treatments (alone or in combination) to control seizures (Kwan et al., 2010). Despite the increasing range of AEDs available, the incidence of drug-resistant epilepsy remains high, and patients are often required to

undergo alternative therapies, such as vagal nerve stimulation (VNS), surgery or the ketogenic diet. VNS uses electrical stimulation to attenuate seizures, and although minimally invasive, it provides modest efficacy and is currently limited to patients who experience a specific seizure classification (i.e. focal onset epilepsy) (Binnie, 2000; Morris & Mueller, 1999). Surgery offers the most aggressive intervention, involving resection of brain tissue thought to be the focus of seizures. Whilst highly effective, much like VNS, patients with focal onset epilepsy are most amenable to surgery, thus making it an unsuitable procedure for all epilepsy patients (Téllez-Zenteno, Dhar, & Wiebe, 2005). The ketogenic diet, however, remains a treatment option for a wide range of epilepsies, and whilst complex to maintain, it offers an alternative non-invasive, nonpharmacological therapy to drug-resistant epilepsy.

With the mechanisms of drug-resistance largely unclear and data conflicting on the factors associated with poor responsiveness to drugs (Mohanraj & Brodie, 2013), there remains a need to develop effective therapies for drug-resistant epilepsy. The broad-ranging impact of the ketogenic diet, however, provides a suitable avenue for the advancement of a therapeutic intervention that can be geared towards drug-resistant patients.

1.4.1 The Ketogenic Diet (KD)

Since antiquity, fasting has been known to exert a beneficial effect on seizures in epilepsy patients. In the 1920s, medical interest in these effects re-emerged (Geyelin, 1921), and the ketogenic diet (KD) was developed to simulate the metabolic profile of fasting (Wilder, 1921). A high-fat, low-carbohydrate, low-protein regimen, the KD induces ketone body generation from fats to provide an alternative fuel source during glucose restriction. This form of the diet, known as the classical KD, traditionally

provides long-chain fats in a 4:1 or 3:1 ratio (in grams) to carbohydrates plus protein combined, with 90% of daily energy intake from fat (Kossoff et al., 2009; Neal, 2012b). Patients undergo ketosis as a result, producing elevated levels of ketone bodies from the high fat intake, lending the diet its name.

1.4.2 Medium-chain Triglyceride Ketogenic Diet (MCT KD)

With the restrictive nature of the classical KD, several variations of the diet have since emerged, including the medium-chain triglyceride ketogenic diet, the modified Atkins diet and the low-glycaemic index treatment. Of particular interest is the medium-chain triglyceride ketogenic diet (MCT KD), an alternative diet developed in the 1970s (Huttenlocher, Wilbourn, & Signore, 1971). In the MCT KD, fats are provided by medium-chain triglycerides (MCTs), generally in the form of an MCT oil or emulsion composed of the saturated medium-chain fatty acids octanoic acid (~60%), an eight-carbon chain, and decanoic acid (~40%), a ten-carbon chain. Rapidly absorbed and metabolised by the body, MCTs are more ketogenic than LCTs, yielding greater amounts of ketone bodies per kilocalorie of energy. Consequently, the MCT KD is favoured for its reduced carbohydrate and protein restriction, with approximately 60-80% of energy intake required from fat (Neal, 2012b), making it more palatable than the classical KD (Figure 1.4). Moreover, the MCT KD relies on a percentage of calories to calculate MCT intake instead of ratios, allowing flexible modification of the diet. Accordingly, MCT intake generally varies from 30-60%, based on patient response and tolerability, with the remainder supplemented by LCTs (Kossoff et al., 2009; Neal, 2012b; Schwartz et al., 1989b).

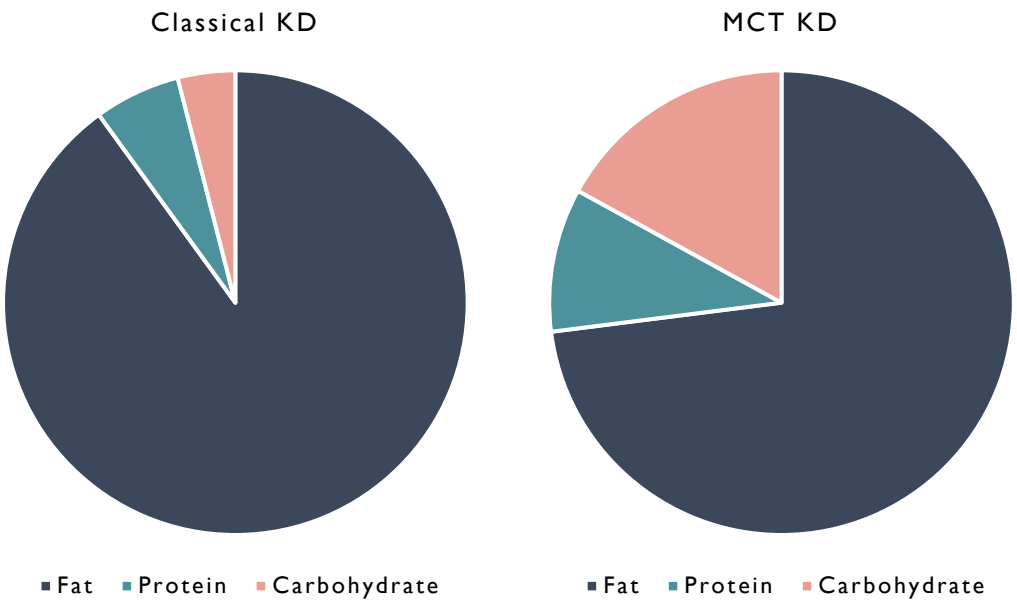

FIGURE 1.4 Typical compositions of the classical 4:1 ratio and MCT KDs. In the classical 4:1 ratio KD, the approximate percentages of dietary energy provided are 90% fat, 6% protein and 4% carbohydrate, whilst the MCT KD provides 73% fat, 10% protein and 17% carbohydrate (Neal 2012).

1.4.2.1 Fatty Acid Digestion and Transport

As described above, MCTs are utilised in the MCT KD for their increased ability to generate ketone bodies, in comparison to LCTs. When dietary triglycerides are consumed, they are hydrolysed by pancreatic lipoprotein lipases. MCTs are fully degraded into free fatty acids, whilst LCTs are broken down into monoacylglycerol and free fatty acids. MCFAs are then absorbed directly into the bloodstream and delivered to the liver via the hepatic portal vein. Meanwhile, long-chain fatty acids (LCFAs) and monoacylglycerol are incorporated into lipoproteins called chylomicrons and transported to the hepatic portal via the lymphatic system before reaching the liver. As a result, MCFAs are metabolised more readily than LCFAs due to more efficient absorbance into the bloodstream. Within the liver, fatty acids are generally metabolised through β-oxidation to generate ketone bodies.

1.4.2.2 Fatty Acid β-Oxidation

In addition to differing delivery systems into the liver, the mechanisms controlling MCFA and LCFA β-oxidation also differ. Fatty acid β-oxidation takes place in the mitochondrial matrix. However, fatty acid entry into the mitochondria is regulated according to fatty acid chain length (Kerner & Hoppel, 2000). Prior to entry into the mitochondria, both LCFAs and MCFAs are linked to CoA, a process that takes place on the outer mitochondrial membrane (Figure 1.5). This reaction is driven by acyl CoA synthetase and ATP, forming fatty acyl CoAs upon activation (Pratt & Cornley, 2014). Activated LCFAs are required to enter mitochondria via the carnitine shuttle, whilst activated MCFAs can enter independently of carnitine.

Prior to entry into the mitochondrial matrix, activated LCFA must be conjugated to carnitine to form acyl carnitine, a reaction catalysed by carnitine palmitoyltransferase I (CPT1), bound to the outer mitochondrial membrane. The long-chain fatty acyl carnitine is shuttled through the inner mitochondrial membrane via carnitine acyl carnitine translocase (CAT). Once in the mitochondrial matrix, the carnitine is removed from the acyl group and a fatty acyl CoA is formed once more, via carnitine palmitoyltransferase II (CPT2). The long-chain fatty acyl CoA can now undergo β-oxidation.

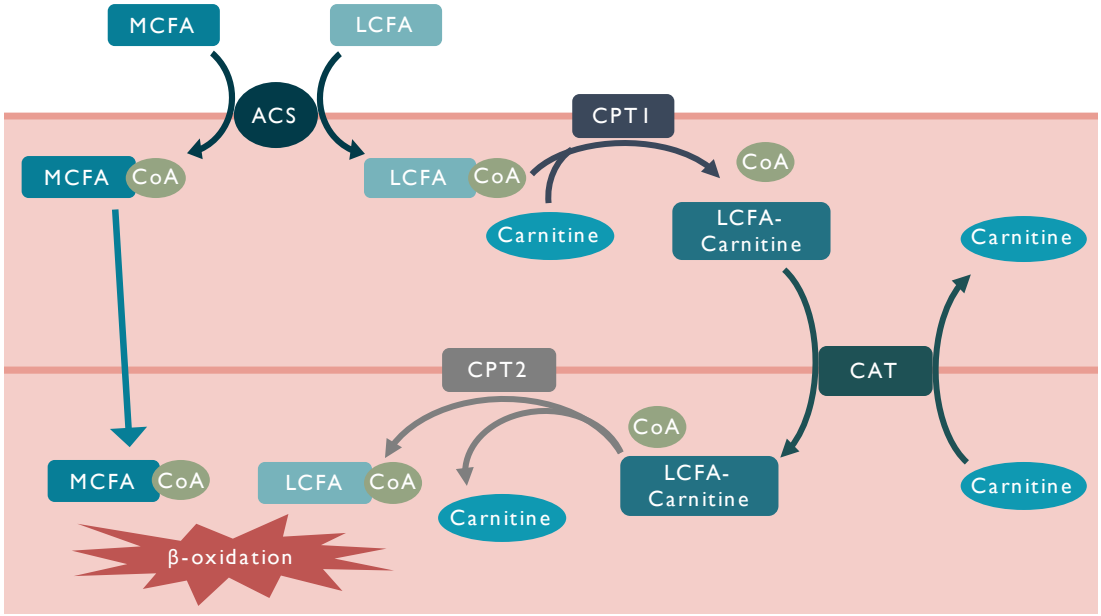

FIGURE 1.5 Overview of long-chain fatty acid entry into mitochondria via the carnitine shuttle. (Abbreviations: MCFA, medium-chain fatty acid; LCFA, long-chain fatty acid; ACS, acyl CoA synthetase; CPT1, carnitine palmitoyltransferase I; CAT, carnitine acyl carnitine translocase; CPT2, carnitine palmitoyltransferase II.)

Fatty acid β-oxidation consists of four major steps in order to produce acetyl CoA (Figure 1.6). The pathway begins by oxidation of the fatty acyl CoA by acyl CoA dehydrogenase, forming an enoyl CoA with a trans double bond between C-2 and C-3. Two electrons are also transferred to FAD to yield $FADH_2$, which delivers them to CoQ through a series of steps. Next, the trans double bond of the enoyl CoA is hydrated by enoyl CoA hydratase, producing 3-hydroxyacyl CoA. This is also oxidised, this time by 3-hydroxyacyl CoA dehydrogenase, yielding a ketoacyl-CoA and transferring electrons to NAD^+. In the final step of this cycle, the enzyme thiolase catalyses the cleavage of ketoacyl-CoA to produce an acetyl CoA and a fatty acyl CoA shortened by two carbons. This process repeats itself once more with the shortened fatty acyl CoA, the β-oxidation pathway cycling continuously until only acetyl CoA remains. MCFAs and LCFAs undergo β-oxidation in the same manner, differing only in the acyl CoA dehydrogenase

used (medium-chain acyl CoA dehydrogenase for MCFAs and long-chain acyl CoA dehydrogenase for LCFAs).

With rapid uptake into the liver and the ability to bypass the carnitine shuttle to enter mitochondria for β-oxidation, MCFAs can more efficiently generate ketone bodies, producing more ketone bodies than LCFAs per kilocalorie of energy. In addition to hepatic metabolism, MCFAs can also readily cross the blood-brain barrier (Olendorf, 1971, 1973; Spector, 1988), permitting further β-oxidation within the brain, where MCFAs have been shown to contribute approximately 20% of brain oxidative energy production (Ebert, Haller, & Walton, 2003).

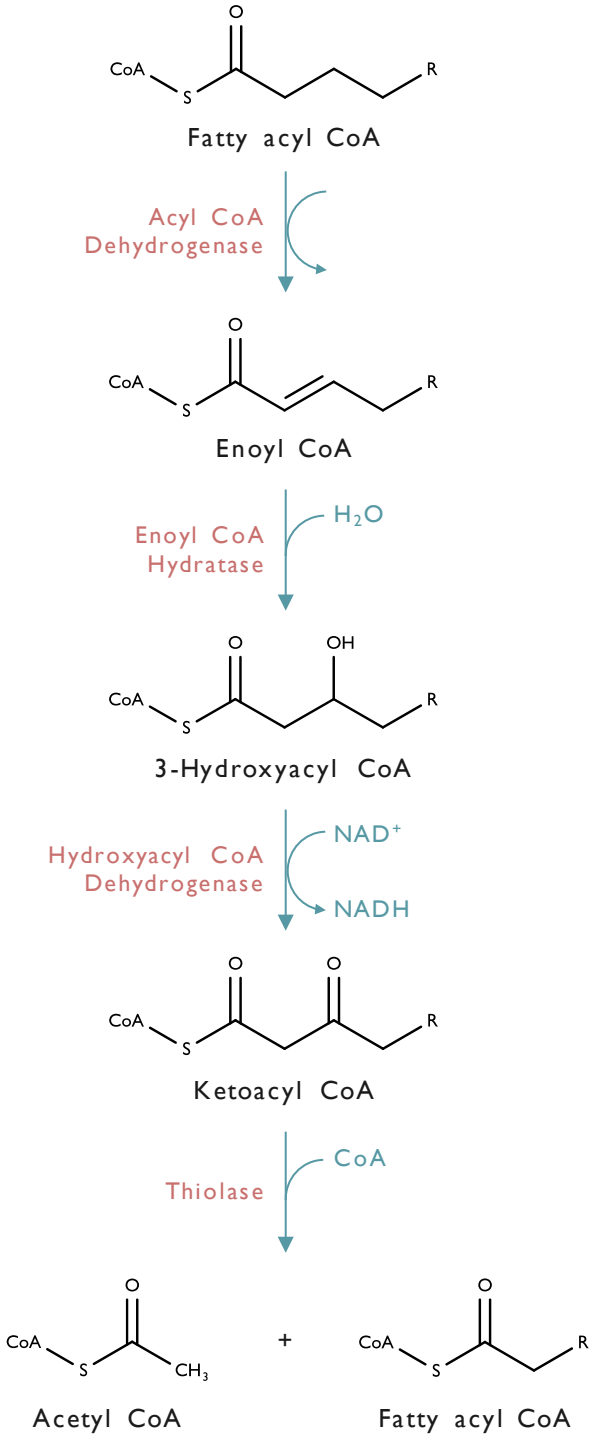

FIGURE 1.6 Fatty acid β-oxidation pathway.

1.4.3 Efficacy of the KD and MCT KD

Primarily a paediatric treatment option, the KD is highly effective in children, with approximately half of all patients showing a ≥50% seizure reduction whilst on the diet and a proportion of patients also becoming seizure-free (Keene, 2006; Kossoff, 2012). Whilst the diet also appears to have an effect in adults (Cervenka et al., 2016; Lambrechts et al., 2012; Schoeler et al., 2014; Sirven et al., 1999), the KD is not frequently offered to adult patients. Lack of efficacy in adults has been posited as a cause for this disparity, with some studies suggesting that patient response is less favourable in adolescents and adults (Coppola et al., 2002; Freeman et al., 1998). This may reflect an age-dependent metabolic capacity to extract ketone bodies into the brain (Morris, 2005), putting children at an advantage over adult populations. However, lack of compliance, due to the rigidity of the KD, and poor tolerability may simply be responsible for the perceived inefficacy in adults, as opposed to physiological and metabolic differences (Mosek et al., 2009; Schwartz et al., 1989b).

In the MCT KD, seizure control studies report high efficacy in patients, with at least 50% of patients responding to the diet (≥50% seizure reduction) (Huttenlocher et al., 1971; Lambrechts et al., 2015; Ross et al., 1985; Sills, Forsythe, & Haidukewych, 1986; Wibisono et al., 2015). Similar effects have also been observed in experimental rodent studies (Likhodii et al., 2000; Nakazawa, Kodama, & Matsuo, 1983; Thavendiranathan et al., 2000). Efficacy of the MCT KD in patients has been found to be comparable to that of the classical KD, despite the differing fat components of the two diets (Neal et al., 2009; Schwartz et al., 1989b; Wibisono et al., 2015). Thus, with its more flexible approach to dietary management, the MCT KD remains a more favourable treatment option to the classical KD.

1.5 MECHANISMS OF ACTION OF THE MCT KD

Despite the efficacy of the MCT KD at reducing seizures, the precise mechanisms of action remain unknown. Furthermore, the MCT KD is frequently associated with a range of gastrointestinal side effects and poor tolerability in patients (Kang et al., 2004; Kossoff et al., 2009). Consequently, compliance rates are low amongst patients, necessitating the need for the development of novel treatments to enhance or replace the MCT ketogenic diet.

A number of mechanisms of action have been proposed for its anticonvulsant and antiepileptic effects, including alterations to mitochondrial bioenergetics and cellular energy metabolism, neurotransmitter levels and antioxidant activity (Rho & Sankar, 2008). The KD has been found to increase mitochondrial biogenesis in the brains of rats (Bough et al., 2006), with mitochondrial enrichment proposed to contribute to the antiepileptic effects of the diet by targeting mitochondrial bioenergetics and metabolism, decreasing brain excitability. The KD has also been found to increase the ratio of ATP:ADP in rats (DeVivo et al., 1978), increasing brain energy capacity. Changes in glucose oxidation and cellular energy metabolism incurred through the diet may also alter neurotransmitter modulation, with generation of γ-aminobutyric acid (GABA), a neurotransmitter involved in inhibitory synaptic transmission, dependent on TCA cycle activity (Waagepetersen et al., 1999). Increased GABA levels have been observed in the cerebrospinal fluid of KD patients (Dahlin et al., 2005), and in experimental mouse studies (Calderón et al., 2017), with changes in brain GABA also measured in KD patients using magnetic resonance spectroscopy (Wang et al., 2003). Moreover, increased antioxidant capacity and reduced ROS generation has been reported in KD animal studies (Jarrett et al., 2008; Sullivan et al., 2004).

How these effects are specifically exerted by the KD have yet to be fully elucidated. The biochemical changes associated with the KD have been a focal interest of studies, particularly in regard to direct anti-seizure effects. Ketone bodies, a hallmark feature of the KD, have been the primary subject of initial studies into the mechanisms of the KD. In more recent years, however, there has been a growing interest in the potential role of fatty acids in the KD effects, particularly medium-chain fatty acids such as octanoic and decanoic acid.

1.5.1 Ketone Bodies

Increased levels of plasma and urinary ketone bodies are a key clinical marker of the KD and MCT KD. The ketone bodies β-hydroxybutyrate, acetoacetate and acetone (Figure 1.7) accumulate during glucose restriction, resulting in ketosis (McNally & Hartman, 2012).

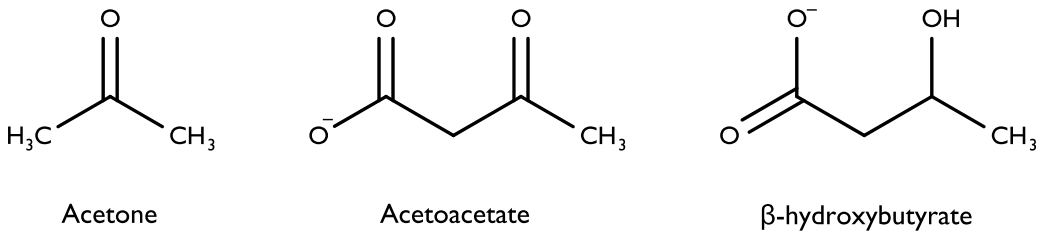

FIGURE 1.7 Chemical structures of the ketone bodies, acetone, acetoacetate and β-hydroxybutyrate.

During the diet, where glucose consumption is restricted and fat intake is increased, acetyl CoA synthesis from fatty acids exceeds TCA cycle activity (McNally & Hartman, 2012; McPherson & McEneny, 2012). This acetyl CoA is then used to generate ketone bodies in a process known as ketogenesis, which takes place in hepatic mitochondria (Figure 1.8).

Two molecules of acetyl CoA are condensed by a thiolase enzyme to form a four-carbon acetoacetyl-CoA. The enzyme HMG-CoA synthase then catalyses the condensation of this compound with an additional molecule of acetyl CoA, producing the six-carbon β-hydroxy-β-methylglutaryl-CoA (HMG-CoA). HMG-CoA lyase then degrades HMG-CoA into acetoacetate and acetyl CoA. Acetoacetate may then be reduced to β-hydroxybutyrate by β-hydroxybutyrate dehydrogenase, and may also undergo non-enzymatic decarboxylation to acetone (responsible for the distinctive "keto breath" observed with patients in ketosis) and CO_2. Approximately 40% of acetoacetate produced is thought to undergo conversion to acetone (Reichard et al., 1979), which builds up in the plasma during the KD (Seymour et al., 1999). These ketone bodies are soluble and can pass into the blood-brain barrier with ease, allowing for their use as fuels in brain cells, where they are converted back to acetyl CoA (Morris, 2005). Here, β-hydroxybutyrate is oxidised back to acetoacetate via β-hydroxybutyrate dehydrogenase, followed by the conversion of acetoacetate to acetoacetyl-CoA using a CoA group donated by succinyl CoA, a process catalysed by β-ketoacyl-CoA transferase. Using a free CoA group, acetoacetyl-CoA is then cleaved by thiolase to produce two acetyl CoA molecules, which can then be utilised in the TCA cycle for subsequent ATP synthesis. Acetone is thought to be metabolised through a number of different pathways. The enzyme acetone monooxygenase converts acetone to acetol, which is subsequently converted into either two-carbon (propanediol) or three-carbon (methylglyoxal) fragments that are then processed by several separate pathways, ultimately producing pyruvate (Kalapos, 2003). Part of this pyruvate is then processed into glucose, or converted into acetyl CoA by the pyruvate dehydrogenase complex (Berg et al., 2012; Kalapos, 2003), contributing towards the TCA cycle.

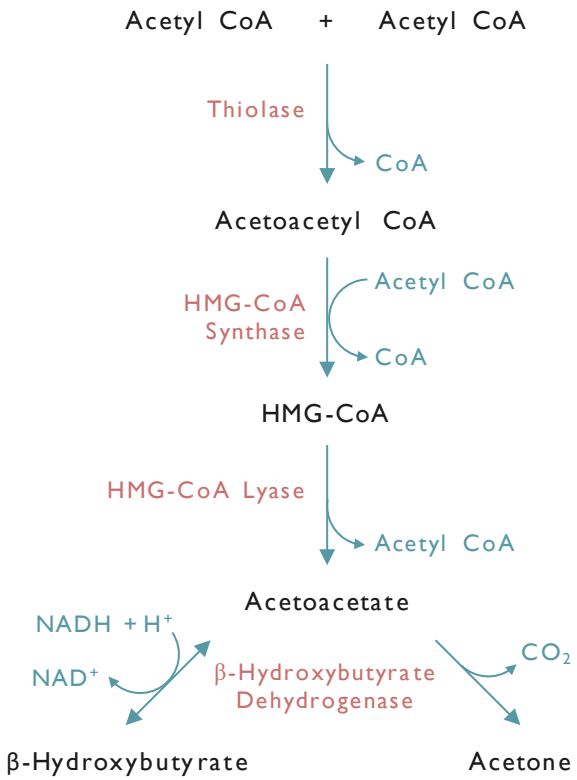

FIGURE 1.8 The generation of ketone bodies through ketogenesis.

Consequently, ketone bodies have been postulated to play a direct role in seizure control, with plasma levels of all three ketone bodies found to rise during the KD (McNally & Hartman, 2012). Evidence suggests that acetone and acetoacetate may have anticonvulsant properties in several experimental models (Gasior et al., 2007; Likhodii et al., 2000; Rho et al., 2002), whilst data on acetoacetate effects appear to be incongruent (Likhodii, Nylen, & McIntyre Burnham, 2008; Rho et al., 2002; Thio, Wong, & Yamada, 2000). It is also worth noting that the concentrations of acetone utilised in these studies to achieve effective seizure control may exceed those found in the brains of patients on the KD (Seymour et al., 1999). Additionally, no anticonvulsant effect has been observed with β-hydroxybutyrate (Rho et al., 2002; Samala, Willis, & Borges, 2008; Thio et al., 2000). Whilst it may not have a direct effect on seizures, β-hydroxybutyrate has been postulated to exert an indirect effect on epilepsy by affecting

brain amino acid handling, increasing GABA levels in the brain and reducing the availability of glutamate, an excitatory neurotransmitter (Erecińska et al., 1996; Lund et al., 2009; Yudkoff et al., 2001).

Although the role of ketone bodies in the effects of the KD remains unclear, maintaining ketosis appears to be a precursor to seizure control, where carbohydrate consumption can result in the temporary loss of seizure control (Huttenlocher, 1976). However, studies investigating the relationship between ketone levels and seizure control are conflicting. Whilst some studies have suggested that increased β-hydroxybutyrate levels correlate with improved seizure control (Gilbert, Pyzik, & Freeman, 2000; Huttenlocher, 1976; van Delft et al., 2010), with a suggested threshold of 4mM in blood required (Gilbert, Pyzek, & Freeman, 2000), others have shown poor correlation between ketosis and seizure control (Fraser et al., 2003; Likhodii et al., 2000; Ross et al., 1985; Schwartz, Boyes, & Aynsley-Green, 1989a; Thavendiranathan et al., 2000).

1.5.2 Medium-Chain Fatty Acids (MCFAs)

Whilst increased ketone body levels are generally associated with the KD and MCT KD, elevated blood levels of medium-chain fatty acids (MCFAs) have also been observed in patients on the MCT KD (Haidukewych, Forsythe, & Sills, 1982; Sills et al., 1986). In the study conducted by Haidukewych et al. (1982), patients on the MCT KD were required to supplement the diet with MCT oil containing approximately 80% octanoic acid (C8) and 20% decanoic acid (C10). In these patients, plasma levels of C8 and C10 were found to range at 30-861μM and 23-553μM respectively, with mean concentrations of 307μM C8 and 157μM C10. Sills et al. (1986) examined the association between seizure control and MCFA blood levels, but no correlation was

found. Since these findings, little more was done to further investigate the potential roles of C8 and C10 in the MCT KD. In recent years, however, there has been a growing interest in C8 and C10, with increased evidence suggesting direct and indirect effects on seizure control.

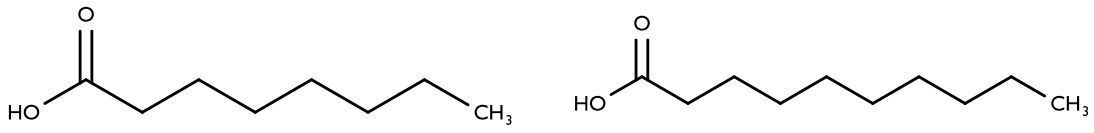

Octanoic Acid (C8) Decanoic Acid (C10)

FIGURE 1.9 Chemical structures of octanoic (C8) and decanoic (C10) acids.

1.6 THE ROLE OF C8 AND C10 IN THE MCT KD

Recent studies into the neuronal and peripheral effects of C8 and C10 provide novel insight into the key roles of MCFAs in the MCT KD, particularly in regard to seizure control and mitochondrial function. Most pertinent, however, is that the data is indicative of a disparity in effect between C8 and C10, despite the elevation of patient plasma levels of both fatty acids. Here, these findings are reviewed, introducing the therapeutic potential that these fatty acids may have in epilepsy treatment.

Experimental seizure studies reveal a direct role of C8 and C10 in seizure control, potentially contributing to the clinical efficacy of the MCT KD. In animal models examining the role of C8, acute and chronic administration of C8 was found to increase seizure threshold in 6-Hz psychomotor and pentylenetetrazole (PTZ) seizure tests (McDonald et al., 2014; Wlaź et al., 2012), with an adenosine receptor-dependent effect on seizure threshold also observed in a glucose-restricted 6-Hz seizure model

(Socała et al., 2015), although no effect was observed with the maximal electroshock seizure threshold (MEST) tests (Wlaź et al., 2012). Moreover, data surrounding the anticonvulsant profile of C8 appear to be inconsistent, with other studies reporting no effect of C8 on seizure control (Chang et al., 2012, 2016; Tan et al., 2017).

C10 has also been shown to exert seizure control in a number of seizure models. In *ex vivo* hippocampal slices, acute application of C10 was found to exert complete seizure inhibition in PTZ- and low magnesium-induced seizures (Chang et al., 2012, 2016). In animal models, acute C10 administration increased seizure threshold in the 6-Hz and MEST tests, although no effect was observed with PTZ-induced seizures (Wlaź et al., 2015), whilst mice fed chronically with a C10 triglyceride-enriched chow were also found to exhibit improved seizure tolerance (6-Hz test) and increased latency to seizures (fluorothyl test) (Tan et al., 2017), suggesting that C10 activity may vary with seizure type. Tan et al. (2017) investigated the *in vivo* effects of C10 on glycolytic enzymes, but found no changes in activity, suggesting that C10 may affect seizure generation independently of this pathway.

Further highlighting the potent anti-seizure effects of C10 is the recent finding that the fatty acid acts as a selective inhibitor of the α-amino-3-hydroxy-5-methyl-4-isoxazolepropionic acid receptor (AMPA) receptor (Chang et al., 2016). A receptor for the neurotransmitter glutamate, AMPA receptors mediate excitatory synaptic transmission and are thus involved in seizure generation. C10 inhibition of AMPA receptors was found to be non-competitive to glutamate, also occurring at concentrations reported in patient plasma, suggesting that this mechanism may underlie the anticonvulsant efficacy observed with the MCT KD.

Whilst both C8 and C10 appear to exhibit anti-seizure properties, differences in effect on mitochondria are apparent. Previously, in this laboratory, C10 was found to significantly alter mitochondrial function in the human neuroblastoma cell line SH-SY5Y, as well as in human fibroblast cells (Hughes et al., 2014; Kanabus et al., 2016). Treatment of these cells with 250μM C10 over the course of 6 days was shown to significantly increase mitochondrial enrichment, as measured by the activity of mitochondrial enzyme marker, citrate synthase. Interestingly, this marked increase in activity was not observed with C8 treatment. Additionally, C10, but not C8, was found to cause a pronounced increase in complex I activity, potentially suggesting increased mitochondrial function. C10 treatment, but not C8, also amplified activity of the antioxidant, catalase. These C10 effects on citrate synthase activity and catalase were found to be mediated by the peroxisome proliferator-activated receptor gamma (PPARγ), a nuclear receptor involved in mitochondrial regulation and neuroprotection (Berger & Moller, 2002). Interestingly, C10 has been identified as a PPARγ agonist, binding directly to the receptor to activate it (Malapaka et al., 2012), suggesting that the fatty acid may potentially play a role in the increased mitochondrial biogenesis associated with the KD (Bough et al., 2006). Furthermore, the ketone bodies β-hydroxybutyrate and acetoacetate were not found to have any effects in this study.

Increased mitochondrial biogenesis may exert beneficial effects on brain energy metabolism by increasing ATP availability, and consequently, improving seizure threshold. Increased respiration, suggesting increased mitochondrial function, has also been observed in C10-treated astrocytes (Tan et al., 2017). In addition to improved energy availability, antioxidant effects of C10 suggest a potential neuroprotective effect of the fatty acid. Increased antioxidant status *in vivo* has been reported following C10-enriched feeding of rodent models, with increased catalase, superoxide dismutase,

glutathione reductase and glutathione peroxidase activity, as well as reduced lipid peroxidation, observed in brain tissue and increased antioxidant status in plasma (Sengupta & Ghosh, 2012; Sengupta, Ghosh, & Bhattacharyya, 2014; Tan et al., 2017), further corroborating previous reports (Hughes et al., 2014). C8 administration has also been found to improve antioxidant status *in vivo* (Sengupta & Ghosh, 2012; McDonald et al., 2014), suggesting that both fatty acids may contribute to the antioxidative and neuroprotective effects observed with the diet.

In the brains of mice fed a C10-enriched chow, the concentration of the fatty acid has been found to average 240μM (Wlaź et al., 2015), a value that corresponds closely with the required concentration for mitochondrial proliferation and increased antioxidant activity (Hughes et al., 2014). This concentration also permits AMPA receptor inhibition, and reflects the range of C10 observed in MCT KD patient plasma, suggesting that it may be possible to achieve these levels in human brains. However, current understanding of MCT metabolism would suggest that MCFAs are primarily oxidised to ketone bodies, in contrast to the observed accumulation of C10 in rodent brains.

Moreover, whilst this data suggests the potential for C10 to directly contribute to seizure control and neuroprotection in experimental studies, how this may translate to patients has yet to be investigated. In light of this, a C10-enriched MCT product, named Betashot, was recently developed by nutritional company Vitaflo International Ltd, to be used as a supplement to the MCT KD. The increased C10 content in the product raises the potential for improved efficacy of the MCT KD. At the time of writing, a feasibility study was launched, assessing the clinical biochemical effects of Betashot, as well as compliance, tolerability and palatability, in adult and children epilepsy patients.

Thus, in view of this, this thesis aims to further elucidate the *in vitro* neuronal effects of C10 on mitochondrial content and function, including mitochondrial membrane potential and cellular energy charge, and delineate the metabolic fate of C10 that leads to its elevated levels in the brain. Understanding this may provide further insight into how C10 may affect brain energy metabolism, as well as its impact on its mitochondrial and anti-seizure targets. For these studies, the human neuroblastoma cell line SH-SH5Y was utilised. A well-characterised cell line, SH-SY5Y cells possess a range of biochemical, molecular and functional properties associated with neurons (Kovalevich & Langford, 2013; Ross, Spengler, & Biedler, 1983; Xie, Hu, & Li, 2010), and are thus frequently employed as experimental models in neurological studies. Whilst the use of an immortalised cell line affords considerable practical advantages, cell lines are not without their limitations, including differences in neuronal marker expression and the lack of heterogeneity typically present in neuronal phenotypes (Audesirk, 2010), therefore requiring careful interpretation of experimental data. These limitations may potentially be addressed through numerous methods, such as differentiation of SH-SY5Y cells to confer a more mature neuronal phenotype, the use of additional cell lines in conjunction with SH-SY5Y, or culture of primary neurons. However, for this thesis, undifferentiated SH-SY5Y cells were used to ensure consistency and comparability with the work of Hughes et al. (2014), as well as to develop a more comprehensive understanding of the effects of C10 within this model. In addition to examining the *in vitro* effects of C10, this thesis also aims to evaluate the biochemical effects of the C10-enriched MCT formulation Betashot in epilepsy patients, including β-hydroxybutyrate levels, lipid profiles and acyl carnitine profiles, as well as develop a quantitative method of analysis to assess MCFA plasma levels in participants.

1.7 AIMS

- Since C10 exerts a range of pro-mitochondrial effects in neuronal cells, this thesis aims to further characterise the effects of C10 on mitochondrial content and function in human neuroblastoma SH-SY5Y cells, examining the effects of treatment on the mitochondrial content marker citrate synthase, mitochondrial membrane potential and cellular energy charge.
- To understand how C10 may exert its effects within the brain, this thesis also aims to determine the neuronal metabolic fate of C8 and C10, exploring in detail the mitochondrial β-oxidation of the two MCFAs in SH-SY5Y cells.
- With evidence suggesting that C10 may exert a range of potentially anti-epileptic effects, C10-enrichment of MCT formulae may provide an effective alternative to current mainstream MCT products. This thesis aims to evaluate the biochemical effects of a C10-enriched MCT formulation, Betashot, on adult and child epilepsy participants in a feasibility study. To aid analysis, this thesis also aims to develop a quantitative GC-MS method to analyse and monitor MCFA levels in the plasma of patients involved in the study.

CHAPTER 2

Materials and Methods

2.1 MATERIALS

Unless otherwise stated, all reagents were purchased from Sigma-Aldrich (Poole, UK) or from ThermoFisher Scientific (Paisley, UK). The human neuroblastoma cell line, SH-SY5Y, was purchased from the European Collection of Cell Cultures (Public Health England, Salisbury, UK).

2.2 TISSUE CULTURE

2.2.1 SH-SY5Y Cell Line

SH-SY5Y is a human neuroblastoma cell line, originally derived as a subline from the SK-N-SH cell line. Established from a metastatic bone marrow biopsy in 1970, the parental SK-N-SH line comprised two morphologically distinct cell types/phenotypes, neuroblast-like and epithelial-like. The neuroblast-like cells were serially subcloned, thrice, into SH-SY, SH-SY5 and eventually SH-SY5Y lines (Biedler et al., 1978).

Biochemically, SH-SY5Y cells exhibit a range of neuronal properties, and are known to express activities for tyrosine hydroxylase and dopamine-β-hydroxylase, a trait characteristic of catecholaminergic neurons (Biedler et al., 1978; Ross et al., 1983). Moreover, they have also been found to be able to convert glutamate to the neurotransmitter GABA.

Morphologically, SH-SY5Y cells are characterised by neuroblast-like cell bodies with neurite-like projections, also expressing immature neuronal markers (Kovalevich & Langford, 2013). However, with a number of methods, they can also be differentiated into more mature neuron-like cells, defined by specific neuronal markers and phenotypes. Cultures of undifferentiated SH-SY5Y cells contain both adherent and suspension cells. However, for the purpose of this thesis, only adherent cells were used.

Furthermore, loss of neuronal characteristics has been described with increasing passage numbers. Therefore, use of cells was also limited to passages 20-24 for all experimental procedures.

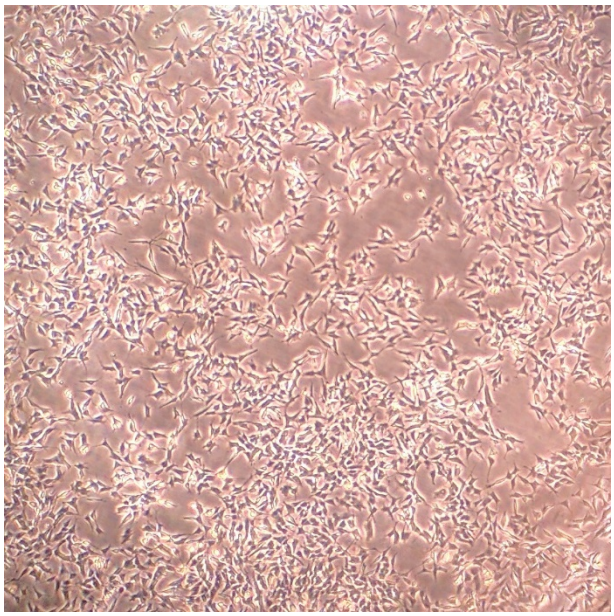

FIGURE 2.1 SH-SY5Y human neuroblastoma cells under a light microscope.

2.2.2 Cell Recovery and Seeding

Frozen cells were thawed rapidly at 37°C and immediately transferred to a falcon tube containing 9ml complete growth medium, comprised of 1:1 DMEM/F12 media, containing 17.5mM glucose and supplemented with 100ml/L heat-inactivated foetal bovine serum (FBS) and 10ml/L 200mM L-glutamine. Cells were gently mixed in the medium, before centrifugation at 500xg for 4 minutes. The cell suspension was removed and cells were resuspended in fresh growth medium, before transfer to a T75 flask. All cells were maintained in a humidified atmosphere at 37°C and 5% CO_2. The next day, the medium was changed to remove traces of dimethyl sulfoxide (DMSO)

present from the freezing medium. Cells were left to grow until 80-90% confluency before subculture.

2.2.3 Cell Subculture

Cells were subcultured by removing growth medium and gently washing with 10ml/flask Mg^{2+}/Ca^{2+}-free Dulbecco's phosphate-buffered saline (DPBS). The DPBS was removed and the cells then lifted with 2ml 0.25% trypsin-EDTA, before suspension in 8ml complete growth medium to inactivate the trypsin. This cell suspension was then centrifuged in a falcon tube for 4 minutes at 500xg. After removing the supernatant, the cells were suspended in a known volume of fresh medium and counted using Trypan Blue exclusion, testing for viability. A known volume of the cell suspension was mixed 1:1 with 0.4% Trypan Blue solution and counted with a Bio-Rad TC20™ Automated Cell Counter (Hemel Hempstead, UK). Cells were then seeded at a density of 5-10 x 10^3 cells/cm^2 in either T25 or T75 flasks and made up to a final volume of 5-10ml with fresh growth medium. Cells were cultured until 80-90% confluent at 37°C and 5% CO_2, refreshing medium every 2-3 days.

2.2.4 Cell Cryopreservation

Cells at low passage number were frequently cryopreserved and stored for future use. Confluent cells were passaged as described above. However, after counting, cells were centrifuged for 4 mins at 500xg and the supernatant discarded. The cell pellet was then suspended in a known volume of cold Gibco™ Recovery™ Cell Culture Freezing Medium and stored in 1ml aliquots in cryovials containing approximately 1 x 10^6 cells/ml. Cells were then frozen immediately at -80°C in a Mr Frosty™ Freezing Container (Fisher Scientific UK Ltd, Loughborough, UK) and left overnight. After 24h, the cells were then transferred into liquid nitrogen for long-term storage.

2.2.5 Mycoplasma Testing

Mycoplasma infections are a frequent issue in tissue culture and can cause a myriad of problems, from interference with cell function and gene expression to cell growth and survival (Drexler & Uphoff, 2002). Resistant to antibiotics, Mycoplasma are also undetectable by the naked eye, requiring routine testing for infection. SH-SY5Y cells were periodically tested for Mycoplasma contamination using the MycoAlert™ mycoplasma detection kit (Lonza, Slough, UK), following manufacturer instructions. The test kit detects Mycoplasma through a luminescence assay, that exploits the reaction of mycoplasmal enzymes with MycoAlert substrate to catalyse the conversion of ADP to ATP, with changes in ATP levels used to indicate Mycoplasma contamination.

Cells were tested once deemed confluent, prior to subculture, with medium unchanged for at least 48h prior to testing. Without touching the cell monolayer, 1ml of culture medium was removed from flasks and transferred to a sterile microtube. The sample was centrifuged for 3 mins at 500xg and 100µl supernatant was transferred to a flat clear-bottom 96-well plate with opaque white walls. MycoAlert buffer (100µl) was utilised as a negative control, whilst 100µl positive control, provided by the kit, was also added to the plate. To each well, 100µl MycoAlert reagent was added, which had been previously reconstituted and equilibrated in the assay buffer provided as per manufacturer instructions. Samples were incubated for 5 mins at room temperature, before measuring luminescence with a 1 second integrated reading on an Infinite F200 PRO plate reader (Tecan, Männedorf, Switzerland). This measurement was deemed Reading A. To the same wells, 100µl reconstituted MycoAlert substrate was added, with samples incubated for 10 mins at room temperature. A final luminescence reading, denoted Reading B, was measured and the ratio of luminescence detected at

Reading B to Reading A was calculated. This ratio was then utilised to determine mycoplasma infection based on the range provided by the manufacturer.

2.3 CELL TREATMENT

2.3.1 SH-SY5Y Treatment with C8 and C10

Stock solutions of 50mM C8 and C10 were prepared in DMSO, sterile-filtered and stored in aliquots at -20°C. Cells were passaged as previously described and seeded at 5 x 10^3 cells/cm^2 in T25 flasks. They were then treated with 5ml complete growth medium, containing 25µl of either vehicle control DMSO, C10 or C8. Cells were incubated for 6 days, with day of seeding considered day 0. Treatment medium was refreshed every two days. Cells were harvested on day 6 as described below.

2.3.2 Cell Harvesting

To harvest cells for analysis at the end of experimental procedures, cells were washed with 5ml DBPS and lifted with 1ml 0.25% trypsin-EDTA. The cells were suspended in 5ml fresh culture medium, centrifuged for 4 minutes at 500xg and the supernatant removed. Without breaking the pellet, the cell pellet was gently washed once with 2-3ml DPBS and the DPBS removed. The pellet was then suspended in a known volume of cold protein isolation buffer, composed of 320mM sucrose, 10mM Tris and 1mM EDTA in Milli-Q water (pH 7.4). The cell suspension was divided into two aliquots where necessary, for enzymatic assays and protein quantification. Samples were immediately frozen in dry ice and then stored at -80°C until further analysis.

2.4 CITRATE SYNTHASE ACTIVITY ASSAYS

2.4.1 Principle

Citrate synthase (EC 4.1.3.7) is a mitochondrial enzyme that catalyses the first step of the TCA cycle, the condensation of acetyl CoA with oxaloacetate to produce citrate and free CoA (CoA-SH). Located in the mitochondrial matrix (Marco et al., 1974), citrate synthase activity can be utilised as a biochemical measure of mitochondrial content (Hughes et al., 2014; Jacobs et al., 2013; Larsen et al., 2012), and is used as a validated diagnostic marker in accredited mitochondrial services in the NHS. The activity of the enzyme can be determined using a colorimetric method described by Shepherd and Garland (1969), which measures the reaction between CoA-SH, generated from citrate synthase enzyme activity, and the reagent 5,5'-dithio-bis-(2-nitrobenzoic acid) (DTNB or Ellman's reagent) (Shepherd & Garland, 1969). This produces 5-thio-2-nitrobenzoate (TNB) (Figure 2.2), a by-product with an absorbance at 412nm and an absorbance intensity proportional to citrate synthase enzyme activity.

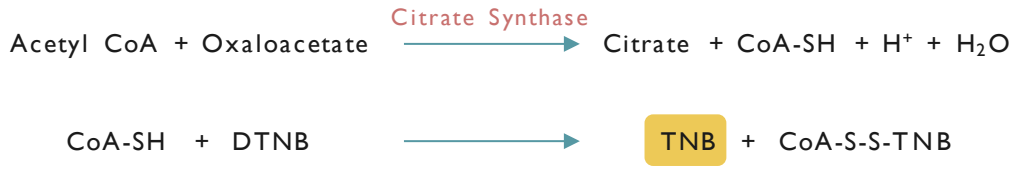

FIGURE 2.2 Citrate synthase assay reaction. CoA-SH produced from the reaction between acetyl CoA and oxaloacetate, catalysed by citrate synthase, reacts with DTNB to produce the yellow by-product TNB, which is then measured spectrophotometrically.

2.4.2 Citrate Synthase Activity in SH-SY5Y Cells

Citrate synthase (CS) enzyme activity was assessed using an Uvikon XL spectrophotometer (Secomam, Ales, France). Assays were carried out at 37°C and samples were assayed in duplicate. CS assay buffer (100mM Tris, 0.1% v/v Triton X-

100, in Milli-Q water, pH 8.0), was warmed to 37°C and kept at that temperature throughout the duration of the procedure. A stock of 10mM acetyl CoA was prepared in Milli-Q water, aliquoted and stored at -20°C until use, during which aliquots were thawed at room temperature and then kept in ice. Prior to each experiment, 20mM DTNB and 20mM oxaloacetate were freshly prepared in Milli-Q water and kept in ice.

To 1.5ml polystyrene cuvettes, 10µl acetyl-CoA and 10µl DTNB were added. Cell samples were thawed at 37°C and diluted appropriately with protein isolation buffer, before adding 20µl of the diluted sample to cuvettes. Samples were immediately frozen in dry ice after use. To sample cuvettes, 950µl citrate synthase assay buffer was added, with 960µl added to reference cuvettes. Samples were blanked to reference cuvettes containing the cell sample and all reagents, except for oxaloacetate. Reagents were mixed in the cuvettes by inversion and baseline citrate synthase activity was measured in each sample for 3 minutes at 412nm. Once determined, the reaction was started by adding 10µl of oxaloacetate to sample cuvettes and inverting each cuvette to mix. Sample absorbance was measured immediately afterwards for 10 minutes at 30 second intervals, with samples assayed in duplicate. CS activity was calculated using the Beer-Lambert law (Equation 2.1) and expressed in nmol/min/mg, normalised to protein content in each sample. Normalising CS activity to protein content takes into consideration that enzymes are proteins, but also provides a standardised approach measurable against publications (De Vogel-Van Den Bosch et al., 2011; Gegg et al., 2010; Hughes et al., 2014; Kanabus et al., 2016; Kudin et al., 2002) and the procedures employed in specialist NHS-accredited laboratories that support the NHS Highly Specialised Service for Rare Mitochondrial Disorders.

$$\frac{\Delta A}{\varepsilon\, l} = \Delta c$$

EQUATION 2.1 Beer-Lambert law. CS activity was calculated using the Beer-Lambert law, where ΔA = change in absorbance, ε = extinction coefficient of TNB (13,600 M^{-1} cm^{-1}), *l* = path length (1cm) and Δ*c* = enzyme activity in mole/min/L.

Pooled control SH-SY5Y cell samples were used to generate quality control (QC) samples for CS activity within the working range of the assay, with enzyme activity cross-validated at the Neurometabolic Unit, National Hospital for Neurology and Neurosurgery. CS activity of QC samples were determined prior to each assay of experimental samples, with control limits set as the mean ± 2SD (CV 4.85%).

Linearity of CS activity to protein content was also determined in SH-SY5Y cells to validate the assay, consistent with practice employed in NHS-accredited laboratories. A control sample with a known protein concentration was serially diluted in protein isolation buffer and the CS activity of each dilution was measured. CS activity was found to strongly correlate with protein content (r^2 = 0.9988) in the concentration range used (Figure 2.3).

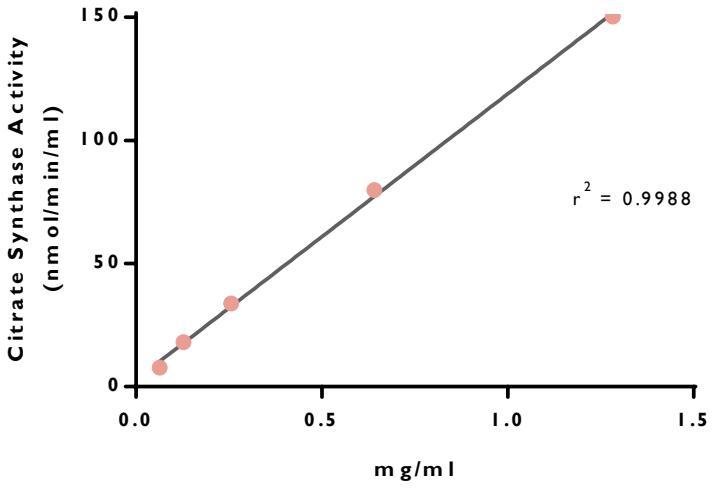

FIGURE 2.3 Linearity between citrate synthase (CS) activity and protein concentration in a typical SH-SY5Y cell sample. A typical control SH-SY5Y sample was serially diluted in protein isolation buffer and the CS activity of each dilution was determined. Linear regression analysis showed a strongly linear relationship between CS activity and protein content in cells (r^2 = 0.9988).

2.4.3 Citrate Synthase Activity in White Blood Cells

White blood cell pellets were obtained from anonymised surplus patient samples from Chemical Pathology, Great Ormond Street Hospital, and stored at -80°C until use. The method described above was used to determine CS activity in white blood cell samples, with cell samples diluted appropriately in Milli-Q water. QCs comprised of pooled white blood cell samples were generated and cross-validated as described above. CS activity of QC samples was determined prior to each assay of experimental samples, with control limits set as the mean ± 2SD (CV 6.04%). A reference range for CS activity in WBCs was established from 17 samples from patients with no evidence for alteration in mitochondrial function or diagnosis of epilepsy, with activities ranging from 102-242 nmol/min/mg (mean ± 2SD).

Linearity of CS activity to protein content in white blood cells was measured with a control sample of known protein concentration, as described above. CS activity was found to be highly linear with protein content (r^2 = 0.9955) in the concentration range used (Figure 2.4).

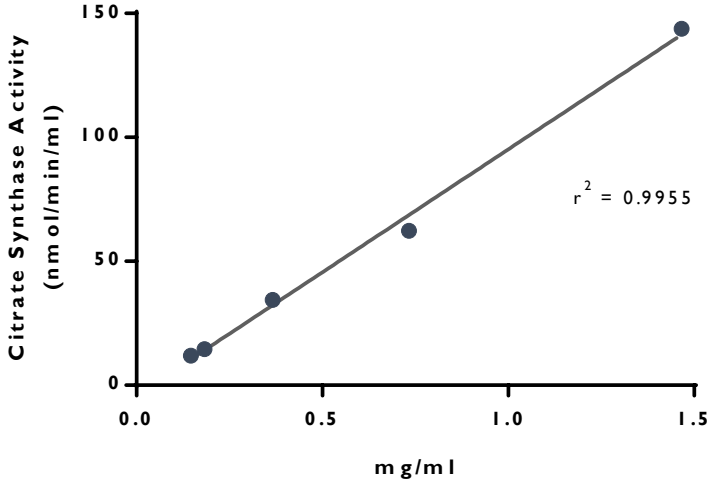

FIGURE 2.4 Linearity between citrate synthase (CS) activity and protein concentration in a typical white blood cell sample. A typical control patient white blood cell sample was serially diluted in Milli-Q water and the CS activity of each dilution was determined. Linear regression analysis showed a strongly linear relationship between CS activity and protein content in cells (r^2 = 0.9955).

2.5 TOTAL PROTEIN QUANTIFICATION

2.5.1 Principle

Total protein content of cells was quantified using the Bradford assay. Based on a method developed by Bradford (1976), the assay relies on a colorimetric shift observed when Bradford Reagent, containing the dye Coomassie Brilliant Blue G-250, is added to protein samples. In acidic solutions, Coomassie Brilliant Blue G-250 exists in a red-brown cationic form, which converts to a stable blue anionic form when it binds to proteins, primarily interacting with arginine, whilst also binding other basic and aromatic amino acid residues to an extent (Bradford, 1976; Compton & Jones, 1985).

This visible colour change is accompanied by a shift in absorbance maximum from 465nm to 595nm, with the protein-dye complex detected at 595nm.

2.5.2 Bradford Assay

A stock solution of 0.2mg/ml bovine serum albumin (BSA) was prepared in Milli-Q water, aliquoted and frozen at -20°C for up to 6 months. Cell samples were assayed against a BSA standard curve, generated from diluting the stock solution in Milli-Q water, at a range of 0-200µg/ml. To a clear flat-bottom 96-well plate, 20µl of BSA standards were added in duplicate. Milli-Q water was used for blanks. A known volume of cell sample was transferred to a fresh microtube and frozen in dry ice, followed immediately by thawing at 37°C. This freeze/thaw process was repeated three times. The sample was diluted appropriately in Milli-Q water and 20µl of diluted sample was then added in triplicate to the 96-well plate. Bradford Reagent was warmed to room temperature and 180µl of the reagent was added to each well. Samples and reagents were gently mixed together, prior to incubating at room temperature for 5 minutes. Absorbance was then measured at 595nm in an Infinite F200 PRO plate reader and final readings utilised to determine sample protein concentration alongside the generated standard curve (Figure 2.5).

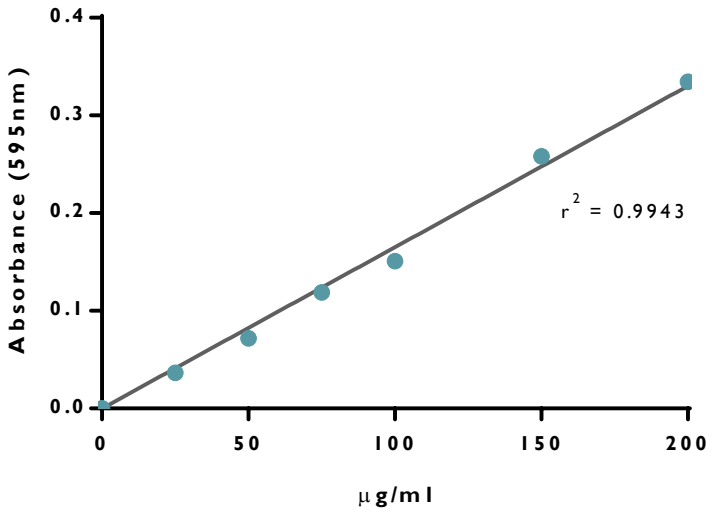

FIGURE 2.5 Typical BSA standard curve with the Bradford protein assay.

2.6 FLOW CYTOMETRY FOR MITOCHONDRIAL MEMBRANE POTENTIAL

2.6.1 Principle

The mitochondrial membrane potential of SH-SY5Y cells was measured using tetramethylrhodamine ethyl ester (TMRE), a cationic fluorescent dye that readily accumulates in the active mitochondria of live cells. A lipophilic compound, TMRE is taken up into the mitochondrial matrix due to its charge and solubility and equilibrates across the inner mitochondrial membrane in a Nernstian manner (Perry et al., 2011). It accumulates in the mitochondrial matrix inversely to the negatively charged mitochondrial membrane potential, with greater uptake observed in mitochondria with more polarised mitochondrial membrane potential (hyperpolarisation), whilst mitochondria with decreased membrane potential (depolarisation) exhibit lower uptake of TMRE. Consequently, changes in mitochondrial membrane potential can be detected with the dye using flow cytometry.

Flow cytometry is an analytical tool that utilises lasers to measure the characteristics of cells and their components, and is capable of measuring a vast number of parameters simultaneously within a single cell. Lasers are used to excite fluorochromes, such as TMRE, that are bound to or associated with cellular components, and the fluorescence intensity measured. Cell suspensions of stained cells are injected into the flow chamber of the flow cytometer, where sheath fluid is used to hydrodynamically focus the suspension into a single-file stream of cells. As the cells flow through the stream, they intercept a laser beam, one cell at a time, scattering light and emitting fluorescence. The scattered light is collected by two detectors that measure forward scatter (FSC) and side scatter (SSC), with FSC correlating with cell size and SSC with cell structure and granularity. Differences in FSC and SSC can be used to distinguish different populations of cells. Fluorescence emitted by the excited fluorochromes is also detected simultaneously, when positively stained cells pass through lasers with a corresponding excitation wavelength. Scattered light and fluorescence emission are channelled through a series of filters and mirrors that direct specific wavelengths of emitted light to specified optical sensors called photomultiplier tubes (PMTs). PMTs convert the detected light into electrical signals, or events, which are then processed digitally into a measurable readout (Figure 2.6).

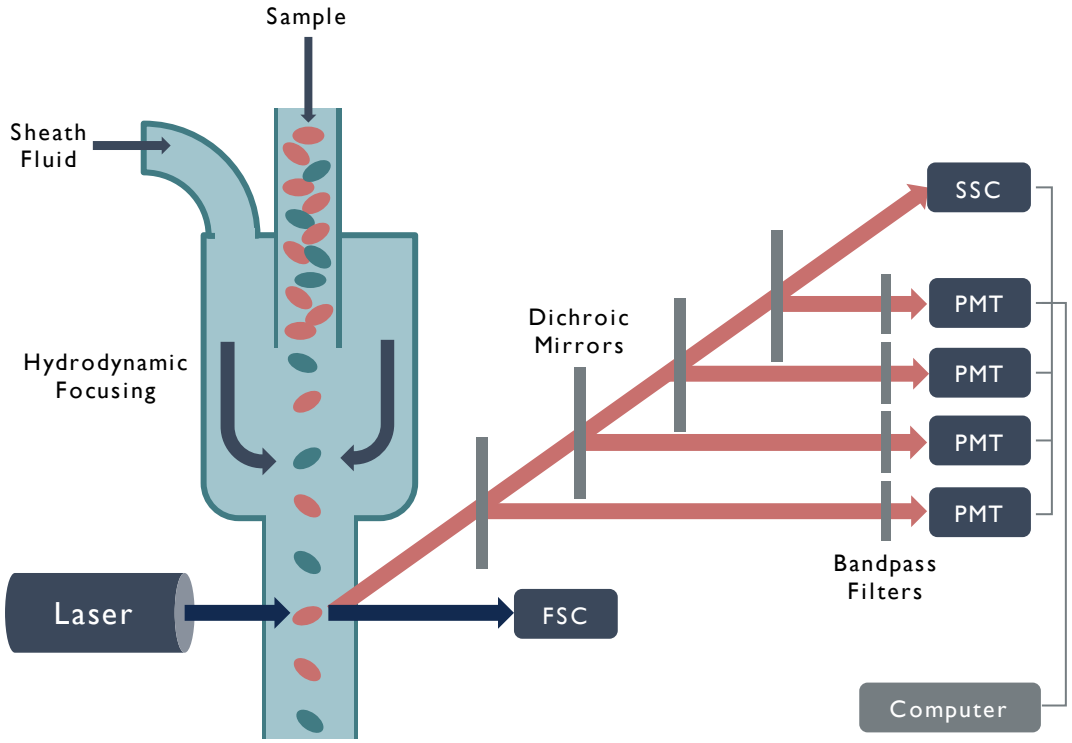

FIGURE 2.6 Schematic of a flow cytometer. Upon excitation, cells stained with fluorochromes emit fluorescence, which then passes through a series of dichroic mirrors, which reflects specific wavelengths of light to a PMT and lets the remaining light pass through. The reflected light then crosses through a bandpass filter which only allows wavelengths within a certain range to transmit to the PMT.

For the purpose of measuring changes in mitochondrial membrane potential, a BD FACSCalibur™ flow cytometer (BD Biosciences, San Jose, CA, USA) was used. TMRE has excitation/emission wavelengths of 549/575nm and is excited by the blue argon laser (488nm), emitting a red-orange fluorescence that can be detected by the PMT in the FL2 (585/42nm) channel. To confirm accurate interpretation of changes in TMRE fluorescence and determine the validity of the TMRE concentration used, pharmacological controls were utilised to examine bidirectional changes in mitochondrial membrane potential. Carbonyl cyanide 4-(trifluoromethoxy)phenylhydrazone (FCCP) is a lipid-soluble ionophoric oxidative phosphorylation uncoupler. A weak acid, it transports protons across the inner

mitochondrial membrane (Benz & McLaughlin, 1983), before leaving as an anion (Lee & O'Brien, 2010), disrupting the proton gradient and dissipating the mitochondrial membrane potential. Conversely, the antibiotic oligomycin A can be used to demonstrate hyperpolarisation of the mitochondrial membrane potential. It acts by binding to the F_0 subunit of ATP synthase, blocking the proton channel and thereby inhibiting proton translocation into the mitochondrial matrix (Lee & O'Brien, 2010), resulting in increased polarisation of the mitochondrial membrane potential. Thus, FCCP and oligomycin A can be used to either decrease or increase TMRE staining.

Finally, dead cells often bind non-specifically to fluorochromes, generating artefacts and false positive results. TO-PRO®-3 Iodide is a carbocyanine monomer, impermeant to live cells, that specifically stains nucleic acids (Bink et al., 2001) and can be used as a viability dye to differentiate live and dead cells. With excitation/emission wavelengths of 642/661nm, it emits a far-red fluorescence that can be detected on the FL4 (661/16nm) channel on the FACSCalibur, allowing complete separation of fluorescence from TMRE.

2.6.2 Reagent Preparation

A stock solution of 100µM TMRE was prepared in DMSO, aliquoted and stored, protected from light, at -20°C for up to 3 months. FCCP and oligomycin A were also prepared as 10mM and 1mM stock solutions, respectively, in DMSO before being aliquoted and stored away from light at -20°C. Staining buffer was prepared from sterile phenol red-free Hank's Balanced Salt Solution (HBSS), containing magnesium and calcium chloride, and 2% FBS. Staining buffer was stored at 4°C for up to 1 month. A pre-purchased 1mM stock solution of TO-PRO-3 iodide in DMSO was diluted to a 1µM

working stock solution in staining buffer. This 1µM stock solution was then aliquoted and stored at -20°C, protected from light, until further use.

2.6.3 Flow Cytometry Sample Preparation

The final concentration of TMRE used was optimised through flow cytometry analysis, and selected for the concentration that provided an adequate fluorescence signal without quenching. To further validate this and to determine that changes in TMRE can be interpreted as predicted, cells were pre-treated with the pharmacological controls FCCP and oligomycin A prior to TMRE staining. For pharmacological control testing, SH-SY5Y cells were seeded in T25 flasks, as described in Sections 2.2.2 and 2.3.1, and grown until confluent. Once confluent, medium was removed and cells were washed with 5ml DPBS. Cells were then treated with 5ml HBSS containing a final concentration of either 1µl/ml vehicle DMSO, 10µM FCCP or 1µM oligomycin A (Schneider et al., 2011). Cells were incubated for 10 mins at 37°C and 5% CO_2, after which cells were removed and washed with 5ml DPBS. The DPBS was then removed and the cells lifted with 1ml 0.25% trypsin-EDTA, and the trypsin inactivated with 5ml complete growth medium. Cells were then transferred to a falcon tube and counted as described in Section 2.2.3, prior to centrifugation for 4 mins at 500xg. After removing the supernatant, the cell pellet was gently washed with DPBS and then suspended in 1ml pre-warmed staining buffer. Based on the cell count of each sample, a volume of cell suspension containing 100,000 cells was transferred to fresh microtubes. The cells were then centrifuged for 1 min at 8000xg. The staining buffer was gently removed and the cells resuspended in 200µl pre-warmed staining buffer containing a final concentration of 500nM TMRE, to ensure consistent staining of cells. Cells were then incubated for 15 mins at 37°C and 5% CO_2, protected from light. After incubation, the cell suspensions were centrifuged once more for 1 min at 8000xg, and the supernatant

removed. Cell pellets were gently washed, and then resuspended in 100µl staining buffer containing a final concentration of 50nM TO-PRO-3 iodide. Samples were kept on ice, protected from light, and immediately transferred to the FACSCalibur for analysis.

Cells treated with C8 and C10 were handled in a similar manner as described above. However, following trypsination, cells were suspended in 10ml complete growth medium and halved into two separate aliquots, with one aliquot of cells harvested as described in Section 2.3.2 for CS activity analysis, as outlined in Section 2.4.2, and the other aliquot counted and processed for TMRE staining and mitochondrial membrane potential analysis.

2.6.4 Flow Cytometry Data Acquisition and Analysis

TMRE-stained cells were transferred either to a round-bottom 96-well plate or round-bottom polystyrene tubes for analysis on the FACSCalibur. Control cells, treated with TO-PRO-3 iodide alone, were also analysed alongside TMRE-stained samples to account for cellular autofluorescence. As previously highlighted, the FACSCalibur flow cytometer contains a blue argon laser with a 488nm wavelength, as well as a red diode laser with a wavelength of 635nm. TMRE fluorescence emission was analysed via the FL2 channel, containing a 585/42nm band pass filter, whilst TO-PRO-3 iodide fluorescence was measured via the FL4 channel, with a 661/16nm band pass filter. FSC and SSC data were also measured from each sample. BD CellQuest™ Pro software (BD Biosciences, San Jose, CA, USA) was used to optimise flow cytometer detection parameters and for data acquisition. Live cells were distinguished from dead cells using TO-PRO-3 iodide staining, and used to collect 10,000 live events. Data was then analysed using FlowJo v9 software (Tree Star, Inc., Ashland, OR, USA), with median

fluorescence intensity in live cells determined for each treatment. For C8- and C10-treated cells, median fluorescence intensity was then normalised against the corresponding CS activities to account for potential differences in mitochondrial content between cells.

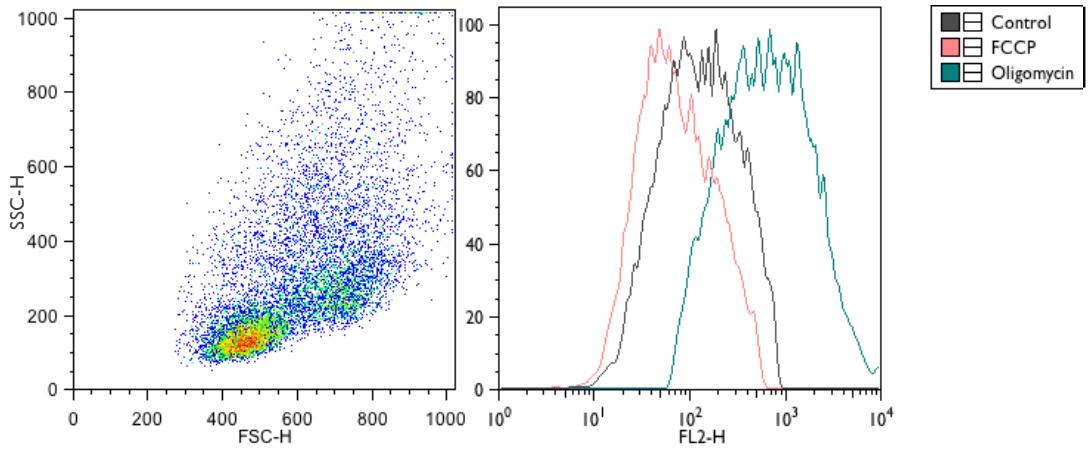

FIGURE 2.7 Typical flow cytometry pseudocolour plot and histogram of TMRE-stained SH-SY5Y cells. The pseudocolour plot, obtained from control cells, shows all detected events plotted against FSC and SSC. The histogram represents a set of cells from an individual experiment treated with FCCP and oligomycin. The shift in peaks indicates the direction of change in fluorescence, with FCCP-treated cells showing a decrease in fluorescence and oligomycin-treated cells showing an increase in fluorescence compared to the control.

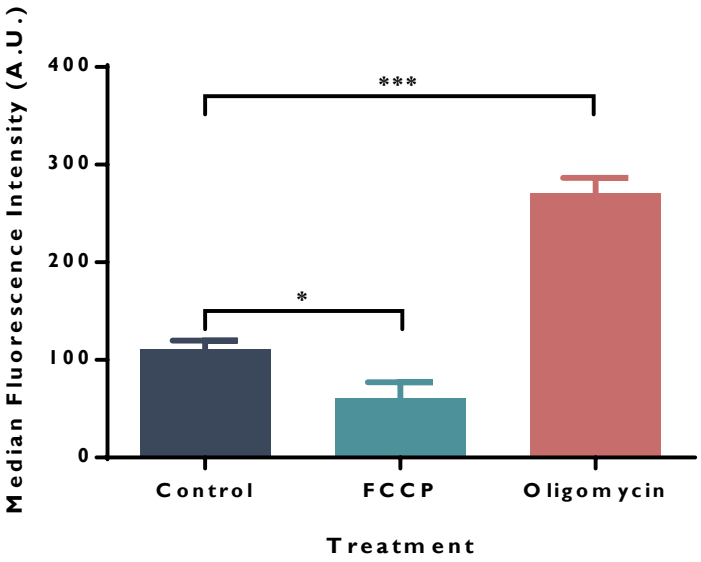

FIGURE 2.8 Change in TMRE median fluorescence intensity of SH-SY5Y cells treated with FCCP and oligomycin. Cells treated with 10μM FCCP and 1μM oligomycin and stained with TMRE showed a shift in median fluorescence intensity, indicating changes to mitochondrial membrane potential. FCCP depolarised and oligomycin hyperpolarised the mitochondrial membrane potential under these conditions. Data represents mean ± SEM of three individual experiments (n=3).

2.7 MEASUREMENT OF ENERGY CHARGE BY HPLC

2.7.1 Principle

The energy charge is a measure of the energetic state of cells, based on the ratio of ATP to ADP and AMP present in the cellular adenylate pool (Atkinson, 1968), and is defined by the following equation:

$$\frac{[ATP] + 0.5[ADP]}{[ATP] + [ADP] + [AMP]}$$

EQUATION 2.2 Cellular Energy Charge

To determine these ratios, ATP, ADP and AMP levels were measured using reversed phase high-performance liquid chromatography (HPLC), coupled to a fluorescence detector. Reversed-phase HPLC is an analytical chromatographic technique capable of

separating and quantifying mixtures of compounds, based on surface hydrophobicity (Boone & Adamec, 2016; Canene-Adams, 2013). It relies on the use of a nonpolar stationary phase, upon which analytes adsorb to, and a polar mobile phase to separate them. The stationary phase is generally composed of a silica column packed with alkyl chains, typically C18 in length (Boone & Adamec, 2016). Analytes are separated according to polarity, with non-polar compounds adsorbing more readily to the stationary phase than polar compounds, resulting in longer retention times. Following separation, the analytes can then be detected by a detector, which converts the signals into an electrical output that is generated into a chromatogram by the data system. For the measurement of adenine nucleotides, a fluorescence detector was utilised due to its sensitivity at detecting very low sample levels (Swartz, 2010). Fluorescence detectors measure fluorescence emission from analytes following excitation at a high energy wavelength and can therefore be used to detect compounds that are autofluorescent or have been modified to fluoresce. To detect the adenine nucleotides, the compounds were derivatized with chloroacetaldehyde to produce fluorescent 1,N^6-ethenoderivatives. This reaction forms an etheno bridge on the purine ring of the adenine group, between the 1st nitrogen and the amino group nitrogen on carbon 6, as represented in Figure 2.9, and is specific to adenines and cytidines (Kochetkov, Shibaev, & Kost, 1971). Adapted from Bhatt et al. (2012), this method was further developed and validated by Dr Simon Eaton and Dr Michael Orford.

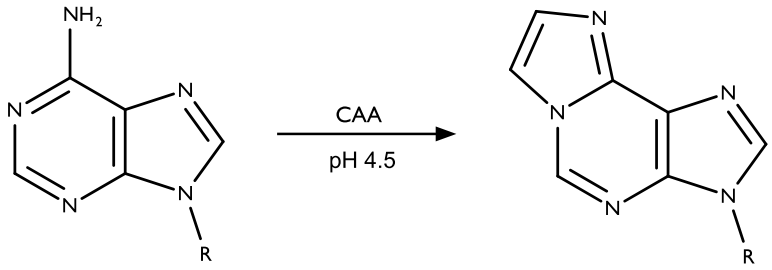

Figure 2.9 Derivatization of adenine purine ring with chloroacetaldehyde. The reaction forms an etheno bridge between N^1 and the amino group nitrogen on C^6, resulting in a fluorescent ethenoderivative that can be detected via a fluorescence detector.

2.7.2 Reagent Preparation

For sample extraction, 1M perchloric acid was prepared by diluting 70% perchloric acid (BDH Chemicals, VWR, Lutterworth, UK) in Milli-Q water, and stored at 4°C to maintain the cold temperature necessary for extraction. A solution of 0.5M potassium hydrogen carbonate ($KHCO_3$) in 1M potassium hydroxide (KOH) (BDH Chemicals, VWR, Lutterworth, UK) was also prepared in Milli-Q water for sample processing, and stored at room temperature. For derivatization, 1M sodium acetate (VWR, Lutterworth, UK) was prepared in Milli-Q water and the pH adjusted to 4.5 with acetic acid, before storing at room temperature. These reagents were stored in these conditions for up to 3 months. A 4M solution of chloroacetaldehyde (CAA) was prepared in Milli-Q water and stored at room temperature for up to one week. If discolouration was observed prior to that, the solution was discarded and prepared from fresh. The HPLC mobile phase consisted of two buffers, Mobile Phase A and Mobile Phase B. Mobile Phase A was prepared from 0.2M potassium phosphate (VWR, Lutterworth, UK) in Milli-Q water, with pH adjusted to 5.0 with KOH. Mobile Phase B was composed from 0.2M potassium phosphate (pH 5.0) with 10% acetonitrile (Fisher

Scientific UK Ltd, Loughborough, UK), with pH adjusted as previously described for Mobile Phase A.

2.7.3 Sample Treatment and Extraction

Cells were seeded at a density of 5 x 10^3 cells/cm^2 in 6-well plates and treated with DMSO, C8 and C10 as specified in Section 2.3.1. At the end of treatment, on day 6, medium was removed and cells were quickly washed with 1ml DPBS. The plate was immediately placed on ice and 1ml ice cold 1M perchloric acid was added directly to each well. Cells were then scraped and transferred to microtubes, and the cell extracts frozen at -20°C until processing.

To process the samples, 250µl of the cell extract was transferred to a new microtube, and 200µl 0.5M $KHCO_3$ in 1M KOH was added. Samples were vortexed and centrifuged for 5 mins at 13,000xg to remove precipitated proteins and potassium perchlorate. The supernatant was collected to a new microtube with 100µl transferred to a glass vial for derivatization. The remaining supernatant was stored at -20°C for future use if necessary.

2.7.4 Derivatization and HPLC Analysis

For derivatization, 100µl 1M sodium acetate (pH 4.5) and 10µl 4M CAA were added to the glass vial containing 100µl of supernatant. After thorough mixing, the samples were heated for 40 mins at 60°C. At the end of incubation, samples were immediately placed on ice for 5 mins to stop the reaction, before being transferred to the HPLC autosampler tray, pre-cooled to 4°C, for analysis.

Reversed-phase HPLC analysis was carried out in a JASCO Automated HPLC System (JASCO UK Ltd., Great Dunmow, UK), comprised of an AS-950 Intelligent Sampler, PU-1580 Intelligent HPLC Pump, CO-1560 Intelligent Column Thermostat, DG-1580-53 3-Line Degasser and MD-1510 Multiwavelength Detector, coupled to a PC for analysis.

After loading to the autosampler tray, 20µl of sample was injected into a Hypersil™ ODS C18 column (3µm particle size, 150mm column length, 4.6mm I.D), with the column thermostat set to 25°C. The mobile phase flow rate was set to 0.8ml/min, with the gradients outlined in Table 2.1 utilised for sample runs, lasting 37 mins each.

TABLE 2.1 HPLC mobile phase gradients applied to each sample run.

Time (min)	Mobile Phase A (%)	Mobile Phase B (%)
0	100	0
31	89	11
36	80	20
37	100	0

Detection with the fluorescence detector was set to 290nm excitation and 415nm emission. Data was collected and analysed with EZChrom Elite v3.17 software (Agilent Technologies, Santa Clara, CA, USA). Peak integration from the generated chromatograms was then utilised to calculate the energy charge of cells, using Equation 2.2. A typical chromatogram observed in control SH-SY5Y cells, displaying ATP, ADP and AMP peaks, is exemplified in Figure 2.10.

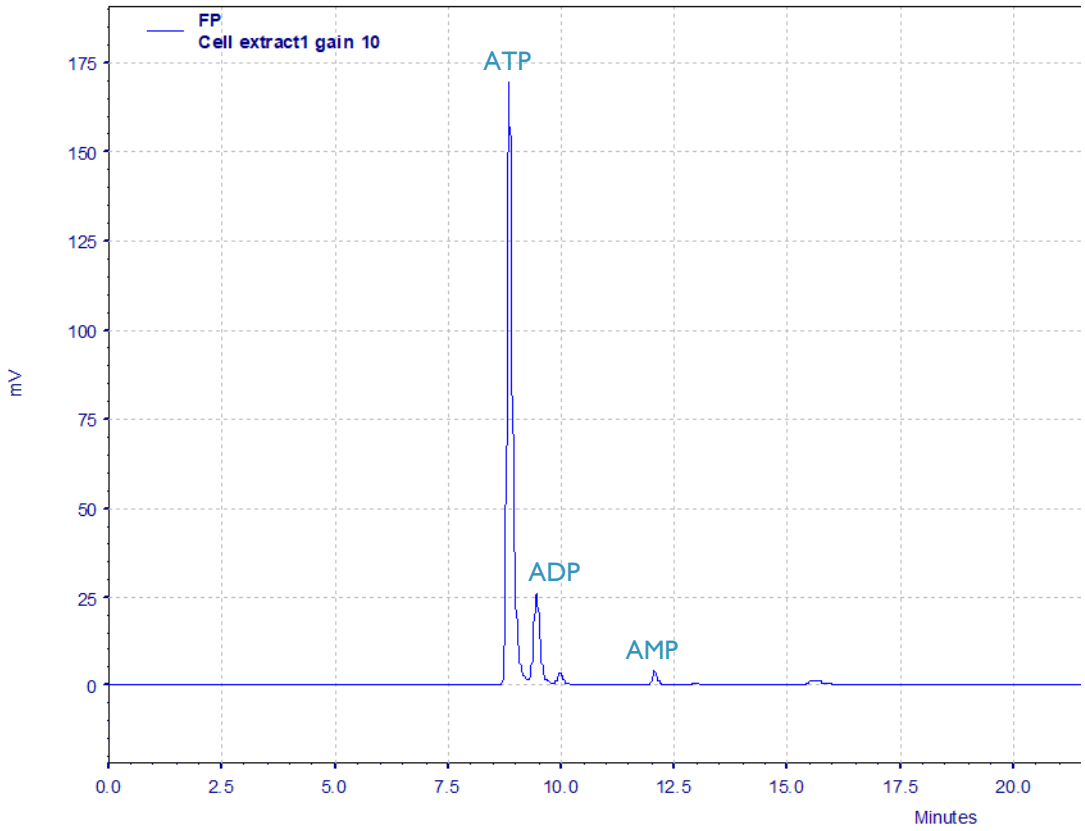

FIGURE 2.10 Typical HPLC chromatogram representative of ATP, ADP and AMP levels in control SH-SY5Y cells. Each peak was integrated to obtain peak area for each compound, which was then utilised to determine the energy charge according to Equation 2.2.

2.8 STATISTICS

Results throughout this thesis are expressed as the mean ± SEM. Unless otherwise stated, statistical analyses for two groups were performed using an unpaired Student's t-test. For multiple comparisons, statistical analysis was carried out with one-way Analysis of Variance (ANOVA,) followed by a Tukey's post-test, unless otherwise stated. Statistical significance was considered when $p<0.05$. As these analyses are parametric tests, they assume that the data analysed follow a Gaussian distribution. The D'Agostino-Pearson Omnibus K2 test for normality was run prior to analysis to determine that the data were not inconsistent with a Gaussian distribution. Where skewness and kurtosis were detected, data were also transformed, with the

transformations utilised described where applicable. For patient data in Chapter 6, repeated-measures ANOVA was also considered where data were matched between treatments for the same patients and carried out where applicable. However, given the nature of the study and continuous participant drop-out, unpaired measurements were carried out for most datasets. Justification for the statistical analyses employed for this data is further clarified in Section 6.3.8. All statistical analyses were performed using the GraphPad Prism software (San Diego, CA, USA).

CHAPTER 3

Effects of Decanoic Acid on Mitochondrial Citrate Synthase, Mitochondrial Membrane Potential and Energy Charge in SH-SY5Y Cells

3.1 BACKGROUND

Mitochondrial dysfunction has been strongly implicated in epilepsy. Whilst an exact causal relationship between seizure generation and mitochondrial dysfunction has yet to be elucidated, targeting mitochondria may provide a useful avenue for the development of neuroprotective therapies. Depressed mitochondrial respiration has been implicated in seizure generation, with complex I deficiencies also linked to mitochondrial epilepsies (Kanabus et al., 2016; Kanabus, Heales, & Rahman, 2014; Rahman, 2012). Furthermore, ROS are speculated to contribute to seizure development (Folbergrová & Kunz, 2012), as mitochondrial dysfunction can expose cells to oxidative damage, leaving neuronal cells vulnerable to aberrant excitatory activity and neurodegeneration. Likewise, epileptiform activity can also result in mitochondrial damage through oxidative stress (Chang & Yu, 2010; Frantseva et al., 2000; Waldbaum & Patel, 2010), resulting in a vicious and deleterious cycle of seizure activity and mitochondrial dysfunction.

Previous work in this laboratory by Hughes et al. (2014) demonstrated the pro-mitochondrial effects of C10, with its ability to increase complex I activity, catalase activity and mitochondrial content. The latter, in particular, was found to be mediated by PPARγ, a nuclear receptor involved in mitochondrial biogenesis and regulation. With C10 known to act as a PPARγ ligand (Malapaka et al., 2012), the fatty acid may play an underlying role in the increased mitochondrial biogenesis associated with the MCT KD (Bough et al., 2006).

However, whilst improving mitochondrial function and increasing content may be beneficial, the long-term impact and potential disadvantages of mitochondrial accumulation have yet to be fully considered. Thus, with this thesis building on the

work of Hughes et al. (2014), this chapter aims to further observe and evaluate the effects of C10 on mitochondrial content in SH-SY5Y cells, as measured by citrate synthase activity. Interestingly, at the commencement of this study, populations of SH-SY5Y cells that differed by control citrate synthase activity were identified, including: cells with levels comparable to the activities reported by Hughes et al. (2014), cells with much higher control activities, and cells that exhibited intermediate values. The effects of C10 treatment on mitochondrial content across these different levels of control citrate synthase activity were assessed and the potential involvement of mitophagy as an additional regulatory mechanism was also considered, with the use of an inhibitor of mitophagy, Mdivi-1 (Cassidy-Stone et al., 2008; Kim et al., 2016; Rosdah et al., 2016).

In addition to this, C10 effects on mitochondrial function were also explored within this chapter. In view of the key role of mitochondrial membrane potential ($\Delta\Psi_m$) as an indicator of mitochondrial function, with its involvement in oxidative phosphorylation, the effects of C10 on $\Delta\Psi_m$ were evaluated. Interlinked with oxidative phosphorylation capacity to generate ATP, $\Delta\Psi_m$ is also closely associated with apoptosis and ROS generation. Indeed, increased $\Delta\Psi_m$ can lead to increased ROS (Zorova et al., 2017), whilst oxidative damage of mitochondrial components, such as electron transport chain complexes, can also result in depolarisation of $\Delta\Psi_m$, where prolonged dissipation of $\Delta\Psi_m$ is capable of triggering apoptosis (Ly, Grubb, & Lawen, 2003). Thus, with C10 reported to increase catalase activity and brain antioxidant status (Hughes et al., 2014; Sengupta & Ghosh, 2012; Sengupta, Ghosh & Bhattacharyya, 2014), measuring potential changes in $\Delta\Psi_m$ may provide further insight into the effects of C10 on mitochondrial function. In conjunction with this, energy charge, a measure of the energetic state of cells based on the adenylate system, was also assessed with C10

treatment. Furthermore, as it is a major component of MCT oil in the MCT KD, the effects of C8 on mitochondrial content and function were also examined alongside C10.

3.2 AIMS

- To determine the effects of C10 treatment on citrate synthase activity in SH-SH5Y cells differing in control citrate synthase activities.
- To explore the regulatory mechanisms behind the effects of C10 treatment on mitochondrial content.
- To investigate the effects of C8 and C10 on mitochondrial function, via $\Delta\Psi_m$ and cellular energy charge.

3.3 METHODS

3.3.1 Materials

All reagents were purchased as described in Section 2.1.

3.3.2 Cell Treatment with C8 and C10

SH-SY5Y cells were cultured and treated as described in Section 2.3.1 in 6-well plates, T25 or T75 flasks, where appropriate, at a cell density of 5 x 10^3 cells/cm^2. Cells were treated for 6 days with C8 or C10 at a final concentration of 250μM, with DMSO used as a vehicle control. On day 6 of treatment, cells were harvested in a known volume of protein isolation buffer, as described in Section 2.3.2.

3.3.3 Mitophagy Inhibition with Mdivi-1

To examine the role of mitophagy on the effects of C10, a mitochondrial fission inhibitor, Mdivi-1, was used. Stock solutions of 2mM and 4mM of Mdivi-1 were

prepared in DMSO and aliquoted prior to storage at -20°C. An additional stock solution of 100mM C10 was also prepared and stored as outlined in Section 2.3.1. Various treatment conditions were examined, including treating cells with Mdivi-1 alone and in conjunction with C10. Cells were cultured in T25 flasks and treated with DMSO vehicle control or 250μM C10 for 6 days, as described above. On days 4 and 5 of treatment, cells pre-treated with either DMSO vehicle control or 250μM C10 were subjected to treatment with Mdivi-1 alone or with C10 for 48h and 24h, with Mdivi-1 at a final concentration of 10μM. Total treatment volume was always maintained at 5μl/ml for all conditions. On day 6 of treatment, cells were harvested in 250μl protein isolation buffer as outlined in Section 2.3.2.

3.3.4 Citrate Synthase Enzyme Activity Assay

Citrate synthase enzyme activity assays were carried out as described in Section 2.4.2 and normalised against protein content.

3.3.5 Protein Quantification

Protein content of samples was determined using the Bradford assay, as outlined in Section 2.5.2.

3.3.6 Mitochondrial Membrane Potential Analysis with TMRE

Mitochondrial membrane potential was analysed in C8- and C10-treated cells by FACS analysis using TMRE, as described in Section 2.6, with median fluorescence intensity normalised against CS activity.

3.3.7 Energy Charge Determination via HPLC

Cellular energy charge in C8- and C10-treated cells was determined by ATP, ADP and AMP measurement via HPLC using the methods described in Section 2.7.

3.3.8 Statistical Analysis

All data were statistically analysed as described in Section 2.8. Linear regression analysis and runs tests were also performed using GraphPad Prism 6. Data were specifically transformed prior to analysis where necessary.

3.4 RESULTS

3.4.1 Differential Effects of C10 on Citrate Synthase (CS) Enzyme Activity

Studies have shown that C10 elicits increased citrate synthase (CS) activity in both neuronal SH-SY5Y cells and fibroblast cells, after treatment for 6 days at a reported concentration of 250μM (Hughes et al., 2014; Kanabus et al., 2016). The initial aim of this study was to replicate these findings, and subsequently build on this observation relating to effects upon CS activity. However, at the commencement of this study, scrutiny of the control CS activity revealed distinctive populations of cells with widely varying CS activities. Control CS activity measured was found to span a wide range of values. Based on this, cells within the data set could be divided into approximately 2 populations. In one population, cells displayed CS activities comparable to those reported by Hughes et al. (2014), whilst in another, cells were found to have much higher control CS activities. In addition to these two groups, many cells also exhibited CS activities that fell within the middle of this range. Overall, C10 treatment was found to have no significant effect on CS activity (Figure 3.1A). However, upon examining the

data in further detail, a differential effect of C10 on CS activity within these cells was observed, with C10 treatment either increasing or decreasing CS activity. To further analyse this observation, the data were divided into two separate groups based on control CS activity. A CS activity of 130 nmol/min/mg was determined as a cut-off point, based on the data published by Hughes et al. (2014) and documented in the PhD thesis by Hughes (2014), where reported control CS activities were always below this level. In 7 out of 20 experiments, control CS activity was observed to be below this cut-off point. In these cells, C10 treatment was found to increase CS activity by an average of 24±7 nmol/min/mg, the overall effect of which was statistically significant with a paired analysis (*$p<0.05$) (Figure 3.1B). Conversely, in the remaining data sets (n=13) (Figure 3.1C), where control CS activity was higher than the cut-off point, C10 treatment significantly decreased CS activity (**$p<0.01$) by a mean of 32±9 nmol/min/mg, indicating that the effects of C10 on mitochondrial content may be divergent. It is of note that the CS activities measured here were normalised to protein content to take into consideration the nature of enzymes as proteins, and provide a standardised approach measurable against the data published by Hughes et al., (2014) and comparable to protocols employed in the literature (De Vogel-Van Den Bosch et al., 2011; Gegg et al., 2010; Kanabus et al., 2016; Kudin et al., 2002). In addition, assessment of CS activity, employed as described here, is used as a validated (accredited) marker of mitochondrial enrichment in the nationally commissioned (NHS England) diagnostic service for mitochondrial disorders.

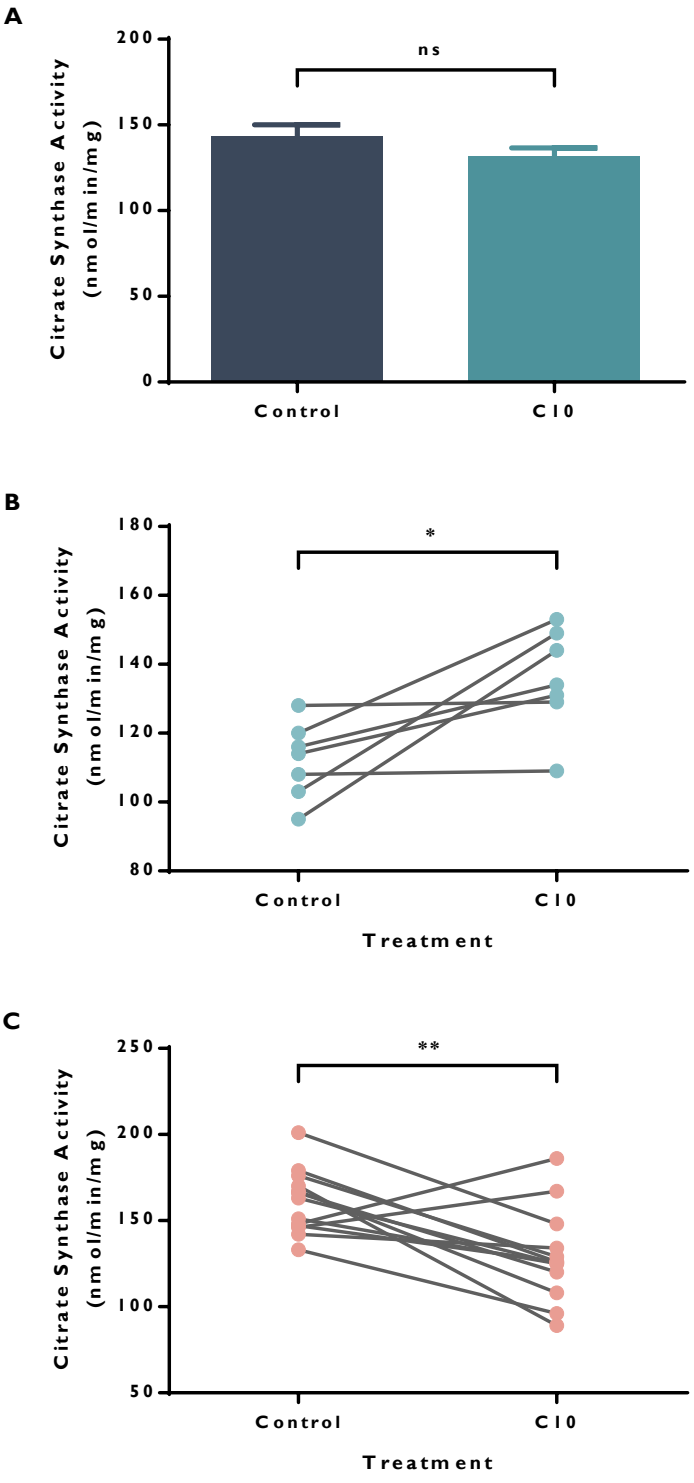

FIGURE 3.1 C10 treatment exerts a differential effect on CS activity in SH-SY5Y cells. Cells treated for 6 days with 250μM C10 displayed a differential change in CS activity following treatment. These changes could be separated into two separate groups. A) Overall, no significant changes in CS activity were found with C10 treatment (n=20). B) Samples were separated into two groups based on control CS activity, with 130 nmol/min/mg utilised as a cut-off point based on Hughes et al. (2014). Here, samples with control activities below this cut-off (n=7)

were analysed. Analysis with a paired Student's t-test found that C10 treatment significantly increased CS activity in these cells (*$p<0.05$). C) Samples with control CS activities above the 130 nmol/min/mg cut-off point (n=13) were found to exhibit a significant decrease in CS activity following C10 treatment (**$p<0.01$) when analysed with a paired t-test. Data are represented as mean ± SEM, obtained from 20 independent experiments overall.

To further delineate the differential effects of C10, the role of cell control CS activity in treatment outcome was also closely examined. Changes in CS activity following C10 treatment were compared to initial control levels in cells (Figure 3.2). Interestingly, a strong linear effect was observed ($r^2 = 0.6402$, ***$p<0.001$), with changes in CS activity following C10 treatment negatively correlating with control levels in control cells. These changes in CS activity observed after C10 treatment were found to decrease as control CS activity increased. C10 treatment also appeared to increase CS activity when control levels were below a certain threshold, approximately determined as 138 nmol/min/mg by linear regression analysis. At this approximate threshold, cells appeared to exhibit little to no change in CS activity with C10 treatment. Furthermore, cells with control levels higher than this threshold generally exhibited decreased CS activity following C10 treatment.

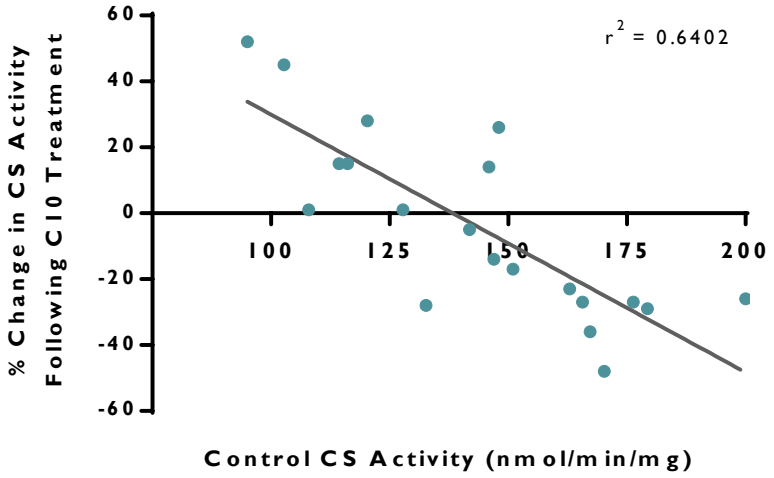

FIGURE 3.2 The effects of C10 on CS activity are dependent on initial control CS activity levels. Linear regression analysis was performed and a strong linear correlation was observed (r^2=0.6402). CS activity increased with C10 treatment when control levels were below a certain threshold. Above this level, CS activity was found to decrease with C10 treatment. This threshold was approximately determined as 138 nmol/min/mg, using the following equation of the line (y = -0.78x+107.9). An F-stop test indicated that the slope was significantly non-zero (***p<0.001), whilst a runs test was also performed to determine deviation from the line, which was found to be non-significant.

With the data potentially suggesting a differential effect of C10 treatment on CS activity, an attempt was made to calculate the EC_{50} of C10 on CS activity, the concentration that C10 is estimated to give a half-maximal response. In a pilot study, SH-SY5Y cells were treated for 6 days with C10 at a range of concentrations up to 250μM and CS activity then measured. Dose-response curves were obtained and compared from two independent experiments where an overall positive (n=1) and negative (n=1) effect of C10 treatment were found. A dose-response effect appeared to be observed in each of the experiments, with increasing concentrations of C10 either sequentially raising CS activity (positive response) or reducing CS activity (negative response) compared to the control. In the positive response dataset, control CS activity was measured at 103 nmol/min/mg, rising to 149 nmol/min/mg following 250μM C10

treatment, whilst in the negative response dataset, control CS activity was 155 nmol/min/mg, with 250μM C10 treatment reducing it to 89 nmol/min/mg.

To estimate the EC_{50} of C10, the data were first transformed by taking $\log_{10}$[C10] and then plotting against normalised values of CS activity, designating 0% and 100% as minimal and maximal responses for each dataset (Motulksy and Christopoulos 2004). Sigmoidal curves were generated for each treatment response (positive response, r^2=0.9862; negative response, r^2=0.8778), with each curve indicating opposite treatment effects of C10. These were then used to estimate the EC_{50} for both the positive and negative responses to C10 treatment. Comparison of fits statistical analysis suggested a model where logEC_{50} was found to be identical for each curve, as observed by the intersection of the lines in Figure 3.3. With this assumption in mind, best-fit EC_{50} of C10 was estimated at 129μM for both positive and negative responses. However, as these curves were generated from one replicate in each experiment, the calculated EC_{50} must be considered a preliminary estimate.

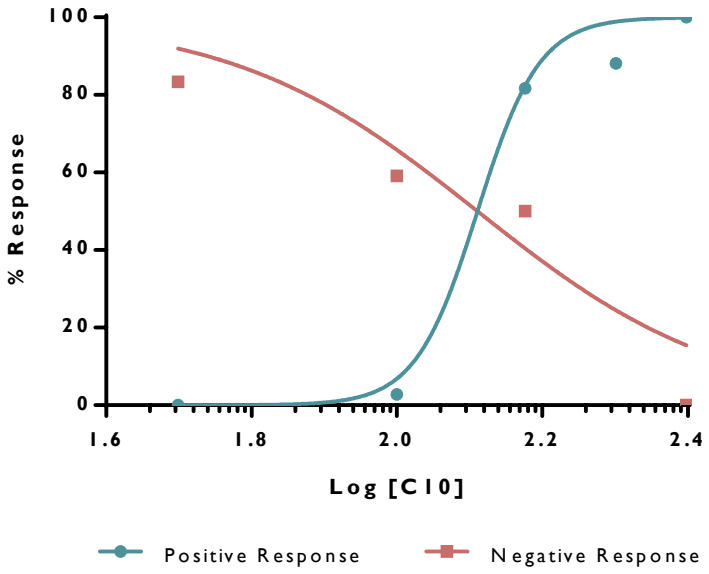

FIGURE 3.3 Preliminary dose response curves for the differential effects of C10 on CS activity. SH-SY5Y cells were treated for 6 days with 0-250μM C10 and CS activity measured. Data represent single points from one independent experiment for each curve (n=1). Analysis of the dose response curves (positive response r^2=0.9862; negative response r^2=0.8778) via comparison of fits suggested that logEC_{50} was the same for both positive and negative responses, with EC_{50} estimated at 129.0μM.

3.4.2 Effects of C8 on Citrate Synthase Enzyme Activity

To determine if these effects were unique to C10, SH-SY5Y cells were treated with 250μM C8 for 6 days and CS activity was measured (Figure 3.4). No significant changes in overall CS activity were observed following C8 treatment in these cells. Furthermore, no apparent effects on CS activity were found within individual experiments, suggesting that the ability of C10 to both increase and decrease CS activity in cells is associated with C10 rather than C8.

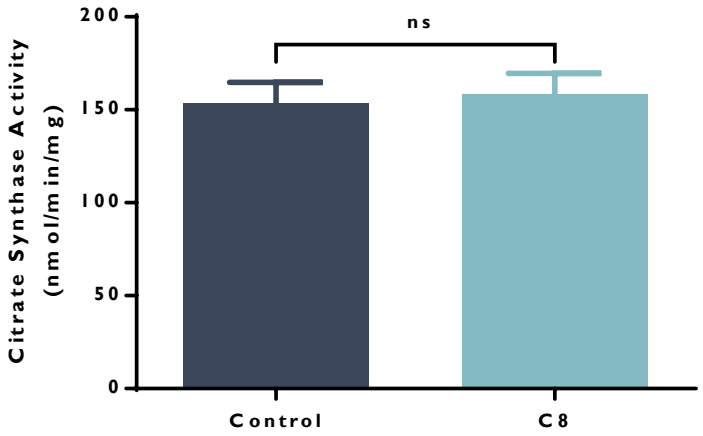

FIGURE 3.4 CS activity in SH-SY5Y cells following 250μM C8 treatment for 6 days. No significant changes in CS activity were found with C8 treatment. Data are expressed as mean ± SEM of 11 independent experiments (n=11). The percentage change of CS activity following C8 treatment was also analysed (data not shown), with a poor correlation determined (r^2=0.0876) through linear regression analysis.

3.4.3 Effects of C10 on Citrate Synthase Activity Following Pharmacological Inhibition of Mitophagy with Mdivi-1

With the observed data suggesting a differential impact of C10 on CS activity, it was hypothesised that mitophagy regulation may play a role in the effects of C10. To understand the mechanisms underlying these effects, pharmacological inhibition of mitophagy was considered. However, pharmacological approaches to inhibiting mitophagy are limited. Whilst most commonly used inhibitors, such as bafilomycin A1 and chloroquine, are effective at halting mitophagy, they are typically nonspecific and inhibit general autophagic and lysosomal processes within cells (Georgakopoulos, Wells, & Campanella, 2017; Tasdemir et al., 2008). Thus, with very few inhibitors available to selectively block mitophagy without affecting autophagy, disrupting mitochondrial fission may be used as an alternative approach.

Mitochondrial fission is a key component of mitochondrial homeostasis, and facilitates quality control by removing damaged mitochondria through mitophagy. Upon loss of membrane potential, damaged mitochondria are subject to fission, generating small daughter mitochondria which are then cleared via mitophagic processes, leaving behind mitochondria with intact membrane potential. This process of fission is regulated by the GTPase dynamin-related protein (Drp1), which polymerises into a ring-like structure around the outer mitochondrial membrane that constricts to induce mitochondrial fission (Rosdah et al., 2016). Loss of Drp1 function has been shown to prevent mitophagy, suggesting that mitophagy may be dependent on prior mitochondrial fission (Ikeda et al., 2015; Kageyama et al., 2014; Twig et al., 2008). Mdivi-1 (mitochondrial division inhibitor-1) can be used to pharmacologically inhibit mitochondrial fission. Mdivi-1 is a reversible selective inhibitor of Drp1 that binds to an allosteric site fundamental to its polymerisation, disrupting Drp1 self-assembly into the ring structure for fission and consequently suppressing GTPase activity (Cassidy-Stone et al., 2008).

In a preliminary study investigating the potential role of mitophagy, SH-SY5Y cells were treated with 250μM C10 and vehicle control for 6 days, with and without 10μM Mdivi-1 treatment for 24h and 48h. The concentration used and duration of treatment with Mdivi-1 was based on publications that utilised SH-SY5Y cells (Gan et al., 2014; Park et al., 2015; Saez-Atienzar et al., 2014; Solesio et al., 2012), and CS activity was examined following treatment. No significant changes in CS activity were observed with all treatments, including with C10 alone (Figure 3.5). Further examination of individual replicate data suggested differences in control CS activity, and thus some variability in response to C10 treatment (data not shown). However, the lack of effect

observed with both 24h and 48h Mdivi-1 treatments indicates that the inhibitor may have been ineffective in these cells at the concentration and treatment length used.

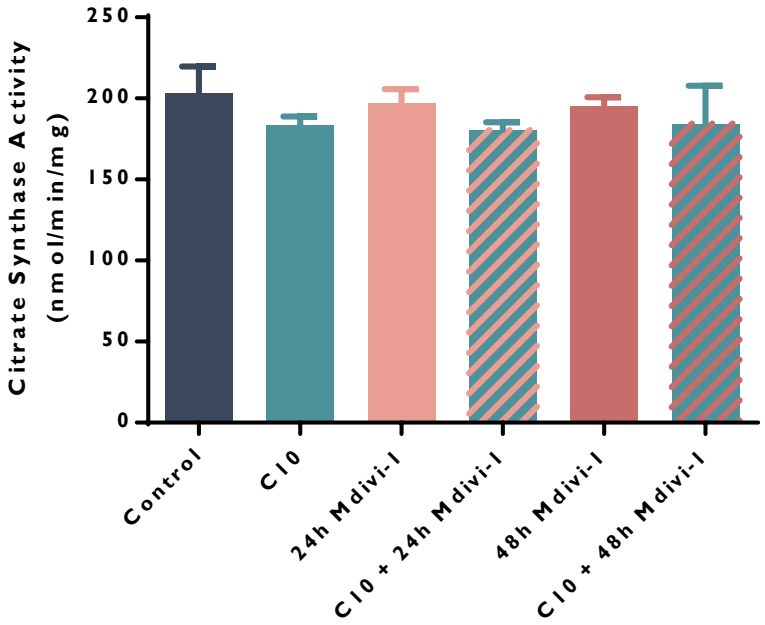

FIGURE 3.5 CS activity in SH-SY5Y cells following 6-day treatment with 250μM C10, 24h 10μM Mdivi-1 alone or with C10, and 48h 10μM Mdivi-1 alone or with C10. No significant changes in CS activity were found with all treatment conditions. Data are expressed as mean ± SEM of 3 independent experiments (n=3).

3.4.4 Effects of C8 and C10 on Mitochondrial Membrane Potential (ΔΨm)

Mitochondrial membrane potential ($\Delta\Psi_m$) can be used an indicator of mitochondrial and cellular function. To examine the effects of C10 on mitochondrial function, the mitochondrial membrane potential ($\Delta\Psi_m$) of cells treated with 250μM C10 for 6 days was assessed. Given the role of C8 in the MCT KD as a component of MCT oil, the effects of 250μM C8 treatment were also investigated and compared to C10. Using the $\Delta\Psi_m$-dependent fluorescent probe tetramethylrhodamine ethyl ester (TMRE), changes in $\Delta\Psi_m$ were measured by flow cytometry. A lipophilic cation, TMRE is readily

sequestered by mitochondria and accumulates inversely to $\Delta\Psi_m$ according to the Nernst equation (Perry et al., 2011). The more polarized mitochondria are, the more the dye will accumulate in the mitochondrial matrix, whilst depolarization of mitochondria results in less dye accumulation. This translates directly into fluorescence emitted by the probe.

The median fluorescence intensity was measured for each treatment, and the values then normalised to citrate synthase activity (nmol/min/ml) to account for differences in mitochondrial content. As an enzyme exclusive to mitochondria, CS activity was used as a measure of mitochondrial content, as validated in the literature (Hughes et al., 2014; Jacobs et al., 2013; Larsen et al., 2012) and in accordance with practice in Highly Specialised NHS-accredited laboratories for mitochondrial services. C10 treatment was found to significantly increase $\Delta\Psi_m$ in these cells (*$p<0.05$) (Figure 3.6), potentially indicating improved mitochondrial function in these cells. Conversely, C8 treatment did not result in any significant changes to $\Delta\Psi_m$ when compared to the control, with overall $\Delta\Psi_m$ found to be similar to that of control cells.

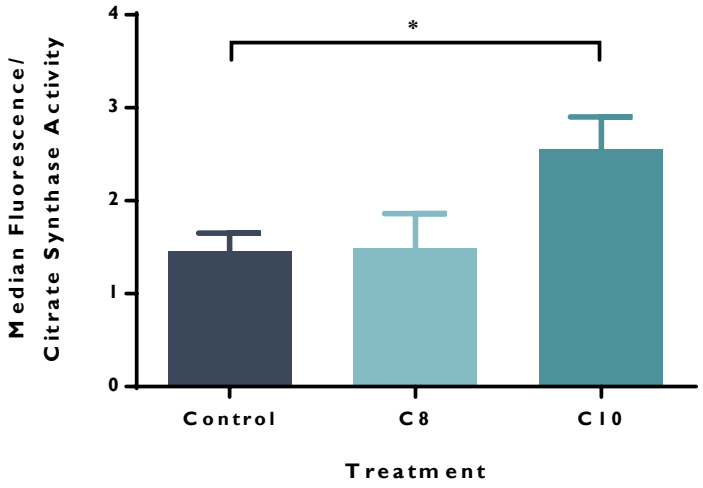

FIGURE 3.6 The effects of C8 and C10 treatment on mitochondrial membrane potential ($\Delta\Psi_m$) in SH-SY5Y cells. No significant changes to $\Delta\Psi_m$ were found with 250μM C8 treatment, whilst a significant increase in $\Delta\Psi_m$ was observed with 250μM C10 (*$p<0.05$). Data are expressed as mean ± SEM of 6-9 independent experiments (n=6-9).

3.4.5 Energy Charge in C8- and C10-treated Cells

Maintaining a high ratio of ATP:ADP and ATP:AMP is of critical importance to cell health. Energy charge (also known as adenylate charge) can be used as a linear measure of the energetic state of cells, reflecting the levels of ATP, ADP and AMP present. Expressed as a ratio ranging from 0-1.0, a system that contains only ATP in its adenylate pool will have an energy charge of 1.0, whilst a fully discharged system containing only AMP will have a charge of 0 (Atkinson, 1968; Hardie & Hawley, 2001). Most cells will express an energy charge of 0.8-0.95. The energy charge of cells treated with 250μM C8 and C10, for 6 days, was assessed using HPLC (Figure 3.7). Mean energy charge for each treatment was calculated as 0.93±0.005 in control cells, 0.93±0.002 in C8-treated cells and 0.92±0.004 in C10-treated cells, with no significant changes in energy charge found with both C8 and C10 treatments compared to the control. This indicates that neither C8 nor C10 affect the overall ratios of ATP to ADP

and AMP in cells. Other work on SH-SY5Y cells has shown that 48h rotenone treatment decreases energy charge to approximately 0.85 (Mesfer Al-Shahrani, personal communication).

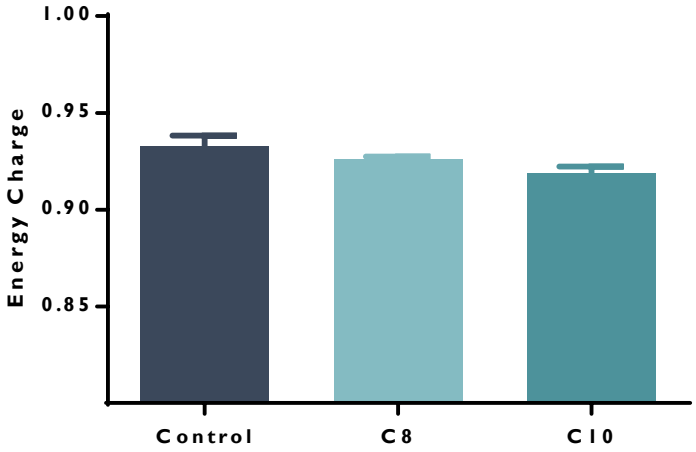

FIGURE 3.7 The energy charge of control, C8- and C10-treated cells. Cells were treated for 6 days with 250μM C8 and C10. Relative quantities of ATP, ADP and AMP were obtained via HPLC and the mean energy charge quantified for each treatment. No significant differences were observed for both C8 and C10 treatments. The following mean energy charge for each treatment were obtained: 0.93±0.005 in control cells, 0.93±0.002 in C8-treated cells and 0.92±0.004 in C10-treated cells. Data are expressed as mean ± SEM of 7-9 independent experiments (n=7-9). Data were also transformed prior to statistical analysis using the function $y = \sqrt{y}$ to account for skewness of normality.

3.5 DISCUSSION

C10 has been reported to exhibit a range of effects on neuronal mitochondrial content and function, including PPARγ-mediated increases in CS activity (Hughes et al., 2014). These effects were also reportedly mimicked in fibroblast cells, suggesting the capacity of C10 to affect non-neuronal cells in a similar manner (Kanabus et al., 2016). Nonetheless, whilst increased CS activity, suggestive of increased mitochondrial content, may potentially be of benefit to cells, uncontrolled mitochondrial biogenesis could also prove to be detrimental (e.g. through excess ROS accumulation). Enhanced

antioxidant reserves and PPARγ-dependent catalase activity are observed with C10 treatment, however, potentially inferring a balanced cellular response to C10-induced mitochondrial enrichment.

In this chapter, cellular response to C10 treatment was further characterised. CS activity was analysed as a measure of mitochondrial enrichment in these cells. An exclusive mitochondrial enzyme (Marco et al., 1974), CS activity is a biomarker of mitochondrial content (Hughes et al., 2014; Jacobs et al., 2013; Larsen et al., 2012), also used as a diagnostic marker in specialist accredited mitochondrial services in the NHS. Analysis of CS activity in SH-SY5Y cells, and use of the same methods, also allowed direct comparison with data reported by Hughes et al. (2014). At the commencement of this study, populations of SH-SY5Y cells were observed that varied in control CS activities, with values ranging from those corresponding with reports by Hughes et al. (2014) to relatively higher CS activities. The effects of C10 treatment on these cells was analysed in relation to control CS activities, using data by Hughes et al. (2014) and Hughes (2014) to determine a cut-off threshold for control activities. The difference in control CS activity between cells was found to be associated with the differential effects of C10 treatment, with the outcome of C10 treatment on CS activity strongly dependent on initial levels in control cells. In cells that exhibited high control CS activities (relative to published values by Hughes et al. (2014) and the specified cut-off point), C10 treatment was found to significantly reduce CS activity. However, when control CS activity was found to be below the threshold, and similar to those reported by Hughes et al. (2014), the converse effect was observed, with C10 increasing mitochondrial content. Moreover, in cells that displayed control CS activities close to the threshold, C10 generally exerted minimal change to CS activity. This suggested a balancing effect, with C10 proposed to regulate mitochondrial content to optimal

levels. Nonetheless, the possibility of these observed effects reflecting a regression to the mean cannot be discounted. Further experiments, including increased replication and consideration for the influence of potential covariates, are necessary to exclude this possibility. Interestingly, these findings also appeared to be paralleled in a pilot study examining the dose-response effects of C10 treatment on CS activity. In independent experiments, C10 treatment exerted a dose-dependent differential effect on CS activity: in positively responding cells, increasing concentrations of C10 also increased CS activity, whilst in negatively responding cells, increased C10 concentrations resulted in decreased CS activity. In each of these datasets, initial control CS activities and the following response to 250μM C10 corresponded to the observed paradigm described above. When plotted together, the two dose-response curves mirror one another, reflecting the contrasting effects of C10 according to control CS activities. The EC_{50} of C10 estimated from these curves also suggests that the differential effects of the fatty acid may occur at approximately the same concentration for both positive and negative responses. However, the preliminary nature of this experiment and the limited replicates necessitates the need for further work before conclusions can be made to elucidate the exact dose-response effects of C10 treatment within these cell populations. In contrast, C8 was not found to exert the same effect on CS activity, supporting previous work that the reported effects are specific to C10. Building on the evidence that C10 elicits mitochondrial biogenesis via PPARγ (Hughes et al., 2014), it was thus hypothesised that the effects of C10 may also employ additional cellular mechanisms involved in mitochondrial regulation.

One such mechanism speculated to be involved was mitophagy, a branch of autophagy that involves the selective clearance of mitochondria via autophagosomes (Youle & Narendra, 2011). Mitophagy is a key element of mitochondrial quality control and

regulation, and works alongside mitochondrial biogenesis to remove damaged mitochondria and modulate mitochondrial content in response to cellular metabolic demand and stress. Thus, the interplay of mitophagy and mitochondrial biogenesis carefully balances mitochondrial quantity and quality, and maintains cellular homeostasis (Palikaras, Lionaki, & Tavernarakis, 2015a; Palikaras & Tavernarakis, 2014) (Figure 3.8). Therefore, the observed differential effects of C10 on CS activity may integrate the mechanisms involved in these two processes.

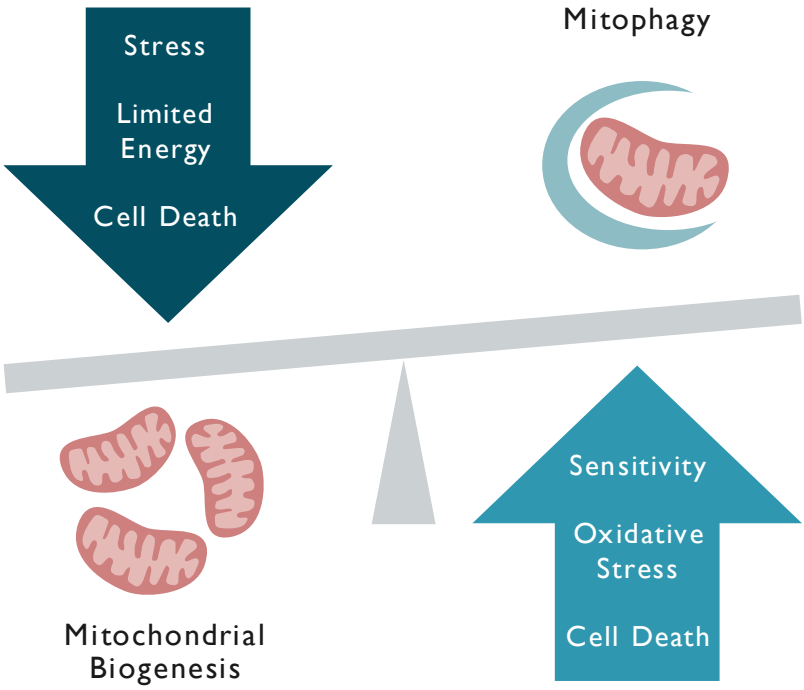

FIGURE 3.8 The balance in the relationship between mitochondrial biogenesis and mitophagy. Excess mitochondrial clearance through mitophagy can leave cells under stress and with a limited energy supply, eventually leading to cell death. Similarly, excess mitochondrial biogenesis can increase cellular sensitivity and oxidative damage, also leading to cellular degeneration and death.

To initially test this hypothesis, the role of mitophagy in the differential effects of C10 was explored pharmacologically using an inhibitor of mitophagy. The Drp1 inhibitor, Mdivi-1, was used in an attempt to indirectly inhibit mitophagy through the

obstruction of mitochondrial fission. Cells were treated for 6 days with 250μM C10 and vehicle control, and then with 10μM Mdivi-1 for 24h and 48h prior to harvesting. Preliminary data suggested no significant overall changes in CS activity with all the treatment conditions tested. Variability in C10 effect was observed in individual independent replicates, which may be due to the dependency of C10 effects on control CS activity, which was also found to vary across independent experiments. Given the preliminary nature of these experiments, further work is also needed to optimise the treatment conditions utilised. The parameters used were based on the literature available for SH-SY5Y cells (Gan et al., 2014; Park et al., 2015; Saez-Atienzar et al., 2014; Solesio et al., 2012), and were thus assumed to be effective for inhibition of mitophagy. However, the lack of observed effect with Mdivi-1 treatment suggests that the concentrations and conditions used may not have been sufficient for effective inhibition of mitochondrial fission, and thus mitophagy, in this cell line. Furthermore, it is worth noting that whilst CS activity may be used as a measure of mitophagy (Gegg et al., 2010; Ivankovic et al., 2016), quantifying CS activity alone may not be a sufficient marker for the effects of Mdivi-1. Measurement of changes to Drp1 function, mitochondrial structure or expression of mitophagy markers, such as components of the PINK1/Parkin pathway, would need to be examined to determine the effective inhibition of fission/mitophagy with Mdivi-1. In addition to mitophagy, consideration for the potential role of non-specific autophagy in the observed C10 effects on CS activity is also needed, which may also be investigated pharmacologically using general autophagy inhibitors, such as bafilomycin A1 and chloroquine.

Whilst C10 has been shown to exert a differential effect on neuronal citrate synthase activity, understanding how C10 also impacts mitochondrial function is of critical importance. To assess this, $\Delta\Psi_m$ was used as a parameter of mitochondrial function.

Established as a consequence of proton pumping across the inner mitochondrial membrane by complexes I, III and IV, $\Delta\Psi_m$ provides energy for ATP generation via ATP synthase (see Chapter 1). Not only does $\Delta\Psi_m$ influence ATP synthesis, it is also required for control of ionic flux and mitochondrial Ca^{2+} accumulation, ROS production and apoptosis (Zorova et al., 2017). Thus, $\Delta\Psi_m$ is critical to cell function, and aberrant changes to $\Delta\Psi_m$ may result in impaired ATP production and ROS generation, consequently leading to dysfunctional cellular homeostasis and/or cell death. Moreover, defective mitochondria can also be marked by changes to $\Delta\Psi_m$, particularly reductions in potential (i.e. depolarisation).

In SH-SY5Y cells, $\Delta\Psi_m$ was significantly increased with C10 treatment, whilst C8 was observed to have no overall effect. Interestingly, with all values normalised to CS activity, the elevated $\Delta\Psi_m$ with C10 treatment was found to be independent of mitochondrial content. Increased $\Delta\Psi_m$ suggests potentially increased mitochondrial function and ATP production, which may allow cells to more sufficiently meet energy demands. Elevated respiratory activity, however, may amplify ROS generation in cells, and whilst it may be argued that this may lead to oxidative damage, the increased catalase and antioxidant activities reported with C10 may protect against this (Hughes et al., 2014; Sengupta & Ghosh, 2012; Sengupta, Ghosh & Bhattacharyya, 2014). Furthermore, raised $\Delta\Psi_m$ may also indicate improved capacity of mitochondria to maintain $\Delta\Psi_m$, such as through reduction of proton leakage from the intermembrane space into the mitochondrial matrix. This process is generally maintained by mitochondrial uncoupling proteins (UCPs), although it has been reported that C10 treatment *in vivo* may not affect UCP expression in the brain (Tan et al., 2017). Ultimately, however, C10 appears to increase $\Delta\Psi_m$ irrespective of CS activity in cells, suggesting that C10 may have the ability to optimally influence mitochondrial content

in cells to potentially generate mitochondria that are more efficient at maintaining $\Delta\Psi_m$, with potentially increased mitochondrial function and energy capacity as a consequence.

Although increased $\Delta\Psi_m$ with C10 treatment may suggest enhanced ATP production, the energy charge of cells was also determined as an additional measure of cell function, to provide further insight into the ratios of ATP, ADP and AMP present within cells. Control, C8- and C10-treated cells were all found to maintain high ratios of ATP to ADP and AMP, and no significant differences were observed between treatments. This indicates that the fatty acids did not affect the distribution of the nucleotides within the adenylate pool. Maintaining a high ratio of ATP to ADP and AMP is of critical importance, as most energy-dependent processes are driven by ATP. The lack of change in energy charge, in conjunction with the increased $\Delta\Psi_m$ observed with C10 treatment, also suggest that energy is tightly controlled within mitochondria, with any changes in ATP reflected by changes in ADP and AMP. This may occur through regulatory mechanisms such as AMP-activated protein kinase (AMPK) signalling, a metabolic sensor also involved in mitochondrial quality control (Cantó & Auwerx, 2009; Hardie & Hawley, 2001), or the translocation of ATP and ADP into and out of mitochondria via ADP/ATP carriers (Klingenberg, 2008), tightly maintaining cellular bioenergetic homeostasis and the adenylate pool. It may be of interest to quantify the abundance of each nucleotide following C8 and C10 treatment to gain a broader picture of the energetic capacity of cells. Furthermore, as these experiments were carried out under basal conditions, it may be worth examining the effects of these fatty acids on energy charge under stress conditions, as energy charge is thought to remain constant under normal conditions (Hardie & Hawley, 2001). With C10 potentially influencing mitochondrial content, as judged by CS activity, and potentially improving

mitochondrial function through increased complex I activity, catalase activity and $\Delta\Psi_m$, it may be hypothesised that C10 may generate a more efficient system capable of withstanding stress. However, further work is needed to determine this and, in particular, the potential relationships between the effects of C10 on CS activity, $\Delta\Psi_m$ and energy charge. Additional consideration for the potential effects of C10 on mitochondrial pH may also be useful to analyse. Mitochondrial pH, and the chemical gradient associated with it, play a key role in the generation of the proton-motive force that drives ATP synthesis, as well as the flux of ions and metabolites across the inner mitochondrial membrane (Santo-Domingo & Demaurex, 2012). Whilst it may be predicted that the increased $\Delta\Psi_m$ observed with C10 may suggest increased mitochondrial pH, changes in $\Delta\Psi_m$ do not always mirror changes in mitochondrial pH (Perry et al., 2011). For these experiments, pH-sensitive probes could be utilised to measure any potential effects of C10 treatment on mitochondrial pH and examine how these relate to the effects observed thus far in this thesis.

To summarise, the data suggests a clear differential effect of C10 on CS activity in SH-SY5Y cells, suggesting the potential for C10 to balance neuronal mitochondrial content. The relationship between mitochondrial biogenesis and mitophagy plays a pivotal role in cellular homeostasis, and whilst this mechanism was explored within this chapter, it remains unclear if C10 exerts its balancing effects on mitochondrial content through this system (Figure 3.9). What is clear, however, is that this balance is necessary for optimum cellular function. In addition to its differential effects on mitochondrial content, as measured through CS activity, C10 also increases $\Delta\Psi_m$ independently of CS activity. Moreover, these effects occur without affecting the energy charge within cells. Consequently, the data suggests that C10 treatment may result in the generation of more efficient mitochondria with improved functional and

respiratory capacity. Thus, with the ability of C10 to balance mitochondrial content and function to optimum levels, the fatty acid may prove a promising intervention against mitochondrially-compromised neurological conditions, including drug-resistant epilepsy.

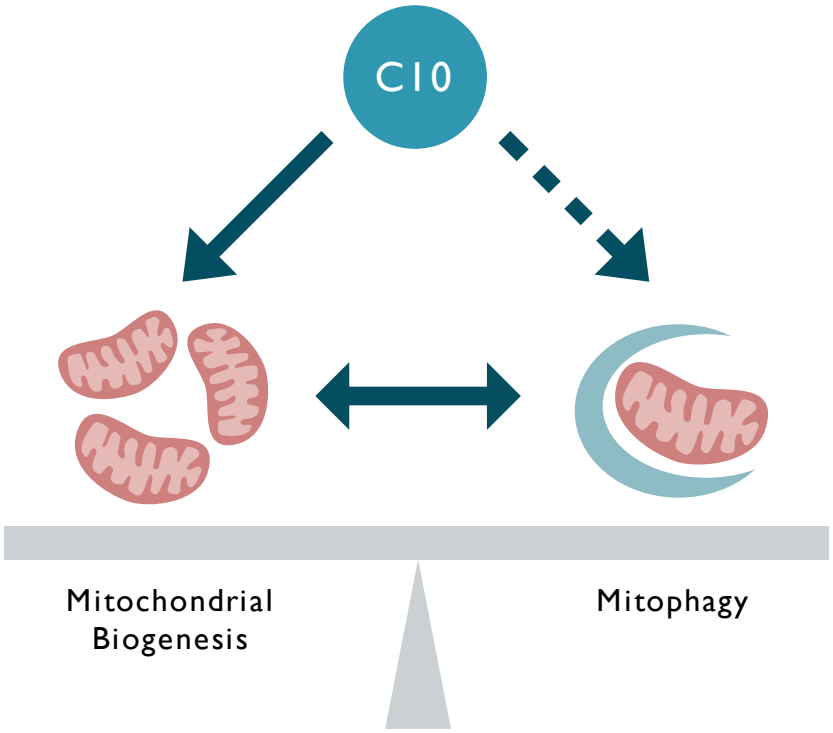

FIGURE 3.9 The potential regulatory effects of C10 on mitochondrial content. The differential effects of C10 may potentially regulate the balance of mitochondrial content through the processes of mitochondrial biogenesis and mitophagy, although this has yet to be confirmed. Maintaining this balance is crucial for cellular homeostasis and optimum mitochondrial function.

CHAPTER 4

The β-Oxidation of Decanoic and Octanoic Acids in SH-SY5Y Cells

4.1 BACKGROUND

Despite the growing interest in the potential anti-seizure effects of C8 and C10, little is known about the precise metabolic fate of these two compounds in the brain. In patients receiving the MCT KD, it is known that both C8 and C10 levels are elevated in the blood (Haidukewych et al., 1982; Sills et al., 1986). Whether these levels are reflected in patient brains remains unknown, and very few studies have investigated if this accumulation is also paralleled within the brains of animal models. However, in two separate studies by Wlaź et al. (2012, 2015), C8 and C10 levels were determined in the plasma and brains of mice following either a C8-enriched or C10-enriched diet. In both studies, C8 and C10 were found to accumulate in mouse brain and plasma in a time-dependent manner. Mean C8 levels were found to reach 500μM in plasma and 250μM in the brain. Interestingly, the concentration of C10 in mouse brain and plasma was found to reach a mean level of 240μM and 410μM, respectively, reflecting the blood levels reported in MCT KD patients, as well as corresponding closely with the optimum concentration (250μM) required for mitochondrial proliferation, increased catalase activity and AMPA receptor inhibition cited in previous reports (Hughes et al., 2014; Kanabus et al., 2016; Chang et al., 2016) and used throughout this thesis.

However, as MCFAs are typically rapidly oxidised or converted to ketone bodies, do sufficient levels of C10 accumulate in the brain to allow it to exert its effects within neurons? Furthermore, as MCT oils used in the MCT KD vary in ratio of C8 and C10 (Marten, Pfeuffer, & Schrezenmeir, 2006; Rogawski, 2016), does the presence of C8 further affect C10 metabolism? To address these questions, the β-oxidation rates of C8 and C10 in SH-SY5Y cells were assessed in this chapter using gas chromatography isotope-ratio mass spectrometry (GC-IRMS). A highly-specialised tool, GC-IRMS can be used to precisely determine the relative ratios of stable isotopes of light elements,

such as carbon ($^{13}C/^{12}C$), nitrogen ($^{15}N/^{14}N$), oxygen ($^{18}O/^{16}O$) and hydrogen ($^{2}H/^{1}H$), within mixtures (Muccio & Jackson, 2009). To utilise this feature, ^{13}C-labelled C8 and C10 were used to evaluate the absolute β-oxidation rates of these compounds. As these compounds are broken down during β-oxidation and fed into the TCA cycle, $^{13}CO_2$ is released into culture medium, which contains unlabelled bicarbonate. The changes in $^{13}C/^{12}C$ ratio in the medium are measured over time and from this the absolute β-oxidation rates of the compounds can be determined (Figure 4.1). This method can also be utilised to examine the metabolism of other ^{13}C-labelled compounds, with the oxidation of ^{13}C-labelled glucose measured alongside that of C8 and C10, to identify the fuel preference of SH-SY5Y cells. In addition to this, as C10 may be a key component in understanding the mechanisms of the MCT KD, this chapter also explored whether C8 exerts any sparing effects on C10 β-oxidation when administered in an 80:20 ratio of C10 to C8, reflecting the content of the two fatty acids in C10-enriched MCT product Betashot. Elucidating this relationship between C8 and C10 within MCT oil may provide a further basis for the push towards more C10-enriched formulations. Furthermore, the carnitine-dependence of C8 and C10 β-oxidation was also investigated, utilising ^{13}C-labelled long-chain fatty acid palmitic acid (C16) as a control and pharmacologically blocking CPT1 activity. Examining the role of the carnitine shuttle in C8 and C10 β-oxidation may provide further mechanistic insight into how C10 accumulates within the brain. The findings from this chapter were published in Khabbush et al. (2017) in *Epilepsia*.

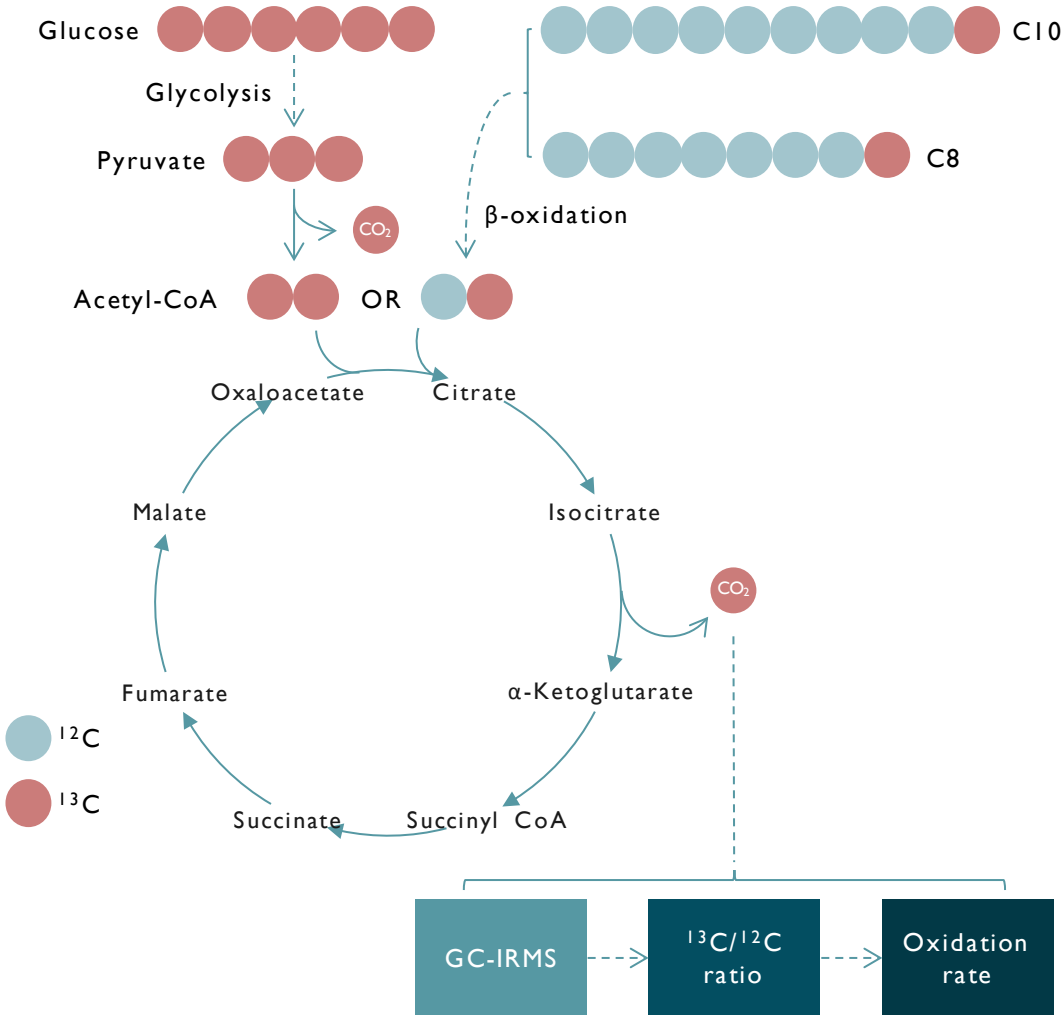

FIGURE 4.1 Determining the oxidation rates of glucose, C8 and C10 using ^{13}C-labelled compounds. Labelled glucose and C8/C10 are broken down by glycolysis/pyruvate dehydrogenase activity and β-oxidation, respectively, to form ^{13}C-labelled acetyl CoA. The ^{13}C-acetyl CoA then feeds into the TCA cycle where it is further utilised in the formation of TCA cycle substrates. This results in the production of $^{13}CO_2$, which dissolves into culture medium and is later released for GC-IRMS analysis.

4.2 METHODS

4.2.1 Materials

Stable isotope-labelled compounds, [U-^{13}C]glucose, [1-^{13}C]decanoic acid ([1-^{13}C]C10) and [1-^{13}C]octanoic acid ([1-^{13}C]C8) were purchased from Cambridge Isotopes Laboratories, Inc. via CK Isotopes (Ibstock, UK). [U-^{13}C]palmitic acid ([U-^{13}C]C16) was purchased from Larodan (Malmö, Sweden) and used as a 5:1 complex (molar ratio) with fatty acid-free bovine serum albumin. All other reagents were purchased as described in Section 2.1.

4.2.2 Experimental DMEM Preparation

All experimental procedures were carried out with the use of a specifically formulated glucose-free DMEM medium, containing a final concentration of 15mM HEPES, 2.9mM sodium bicarbonate, 2mM L-glutamine, 0.5mM sodium pyruvate and 21.5µM phenol red. The experimental DMEM was adjusted to a pH of 7.4 and then sterile-filtered before storage at 4°C for up to three months.

4.2.3 Stable Isotope-labelled Reagent Preparation

A stock solution of 134.3mM [U-^{13}C]glucose was prepared by dissolving with experimental DMEM medium and then frozen in aliquots at -20°C. To determine the β-oxidation rates of C8 and C10, stock solutions of 50mM [1-^{13}C]C10 and 50mM [1-^{13}C]C8 were prepared in DMSO, sterile-filtered and then stored in aliquots at -20°C for up to one month. For the C8 and C10 co-incubation treatments, additional stock solutions of 25mM C8 and 100mM [1-^{13}C]C10 were also prepared and stored in the same manner.

4.2.4 Cell Culture

SH-SY5Y cells were cultured as outlined in Section 2.2, and seeded at a density of $1x10^4$ cells/cm^2 in 6-well plates. Fresh complete growth medium was made up to a final volume of 2ml per well and cells were cultured for 5 days prior to all experiments. Medium was refreshed every two days and the same starting number of cells was used for each investigation.

4.2.5 Stable Isotope-labelled Glucose, C8 and C10 Treatment

On day 5 of culture, complete growth medium was removed and cells washed once with DPBS. Cells were then incubated with 2ml of experimental DMEM medium, supplemented with 10% FBS and 3mM D-glucose, for 20h at 37°C and 5% CO_2. After 20h, the medium was removed and cells washed once with DPBS. To each well, 3ml of DMEM was then added containing either 3mM [U-^{13}C]-glucose and vehicle control DMSO, 3mM unlabelled D-glucose and 250µM [1-^{13}C]C10 or 3mM unlabelled D-glucose and 250µM [1-^{13}C]C8. The amount of vehicle control DMSO and stable isotope-labelled fatty acids added was kept at the same total volume throughout. Wells were then sealed with a 3ml layer of heavy mineral oil in order to prevent the loss of $^{13}CO_2$ through gas exchange between the medium and the atmosphere (Will et al., 2006). This approach also prevented crossover of $^{13}CO_2$ between wells. Trapped $^{13}CO_2$ may potentially affect the pH of medium, although visible changes in medium pH over the course of the experiment were not observed with the phenol red indicator. Cells were incubated at 37°C for 6 hours, with 100µl of medium sampled from each well at hourly intervals. Sampled medium was immediately stored in rubber-sealed Exetainer™ vials (Labco Ltd, Ceredigion, UK) and kept at -20°C until analysis.

4.2.6 C10 and C8 Co-treatment

The effect of co-treating C10 and C8 in an 80:20 ratio on C10 β-oxidation in SH-SY5Y cells was also explored, paralleling the MCT content in C10-enriched Betashot. Cells were cultured and incubated for 20h prior to the experiment as previously described. After washing the cells, medium was then replaced with 3ml experimental DMEM containing either 3mM [U-^{13}C]glucose and vehicle control DMSO, or 3mM unlabelled D-glucose with either a final concentration of 250μM [1-^{13}C]C10, or 250μM [1-^{13}C]C10 plus 62.5μM C8, added at a fixed total volume. Wells were then sealed with heavy mineral oil, cells incubated and medium sampled as previously outlined.

4.2.7 Preparation of [U-^{13}C]-Palmitic Acid

[U-^{13}C]palmitic acid was neutralised with 0.35M NaOH and made to a concentration of 17.5mM in water, before heating to 70°C until fully dissolved. Fatty acid-free bovine serum albumin (BSA) was then dissolved to a concentration of 3.5mM in water at 37°C. Swirling gently, [U-^{13}C]-palmitate ([U-^{13}C]-C16) was then slowly added 1:1 to BSA at 37°C, forming an 8.75mM [U-^{13}C]C16:BSA complex (5:1 molar ratio fatty acid:BSA). An additional stock solution of 1.75mM BSA in water was also prepared. Both solutions were aliquoted and stored at -20°C until further use.

4.2.8 CPT1 Inhibitor Viability Assay

CPT1 inhibition in SH-SY5Y cells was achieved using the inhibitor etomoxir. A stock solution of 50mM etomoxir was prepared in sterile cell culture grade water and stored in aliquots at -20°C. Cells were cultured as described above and medium replaced on day 5 with experimental DMEM containing 3mM D-glucose and 10% FBS, with or without 50μM etomoxir. Cells were incubated for 20h at 37°C and 5% CO_2, and then for a further 6h at 37°C with 50μM etomoxir in experimental DMEM medium with

3mM D-glucose and without FBS. At the end of incubation, medium was removed and cells lifted with 1ml 0.25% trypsin-EDTA, suspended in 4ml culture medium and centrifuged for 4 minutes at 500xg. After pelleting, the supernatant was discarded and cells were suspended in 1ml of fresh culture medium. Viability of cells was then assessed using Trypan Blue exclusion (Section 2.2.2).

4.2.9 CPT1 Inhibition Assay

Cells were cultured as previously described. On day 5 of culture, complete growth medium was replaced with 2ml experimental DMEM medium containing 3mM D-glucose and 10% FBS. Cells were incubated with or without the presence of 50μM etomoxir for 20h at 37°C and 5% CO_2. Medium was then removed and replaced with 3ml DMEM, containing 3mM [U-^{13}C]glucose and vehicle control DMSO or 3mM D-glucose with either 250μM [1-^{13}C]C10, [1-^{13}C]C8 or [U-^{13}C]C16, with 50μM etomoxir also added back to pre-treated cells. Wells were then sealed with heavy mineral oil, with the cells incubated and the medium sampled as previously described.

4.2.10 Measurement of $^{13}CO_2$ Release

Samples were thawed at room temperature and 100μl 1M hydrochloric acid was injected through the rubber septum into each Exetainer vial to release CO_2 from the medium. Vials were centrifuged for 30 seconds at 500xg to collect the acid and medium to the bottom of the vial and ensure thorough mixing. Samples were then analysed on a GasBench II coupled to a Thermo Delta-XP isotope-ratio mass spectrometer (Thermo-Finnigan, Bremen, Germany). Helium was used to flush sample vials and ten repeat injections with a 50μl loop were carried out per sample, with $^{13}CO_2/^{12}CO_2$ ratios measured against international standard Vienna Pee Dee Belemnite (VPDB) using a calibrated CO_2 reference gas. Following this, $^{13}CO_2/^{12}CO_2$ ratios were then converted

to mole percent excess using absolute molar ratio of ^{13}C to ^{12}C (0.0111796) in VPDB. The change in mole percent excess was then converted to pmol CO_2 generated using the volume of medium and concentration of bicarbonate (2.9mM) present, which was then corrected for the number of labelled carbon atoms (1 for C8 and C10, 6 for glucose and 16 for palmitate) to obtain pmol substrate oxidised. The following example further explains this:

For [U-^{13}C]glucose:

+2063 ‰ vs. VPDB is equivalent to 3.3% enriched, or an excess enrichment of 2.22%. As the concentration of bicarbonate was 2.9mM in a volume of 3ml, the total $^{13}CO_2$ generated was:

$$(2.9 \times 3) \times (2.22 / 100) = 0.193 \text{ micromoles} = 193 \text{ nmoles } ^{13}CO_2$$

As each glucose has 6 labelled carbons, 6nmol $^{13}CO_2 \equiv$ 1nmol [U-^{13}C]glucose

$$193 \text{ nmoles } ^{13}CO_2 \equiv 193/6 = 32.2 \text{ nmol glucose}$$

This was in 6 hours, so the rate of glucose oxidation = 32.2 / 6 = 5.4nmol/hour, or 5400pmol/hour.

4.2.11 Statistical Analysis

Statistical analysis was performed as described in Section 2.8.

4.3 RESULTS

4.3.1 Oxidation rates of Glucose, C8 and C10 in SH-SY5Y cells

^{13}C-labelled compounds permit the measurement of cellular oxidation rates of glucose, C8 and C10 via CO_2, the release of which emanates from pyruvate dehydrogenase

activity and the TCA cycle following glucose oxidation, and the TCA cycle following C8/C10 β-oxidation. $^{13}CO_2$ release over 6 hours was used to determine and quantify the rate of cellular oxidation of each compound, with the number of ^{13}C labels in each molecule accounted for during calculations. Cells were treated with 3mM ^{13}C-labelled glucose to replicate physiological levels observed in patients under the MCT KD, with unlabelled 3mM glucose used in the presence of ^{13}C-labelled C10 and C8. ^{13}C-labelled C10 and C8 were added separately to a final concentration of 250μM, reflecting the concentration of C10 used throughout this thesis and previously determined for optimum effects upon mitochondria and antioxidant status (Hughes et al., 2014). Furthermore, this also replicates the brain concentration achieved in mice following peripheral C10 administration (Wlaź et al., 2012, 2015). For each molecule studied, $^{13}CO_2$ release was linear for the 6-hour incubation. As expected, the rate of glucose oxidation was markedly faster than that of either C8 or C10 (Figure 4.2). However, C8 and C10 were found to be differentially oxidised in these cells, with C10 β-oxidation significantly lower than that of C8, by approximately 80%. This suggests that C8 may be preferentially oxidised in SH-SY5Y cells. The oxygen consumption of glucose, C8 and C10 oxidation relative to the data above was also determined, and calculated assuming a stoichiometry of 6 moles O_2 to 1 mole glucose ($C_6H_{12}O_6 + 6O_2 \rightarrow 6\ CO_2 + 6H_2O$), 11 moles O_2 to 1 mole C8 ($C_8H_{16}O_2 + 11O_2 \rightarrow 8CO_2 + 8H_2O$) and 14 moles O_2 to 1 mole C10 ($C_{10}H_{20}O_2 + 14O_2 \rightarrow 10CO_2 + 10H_2O$). Glucose oxidation was estimated to consume 28.2±1.8 nmol O_2/h, whilst C8 consumed 13.5±0.9 nmol/h and C10 only 3.5±0.3 nmol/h, further indicating the preferential oxidation of C8 to C10. Furthermore, despite the low absolute oxidation rate of C8 compared to glucose (75% lower cf. glucose), the oxygen consumption of C8 oxidation also appeared to be almost half that of glucose.

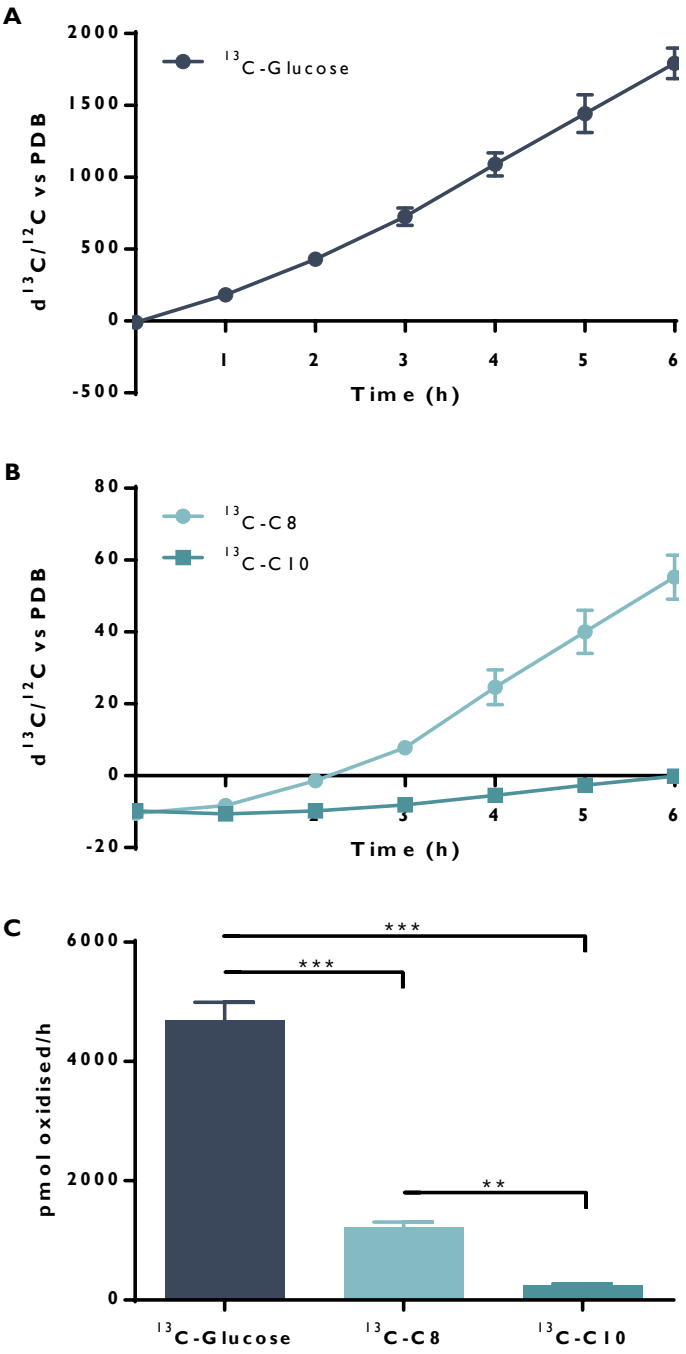

FIGURE 4.2 Absolute oxidation rates of ^{13}C-labelled 3mM glucose, 250µM C8 and 250µM C10 in SH-SY5Y cells per hour. A, B) Time course of $^{13}CO_2/^{12}CO_2$ release over 6h for each ^{13}C-labelled molecule. C)The oxidation rate of [1-^{13}C]C10 was found to be significantly lower than that of [U-^{13}C]glucose (***p<0.001) and [1-^{13}C]C8 (**p<0.01), with [U-^{13}C]glucose oxidised at 4693±301 pmol/h, [1-^{13}C]C8 at 1225±85 pmol/h and [1-^{13}C]C10 at 249±23 pmol/h. Data are expressed as mean ± SEM of 5 independent experiments (n=5), each performed in 4 replicate wells.

4.3.2 Effect of co-treatment of C8 and C10 on β-oxidation

Current MCT KD preparations are composed of a mixture of C8 and C10 at varying ratios. In light of this, we examined the effects on [1-^{13}C]C10 β-oxidation when SH-SY5Y cells were treated with 62.5μM unlabelled C8, reflecting a move towards a more C10-enriched formula, such as in Betashot, providing a C10 to C8 ratio of 80:20. Despite the relatively low concentration, C8 addition was found to significantly impair the β-oxidation rate of C10 by 29% (Figure 4.3).

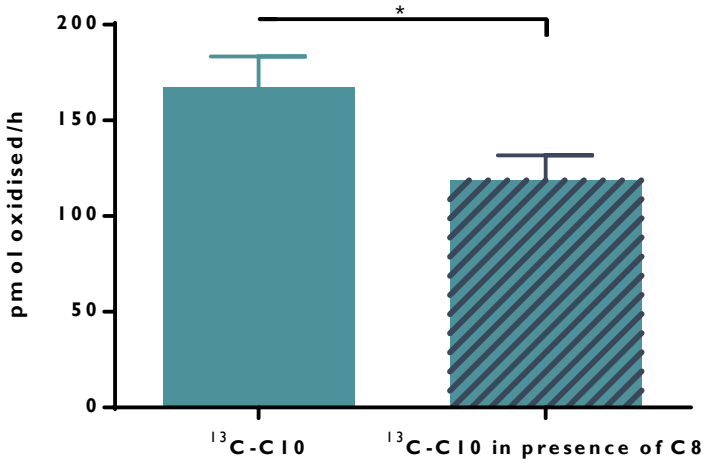

FIGURE 4.3 Effect of C8 co-incubation on β-oxidation of C10 in SH-SY5Y cells. The β-oxidation rate of 250μM [1-^{13}C]C10 (167±16 pmol/h) was significantly reduced (*p<0.05) in the presence of 62.5μM unlabelled C8 (119±13 pmol/h). Data are expressed as mean ± SEM of 4 independent experiments (n=4), each performed in 4 replicate wells.

4.3.3 C10 β-oxidation following CPT1 inhibition

To determine the mechanisms behind the differential β-oxidation of C8 and C10, the potential role of the carnitine shuttle was explored. Whilst long chain fatty acids require this system, medium chain fatty acids are generally considered to be able to enter the mitochondrial matrix in a carnitine-independent manner (Papamandjaris,

MacDougall, & Jones, 1998). Whilst this may be the case for C8, there are reports to suggest that C10, in contrast to C8, may require the carnitine system for complete mitochondrial β-oxidation (Parini et al., 1999). Carnitine palmitoyltransferase I (CPT1) is responsible for transferring fatty acyl groups to carnitine and is the rate-limiting step in carnitine-dependent β-oxidation in mitochondria (Eaton, 2002; McGarry & Brown, 1997; Wolfgang et al., 2006). To evaluate the potential role of CPT1 in C8 and C10 β-oxidation, the well-characterised CPT1 irreversible inhibitor etomoxir was used (Ratheiser et al., 1991; Selby & Sherratt, 1989; Spurway et al., 1997). Through dose-response experiments, [U-^{13}C]palmitic (C16) acid, which is well-known to depend on CPT1 for mitochondrial β-oxidation, was used as a positive control to determine the maximal concentration of etomoxir that could be used to inhibit CPT1 without affecting cell viability (concentrations of 100μM etomoxir and above caused cell death). With the conditions employed, β-oxidation of [U-^{13}C]C16 was reduced by 99%, suggesting complete irreversible inhibition of CPT1 (Table 4.1). Moreover, at the concentration used, etomoxir was observed to have no effect on viability of the SH-SY5Y cells used (control cells % viability = 97.5±0.5%; etomoxir-treated cells % viability = 97.5±0.4%). Under the same conditions, C10 β-oxidation was found to be reduced by 95% in the presence of etomoxir (Table 4.1), whereas C8 β-oxidation was only inhibited by 34%.

TABLE 4.1 Effects of CPT1 inhibition on the β-oxidation rates of C8, C10 and C16 in SH-SY5Y cells.

	Oxidation rate (pmol/h)	
Compound	**- Etomoxir**	**+ Etomoxir**
[1-^{13}C]C8	1139 ± 106	750 ± 63**
[1-^{13}C]C10	198 ± 24	10 ± 9***
[U-^{13}C]C16	224 ± 43	2 ± 2***

Cells were pre-treated for 20h with the irreversible CPT1 inhibitor etomoxir (50μM) and then incubated for 6h with ^{13}C-labelled 250μM C8, C10, or C16:BSA in the presence of 50μM etomoxir. Control cells were processed identically but were pre-treated and incubated in the absence of etomoxir. CPT1 inhibition resulted in a significant reduction (***p<0.001 compared with untreated control cells) in C10 β-oxidation by 95%. The β-oxidation rate of C8 was also significantly reduced by 34% (**p<0.01 compared to untreated control cells). Results are expressed as mean ± SEM of 5 independent experiments (n=5), each performed in duplicate. CPT1 inhibition was confirmed with a significant 99% inhibition of [U-^{13}C]C16 oxidation (***p<0.001 compared to untreated control cells). Results are expressed as mean ± SEM of 3 independent experiments (n=3), each performed in duplicate.

4.4 DISCUSSION

There is growing interest in the mode of action of the MCT KD, particularly in regard to the effects of the medium-chain fatty acid, C10. In contrast to C8, C10 appears to have a number of biological targets that can explain the anti-seizure properties of the diet. However, for C10 to exert its beneficial effects, attaining a sufficiently high concentration within the brain is essential. Existing data suggest that concentrations of up to 250μM C10 are required to facilitate an increase in mitochondrial biogenesis, increased antioxidant capacity and AMPA receptor inhibition (Chang et al., 2016; Hughes et al., 2014; Kanabus et al., 2016). Achieving such a concentration, however, appears to be feasible, as oral administration of C10 in mice leads to mean brain

concentrations of 240μM (Wlaź et al., 2015). The brain:plasma ratios of C10 in mice appear to range from 0.59-0.76, with C8 ranging at 0.41-0.62 (Wlaź et al., 2012, 2015), indicating that both MCFAs have sufficient access to the blood brain barrier for therapeutic compounds (Kulkarni et al., 2016). Therapeutic compounds with a brain:plasma ratio of 0.3-0.5 are thought to have sufficient penetration of the blood brain barrier, whilst compounds with ratios greater than 1.0 can freely cross it. The reported brain:plasma ratios of C10 and C8 corroborate with evidence that suggests MCFAs are able to cross the blood brain barrier via probenecid-sensitive transport system (Spector, 1988), which may control the level of entry of these fatty acids into the brain.

Medium-chain fatty acids are metabolised by β-oxidation resulting in acetyl CoA formation, which can be further metabolised to generate ketones and/or enter the TCA cycle. Since medium-chain fatty acids are able to cross the blood brain barrier (Olendorf, 1971, 1973; Spector, 1988) and the enzymes of β-oxidation are reported to be present in neuronal cells (Reichmann, Maltese, & DeVivo, 1988; Yang, He, & Schulz, 1987), the ability of neuronal-like SH-SY5Y cells to β-oxidise C8 and C10 was evaluated. In light of the accumulation of C10 reported in mouse brain, it was hypothesised that C10 would be relatively spared in neuronal cells.

Utilising ^{13}C-labelled substrates allowed for the precise quantification and comparison of substrate metabolism, by capturing and quantifying the labelled CO_2 released by the cells. Here, [1-^{13}C]C8 and [1-^{13}C]C10 were used, compared with [U-^{13}C]palmitic acid and [U-^{13}C]glucose. Although this could result in potential errors in comparison between the substrates in the case of incomplete oxidation, in non-ketogenic cell types such as neuronal-like cells, oxidation of MCFAs is thought to proceed completely to

acetyl-CoA, and thence oxidation in the TCA cycle, with no significant release of chain-shortened fatty acyl moieties. Thus, release of ^{13}C in the first turn of β-oxidation usually represents complete oxidation of the molecule. If any incomplete oxidation did occur, then the relative rates of C8 and C10 oxidation would be even lower than those observed in this study compared with glucose. Using this approach, glucose metabolism was considerably greater than that of C8 or C10. This was expected, given that it is well established that glucose is the main fuel for neuronal energy metabolism (Dienel & Hertz, 2001; Hall et al., 2012; Lundgaard et al., 2015; Mergenthaler et al., 2013). Whilst showing lower rates of oxidation than glucose, both C8 and C10 were β-oxidised to some extent by the cells. Despite the lower absolute oxidation rate of C8 compared to glucose, the oxygen consumption due to C8 oxidation (~50% of that due to glucose) suggests that C8 may be a significant substrate for ATP generation in these cells. However, it was observed that C10 β-oxidation was markedly lower than that of C8, with relative oxygen consumption also substantially low, suggesting that these two fatty acids are processed differently by SH-SY5Y cells. To ascertain the potential cause for this difference, the involvement of the carnitine shuttle was considered, as C10 is reported to utilise this system for maximal β-oxidation to occur (Parini et al., 1999). Furthermore, C10 oxidation is impaired in inherited disorders of carnitine metabolism (Chalmers et al., 1997). This reliance of C10 upon the carnitine shuttle was further supported by the finding here that CPT1 inhibition, by etomoxir, markedly impaired C10 β-oxidation, whereas C8 β-oxidation appeared mainly CPT1-independent. Whilst etomoxir is a well-characterised CPT1 inhibitor, as reflected by its ability to almost completely abolish C16 β-oxidation, it should be noted that it may have other targets, e.g. by acting as a PPARα agonist, which regulates expression of genes involved in β-oxidation. Relatively prolonged exposure (5 days) has been suggested to lead to up-regulation of fatty acid oxidation (Portilla et al., 2000). However, in the data presented

within this chapter, the converse was apparent, in keeping with CPT1 inhibition. The finding that CPT1 inhibition markedly impaired C10 β-oxidation, whilst C8 β-oxidation was mainly CPT1-independent, suggests that this system in neuronal type cells is essential for maximal catabolism of C10 to occur.

To further explore the potential common metabolic fates of C8 and C10 and the role this may play in the MCT KD, the effect of the presence of C8 on C10 β-oxidation was also investigated. Whilst the composition of MCT oil varies greatly from product to product, an 80:20 ratio of C10 to C8 was selected to underscore a move towards a more C10-enriched formula, whilst also reflecting the content of recently developed MCT product, Betashot. Even in the presence of a relatively low concentration of C8, C10 β-oxidation was significantly inhibited. This observation may suggest that in the MCT KD, the presence of C8 has a sparing effect to further limit the metabolism of C10, thus facilitating its accumulation in the brain and the manifestation of its anti-seizure effects. However, it is possible that other mechanisms could also contribute to the differential metabolism of C8 and C10, such as varying degrees of cellular uptake for the two fatty acids. Further studies, involving cellular fractionation following C8 and/or C10 exposure may therefore be informative. Nonetheless, this finding still demonstrates the potentially promising effects of shifting MCT formulations towards containing higher levels of C10, without foregoing the presence of C8.

To summarise, the data presented here suggest that in a neuronal cell line, C10 and C8 are differentially oxidised. Thus, C8 may be preferentially metabolised and provide energy, whereas, because of its requirement of the carnitine shuttle, C10 is metabolised at a lower rate and can consequently accumulate (Figure 4.4). CPT1 activity in brain is low, and although there is a brain-specific isoform of CPT1 (CPT1c), this isoform has

not been found to demonstrate any enzymatic activity (Dai et al., 2007; Lee & Wolfgang, 2012; Price et al., 2002; Wolfgang et al., 2006, 2008). This hypothesis is further supported by the recent observation that reports, in astrocytes, that C8 is ketogenic whilst C10 is not (Thevenet et al., 2016).

In conclusion, the fatty acid components of the MCT KD are differentially oxidised by neuronal-like cells. The carnitine dependence and sluggish metabolism of C10 provides an explanation for how critical concentrations may occur and permit interaction with key anti-seizure targets. In contrast, C8 may be preferentially metabolised and have two key effects: sparing of C10 by inhibiting C10 β-oxidation and acting as a fuel source for brain energy metabolism.

Whilst this study provides further mechanistic insight into the MCT KD, relevance to understanding the classical KD is not immediately clear. However, the possibility exists that progressive (mitochondrial/peroxisomal) oxidation of the long-chain fatty acid components may occur, leading to C10 formation and eventual neuronal C10 accumulation. Further work is clearly needed to test this hypothesis. Additional alternative mechanisms could also be responsible for efficacy of the classical KD.

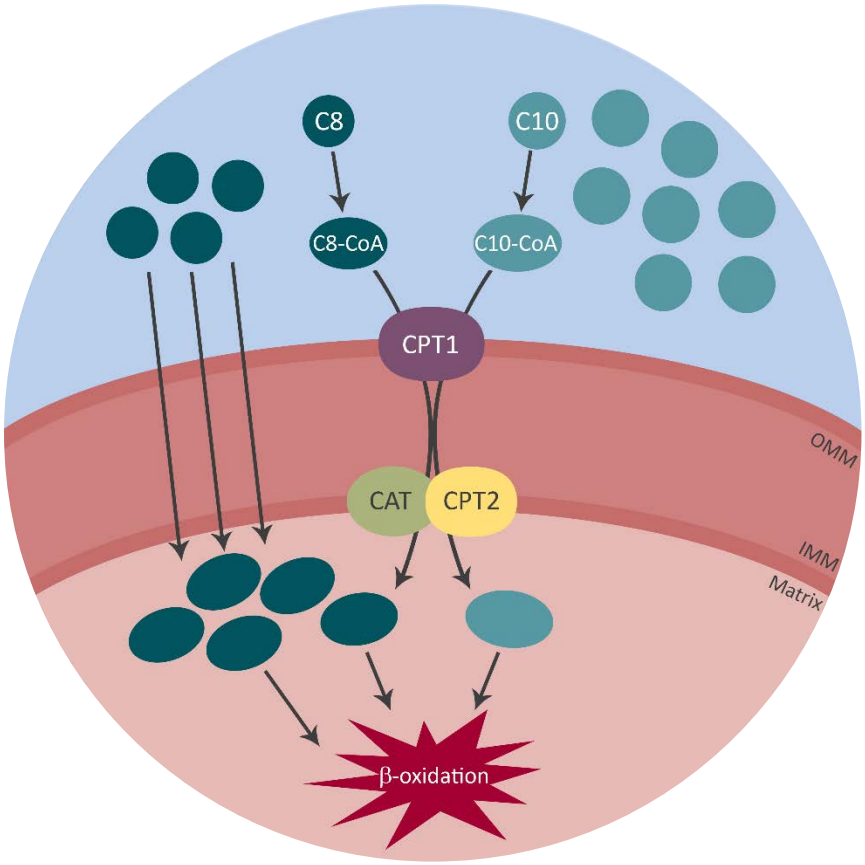

FIGURE 4.4 CPT1-dependent oxidation of C10 may lead to accumulation within the brain. C10 and C8 have differential effects with regard to potential seizure control, e.g. C10 acting as a PPARγ agonist, eliciting improvement in mitochondrial function. For this to occur, a sufficient neuronal concentration of C10 is required. It is proposed that due to its reliance on the carnitine shuttle, β-oxidation of C10 is relatively slow, permitting accumulation of this fatty acid. In contrast, C8 oxidation may proceed in the absence of the carnitine system, contributing to β-oxidation and cellular energy metabolism. In addition, C8 may inhibit any C10 β-oxidation, further contributing to its accumulation. ((C8 acyl-coenzyme A (C8-CoA); C10 acyl-coenzyme A (C10-CoA); carnitine palmitoyltransferase I (CPT1); carnitine-acylcarnitine translocase (CAT); carnitine palmitoyltransferase II (CPT2); outer mitochondrial membrane (OMM); inner mitochondrial membrane (IMM)).

CHAPTER 5

Development of a GC-MS method for quantitative analysis of medium-chain fatty acids in plasma

5.1 BACKGROUND

Using a gas chromatography-based method of analysis, Haidukewych et al. (1982) reported measurable levels of C8 and C10 in the plasma of patients receiving the MCT KD (30-861μM and 23-553μM respectively). With elevated plasma levels of C8 and C10 found in these patients, an additional study was carried out with a cohort of 15 paediatric patients, scrutinising the potential role of the two fatty acids in seizure control, with C8 and C10 serum levels correlated against control of seizures (Sills, Forsythe & Haidukewych, 1986). However, no clear association between serum fatty acid concentration and effect on seizures was established. Since then, little more has been done to investigate any relationship between C8 and C10 blood levels and seizure control. Determining any associations would not only be substantial in providing further insight into the MCT KD, but may also provide a marker of patient compliance to the diet. Moreover, monitoring plasma fatty acid levels is a crucial requirement of the ongoing feasibility study investigating the effects of a C10-enriched MCT formulation, Betashot, in epilepsy patients (see Chapter 6). Therefore, developing a method for the quantitative analysis of C8 and C10 levels in patient plasma is necessary.

For this purpose, gas chromatography mass spectrometry (GC-MS) was selected as the method of choice. A highly sensitive technique, GC-MS can be used to quantify compounds of interest to a strong degree of accuracy. It combines the separation process of gas chromatography with the sensitivity and specificity of mass spectrometry, permitting the identification and quantification of compounds within a mixture.

Analysis through GC-MS can be broken down into several processes (Figure 5.1). Upon injection into the gas chromatograph, samples are vaporised, carried through a capillary column via an inert gas such as helium, and separated per the chemical properties of the compounds. The vaporised compounds are then introduced into the mass spectrometer, where they are fragmented into ions within an ion source and separated by a quadrupole mass analyser, which filters ions according to their mass-to-charge ratios (m/z), before finally reaching the detector (McMaster, 2008). The detector visualises the generated signals into mass spectra which can then be used to identify and quantify compounds in conjunction with their corresponding chromatograms. This characteristic of GC-MS also provides the ability to resolve isotopes, allowing for precise quantification of target compounds by utilising their stable isotope-labelled analogues. Further sensitivity can also be achieved through use of Selected Ion Monitoring (SIM) mode, a feature that enables the GC-MS to detect specific analytes of interest by their m/z. Unlike full scan mode, this focuses detection to specific ions whilst unwanted ions are excluded, allowing a greater proportion of analysis time to be utilised in the detection of ions of interest rather than m/z ratios that are uninformative. As a result, background noise and artefacts are eliminated. This enhanced selectivity and sensitivity makes GC-MS a suitable tool for the detection of low quantities of compounds.

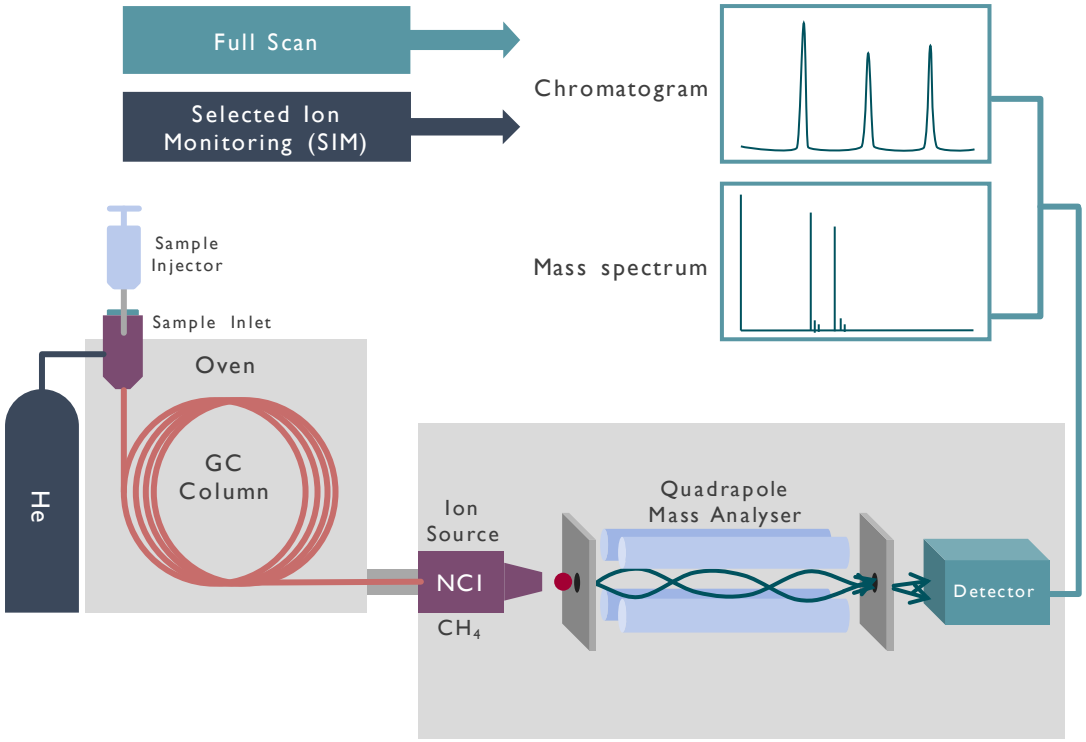

FIGURE 5.1 Schematic layout of GC-MS components and output.

However, the nature of GC-MS analysis necessitates the prior preparation of compounds depending on their chemistry. Free fatty acids are highly polar in nature due to the reactivity of the active hydrogen in the carboxyl group. This causes adsorption of fatty acids to GC columns resulting in poor separation. To prevent this, the functional groups of fatty acids can be chemically derivatized prior to analysis, for example, via esterification, alkylation or silylation (Orata, 2012). This not only improves GC separation, but can also enhance the thermal stability and volatility of the compounds. Traditionally, free fatty acids are esterified into fatty acid methyl esters (FAMEs) with methanol, and then analysed via electron impact ionisation. The active hydrogen of the carboxyl group is replaced with a methyl group, reducing the polarity of the compound and thereby improving separation. Electron impact (EI) ionisation is an energetic ionisation method where an electron beam from a heated metal filament collides with the vaporised analyte and removes an electron to form positively charged

ions. Excess energy from the ionisation technique also results in extensive fragmentation of the analyte, producing daughter ions that can be used to provide structural information of unknown compounds. However, extensive fragmentation can hinder the identification of target compounds, particularly in the case of FAMEs.

Chemical ionisation (CI) can be utilised as an alternative method to analyse free fatty acids. A "soft" ionisation technique, CI relies on a reagent gas, such as methane, to ionise vaporised analytes under high pressure conditions (Kellogg, 2017). The reagent gas, present in high abundance, is first subjected to EI, producing ionised reagent gas plasma. Subsequent collisions between the high-energy reagent gas plasma and the analyte result in the formation of quasimolecular ions, $[M+H]^+$ and $[M-H]^-$, usually through proton transfer or abstraction. Both positive and negative ions are produced simultaneously in CI, and depending on the compound of interest and instrument setup, either positive or negative ions can be selected for detection. Unlike EI ionisation, CI is less harsh, with ionisation occurring at lower energy than in EI, resulting in fewer fragments and yielding quasimolecular ions that can often be detected. Moreover, negative chemical ionisation (NCI) is highly sensitive and selective for compounds with positive electron affinity, producing mass spectra with reduced noise and allowing for analysis with lower detection limits. This is due to the fact that although most compounds can be protonated to produce positive ions, only a few can produce negative ions, thus increasing sensitivity.

Fatty acids can be derivatized for detection with NCI through alkylation, where the active hydrogen is replaced with an alkyl group. Pentafluorobenzyl bromide (PFBBr), an alkylation reagent used to modify carboxylic acids, can be used to achieve this (Orata, 2012). Free fatty acids are derivatized with PFBBr in the presence of

triethylamine, a neutralisation reagent that ensures basic conditions for the reaction to occur. The labile hydrogen is substituted with a pentafluorobenzyl (PFB) group and hydrogen bromide is released as a by-product. The addition of the PFB group reduces the polarity of the fatty acid, and enhances its volatility and thermostability, allowing sufficient analysis by GC-MS. During NCI, this PFB-fatty acid derivative is fragmented into a negatively charged fatty acid quasimolecular ion, $[M-H]^-$, which can then be detected for quantification.

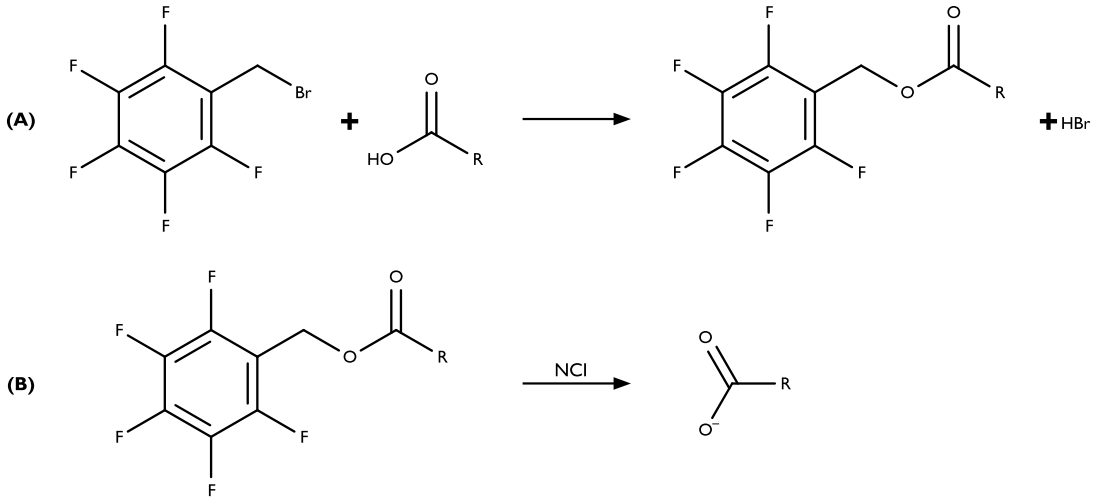

EQUATION 5.1 Pentafluorobenzyl bromide (PFBBr) derivatization of fatty acid carboxyl groups (A) and subsequent fragmentation of fatty acid-PFB derivative during NCI analysis (B). Upon fragmentation, a negatively charged fatty acid ion is produced, which is then detected by the mass spectrometer.

This approach may provide an improved means of accurately measuring medium-chain fatty acids in the plasma of patients on the MCT KD. In this chapter, a GC-MS method for the quantification of octanoic (C8), decanoic (C10) and dodecanoic (C12) acids in patient plasma is outlined, with C12 included to account for its trace presence in mainstream MCT formulations, as well as potential chain elongation of C8 and C10.

Stable isotope-labelled analogues of each fatty acid were utilised as internal standards, with samples analysed following PFBBr derivatization, in conjunction with NCI and SIM, as described above. The accuracy, reliability and reproducibility of this method is investigated and a preliminary reference range for medium-chain fatty acid levels in control patient samples established.

5.2 METHODS

5.2.1 Materials

Stable isotope-labelled internal standard compounds octanoic-d_{15} acid, decanoic-d_5 acid and dodecanoic-d_{23} acid were purchased from QMX Laboratories (Thaxted, UK). Analytical grade ethyl acetate, acetonitrile and triethylamine were purchased from Fisher Scientific (Loughborough, UK). All other reagents were purchased as specified in Section 2.1.

5.2.2 Fatty Acid Standard and Internal Standard Preparation

Deuterated stable isotope-labelled compounds were used as internal standards: octanoic-d_{15} acid (C8-d_{15}), decanoic-d_5 acid (C10-d_5) and dodecanoic-d_{23} acid (C12-d_{23}). Internal standards were prepared as 10mM stock solutions in ethanol. Stock solutions were then further diluted to 1mM and an internal standard working solution was prepared by mixing each internal standard in a 1:1:1 ratio, giving a final concentration of 0.33mM each. Fatty acid standards of octanoic acid (C8), decanoic acid (C10), dodecanoic acid (C12) were also prepared as 10mM stock solutions in ethanol. A fatty acid standard mix was then prepared in ethanol to give a final concentration of 1mM of each fatty acid standard. The internal standard working solution and the fatty acid standard mix were then aliquoted and stored at 4°C for up to 3 months until further use.

5.2.3 Standard Curves

Standard curves for each free fatty acid standard were set up over a range of 0-500μM and always run prior to each batch of samples to limit potential variability in processing and analysis. Using the 1mM fatty acid standard mix, the fatty acids were prepared in ethanol to set up a standard curve, with final concentrations ranging from 25-500μM. To set up a lower range standard curve, a 100μM fatty acid standard mix was prepared by diluting the 1mM standard mix in ethanol. This 100μM fatty acid standard mix was then used to prepare fatty acids in ethanol within a final concentration range of 0-10μM. In stoppered glass tubes, 100μl of the prepared fatty acid standards within the concentration range above were added to 100μl ethanol. To each tube, 30μl of internal standard working solution was then added and the final mixture gently dried down under nitrogen gas at room temperature.

5.2.4 Plasma Fatty Acid Extraction

For the development of this method, anonymised patient samples of lithium-heparin plasma were obtained from Chemical Pathology, Great Ormond Street Hospital for Children. Plasma samples were stored at -80°C until analysis, upon which they were thawed at 37°C and kept on ice. In glass stoppered tubes, 100μl plasma was added to 400μl Milli-Q water and 30μl of the internal standard working solution. Samples were acidified with 125μl 6M HCl, vortexed thoroughly and then extracted with 3ml ethyl acetate with a vortex mixer. The samples were centrifuged for 5 minutes at 1500xg and the upper ethyl acetate layer decanted into fresh glass tubes. The samples were then re-extracted with 3ml ethyl acetate, vortexed and centrifuged once more. The upper ethyl acetate layer was decanted and then combined with the previous. The combined extracted layers were dried with a spatula of anhydrous sodium sulphate, vortexed and

left to sit at room temperature for 5 minutes. The dried samples were then transferred to fresh glass tubes and gently dried down under nitrogen gas at room temperature.

5.2.5 Plasma Recovery of C8, C10 and C12

Plasma samples were spiked with 1mM free fatty acid standard mix containing C8, C10 and C12 at final concentrations of 25µM, 100µM and 200µM. To 100µl plasma, 100µl of 1mM free fatty acid standard mix, 300µl distilled water and 30µl of internal standard working solution were added. Samples were then extracted, processed and dried as previously described. Plasma samples without the addition of fatty acid standards were also processed and analysed alongside the spiked samples to control for the endogenous presence of the free fatty acids.

5.2.6 Derivatization

To derivatize the fatty acids, 2,3,4,5,6-pentafluorobenzyl bromide (PFBBr) was used. PFBBr was prepared as a 10% (v/v) solution in acetonitrile. To tubes of dried down standard curve or plasma samples, 50µl of 10% PFBBr solution was added, followed by 10µl triethylamine (TEA). Tubes were then vortexed and incubated for 15 minutes at room temperature. Samples were then gently dried down under nitrogen gas at room temperature. After drying, samples were redissolved in 100µl ethyl acetate, vortexed and transferred to glass GC autosampler insert vials for analysis.

5.2.7 GC-MS Analysis

All GC-MS analyses were carried out in a Thermo Scientific Trace GC Ultra chromatograph coupled to a Thermo Scientific DSQ II mass spectrometer. After preparation, 2µl of sample was introduced via a split injector (split 100:1, split flow 80ml/min) at 280°C and separated within an Rxi®-5Sil MS fused silica (5%

diphenyl/95% dimethylpolysiloxane) capillary column (30m x 0.25mmID, film thickness 0.25µm) (Thames Restek UK, High Wycombe, UK). Initial oven temperature began at 110°C and was ramped up to 220°C, 10°C per minute, immediately followed by an additional ramp up to 300°C at a rate of 30°C per minute, before ending at a total run time of 13.5 minutes. Helium carrier gas was set at a constant flow rate of 0.8ml/min. The column connected directly to the ion source, at a temperature of 225°C, whilst the MS transfer line was set to 250°C. Samples were ionised through negative chemical ionisation, using methane as the reagent gas, set to a flow rate of 2.0ml/min. Compounds were detected in Selected Ion Monitoring (SIM) mode (Table 5.1) and peak areas were determined using the Thermo Scientific Xcalibur software. Injections were carried out in duplicate for all samples prior to final quantification.

TABLE 5.1 Ions selected for detection in SIM mode during data collection.

Compound	m/z
C8	142.5 – 143.5
C8-d_{15}	157.5 – 158.5
C10	170.5 – 171.5
C10-d_5	175.5 – 176.5
C12	198.5 – 199.5
C12-d_{23}	221.5 – 222.5

5.2.8 Calculations

Standard curves were constructed by calculating the peak area ratio of each free fatty acid to its corresponding internal standard and plotting these values against the set of known concentrations. The standard curves were subject to linear regression analysis and then used to quantify the concentration of fatty acids recovered from plasma samples. Unknown test samples and QC samples were identified by retention times of

peaks and corresponding m/z values. Peak areas were measured and the ratio of fatty acid/internal standard for each fatty acid used to determine final unknown and QC concentrations in samples.

5.3 RESULTS

5.3.1 Fatty acid standard and internal standard detection

To quantify medium-chain fatty acid levels, deuterated stable isotope-labelled analogues (C8-d_{15}, C10-d_5, C12-d_{23}) were utilised as internal standards. Due to their similar physical and chemical properties, stable isotope-labelled analogues effectively behave identically to their unlabelled analyte counterparts. This accounts for any variability in sample extraction, derivatization and GC-MS detection, allowing for accurate and precise quantification of analytes. Using the PFBBr derivatization and NCI method, peaks for the internal standards and the unlabelled fatty acid standards were successfully resolved by GC-MS in SIM. A good degree of separation between peaks was achieved for all compounds, with limited background noise, as exemplified in a representative chromatogram below (Figure 5.2). Retention times, used in conjunction with m/z to identify each compound (Figure 5.3), were also found to be consistent throughout analysis (Table 5.2).

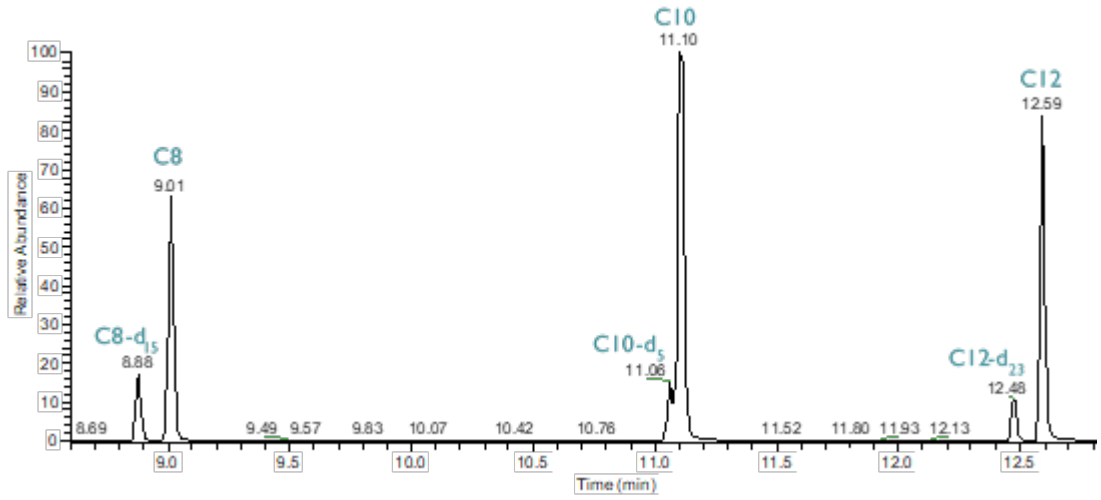

FIGURE 5.2 Typical chromatogram demonstrating peaks obtained for C8-d_{15}, C8, C10-d_5, C10, C12-d_{23} and C12 in SIM.

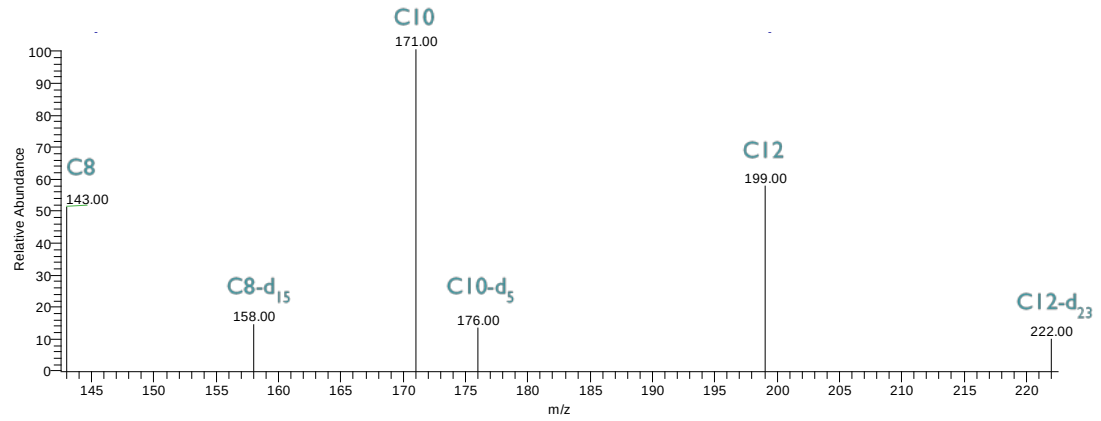

FIGURE 5.3 Combined mass spectrum for the above chromatographic peaks obtained for C8-d_{15}, C8, C10-d_5, C10, C12-d_{23} and C12 in SIM.

TABLE 5.2 Typical retention times for the fatty acids of interest and their corresponding stable isotope-labelled internal standards.

Compound	Retention Time (mins)
C8-d_{15}	8.88
C8	9.01
C10-d_5	11.06
C10	11.10
C12-d_{23}	12.48
C12	12.59

5.3.2 Fatty acid standard curves

For each of the fatty acids of interest, standard curves were established with concentrations ranging from 0-500μM. Peak areas were determined in SIM and the fatty acid/internal standard ratio was calculated to obtain the standard curves. Each standard curve was subject to linear regression analysis, and a strong linear relationship was observed at this concentration range for each fatty acid, where r^2 was always determined to be at least 0.98. Examples of typical standard curves for each of the three MCFAs are provided in Figure 5.4. Standard curves were always run prior to each batch of samples to account for potential in-batch/between-batch variability from processing and GC-MS analysis.

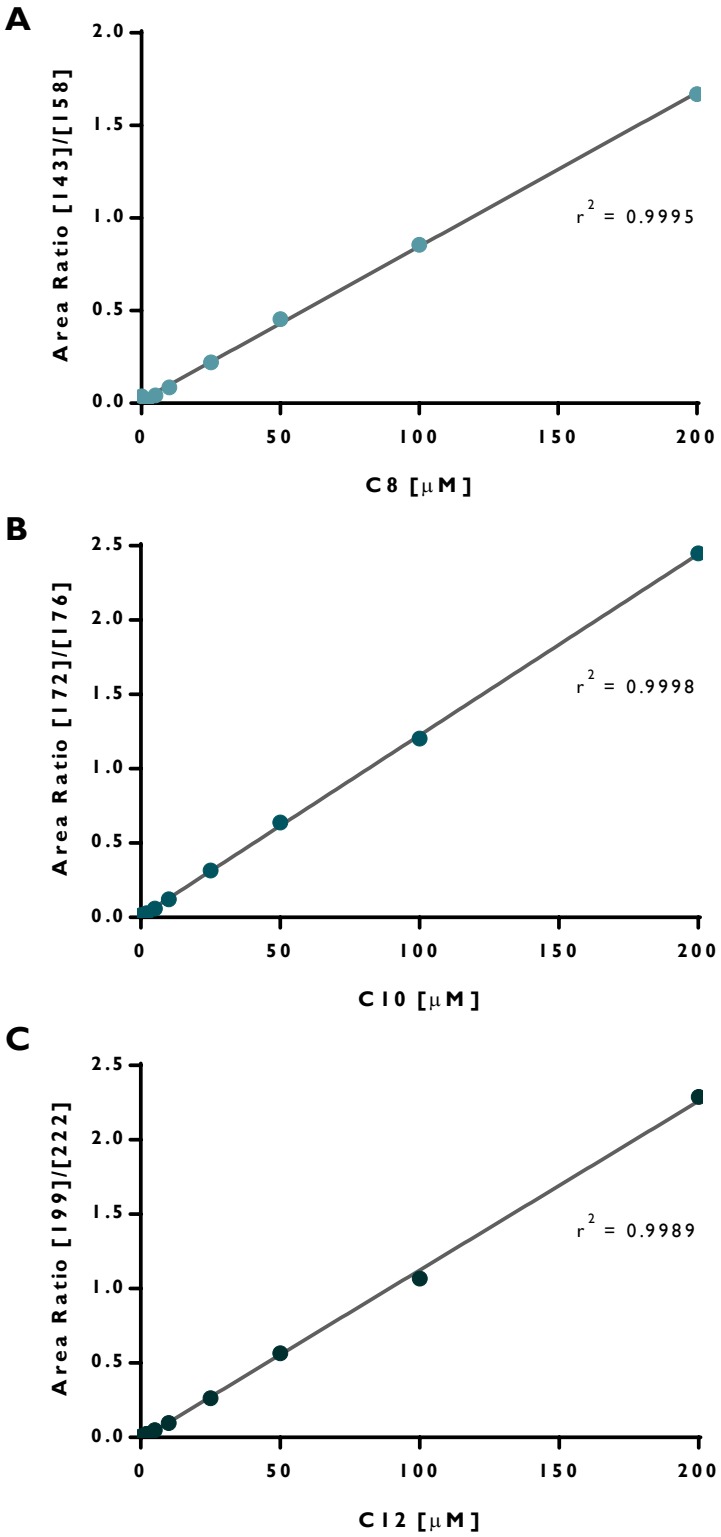

FIGURE 5.4 Typical standard curves for free fatty acids C8, C10 and C12. Standard curves were run prior to analysis of each batch of plasma samples and subject to linear regression analysis.

5.3.3 Fatty acid recovery from plasma

To evaluate the efficacy of the ethyl acetate extraction method, the amount of C8, C10 and C12 recovered from patient plasma was quantified. Patient plasma samples were spiked with known concentrations of each fatty acid and subjected to ethyl acetate extraction, derivatization and GC-MS analysis. Levels of the fatty acids in control plasma were also determined and subtracted from that of the spiked samples before calculating the final recovery rates. These are represented below in Table 5.3. Good recovery rates were achieved for C8, C10 and C12 at all the concentrations tested, averaging at 106%, 104% and 106% respectively. This suggests that this method of extraction and analysis may provide reliable and reproducible measurements of fatty acids in patient plasma.

TABLE 5.3 Recovery rates of known amounts of C8, C10 and C12 from plasma samples. Data are expressed as mean percentage of recovery ± SEM and represent 3-4 independent experiments [n=3-4].

Fatty Acid	Amount spiked (µM)	Mean recovery (%)	Replicates (n)	Overall mean recovery (%)
C8	25	104.4 ± 8.1	4	106 ± 2
	100	110.6 ± 4.8	3	
	200	103.7 ± 0.3	3	
C10	25	113.8 ± 9.3	4	104 ± 5
	100	96.8 ± 0.7	3	
	200	102.2 ± 6.4	3	
C12	25	107.7 ± 8.2	4	106 ± 1
	100	107.3 ± 3.8	2	
	200	103.9 ± 1.1	3	

5.3.4 Free fatty acid levels in control patient plasma

With the standard curves and recovery rates fully determined, control levels of free C8, C10 and C12 were quantified in patient plasma samples. Samples were randomly selected and patients cross-checked for pre-existing metabolic disorders that could affect the data, such as the fatty acid oxidation disorder medium chain acyl-CoA dehydrogenase deficiency (MCADD). Patients undergoing any form of the ketogenic diet were also excluded from analysis. A total of 7 patient plasma samples were analysed, with patients also spanning a broad range of ages. Using the method described above, a reference range for control levels of each of the fatty acids was established (Table 5.4). All three fatty acids were detected at low levels in patient plasma, ranging 6.3-7.8μM for C8, 6.1-10.4μM for C10 and 7.3-17.8μM for C12. No correlation between age, sex and fatty acid levels was observed.

TABLE 5.4 Plasma reference range for control levels of C8, C10 and C12. Control plasma samples assayed, using the method described, yielded reference ranges (min-max) as presented in the table below. Data are expressed as mean ± SEM, representative of 7 individual patients [n=7].

Fatty Acid	Mean concentration (μM)	Reference Range (μM)
Octanoic Acid (C8)	6.9 ±0.6	6.3 - 7.8
Decanoic Acid (C10)	8.2 ±1.6	6.1 - 10.4
Dodecanoic Acid (C12)	11.1±3.5	7.3 - 17.8

5.4 DISCUSSION

With measurable plasma levels of C8 and C10 reported in MCT KD patients, developing a reliable and accurate quantitative method may be beneficial for future clinical investigations into the diet, including the feasibility study into the effects of C10-enriched Betashot in epilepsy patients. Here a GC-MS approach was described that successfully determined the levels of C8, C10 and C12 in patient plasma.

With the ability of GC-MS to detect fatty acids with minimal fragmentation through negative chemical ionisation (NCI), fatty acids were derivatized with PFBBr and TEA. Samples were not saponified before derivatization as MCFAs are found as free fatty acids, rather than esterified, in plasma. Alkylation with PFBBr enabled the fatty acids to form negative ions that were successfully detected at a wide range of concentrations. Chromatograms exhibited sharp peaks with a strong signal and minimal noise. For quantification, this process was coupled with the use of deuterated stable isotope internal standards. The stable isotope standards appeared to behave similarly to their corresponding fatty acid standards at the same concentrations, and the fatty acid/internal standard peak area ratios were found to be strongly linear, allowing accurate fatty acid quantification.

With highly linear standard curves obtained from the method, quantification of C8, C10 and C12 in patient plasma was attempted. Organic solvent extraction, utilising ethyl acetate, was used to separate the fatty acids from the plasma samples. This method delivered highly reproducible results with good recoveries of all three fatty acids of interest. Moreover, the simple and cost-effective procedure excluded the need for more hazardous reagents or additional, and often-times expensive, separation

techniques. After extraction, the fatty acids were derivatized as before and quantified with a standard curve that was run alongside the samples.

Control patients were found to have very low levels of C8, C10 and C12 in their plasma, particularly in comparison to MCT KD patients, where C8 and C10 levels can reach up to 861μM and 553μM respectively (Haidukewych et al., 1982). This is unsurprising as medium-chain triglycerides are not typically found in the predominant fat sources consumed within general Western diets. Despite the low concentrations in control samples, these levels were found to be above the assay's limit of detection, ensuring accurate quantification of the fatty acids. Moreover, the reference ranges established for each fatty acid were relatively narrow, suggesting that individual differences between patients were small. However, it is worth noting that the sample size examined was small and thus insufficient to extrapolate in regard to the general population, and the potential effects of age and sex on plasma C8, C10 and C12 levels.

Finally, the method described appears to provide an effective means of quantifying medium-chain fatty acids in plasma. With the large difference in mean plasma fatty acid levels between control and MCT KD patients, it may be possible to use this method to monitor patient compliance on the diet. Studies have also yet to consider the clinical effects of raised C10 plasma levels on seizures and biochemical outcomes in patients. However, this method will be used to quantify C8, C10 and C12 plasma levels in the feasibility study investigating the effects of C10-enriched Betashot in epilepsy patients. Thus, this method may prove beneficial in elucidating the potential associations, if any, between C8 and C10 plasma levels, seizure control, and additional biochemical outcomes.

CHAPTER 6

Feasibility Study on the Effects of Decanoic Acid-Enriched Betashot, a Food for Special Medical Purposes, in Epilepsy Patients

6.1 INTRODUCTION

MCT oils and emulsions comprise a major element of the MCT KD, providing the key fat component of the diet. Although the MCT KD is recognised for its efficacy in managing drug-resistant epilepsy, its complexity makes it a difficult regimen to follow. Requiring a high degree of dietary restriction and discipline, poor patient compliance is an obstacle to the success of the MCT KD. Administered four times daily, MCT formulations are generally consumed alongside meals, but the distinctive oily taste and texture also pose a challenge to palatability and acceptability. Coupled with the gastrointestinal side effects associated with MCTs, a high discontinuation rate is observed with patients on the MCT KD (Klein, Tyrlikova, & Mathews, 2014; Lambrechts et al., 2012; Liu & Wang, 2012). Thus, alternative or improved approaches to the diet are necessary.

MCT formulations are composed primarily of C8 and C10 medium-chain fatty acids. The ratios of the fatty acids typically vary from product to product (Rogawski, 2016), with many oils and emulsions generally containing C8 to C10 ratios that range from 50:50 to 80:20 (Marten et al., 2006). With the two fatty acids potentially implicated in the mechanisms of the MCT KD, C10 is of particular interest, with its range of antiepileptic effects, including inhibition of the AMPA receptor, increased seizure threshold and increased antioxidant status (Chang et al., 2016; Hughes et al., 2014; Sengupta & Ghosh, 2012; Tan et al., 2017; Wlaź et al., 2015). Moreover, its ability to increase complex I activity (Hughes et al., 2014) and regulate mitochondrial content, as described in Chapter 3, suggests that a move towards more C10-enriched MCT formulations may be beneficial.

With this in mind, a specially-formulated MCT solution was developed by Vitaflo International Ltd, based on in-house data, recent publications, and the work in this laboratory and that of Hughes et al. (2014). Named Betashot, the product is an emulsion containing approximately 33.3% MCT, enriched with C10 at a final C8:C10 ratio of 20:80. Designed to address the issues associated with MCT oils and emulsions, Betashot has been developed as an MCT-based food for special medical purposes (FSMP), and is intended for use by children and adults with epilepsy for the dietary management of their condition. Available in strawberry flavoured and unflavoured versions, Betashot is a thickened, creamy product that is suitable to drink and requires no additional preparation, improving on typical MCT formulations that necessitate prior mixing with food. However, prior to approval for use as part of the MCT KD, the feasibility of Betashot as an FSMP and patient reception to the product must be examined.

To assess the suitability of Betashot in patients, a feasibility study was carried out that aimed to evaluate the compliance, tolerability and acceptability of the product in 40 adult patients and 40 child patients with epilepsy. Participants were required to consume Betashot four times daily for 12 weeks, whilst maintaining a normal diet that restricted intake of high-sugar foods. Typically, the MCT KD provides 30-60% of total caloric intake per day from MCT (Huttenlocher, 1976; Neal, 2012b; Schwartz et al., 1989b). For this study, children were required to consume up to 35% of their daily energy requirement from Betashot by the end of the trial, based on the Estimated Average Requirements (EARs) for their age (Scientific Advisory Committee on Nutrition (SACN), 2011). Adult participants were required to consume 80g/day Betashot by week 12, equivalent to approximately 30-40% EAR, depending on age and sex (Scientific Advisory Committee on Nutrition (SACN), 2011).

In addition to compliance, tolerability and acceptability in patients, adverse events and side effects of Betashot consumption were evaluated in the study. Seizures were also recorded daily by participants in Study Diaries. MCFA levels (C8, C10 and C12) in participant blood plasma were measured throughout the course of the study and a range of biochemical clinical safety measures were also monitored, including the effects of Betashot on ketone body levels, lipid profiles and acylcarnitine profiles. Furthermore, in view of the fact that C10 effect on CS activity was the target of earlier investigations in this thesis, CS activity in participants was also measured during the feasibility study. In this chapter, the biochemical findings of this study are described, and the data summarised and analysed. At the time of writing, the study was ongoing and a total of 60 participants had been recruited. Thus, for the purpose of this thesis, only the data available for these participants were selected for analysis, providing a snapshot of the study.

6.2 AIMS

- To assess the biochemical effects of Betashot in adults and children with epilepsy, examining plasma MCFA levels and biochemical clinical safety measures, and also evaluating compliance, tolerability and acceptability of Betashot in participants thus far.
- To explore the potential effects of Betashot on CS activity in participants.

6.3 METHODS

6.3.1 Materials

Reagents for GC-MS fatty acid analysis were purchased as described in Section 5.2.1. All other reagents were purchased as specified in Section 2.1.

6.3.2 Participants

Children and adults were recruited from outpatient epilepsy clinics at Great Ormond Street Hospital for Children, London, and the National Hospital for Neurology and Neurosurgery, UCLH, London. Children aged 3-18 years and adults over 18 were included in the study if they exhibited symptoms of epilepsy despite anti-epileptic medication. Participants with medical conditions that contraindicate the use of MCT products, such as medium-chain acyl-CoA dehydrogenase deficiency (MCADD) were excluded. In addition, participants who were seizure-free for more than 4 weeks, on the ketogenic diet, or totally enterally fed, as well as pregnant/planning women, were also excluded from the study. As the study was ongoing at the time of writing, specific medical history of participants, including past/ongoing drug treatments and experience of KD therapy, was embargoed from analysis.

6.3.3 Study Protocol

Participants were required to consume Betashot for a total of 12 weeks, whilst following a normal diet with a reduced intake of high-sugar food and drinks. Participants were also required to continue current medications throughout the study unless advised otherwise. Three participant visits took place throughout the course of the trial, at the start of the trial before week 1 (visit A), at week 5 (visit B) and at week 12 (visit C). At visit A, baseline participant measurements were acquired, including anthropometric

values such as height, weight and BMI (Body Mass Index). Urine samples, up to 10ml lithium-heparinised blood samples and dry blood spots were also taken from each participant. Participants were also provided with a Study Diary for daily completion by carers or participants for the duration of the trial. The Study Diary comprised of short questionnaires on gastrointestinal intolerance, side effects, acceptability and intake of Betashot, as well as symptoms of epilepsy, recorded in number of seizures. A 24h diet history was also taken from participants and a simple food frequency questionnaire was administered for dietitians to establish typical nutritional intake. Seizure history and gastrointestinal intolerance symptoms generally experienced by participants were also taken verbally.

Betashot was prescribed to be taken four times daily, before, during or immediately after meals/snacks, including once before sleep. Adult participants were required to introduce Betashot incrementally in the first week, and aimed to take 120ml Betashot by the end of week 1 to provide 40g/day of MCT. As Betashot provides 317kcal/100ml, child participants were required to take the product as a proportion of their daily EAR, calculated from dietary information obtained during visit A. Betashot was introduced incrementally during week 1, with child participants aiming to take a maximum of 17.5% of their EAR from Betashot by the end of week 1.

At visit B, approximately 4-5 weeks into the study, tolerance and compliance were assessed, and gastrointestinal/epilepsy symptoms were reviewed. Urine samples, up to 10ml heparinised blood samples and dry blood spots were also taken from each participant, 2 hours after the consumption of Betashot. Participant weight was also measured. After visit B measurements, the additional introduction of Betashot in participant diets commenced. Adults were required to raise their Betashot

consumption to 240ml/day by the end of the week, to provide an MCT intake of 80g/day. Children were also required to increase the amount of Betashot taken by the end of the week so that 35% of EAR was provided from Betashot. This procedure was required to be followed and maintained from weeks 5 to 12, until visit C. At visit C, by the end of week 12, the previous evaluation methods were applied. Tolerance and compliance were assessed, participant weight was measured and gastrointestinal/epilepsy symptoms were reviewed. Urine samples, up to 10ml heparinised blood samples and dry blood spots were also taken from each participant, 2 hours after the consumption of Betashot. Completed Study Diaries were collected and participants were provided with the option to continue or discontinue with Betashot consumption at the end of the study. Seizure data and quantitative urinalysis were unavailable for analysis at the time of writing.

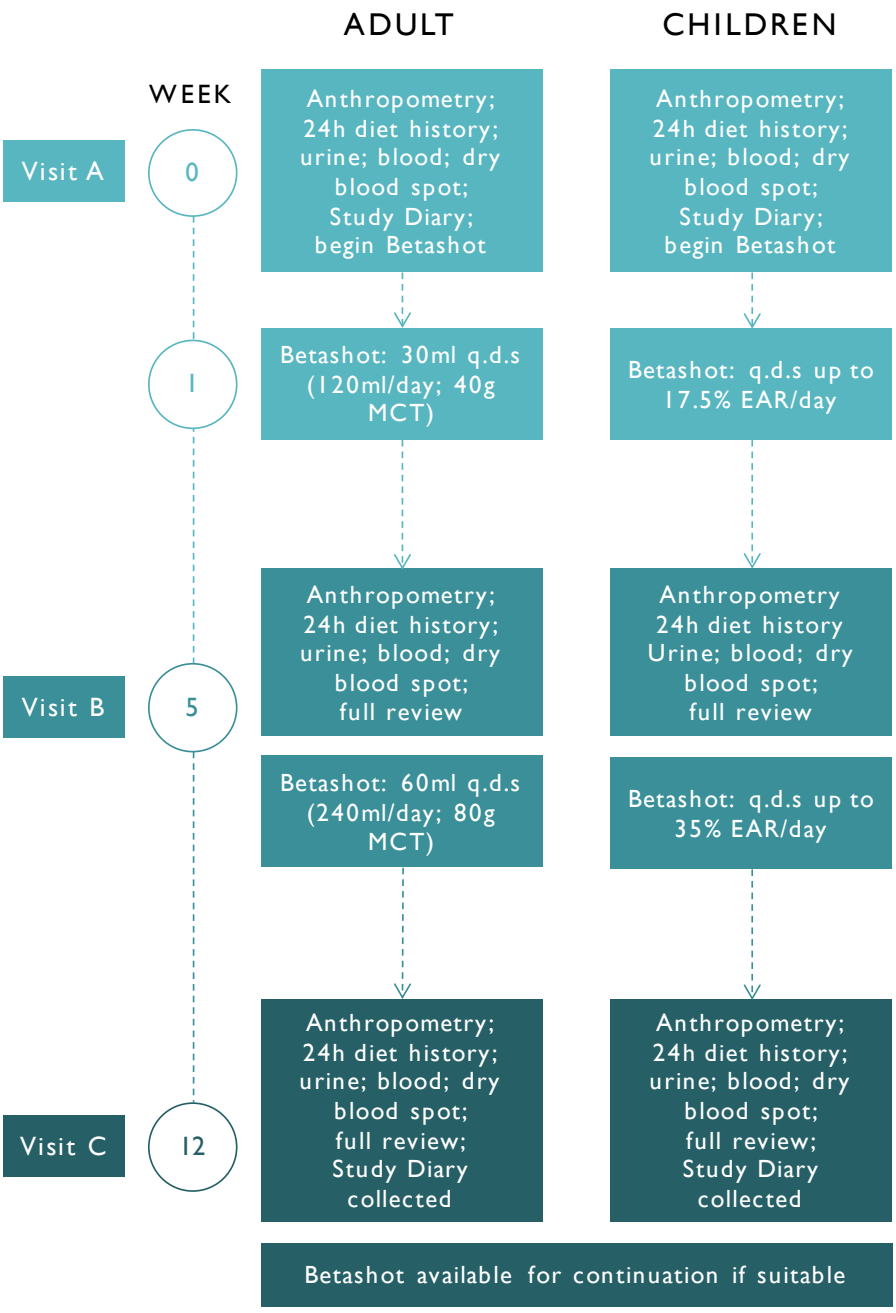

FIGURE 6.1 Breakdown of Betashot study protocol followed by adult and child participants.

6.3.4 Blood Sample Preparation

Fresh whole blood samples, collected in lithium heparin blood tubes, were processed within 24h of collection from participants by Chemical Pathology, Great Ormond

Street Hospital for Children. Plasma and white blood cell samples were collected from the processed blood and stored at -80°C until analysis.

To process samples into plasma and white blood cell fractions, fresh whole blood was transferred to a plastic tube and centrifuged at 1625xg for 10 minutes at 5°C. This procedure separates fresh whole blood samples into distinctive fractions of plasma, white blood cells and red blood cells. The plasma fraction was transferred to a fresh tube and snap frozen in a dry ice/methanol bath before storage. The remaining white blood cell layer was then gently transferred to a clean tube, taking as few red blood cells as possible. Samples and solutions were kept on ice throughout the following procedures. To the white blood cells, 0.5ml 0.9% cold saline solution was added and the cells kept on ice. Approximately 2-3ml 0.9% cold saline solution was then added to the remaining cells in the original blood sample tube and mixed by inversion. Once red blood cells were evenly mixed, the sample was then centrifuged at 1625xg for 10 minutes at 5°C. The saline layer was discarded and any remaining white blood cells transferred to the first yield of white blood cells. An additional 1-2ml of cold 0.9% saline was then added to the tube of combined white blood cells before mixing by inversion. White blood cell samples were then centrifuged once more at 1625xg for 5 minutes at 5°C. Excess saline supernatant was then discarded from the cell sample and 1.5ml cold distilled water was added to wash the white blood cells. The cell samples were gently mixed for 90 seconds, after which 0.5ml cold 3.6% saline solution was added. The cell suspension was mixed by inversion and centrifuged briefly at 1625xg for 40 seconds at 5°C, with excess saline removed afterwards. This process of washing the white blood cells was repeated once more to remove traces of red blood cells, with the cell pellet washed a final time in 1.5ml cold 0.9% saline. Samples were gently mixed and centrifuged at 1625xg for 10 seconds at 5°C. Excess saline solution was discarded

and the white blood cell pellet finally suspended in 50µl cold distilled water before snap freezing and storing as described above.

6.3.5 GC-MS Quantification of Plasma C8, C10 and C12

Free fatty acid levels of C8, C10 and C12 in participant plasma samples were kindly quantified by Dr Michael Orford, using the GC-MS method developed and described in Chapter 5 (Section 5.2).

6.3.6 β-Hydroxybutyrate, Lipid and Acylcarnitine Profiles

To monitor the clinical safety of Betashot, a number of biochemical tests were kindly performed by Chemical Pathology, Great Ormond Street Hospital for Children. This included quantification of plasma β-hydroxybutyrate, triglyceride, non-esterified fatty acids (NEFA) and cholesterol levels. An acylcarnitine profile was also quantified, with the following acylcarnitines included: acetyl carnitine, free carnitine, propionyl carnitine, butyryl carnitine, isovaleryl carnitine, hexanoyl carnitine, octanoyl carnitine, decanoyl carnitine, tetradecenyl carnitine and palmitoyl carnitine. Reference ranges derived in-house from Great Ormond Street Hospital for Children and University College London Hospital labs were utilised for analysis.

6.3.7 CS Activities in White Blood Cells (WBC)

CS activity in participant white blood cell (WBC) samples was determined and normalised to protein content as described in Sections 2.4.2-2.5.2. CS activity was also evaluated in control WBC samples from non-epilepsy patients, obtained from Chemical Pathology, Great Ormond Street Hospital for Children, and anonymised according to official guidance from The Royal College of Pathologists (Wilkins, 2015).

Samples for visits A, B and C from each participant were also always run together to minimise potential batch variation.

6.3.8 Statistical Analysis

Biochemical data included for analysis were obtained from participants determined to be compliant at each of the visits throughout the course of the study. As a consequence, a progressive decrease in n number (individual participants) may be observed with each visit, as mean levels at each visit were only examined from those who complied with the protocol. Although a repeated-measures ANOVA would be the most appropriate statistical test for the study design, this was not usually possible as repeated-measures ANOVA requires a complete dataset with no dropouts. Quantitative data were statistically analysed as described in Section 2.8. One-way ANOVA with repeated measures tests were attempted where appropriate, where matching could be made, as an additional mode of analysis. Qualitative data were described in narrative, summarising observed outcomes.

6.3.9 Ethics

Ethical approval for the study was obtained from the Research Ethics Committee for the centres involved (REC Ref: 15/LO/1979). Adult participants and parents/carers of all child participants were required to provide written informed consent before enrolling in the study. Further details on the study are available on ClinicalTrials.gov (ID: NCT02825745).

6.4 RESULTS

6.4.1 Participant Demographics

At the time of writing, a total of 60 participants were recruited to the study, comprising 33 adults and 27 children. Overall, 27 participants were male (45%) and 32 were female (53%), with one participant's gender unspecified (data unavailable). Mean age was 34.4 ± 1.9 years (19-64 years) for adult participants and 10.4 ± 0.9 years (2-18 years) for child participants. With regards to ethnicity, the majority of participants were White (77%, n=46), whilst eight (13%) were Asian, two (3%) were Black, three (5%) were mixed and one participant was Arab.

TABLE 6.1 Demographics of participants in the Betashot feasibility study.

	n=60	(%)	Mean (y)	Min-Max (y)
Age				
Adults	33	(55)	34.4 ± 1.9	19-64
Children	27	(45)	10.4 ± 0.9	2-18
Gender				
Male	27	(45)		
Female	32	(53)		
Unknown	1	(2)		
Ethnicity				
White	46	(77)		
Black	2	(3)		
Asian	8	(13)		
Mixed	3	(5)		
Arab	1	(2)		

Participants in the study also exhibited a range of seizure types and epilepsy syndromes, with 31 participants experiencing generalised onset seizures, 21 experiencing focal onset seizures, and six participants also experiencing a mixture of both generalised and focal onset seizures, with epilepsy for two participants unspecified. Several participants were diagnosed with non-symptomatic (i.e.

idiopathic) generalised or focal epilepsies (n=11 and n=6 respectively), with one participant exhibiting non-symptomatic generalised and focal seizures. Participants also varied in symptomatic epilepsy syndrome diagnosis, which are detailed in Table 6.2. Dravet syndrome (n=7, all children) was most commonly diagnosed in participants with generalised seizures, whilst structural lesions were the most frequently occurring aetiology for focal onset seizures. Epileptic spasms were also identified in two participants: in one participant with Early Infantile Epileptic Encephalopathy, where the spasms occurred in addition to generalised seizures, and in one participant with an unspecified syndrome, where spasms were the primary seizures experienced.

TABLE 6.2 Participant epilepsy types, grouped by seizure classification and epilepsy diagnosis.

Generalised (n=31)	Focal (n=21)	Generalised/Focal (n=6)	Other (n=2)
Non-symptomatic Generalised (11)	Non-symptomatic Focal (6)	Non-symptomatic Generalised/Focal (1)	Unspecified Syndrome* (1)
Dravet Syndrome (7)	Structural Lesions (10)	Alternating Hemiplegia of Childhood (2)	Not Specified (1)
Early Infantile Epileptic Encephalopathy* (3)	Temporal Lobe Epilepsy (1)	Photosensitive Epilepsy (1)	
GLUT1 Deficiency (2)	Frontal Lobe Epilepsy (2)	Noonan Syndrome (1)	
Juvenile Myoclonic Epilepsy (2)	Cryptogenic Focal (2)	PCDH19 Epilepsy (1)	
Eyelid Myoclonia with Absences (1)			
Epilepsy with Myoclonic Absence (1)			
Doose Syndrome (1)			
Lennox-Gastaut Syndrome (1)			
Lissencephaly (1)			
Unspecified (1)			

*One participant in each of these groups also exhibited epileptic spasms, which are not specifically classified as they may have a generalised, focal or unknown onset.

6.4.2 Effects of Betashot on Anthropometry

Change in weight by the end of the study was found to vary between participants. In the adult cohort, mean baseline weight was 73.8 ± 3.2 kg (n=32), with mean baseline BMI at 26.0 ± 1.1 kg/m^2 (n=27). At visit C, mean weight was 68.9 ± 3.8 kg (n=14) and mean BMI was 24.3 ± 1.4 kg/m^2 (n=11), with no significant difference in mean participant weight between visits A and C. From the data available for participants who completed the study, a mean weight gain of 0.27 ± 0.8 kg (n=13) was observed, with the maximum weight gain at 4.7kg (visit A BMI 18.2 kg/m^2), and the maximum weight loss at 4kg (visit A BMI 22.2 and 31.3 kg/m^2). Anthropometry data for children were unavailable at the time of writing.

6.4.3 Participant Compliance and Tolerability

A total of 28 participants completed the 12-week study, including 14 adults and 14 children. Five participants (3 adults, 2 children) were still in treatment at the time of writing. Several participants (9 adults, 6 children; 54%) who completed the study also continued Betashot treatment after the 12-week study period. Out of 60 participants, there were 27 withdrawals (45%) in total (16 adults, 11 children), nine of which occurred prior to the commencement of the study (Table 6.3). This included four adult participants screened as potentially MCADD positive at the start of the study, necessitating exclusion, three adults who withdrew their consent and one adult who was unable to bleed, whilst one child had to withdraw from the study for other reasons. Of the 18 participants (30% drop-out) who withdrew prior to the end of the study, the reasons for withdrawal varied (Table 6.4). This mid-trial drop-out rate observed thus far is not unlike that seen in clinical KD trials. For adults, gastrointestinal (GI) side effects were cited most frequently as the cause for withdrawal (n=7), whilst two participants also complained of a sore throat from Betashot consumption. One

participant also disliked the taste of Betashot, finding the product unpalatable. In children, lack of appetite (n=3) and GI side effects (n=3) were cited most often, and one child also disliked the taste of Betashot. Behavioural changes, particularly aggression and hyperactivity, were also reported in children, whilst two participants reported worsened seizures during the study.

TABLE 6.3 Participant compliance in the Betashot feasibility study.

Compliance	Adults (n=33)	Children (n=27)
Completed 12 weeks	14	14
Ongoing/in treatment	3	2
Withdrew prior start of study	8	1
Withdrew prior end of study	8	10
Continued after end of study	9	6

TABLE 6.4 Participant reasons for withdrawal from the study. A total of 27 participants withdrew from the study, with 18 participants (30% drop-out) withdrawing after commencing the study. The causes for withdrawal are tallied below. Some participants cited more than one reason for withdrawal.

Reason for Withdrawal	Adults (n)	Children (n)
Withdrawal prior start of study		
MCADD	4	0
Unable to bleed	1	0
Consent withdrawn	3	0
Other	0	1
Withdrawal prior end of study		
GI side effects	7	3
Loss of appetite	0	3
Sore throat	2	0
Disliked Betashot taste	1	1
Seizures worsened	0	2
Behavioural problems	0	2

6.4.4 GI Side Effects

GI side effects experienced by participants during the study included diarrhoea, nausea and vomiting, abdominal pain, reflux, bloating, and constipation. With 10 participants citing GI side effects as a cause for withdrawal from the study, GI side effects were also examined in participants who completed the 12-week study. Of the 28 participants who completed the trial, nine participants cited GI problems at visit C, with one participant also experiencing loss of appetite with Betashot. Eight participants experienced no GI side effects at visit C, whilst data for the remaining 8 participants were unavailable at the time of writing. GI side effects were found to improve with lower doses of Betashot in some participants, whilst for others, symptoms resolved over the course of the study.

6.4.5 C8, C10 and C12 Levels in Participant Plasma

Free fatty acid levels of C8, C10 and C12 were analysed via GC-MS in the plasma samples of participants taken at each visit. Participant compliance was cross-checked and only data from those deemed to be compliant at each of the visits (B and C) were included for analysis, as reflected in the decreasing n number with each visit. Baseline levels for all three fatty acids appeared to be similar to those found in control patients, as reported in Chapter 5. C8 and C10 levels increased with each visit, paralleling the increasing amount of Betashot administered to participants over the course of the study. Significant rises in C8 and C10 levels were observed between visit A and visit B, as well as between visit A and visit C ($p<0.001$), with a significant increase in C10 also observed between visits B and C ($p<0.01$) (Figure 6.2A-B). Mean plasma levels of C8 in participants were 5.6±0.6μM at visit A, 31.6±5.0μM at visit B and 46.1±8.5μM at visit C. C10 levels in participants were found to average at 4.7±0.6μM at visit A, 96.0±11.9μM at visit B and 149.2±21.6μM at visit C. By visit C, C8 and C10 levels

ranged from 11.6-118.6μM and 35.3-293.5μM (min-max), respectively. C12 plasma concentration was measured to account for trace levels in Betashot and to examine potential chain elongation of C8 and/or C12. No significant changes in participant C12 levels were observed over the course of the study, remaining at baseline levels throughout (Figure 6.2C). C12 levels at visits A, B and C were reported at 6.9±1.1μM, 4.9±0.6μM and 4.0±0.3μM, respectively, with visit C levels ranging from 2.0-5.6μM (min-max). Proportions of C8, C10 and C12 in plasma at visits A, B and C were also compared. At visit A, plasma MCFA comprised 28±1.5% C8, 32±2.4% C10 and 40±2.1% C12, with 25±1.7% C8, 71±1.9% C10 and 5±0.8% C12 at visit B, whilst at visit C, plasma MCFA consisted of 22±1.1% C8 and 75±1.1% C10, with C12 making up only 2±0.3% (Table 6.5).

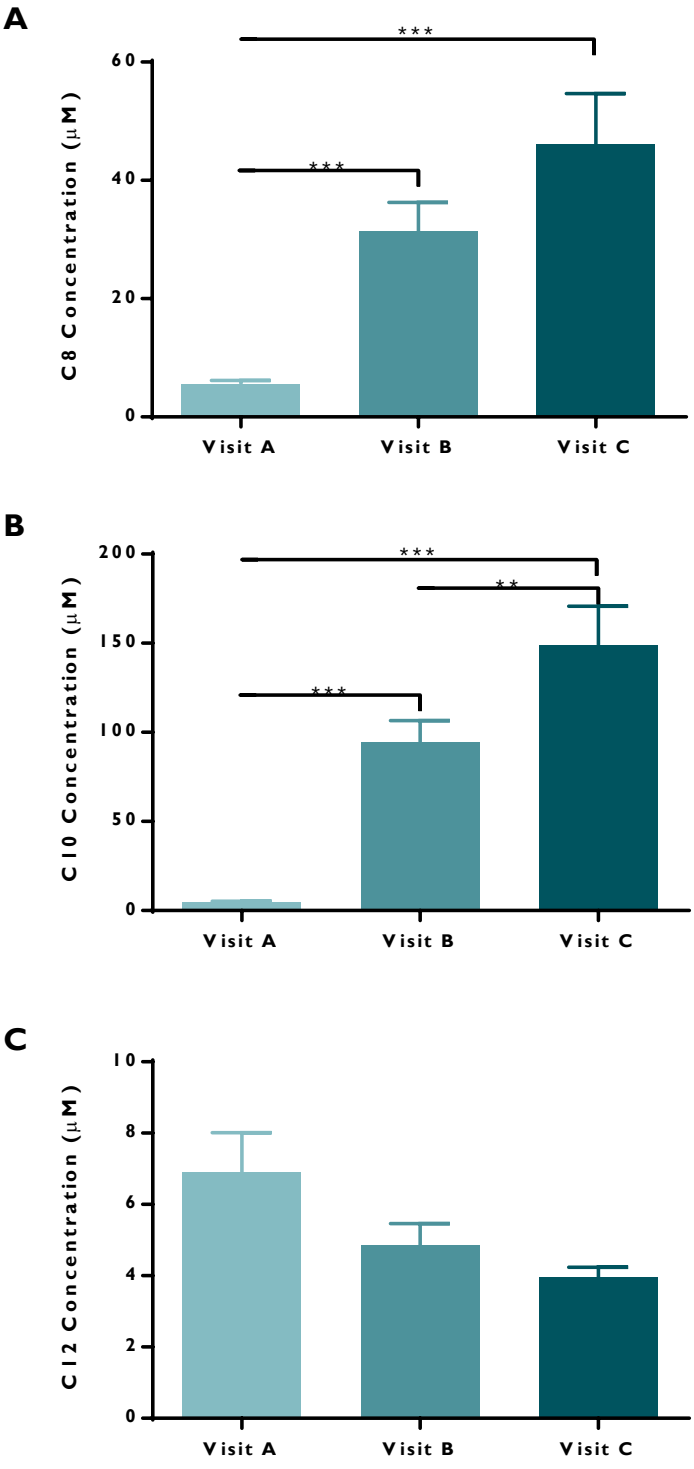
A
***
***
60
40
20
0
C8 Concentration (μM)
Visit A
Visit B
Visit C
B
***
**
***
200
150
100
50
0
C10 Concentration (μM)
Visit A
Visit B
Visit C
C
10
8
6
4
2
0
C12 Concentration (μM)
Visit A
Visit B
Visit C

FIGURE 6.2 Free C8, C10 and C12 levels in participant plasma. Fatty acid plasma levels were quantified at each of the three visits. A) C8 levels were found to significantly rise from 5.6±0.6μM at visit A to 31.6±5.0μM at visit B and 46.1±8.5μM at visit C (***p<0.001). B) C10 levels were also found to significantly increase from 4.7±0.6μM at visit A to 96.0±11.9μM at visit B and 149.2±21.6μM at visit C (***p<0.001), with a significant difference in C10 levels also observed between visits B and C (**p<0.01). C) Conversely, no significant changes in C12 levels were observed throughout the visits, with mean C12 levels of 6.9±1.1μM, 4.9±0.6μM and 4.0±0.3μM at visits A, B and C, respectively. Data represent mean ± SEM of individual participants at visit A (n=44), visit B (n=27) and visit C (n=14). Samples were only included for participants who completed their specified course for visit B and C, respectively, and consumed Betashot up to 2 hours before blood sampling.

TABLE 6.5 Proportion of C8, C10 and C12 in plasma during each of the three visits. Proportions were calculated as a percentage of total free C8, C10 and C12 levels in plasma, with data representing mean ± SEM of individual participants at visit A (n=44), visit B (n=27) and visit C (n=14).

	C8 (%)	C10 (%)	C12 (%)
Visit A	32 ± 2.4	28 ± 1.5	40 ± 2.0
Visit B	25 ± 1.7	71 ± 1.9	5 ± 0.8
Visit C	22 ± 1.1	75 ± 1.1	2 ± 0.3

6.4.6 Effects of Betashot on Plasma β-Hydroxybutyrate Levels

Plasma β-hydroxybutyrate levels were assessed in samples from participants who were considered compliant at each of the three visits. No significant changes in plasma β-hydroxybutyrate levels were observed in participants at each of the visits, with levels remaining at baseline throughout (Figure 6.3). Levels observed were also maintained at expected physiological levels (<0.4mM), indicating that participants were not in ketosis during the study. The β-hydroxybutyrate concentration typically seen in MCT KD patients is also marked on Figure 6.3 for comparison, which generally ranges from 2-4mM.

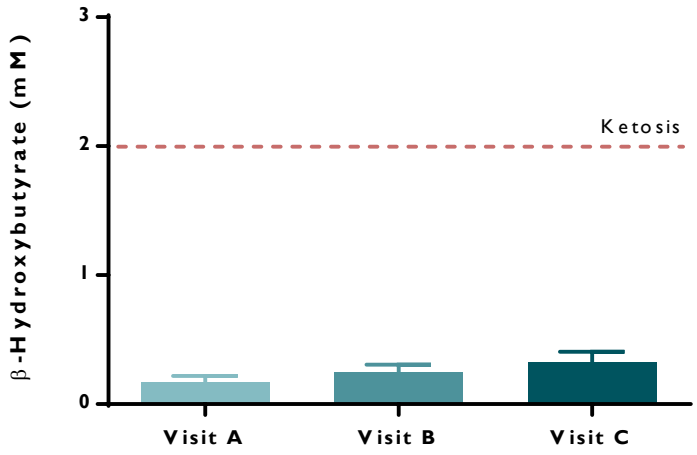

FIGURE 6.3 Plasma β-hydroxybutyrate levels in Betashot participants. No significant changes in β-hydroxybutyrate levels were observed in participants over the course of the three visits. Mean plasma levels at each visit were 0.17±0.05mM at visit A, 0.24±0.06mM at visit B and 0.30±0.07mM at visit C. Levels expressed remained within expected physiological ranges (<0.4mM). These levels were also below the minimum expected threshold for ketosis generally observed in KD and MCT KD patients. Data represents mean mean ± SEM of individual participants at visit A (n=44), visit B (n=28) and visit C (n=18).

6.4.7 Effects of Betashot on Participant Lipid Profiles

To measure the effects of Betashot consumption on the lipid profiles of participants who were deemed compliant at each of the visits, plasma triglyceride (TG), non-esterified fatty acids (NEFA) and total cholesterol levels were quantified (Table 6.6). No significant changes in level were observed for all three parameters assessed, with levels at visits B and C comparable to baseline concentrations. Furthermore, participant TG, NEFA and total cholesterol levels were found to be within expected physiological ranges throughout the course of the study.

TABLE 6.6 BHB, TG, NEFA and Cholesterol levels in participants throughout the course of the study. No significant changes in levels were observed for each of the four compounds between visits. Data represent mean ± SEM of individual participants at visit A (n=44), visit B (n=28) and visit C (n=19).

	Concentration (mM)			
Compound	**Visit A**	**Visit B**	**Visit C**	**Reference Range**
NEFA	0.47 ± 0.04	0.48 ± 0.05	0.50 ± 0.05	0.28-0.89
Triglyceride	1.21 ± 0.09	1.37 ± 0.15	1.25 ± 0.14	< 2.3
Cholesterol	4.59 ± 0.13	4.64 ± 0.15	4.92 ± 0.23	< 5.0

6.4.8 Effects of Betashot on Participant Acylcarnitine Profiles

Dried blood spot acylcarnitine profiles were determined for compliant participants during visits A, B and C (Table 6.7), with adults and children examined separately as acylcarnitine levels are thought to be age-dependent (Table 6.8). In adults, a significant increase ($p<0.05$) in acetyl carnitine levels between visits A and B was observed, although no significant difference was found between visits A and C. Hexanoyl carnitine levels were also found to significantly increase in adults ($p<0.05$), with raised levels observed at visits B and C compared to baseline. For all other acylcarnitines, no significant changes in level were observed in adults over the course of the study. In children, no changes in acylcarnitine levels were detected for all the acylcarnitines tested. Furthermore, acylcarnitine levels were found to be within the expected physiological ranges for both adults and children (Table 6.8).

TABLE 6.7 Acyl carnitine profiles of Betashot participants during visits A, B and C. In adults, acetyl carnitine levels were significantly increased at visit B (*p<0.05), with hexanoyl carnitine levels also significantly raised at visits B and C (*p<0.05), whilst no changes were seen in the remaining acylcarnitines. No significant changes were observed for all acylcarnitines in children. Data represent mean ± SEM of individual participants; adults at visit A (n=22), visit B (n=14) and visit C (n=9); children at visit A (n=23), visit B (n=13) and visit C (n=5). Data for decanoyl carnitine levels are represented by: adults, visit A (n=4), visit B (n=4), visit C (n=6); children, visit A (n=6), visit B (n=6), visit C (data unavailable).

	Adults (μM)			Children (μM)		
Carnitine Species	**Visit A**	**Visit B**	**Visit C**	**Visit A**	**Visit B**	**Visit C**
Free Carnitine	28.14 ± 1.89	30.14 ± 1.75	30.78 ± 2.38	26.87 ± 1.45	31.85 ± 2.24	31.80 ± 2.96
Acetylcarnitine	20.87 ± 0.72	23.54 ± 0.85*	23.51 ± 0.71	22.27 ± 1.17	25.38 ± 1.46	24.80 ± 3.98
Propionylcarnitine	1.21 ± 0.09	1.09 ± 0.10	1.09 ± 0.15	0.88 ± 0.07	1.00 ± 0.09	0.99 ± 0.08
Butyrylcarnitine	0.29 ± 0.02	0.31 ± 0.04	0.31 ± 0.05	0.27 ± 0.03	0.25 ± 0.02	0.25 ± 0.03
Isovalerylcarnitine	0.24 ± 0.02	0.21 ± 0.03	0.24 ± 0.05	0.23 ± 0.03	0.20 ± 0.01	0.19 ± 0.02
Hexanoylcarnitine	0.07 ± 0.004	0.13 ± 0.03*	0.14 ± 0.03*	0.08 ± 0.01	0.09 ± 0.02	0.09 ± 0.02
Octanoylcarnitine	0.15 ± 0.01	0.21 ± 0.04	0.17 ± 0.03	0.14 ± 0.03	0.13 ± 0.02	0.15 ± 0.03
Decanoylcarnitine	0.10 ± 0.02	0.52 ± 0.19	0.38 ± 0.11	0.25 ± 0.15	0.24 ± 0.09	--
Tetradecenoylcarnitine	0.11 ± 0.01	0.11 ± 0.02	0.07 ± 0.004	0.09 ± 0.01	0.09 ± 0.01	0.08 ± 0.01
Palmitoylcarnitine	1.09 ± 0.08	1.00 ± 0.10	0.80 ± 0.06	0.88 ± 0.07	0.95 ± 0.13	0.64 ± 0.05

Table 6.8 In-house reference ranges for dried blood spot carnitine and acylcarnitine levels. No specific reference range was available for adults, therefore ranges for 11y-20y patients were referenced during analysis. For child data, individual levels within the appropriate age range were also examined to account for differences between age groups. All participants analysed within the reported data above (Table 6.7) were not found to have abnormal acylcarnitine profiles.

Carnitine Species	1 y to 11 y (μM)	11 y to 20 y (μM)
Free Carnitine	17 – 55	23 – 75
Acetyl Carnitine	10.0 – 27.8	10.1 – 34.5
Propionyl Carnitine	0.27 – 1.84	0.43 – 2.44
Butyryl Carnitine	0.11 – 0.49	0.10 – 0.53
Isovaleryl Carnitine	0.08 – 0.35	0.06 – 0.31
Hexanoyl Carnitine	0.02 – 0.11	0.02 – 0.18
Octanoyl Carnitine	0 – 0.18	0.04 – 0.20
Decanoyl Carnitine	---	---
Tetradecenoyl Carnitine	0.09 – 0.25	0.02 – 0.21
Palmitoyl Carnitine	0.4 – 1.7	0.5 – 2.2

6.4.9 CS Activities in Control WBC and Baseline Visit Participant WBC

Prior to analysing the potential effects of Betashot on CS activity in participants, CS activity was examined in available baseline (visit A) participant samples alongside non-epilepsy control patient WBC (Figure 6.4). A total of 17 anonymised control samples were obtained and analysed. Given the nature of the anonymization process involved (the WBC samples were remnant diagnostic samples), demographic data was not available for all the control samples analysed. From the available data, the mean age of patients was 42.5 ± 7.0 (n=12), with ages ranging from 1-73 years, whilst gender was split evenly between male (n=6) and female (n=6), with the remainder unknown. In the visit A cohort of Betashot participants, mean age was 31.3 ± 3.2 (n=10), ranging

from 12-45 years, and comprised of 7 males and 3 females. CS activities in both control and Betashot participant WBC samples were found to be independent of age (r^2 = 0.2140 and 0.0633, respectively) (data not shown). Interestingly, in participants in the Betashot study, baseline CS activity (210±17 nmol/min/mg) was observed to be significantly higher ($p<0.05$) than in control patients (172±8 nmol/min/mg). General data on the medical history and health of control patients and participants was embargoed at the time of analysis.

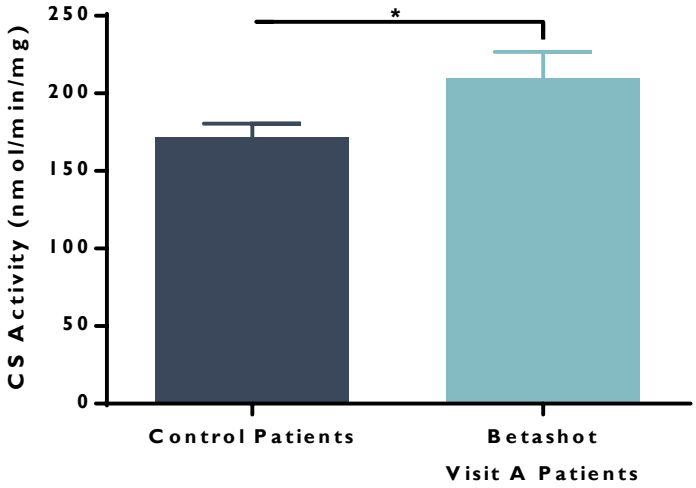

FIGURE 6.4 WBC CS activities in control and Betashot study participant samples. CS activity was examined in non-epilepsy patient samples and compared to baseline (visit A) CS activity in participant samples. CS activity was found to be significantly higher in participant samples (210±17 nmol/min/mg) than in control patient WBC (172±8 nmol/min/mg) (*$p<0.05$). Data are represented as mean ± SEM from 17 control patient samples and 10 participant samples (n=17, n=10).

6.4.10 Effects of Betashot Study on CS Activities in Participant WBC

CS activity in available participant WBC was determined for visits A, B and C to examine the effects, if any, of the study on participant CS activity. Samples analysed were obtained from participants deemed compliant at each of the three visits. The

following activities were quantified for each visit: visit A = 210±17 nmol/min/mg, visit B = 172±12 nmol/min/mg, visit C = 153±7 nmol/min/mg. A decrease in CS activity was observed with each subsequent visit, with a significant reduction in CS activity found between baseline levels (visit A) and visit C ($p<0.05$) (Figure 6.5). To further assess the impact of this effect, the CS activities of visit C were compared to WBC CS activities in control patients. No significant difference in CS activity was found, suggesting that participant samples at visit C and control patient CS activities were comparable in level (Figure 6.5).

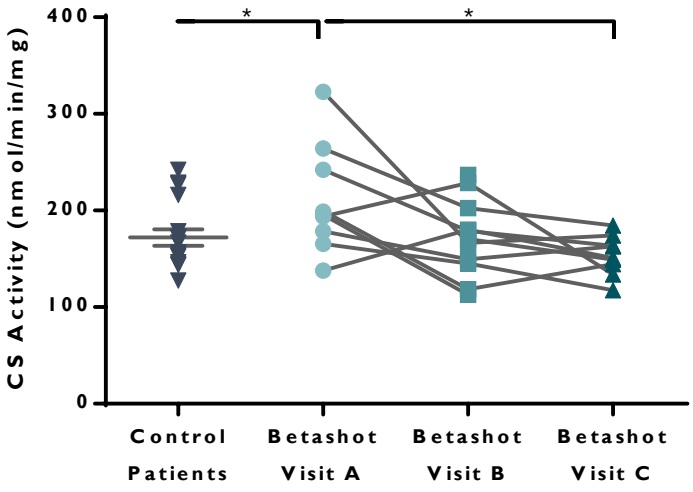

Figure 6.5 CS activity in participant WBC over duration of Betashot study. CS activity was examined in Betashot participant WBC samples from visits A (210±17 nmol/min/mg), B (172±12 nmol/min/mg) and C (153±7 nmol/min/mg). CS activity appeared to decrease at each visit, with a significant reduction in activity found at visit C compared to the baseline (visit A) (*$p<0.05$). Statistical analysis with a repeated measures test (n=8) also revealed a statistically significant reduction (*$p<0.05$) in CS activity between visits A and C. Furthermore, no significant difference in CS activity was found between participant visit C and control patient WBC samples. Data are represented as mean ± SEM from individual participants at visit A (n=10), visit B (n=11), and visit C (n=9), and individual control patients (n=17).

6.5 DISCUSSION

The main purpose of the Betashot study was to assess the compliance, tolerability and acceptability of Betashot, a C10-enriched formulation developed as a food for special medical procedures for adults and children. Study participants were required to consume Betashot over the course of 12 weeks whilst maintaining a normal diet, with blood, urine and dry blood spot samples taken at three visits (visit A at week 0, visit B at week 5 and visit C at week 12). Overall, 60 participants were recruited to the trial, comprising 33 adults and 27 children, with almost equal populations of male and female. Nearly half of participants completed the protocol. However, a large proportion of participants withdrew prior to the end of the study, highlighting potential issues with compliance. A common complaint from participants appeared to cite gastrointestinal problems as a cause for withdrawal, reflecting a primary issue that frequently affects existing MCT KD regimens for epilepsy patients.

However, whilst this feasibility study predominantly focused on participant compliance and tolerability, of particular interest to this thesis were the biochemical effects of Betashot in participants. With seizure data unavailable for analysis until the end of the trial, the effects of Betashot in participants were scrutinised in relation to plasma levels, ketone body, lipid and acylcarnitine profiles, as well as white blood cell citrate synthase activity. Free C8, C10 and C12 levels were quantified in participant plasma over the three visits with increased levels of C8 and C10 observed at visits B and C, indicating elevated fatty acid concentration with increased Betashot consumption in those who adhered to the study protocol. This was in accordance with previous studies that reported elevated levels of C8 and C10 in MCT KD patients (Haidukewych et al., 1982; Sills et al., 1986). The increased Betashot consumption was also reflected in the changes in C8, C10 and C12 proportions in plasma at each visit.

Of the three MCFAs, C12 was predominantly present in plasma at visit A, where it made up 40±2% of the total C8, C10 and C12 pool. However, by visit C, a shift in C8 and C10 proportion was observed, with levels of the two MCFAs paralleling the 20:80 ratio of C8:C10 found in Betashot. In contrast, a lack of change in C12 plasma levels over the course of the three visits suggests that trace levels in Betashot did not affect C12 plasma concentration, with chain elongation of C8 and/or C10 into C12 unlikely to have occurred. Further analysis of potential chain elongation of C8 and/or C10 into LCFAs is required however, as studies have shown MCFAs to stimulate the anabolic pathway of lipogenesis to generate LCFAs (You et al., 1998), and understanding this may glean additional insight into the mechanisms of both the MCT and classical forms of the KD.

Plasma β-hydroxybutyrate levels were also evaluated in participants and was not found to change over the course of the study, with a mean concentration of 0.30±0.07mM observed at visit C. These levels were within expected physiological ranges, indicating no ketosis in participants, whilst typical levels of β-hydroxybutyrate achieved in MCT KD patients generally range from 2-4mM (Gilbert et al., 2000; Kim & Rho, 2008; van Delft et al., 2010). Analysis of plasma β-hydroxybutyrate levels were monitored for future analysis of potential effects of Betashot on seizures in relation to ketone body levels. Furthermore, although participants were not required to undergo any dietary or caloric restriction other than avoidance of high-sugar foods, high fat intake may incur a certain degree of ketogenesis. The limited changes in β-hydroxybutyrate levels, however, are consistent with the findings reported in Chapter 4, indicating the carnitine-dependence of C10 β-oxidation and sluggish metabolism in the presence of C8. How this data associates with seizure control in participants remains to be evaluated however, as seizure data were unavailable for analysis at the time of writing.

Furthermore, the limited changes in plasma β-hydroxybutyrate level were further paralleled by the lack of effect of Betashot on participant NEFA levels in plasma. NEFAs are generally β-oxidised into ketone bodies and the observed lack of change in participant levels suggest limited ketogenesis. TG and total cholesterol levels in Betashot participants were also found to remain at baseline levels over the course of the study, indicating that Betashot may have had no overall effect on participant lipid profiles, reflecting previous findings in MCT KD patients (Lambrechts et al., 2015).

In addition to the lack of effect on participant lipid profiles, Betashot was observed to have little effect on the free carnitine and acylcarnitine profiles of participants, in both adults and children. Changes in acylcarnitine profiles are thought to reflect alterations in fatty acid oxidation caused by high intake of dietary fat (De Vogel-Van Den Bosch et al., 2011; Papamandjaris et al., 2000; Schooneman et al., 2013). No changes in carnitine/acylcarnitine level were seen in children, whilst in adults, increases in acetylcarnitine and hexanoylcarnitine were found. Increased acetylcarnitine levels are generally indicative of increased fatty acid oxidation and ketosis (Neal, 2012a; Schoeler et al., 2017), but this was only observed in adults at visit B and remained within the expected physiological range, in line with the lack of effect of Betashot on β-hydroxybutyrate levels. Raised blood levels of hexanoylcarnitine in adults may reflect the increased intake of MCTs with Betashot consumption, although no changes in octanoylcarnitine levels were found. The disparity between adult and children hexanoylcarnitine levels may be due to age-dependent differences in fatty acid oxidation, where fat oxidation is higher in children than in adults (Kostyak et al., 2007). No significant changes in decanoylcarnitine levels were observed, despite C10 carnitine-dependence. However, available quantitative data for decanoylcarnitine

content in blood were limited, resulting in a very small n number for adults, and no data for visit C in children. Therefore, it is not possible to infer the effects of Betashot on decanoylcarnitine levels in participants.

Finally, in view of the mitochondrial effects of C10 in earlier investigations in this thesis, the effects of Betashot consumption on participant WBC CS activity was examined. Betashot participants were found to exhibit significantly higher levels of CS activity in WBC samples compared to control patient levels, suggestive of increased mitochondrial content. Over the course of the study, however, a decrease in Betashot participant CS activity was observed with each visit. By visit C, CS activity of Betashot participants was found to be comparable to control patient levels. The higher baseline levels of CS activity in Betashot participants may potentially be indicative of mitochondrial accumulation in epilepsy patients, although how this may arise requires further investigation. Indeed, increased mitochondrial content is associated with various mitochondrial epilepsies, such as MERFF and MELAS (Uittenbogaard & Chiaramello, 2014), whilst impaired mitophagy has also been postulated to play a role in epileptogenesis (Ebrahimi-Fakhari et al., 2016; Wu et al., 2017). The findings in this chapter parallel those reported in Chapter 3, where C10 was observed to decrease CS activity in SH-SY5Y cells with high baseline activities. Thus, it may be hypothesised that Betashot consumption may potentially reduce CS activity levels in a similar manner to that seen in neuronal cells, optimising mitochondrial content in peripheral WBCs. However, as the WBC samples obtained from participants are a collection of various WBC subtypes, it remains to be seen if the data reflects changes in CS activity or in WBC populations. The mitochondrial bioenergetic profiles and mtDNA copy number of WBCs are known to vary between WBC subtypes (Chacko et al., 2013; Knez et al., 2016; Kramer et al., 2014), but how this is demonstrated by CS activity has yet

to be fully elucidated. Considering this, it may be possible that the perceived changes in CS activity are not changes in mitochondrial content but simply a reflection of alterations in WBC subtype populations. A WBC differential count of participant samples could provide the necessary information to indicate if the effects of Betashot potentially parallel changes in WBC population. Correlating the effects of Betashot on WBC CS activity with seizure control may also provide further mechanistic insight, as inflammation has been posited to play a key role in epilepsy (see Chapter 7) (Kleen & Holmes, 2008; Vezzani et al., 2011). Changes in WBC CS activity, or WBC populations if determined, may stem from changes to seizures and/or inflammatory responses. Monitoring the plasma levels of proinflammatory markers such as the cytokines interleukin-1β (IL-1β) and interleukin-6 (IL-6), and C-reactive protein (CRP), as well as the anti-inflammatory marker interleukin-1 receptor antagonist (IL-1ra) (Bartfai et al., 2007; Furtado Gouveia et al., 2015), may improve understanding of the WBC effects observed here. To summarise, at the time of writing, the C10-enriched MCT product Betashot appeared to exert a range of biochemical effects in adult and child epilepsy patients. Consumption of Betashot over the course of the study resulted in elevated levels of C8 and C10 in plasma, whilst no change in C12 plasma levels was seen. Proportions of the MCFAs in plasma also reflected the 20:80 ratio of C8:C10 available within the product. Furthermore, ketosis was not observed in participants, as measured by the lack of change in plasma β-hydroxybutyrate levels during the study. Similarly, no changes in NEFA and TG levels were found, whilst negligible changes in free carnitine and acylcarnitine levels in participants were also detected, further corroborating with the lack of ketosis observed. In a cohort of compliant participants, baseline WBC CS activity was found to be significantly higher than control levels. WBC CS activity was found to decrease over the course of the study in participants, suggesting a potential effect of Betashot on mitochondrial content in WBC, as judged

by CS activity. How these biochemical effects of Betashot relate to seizure control in participants remain to be determined.

CHAPTER 7

Discussion

7.1 DISCUSSION

The MCT KD is widely used as a therapy for children with drug-resistant epilepsy. Although its anticonvulsant properties were initially proposed to derive from ketone body generation, seizure control is poorly correlated with plasma ketone body levels (Likhodii et al., 2000; Schwartz et al., 1989a; Thavendiranathan et al., 2000). Whilst the exact mechanisms through which the MCT KD exerts its anticonvulsant effects remain elusive, there is growing interest in the potential roles of MCFAs C8 and C10, both provided in the diet.

Major constituents of MCT oil, elevated levels of C8 and C10 are reported in the plasma and serum of patients receiving the MCT KD (Dean, Bonser, & Gent, 1989; Haidukewych et al., 1982; Sills et al., 1986). Studies into the anticonvulsant and biochemical effects of these two compounds reveal a number of pertinent findings, suggesting both direct and indirect roles for the fatty acids in seizure control. However, despite both these fatty acids being present in the MCT KD, a distinguishable difference in effect between C8 and C10 is apparent. Emerging evidence suggests that C10, and not C8, may be primarily responsible for the beneficial effects associated with the diet. Whilst C8 has been shown to be anticonvulsant in some studies, also improving brain antioxidant activity (McDonald et al., 2014; Socała et al., 2015; Wlaź et al., 2012), other reports suggest that C8 has no direct effect on seizure control (Chang et al., 2012; Chang et al., 2015; Tan et al., 2016) and no effect on neuronal antioxidant activity (Hughes et al., 2014).

In contrast to C8, however, C10 appears to have several biological targets that may explain the anti-seizure properties of the diet. In an *ex vivo* model of epilepsy, C10, but not C8, was reported to elicit direct seizure control (Chang et al., 2012), with C10 also

significantly improving *in vivo* seizure tolerance and brain antioxidative capacity (McDonald et al., 2014; Sengupta & Ghosh, 2012; Sengupta et al., 2014; Tan et al., 2017; Wlaź et al., 2015). These observations are further supported by the finding that C10, but not C8, exerts a direct inhibitory effect on the AMPA receptor, providing a direct mechanism through which C10 could elicit seizure control (Chang et al., 2016).

In addition to its anticonvulsant effects, C10 has been found to exert pro-mitochondrial effects not seen with C8 treatment, including increased brain mitochondrial function and ATP synthesis capacity (Tan et al., 2017). Previously in this laboratory, C10, but not C8, was shown to elicit PPARγ-mediated increases in CS activity, increased complex I activity and increased catalase activity, in both neurons and fibroblasts (Hughes et al., 2014; Kanabus et al., 2016), although the findings in this thesis suggest that C10 may also be capable of decreasing CS activity under certain conditions. PPARγ activation is known to modulate mitochondrial biogenesis, suggesting that the PPARγ ligand C10 may be associated with the increased mitochondrial biogenesis observed with the KD (Bough et al., 2006). Further consideration for mitochondria as a potential therapeutic target comes from observations of diminished brain respiratory chain function, in both animal seizure models and samples derived from patients with epilepsy (Cock et al., 2002; Kunz et al., 2000), as well as in mitochondrial epilepsies (Khurana et al., 2008; Lee et al., 2008; Seo et al., 2010). With mitochondrial dysfunction heavily implicated in seizure generation, C10 may not only provide a direct antiepileptic effect against seizures, but also an indirect means of protection via the enhancement of mitochondrial function.

Thus, the primary aim of this thesis was to further elucidate the potential biochemical actions of C8 and C10 in the MCT KD, particularly focusing on the effects of these two

compounds on mitochondria in neurons, their neuronal metabolic fate, and their biochemical effects in drug-resistant epilepsy patients when orally consumed.

Hughes et al. (2014) demonstrated the ability of C10 to increase CS activity in neuronal cell line SH-SY5Y, suggesting the potential enrichment of mitochondria in these cells. CS activity is an exclusive mitochondrial enzyme and is frequently utilised as a biomarker of mitochondrial content (Larsen et al., 2012). In view of this, the effects of C10 on CS activity and mitochondrial function in SH-SY5Y were further characterised. At the commencement of this study, populations of SH-SY5Y cells were observed that differed in control CS activity, with control activity ranging from those reported by Hughes et al. (2014) to relatively higher values. This difference in CS activity between cells was found to strongly correlate with the differential effects of C10 treatment: the effect of C10 treatment on CS activity was dependent on control levels. In cells that exhibited control levels comparable to those reported by Hughes et al. (2014), and below a threshold determined from this publication and Hughes (2014), C10 treatment significantly increased CS activity. Above the threshold for control CS activity, however, and the converse was observed, with C10 treatment significantly reducing CS activity. Populations of cells were also observed with intermediate control CS activities close to this threshold. In these cases, C10 treatment was generally found to exert minimal change to CS activity. Interestingly, under these conditions, C8 was not found to exert the same effects, confirming the effects to be specific to C10, in line with previous work (Hughes et al., 2014; Kanabus et al., 2016). However, these findings contrast strongly with initial expectations that C10 treatment increases mitochondrial enrichment, as reported by Hughes et al. (2014) and supported by Kanabus et al. (2016). However, it is worth noting that Kanabus et al. (2016) observed a pleiotropic effect of C10, where response to treatment in fibroblasts from complex I deficient Leigh

syndrome patients varied according to genetic defect. Furthermore, how these differential effects relate to the evidence that C10 increases mitochondrial function, in respect to complex I and catalase activities, also requires further consideration.

This data suggests that C10 may influence mitochondrial regulation, pointing to a mechanism that results in an optimum population of mitochondria within cells. Pre-existing levels of mitochondria (i.e. control CS activity) may influence how cells adapt to the effects of C10, regulating mitochondrial content accordingly. Increased CS activity may be of benefit, for example, by improving energetic capacity of cells, but excess mitochondrial biogenesis could also prove harmful through ROS accumulation. However, the ability of cells to exert a balanced response to C10 is exemplified through the increased antioxidant activity observed following treatment (Hughes et al., 2014; Kanabus et al., 2016). Therefore, this regulatory response may extend to the mechanisms involved in controlling mitochondrial content in cells. With C10 known to act as a PPARγ agonist, potentially promoting mitochondrial biogenesis (Hughes et al., 2014; Malapaka et al., 2012), it was hypothesised that part of this mechanism may also draw on the innate cellular machinery of mitophagy.

A mitochondrial-specific branch of autophagy, mitophagy is the selective clearance of mitochondria through autophagic processes within cells, where the organelles are engulfed by autophagosomes prior to lysosomal degradation (Youle & Narendra, 2011). An essential cellular pathway, it works in conjunction with mitochondrial biogenesis to maintain mitochondrial content and quality control, removing damaged mitochondria and regulating mitochondrial number in response to cellular and metabolic demand. Whilst mitochondrial biogenesis and mitophagy appear to act as disparate forces, the two processes work hand in hand to carefully balance

mitochondrial content and maintain homeostasis within cells (Palikaras et al., 2015a; Palikaras & Tavernarakis, 2014). The tight coordination between these two opposing processes is crucial, modulating the quality and quantity of mitochondria in response to cellular metabolic state, stress and other signals (Palikaras, Lionaki, & Tavernarakis, 2015b; Zhu, Wang, & Chu, 2013).

Inadequate levels of mitochondria can be detrimental to cellular function, especially in mitochondrial-dependent cells such as neurons. Reduced mitochondrial biogenesis or rapid mitochondrial clearance can be maladaptive in cells, leaving them with a limited capacity to perform. Likewise, mitochondrial accumulation through excess mitochondrial biogenesis or defective mitophagy can also be damaging to cells, potentially exposing them to excess ROS and, in the case of dysfunctional mitochondria, pro-apoptotic mediators (Zhu et al., 2013). An imbalance between mitochondrial biogenesis and mitophagy can lead to cellular deterioration, and has been linked to the development of a number of pathological conditions, including neurodegenerative and cardiovascular diseases (Barbi de Moura, Santana dos Santos, & Van Houten, 2010; Luo et al., 2013; Meyers, Basha, & Koenig, 2013), highlighting the pivotal role of these processes in cellular homeostasis. Therefore, the potential ability of C10 to exploit these processes could prove beneficial.

To initially test this hypothesis, the potential role of mitophagy in the differential effects of C10 was explored through the pharmacological inhibition of mitophagy. A Drp1 inhibitor, Mdivi-1, was utilised as an indirect means of mitophagy inhibition through the obstruction of mitochondrial fission. Cells were treated with various combinations of C10 and Mdivi-1, but results indicated no overall effect on CS activity with either compound. This may be due to the dependency of C10 effects on control

CS activity, which varied across independent experiments. The lack of effect also seen with Mdivi-1 treatment suggested that the concentrations and conditions utilised may not have been optimum for effective inhibition of mitophagy in this cell line. As this was a preliminary experiment, further work is needed to optimise treatment conditions with Mdivi-1. Moreover, testing additional parameters to confirm mitophagy inhibition may be necessary prior to utilising CS activity as a means to measure the effects of mitophagy on mitochondrial content. For example, examination of changes to Drp1 function and specific mitophagy markers, such as PINK1 and Parkin (Jin & Youle, 2012; Narendra et al., 2008; Narendra, Walker, & Youle, 2012), and/or changes to mitochondrial morphology, may demonstrate effective attenuation of mitophagy with Mdivi-1 treatment. In addition to exploring mitophagy pharmacologically, it may also be of value to investigate the differential effects of C10 treatment on mitochondrial regulation pathways, examining any changes to gene and protein expression of both mitophagy and mitochondrial biogenesis markers in conjunction with one another. This approach may provide further insight into the differential effects of C10 on CS activity in SH-SY5Y cells. Furthermore, it could also be postulated that C10-mediated clearance of mitochondria, if any, may occur through a pathway independent of mitochondrial fission (e.g. via non-specific autophagic clearance). General autophagy inhibitors, such as bafilomycin A1 and chloroquine, could be utilised to investigate this, whilst expression of general autophagy markers with C10 treatment could also be examined.

Whilst C10 appears to influence the regulation of mitochondrial content in SH-SY5Y cells, as judged by CS activity, examining its effects on mitochondrial function in relation to this is also necessary. Mitochondrial membrane potential ($\Delta\Psi_m$) was assessed as a parameter of mitochondrial function, in C8- and C10-treated cells. With

its critical involvement in ATP synthesis, mitochondrial Ca^{2+} sequestration and ROS production, $\Delta\Psi_m$ plays an essential role in maintaining cellular homeostasis. Dysfunctional mitochondria can be marked by abnormal changes to $\Delta\Psi_m$, such as prolonged depolarisation, which may lead to impaired mitochondrial function and, eventually, cell death. In SH-SY5Y cells, C10 treatment was found to significantly increase $\Delta\Psi_m$, independently of mitochondrial content, whilst C8 appeared to have no effect. Several implications may be inferred from this finding.

Raised $\Delta\Psi_m$ may indicate potential increased ATP generation and greater capacity to meet energy demands. It is also possible that increased $\Delta\Psi_m$ may allow for amplified ATP-dependent anabolic processes, such as mitochondrial protein synthesis (Fox, 2012). Although increased $\Delta\Psi_m$ is associated with elevated ROS generation in cells, the increased catalase activity and antioxidant capacity shown with C10 treatment may serve to counter this (Hughes et al., 2014; Sengupta & Ghosh, 2012; Sengupta et al., 2014). Furthermore, maintaining increased $\Delta\Psi_m$ and associated mitochondrial function may also be protective against cell death, as loss of $\Delta\Psi_m$ is closely associated with apoptosis and necrosis (Kroemer, Galluzzi, & Brenner, 2007). Interestingly, seizure activity has also been associated with decreased $\Delta\Psi_m$ and impaired mitochondrial bioenergetics in various seizure models (Kann et al., 2005; Kovac et al., 2012; Kudin et al., 2002). How C10 affects $\Delta\Psi_m$ in the context of seizures has yet to be determined, but the ability of the fatty acid to increase $\Delta\Psi_m$ remains an interesting finding.

In addition to increased ATP synthesis, elevated $\Delta\Psi_m$ may suggest improved mitochondrial efficiency and ability to maintain $\Delta\Psi_m$, perhaps through increased mitochondrial coupling efficiency and reduced proton leakage from the

intermembrane space into the mitochondrial matrix. Proton leakage can occur through two pathways: unregulated basal proton leak, and inducible proton leak. Although it contributes a sizeable proportion of resting metabolic rate, basal proton leak occurs through mechanisms not yet fully understood (Jastroch et al., 2010). However, it is thought to be attributed to the abundance of adenine nucleotide translocase (ANT) in the inner mitochondrial membrane, a carrier protein responsible for the translocation of ATP and ADP in and out of the mitochondria (Divakaruni & Brand, 2011; Jastroch et al., 2010). How C10 may influence basal proton leak remains unclear. It may be possible that C10 treatment could alter the fatty acid composition of the phospholipid bilayer of the inner mitochondrial membrane, thereby altering proton conductance. However, only a small percentage of proton leak occurs via the bilayer, and evidence on the influence of fatty acyl composition on proton conductance is conflicting (Divakaruni & Brand, 2011; Jastroch et al., 2010; Porter, Hulbert, & Brand, 1996). Inducible proton leak is generally facilitated through mitochondrial uncoupling proteins (UCPs). Increased expression of UCPs has been associated with the classical KD (Sullivan et al., 2004), with fatty acids (LCFAs and polyunsaturated fatty acids (PUFAs)) also capable of activating them and driving down $\Delta\Psi_m$ (Mookerjee et al., 2010; Wojtczak & Schönfeld, 1993). Whilst one study has shown C8 and C10 to activate UCPs from brown adipose tissue (Winkler & Klingenberg, 1994), little is known about the effects of these fatty acids in neurons. Moreover, MCFAs are not innate uncouplers, lacking protonophoric activity (Shabalina et al., 2008; Wojtczak & Schönfeld, 1993), and are thus thought to be incapable of inducing uncoupling in mitochondria in the absence of UCPs. The lack of effect on $\Delta\Psi_m$ observed with C8 treatment, and the increased $\Delta\Psi_m$ with C10, suggest that neither of the fatty acids affect UCP activity in SH-SY5Y cells. Consistent with this hypothesis is the observation that no changes in UCP gene expression were reported in hippocampal formations of

mice fed a C10-enriched MCT diet (Tan et al., 2017), although no changes in proton leak were also found in this study. Thevenet et al. (2016) also reported no effect on proton leak and $\Delta\Psi_m$ in neurons with C8 and C10 treatment. However, in this report, the acute effects of C8 and C10 treatment were investigated, whilst this thesis examined the effects of chronic 6-day treatment of neurons. Nonetheless, this evidence may suggest that the increased $\Delta\Psi_m$ with C10 observed in SH-SY5Y cells may occur independently of changes to proton leak.

Further evidence to suggest that uncoupling may not occur in these cells was the lack of effect found with C8 and C10 on energy charge in SH-SY5Y cells. Uncoupling generally occurs at the expense of efficient ATP synthesis, but the data indicated that adenine nucleotide distribution was unaffected, with both C8- and C10-treated cells maintaining high ratios of ATP to ADP and AMP, comparable to control cells. However, additional investigations into the effects of C10 on $\Delta\Psi_m$, UCPs and energy charge are required. Furthermore, given the increase in $\Delta\Psi_m$ following C10 treatment, it remains intriguing that energy charge appeared to be unaffected by C10. This may suggest that energy is tightly regulated, with homeostatic mechanisms in place that maintain ADP and AMP levels in response to changes in ATP levels, such as ATP/ADP translocation in and out of the mitochondria, or AMPK signalling, a sensor which regulates ATP and AMP levels reciprocally in response to environmental changes (Hardie & Hawley, 2001). However, the tight regulation of energy charge means that, under normal conditions, it remains very constant (Hardie & Hawley, 2001), suggesting that while C10 appears to increase $\Delta\Psi_m$, any resulting shifts in ATP levels and the adenylate pool may be too subtle to observe under these conditions. Stressing the cells, such as through glucose restriction, to disrupt the balance maintaining the energy charge may be necessary to observe any effects C10 may have on the adenylate pool.

Thus far, the data suggests several intriguing findings with regards to the effects of C10 on mitochondria. The ability to optimally influence mitochondrial content regulation, as judged by CS activity, and increase $\Delta\Psi_m$ independently of CS activity, without hampering energy charge, point towards C10 potentially improving mitochondrial function in SH-SY5Y cells. This raises the promise for C10 to generate a more efficient cohort of neuronal mitochondria that may provide the energy capacity and protection needed to withstand the insult of seizures. Nonetheless, further studies are needed to uncover the associations and potential interplay between these parameters and, in particular, the effects of C10 under stress.

For C10 to exert its effects on mitochondrial content and function, as well as seizure control, achieving a sufficient concentration of 250μM in the brain is necessary. The differential effects of C10 on mitochondrial content, increased $\Delta\Psi_m$ and the reported enhanced complex I and antioxidant activities (Hughes et al., 2014; Kanabus et al., 2016) all required concentrations of up to 250μM C10. AMPA receptor inhibition was also achieved at 300μM (Chang et al., 2016). Whilst C10 levels may elevate in the plasma of patients receiving the MCT KD, why this occurs and how this is paralleled in patient brains remains unknown. However, concentrations of up to 240μM C10 were reported in the brains of mice fed a C10-enriched chow (Wlaź et al., 2015). MCFAs are thought to be β-oxidised into ketone bodies, and with β-oxidation enzymes reported to be present in neuronal cells (Reichmann et al., 1988; Yang et al., 1987), how C10 may accumulate within the brain was explored by evaluating C8 and C10 β-oxidation in SH-SY5Y cells. Glucose metabolism and β-oxidation of the LCFA, palmitate (C16) were also analysed alongside C8 and C10.

Glucose metabolism occurred at a significantly higher rate than that of C8 and C10, as was expected, given that neurons are thought to be primarily dependent on glucose as an energy source (Dienel & Hertz, 2001; Hall et al., 2012; Lundgaard et al., 2015; Mergenthaler et al., 2013). However, most striking was the apparent difference in C8 and C10 β-oxidation observed, with C10 β-oxidation rates substantially lower than that of C8. This raised the possibility that SH-SY5Y cells processed the two fatty acids differently, and this was determined to involve the carnitine shuttle, a system generally utilised in the transport of LCFAs into mitochondria. Although MCFAs are largely thought to enter mitochondria directly, C10 was found to be primarily reliant on the carnitine shuttle, with CPT1 inhibition by etomoxir markedly diminishing C10 β-oxidation. Complete inhibition of CPT1 was also confirmed with the impairment of C16 β-oxidation, further highlighting the parallels of C10 handling to LCFAs. This finding is corroborated by reports of C10 dependence on the carnitine shuttle for β-oxidation (Parini et al., 1999), as well as impairment of its β-oxidation in inherited disorders of carnitine metabolism (Chalmers et al., 1997). In contrast, C8 β-oxidation was found to be only partially dependent on CPT1, explaining the difference in β-oxidation between the two MCFAs.

The effects of co-incubating C8 and C10 in a 20:80 ratio, reflecting the ratios utilised in C10-enriched Betashot, was also found to further reduce C10 β-oxidation in SH-SY5Y cells. The significant inhibition of C10 β-oxidation despite the relatively low concentration of C8 suggests that C8 may exert a sparing effect on C10 β-oxidation. With the partial dependence of C8 on CPT1, substrate competition for carnitine shuttle-mediated transport into the mitochondria may occur, reducing overall C10 β-oxidation. It is also possible that differing cellular uptake for the two fatty acids may exert this difference. Further studies into these possibilities may therefore be

informative. C8 is thought to contribute approximately 20% of brain energy production (Ebert et al., 2003), suggesting the potential for C8 to be preferentially utilised as an energy source, whilst facilitating the accumulation of C10 in the brain. This effect may be further augmented by the low CPT1 activity reported in the brain (Dai et al., 2007; Lee & Wolfgang, 2012; Price et al., 2002; Wolfgang et al., 2006, 2008), potentially reducing the uptake of C10 into mitochondria for β-oxidation. However, whilst neuronal β-oxidation of C10 may be low, astrocytes are thought to be capable of significant MCFA β-oxidation (Auestad et al., 1991). How astrocytes handle C8 and C10 β-oxidation is also a point of consideration and requires further investigation. In a recent publication, however, C8 was found to be ketogenic in astrocytes, whilst C10 did not stimulate ketone body generation, suggesting that the differential β-oxidation of C8 and C10 observed in neurons may also occur in astrocytes (Thevenet et al., 2016).

The differential β-oxidation of C8 and C10 in SH-SY5Y cells demonstrates the potential mechanism through which C10 may accumulate in the brain to reach the concentrations required for its key mitochondrial and anti-seizure effects. Furthermore, the dampening effect of C8 presence on C10 β-oxidation also conveys an additional benefit to developing more C10-enriched MCT formulations. The combination of C8 and C10 may grant the potential for increased C10 accumulation and, therefore, interaction with neuronal mitochondrial and anti-seizure targets, resulting in its potentially differential effects on CS activity, increased complex I and catalase activities, AMPA receptor inhibition and reported seizure control. How this may be of benefit in the context of epilepsy is visualised in Figure 7.1, which provides an overview of the effects of C10, that summarises the experimental findings presented in this thesis, as well as those reported in available publications thus far.

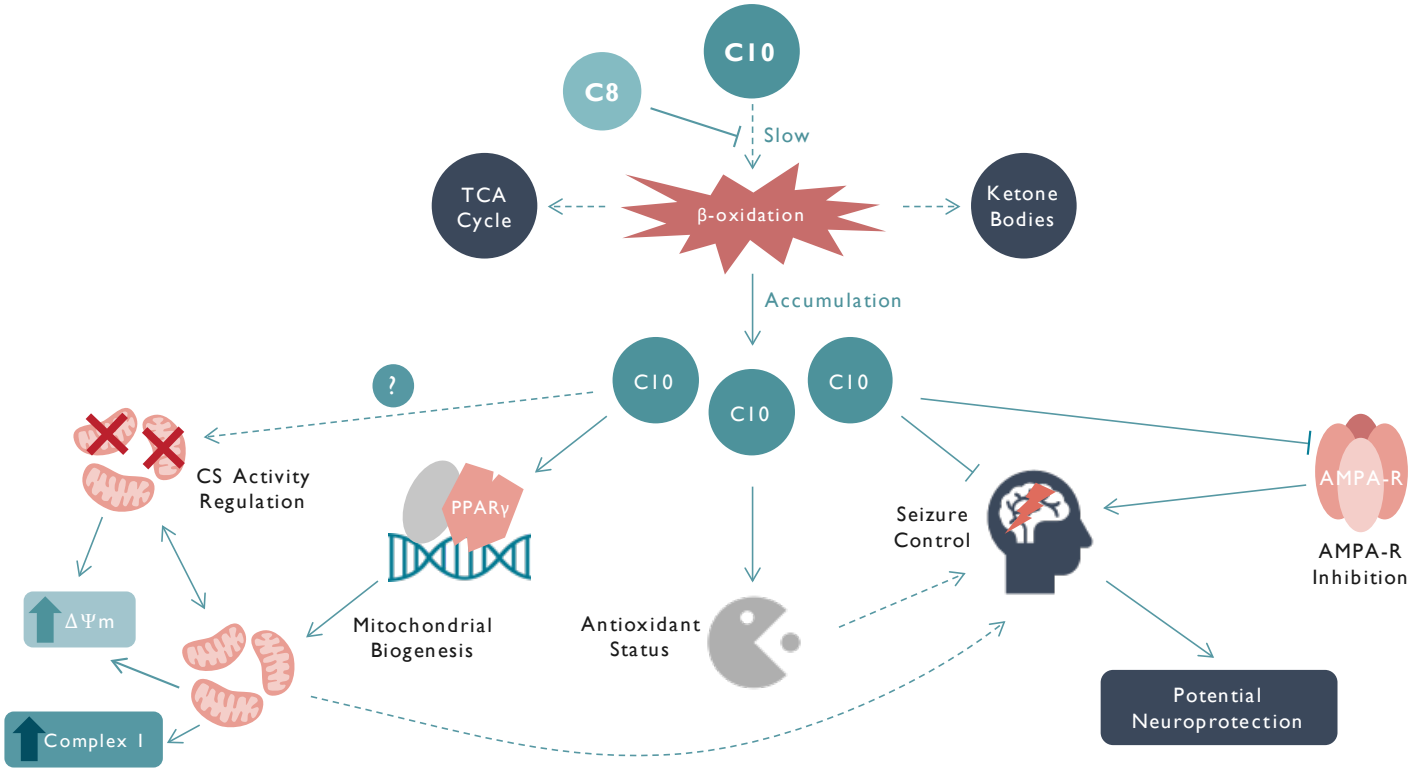

FIGURE 7.1 Schematic overview of the effects of mitochondrial and anti-epileptic effects of C10. Sluggish oxidation of C10, further reduced in the presence of C8, may lead to accumulation of the fatty acid. Once at the critical concentration required, C10 may then promote either mitochondrial biogenesis and/or regulation of mitochondrial content, generating mitochondria with increased $\Delta\Psi_m$ and complex I activities. C10 may also increase activities of catalase and other antioxidants, whilst also inhibiting seizures via AMPA receptor inhibition and/or other mechanisms. As a consequence of these actions, C10 may also potentially lead to neuroprotective effects within the brain.

To assess the impact of a shift in C10 enrichment in MCT formulae, Betashot was developed as an MCT product suitable for consumption as an FSMP. Enriched with a 20:80 ratio of C8 to C10, the effects of Betashot were evaluated in a feasibility study that assessed the compliance, tolerability, and biochemical outcomes in a cohort of 60 adult and children epilepsy patients. This thesis set to determine the biochemical effects of Betashot in participants. A GC-MS method was developed to quantify the levels of C8, C10 and C12 in participant plasma, providing a means through which to assess the metabolic fate of the fatty acids and their potential associated effects. Increased levels of C8 and C10 were observed over the course of the three visits in participants who adhered to study, indicating increased consumption of Betashot as prescribed by the study protocol and reflecting reported findings in MCT KD patients (Haidukewych et al., 1982; Sills et al., 1986). C12 levels were also examined to account for trace levels in Betashot and potential chain elongation of C8 and/or C10. However, concentration of C12 in plasma was not found to significantly change, suggesting that neither trace levels in Betashot, nor chain elongation of C8 and C10 into C12 were significant enough to detect. Further consideration for the potential for C8 and C10 chain elongation into LCFAs is needed however, as synthesis of LCFAs, through de novo lipogenesis and/or chain elongation, has been reported with high intake of MCT (Dell et al., 2001; Hill et al., 1990). Thus, measuring potential changes in plasma LCFAs in Betashot participants may provide further insight into the metabolic fate of the two MCFAs, as well as the efficacy of the classical KD. The GC-MS method developed for the measurement of free MCFAs may be adapted for free LCFA plasma quantification. The possibility remains, however, that LCFA components of the classical KD may be oxidised into C10, leading to its anti-seizure effects, although this necessitates further investigation.

Alongside changes in plasma levels of MCFAs, the effects of Betashot on ketone body generation in participants were also evaluated. Plasma levels of the ketone body β-hydroxybutyrate were assessed and no significant changes in level were observed over the course of the study. With C10 comprising the major component of Betashot, and the lack of carbohydrate restriction applied in the study protocol, this may be in line with the findings in this thesis that show that C10 β-oxidation is carnitine-dependent and further reduced in the presence of C8. This may result in a lower rate of ketogenesis than expected of MCFAs. In addition to this, plasma β-hydroxybutyrate levels found in participants were markedly lower than those typically seen in patients receiving the MCT KD, with Betashot participant levels observed to be within expected physiological ranges. Differences between Betashot participant and MCT KD patient levels may also stem from the higher proportion of C8 present in mainstream MCT formulations, resulting in greater ketogenicity than Betashot. With β-hydroxybutyrate poorly correlating with seizure control in the MCT KD, it remains to be seen if the C10-enriched Betashot exerts an effect on seizures despite a lack of carbohydrate restriction and ketosis. It may be hypothesised that the C10 component of the product, with its reported anticonvulsant effects and ability to inhibit AMPA receptors (Chang et al., 2016; Wlaź et al., 2015), may reduce seizures in participants without the need for dietary restriction. Further analysis of seizure data from participant Study Diaries is required however.

NEFAs, TG and cholesterol levels were also assessed in participant plasma. Increased levels of these parameters are generally associated with a range of adverse effects, including obesity, insulin resistance and cardiovascular disease (Carlsson et al., 2000; McKeigue et al., 1993; Zoratti et al., 2000). In Betashot participants, no significant changes in level were observed at all stages of the study for each of the parameters

tested. These findings are in line with existing reports pertaining to the effects of the MCT KD on blood lipids in humans and animal models (Dell et al., 2001; Lambrechts et al., 2015). Moreover, the lack of change seen with NEFAs may be consistent with the observed limited effect of Betashot on plasma β-hydroxybutyrate levels, as NEFAs are typically precursors to ketone bodies. It is also worth noting that Betashot consumption also appeared to have negligible effect on overall participant weight, which may be associated with blood lipid profiles (Dattilo & Kris-Etherton, 1992).

As previously described, carnitine is a necessary component of LCFA β-oxidation and is involved in the translocation of LCFAs into the mitochondrial matrix (see 1.3.2.2). With acylcarnitines generated from their corresponding fatty acyl-CoAs, it is thought that during increased fatty acid intake, incomplete fatty acid oxidation may lead to acylcarnitine accumulation (Koves et al., 2008). As C10 was found to rely on carnitine for its β-oxidation, the effects of Betashot on the free carnitine and acylcarnitine profiles in participant blood were examined. However, few changes in free carnitine and acylcarnitine levels were found in participants over the course of the study. In children, no changes were seen in any of the parameters tested. In adults, only acetylcarnitine and hexanoylcarnitine levels appeared to increase, potentially reflective of increased MCT consumption, although levels of both acylcarnitines remained within expected physiological ranges. Although the raised acetylcarnitine levels may potentially indicate increased ketone body generation, the changes in β-hydroxybutyrate concentration were negligible. However, in a recent classical KD study in children by Schoeler et al. (2017), acetylcarnitine levels in patients were found to be associated with KD efficacy, where baseline acetylcarnitine was significantly higher in responders than non-responders. This finding was speculated to relate to increased acetylcarnitine/acetyl CoA buffering capacity, as acetylcarnitine equilibrates with

acetyl CoA to maintain ketone body production. Thus, it may be of interest to correlate individual participant acylcarnitine levels with potential seizure control data during the study, despite the lack of observed ketosis.

Furthermore, the overall lack of change in free carnitine and acylcarnitine levels observed in Betashot patients may be suggestive of predominant MCFA fatty acid oxidation, despite the carnitine-dependence of C10. It may be that C8 is primarily β-oxidised, whilst C10 is relatively spared, as reflected in the elevated plasma levels observed. However, the lack of data available on decanoylcarnitine profiles to support this hypothesis prevents further inferences from being drawn. Hypocarnitinaemia is occasionally reported as a secondary effect of the classical KD (Berry-Kravis et al., 2001; Kang et al., 2004), raising the risk of impaired fatty acid oxidation. In the Betashot study, however, all observed levels for free carnitine, as well as acylcarnitines, in both adults and children appeared to be within expected physiological ranges, suggesting no abnormal effects of Betashot consumption on participant carnitine/acylcarnitine profiles.

With C10 reported to exert a range of effects in mitochondria, including the potential regulation of neuronal mitochondrial content, as judged by CS activity, and the increased $\Delta\Psi_m$ shown in this thesis, the effects of Betashot on participant mitochondria were also examined. CS activity in WBCs was measured as a marker of mitochondrial enrichment in a cohort of participants, who were deemed to be compliant, and examined alongside control patient WBC CS activities. Interestingly, baseline CS activities in Betashot participants were found to be significantly higher than in control patients, potentially indicating mitochondrial accumulation in epilepsy patients. Betashot treatment, however, was found to progressively decrease WBC CS activities

in participant samples, ultimately resulting in visit C levels that were not significantly different to control activities. Several hypotheses are proposed to support these findings.

In numerous mitochondrial disorders, elevated mitochondrial content is observed as a response mechanism to mitochondrial dysfunction, where mitochondrial biogenesis is upregulated to compensate for the presence of defective mitochondria and the resulting bioenergetic deficit (Uittenbogaard & Chiaramello, 2014). This maladaptive response is seen in the mitochondrial epilepsies MERFF and MELAS, which are marked by abnormal levels of mitochondria. Conversely, raised mitochondrial content may also be a consequence of impaired autophagy, particularly mitophagy, resulting in ineffective clearance of dysfunctional mitochondria. Defective mitophagy has been implicated in the hippocampus of temporal lobe epilepsy patients (Wu et al., 2017), as well as in neuronal models of tuberous sclerosis complex where mitochondrial accumulation was observed in cells (Ebrahimi-Fakhari et al., 2016), potentially contributing to epileptogenesis. As previously highlighted, the tight coupling between mitochondrial biogenesis and mitophagy is essential for maintaining cellular homeostasis. Thus, disruption of this relationship may lead to mitochondrial accumulation and consequential cellular decline. However, whilst these findings suggest impaired coordination of mitochondrial biogenesis and mitophagy in the brain, how this may apply to WBCs requires further consideration. With C10 previously found to regulate SH-SY5Y CS activity according to control levels, it may be postulated that Betashot exerts a restorative effect on CS activity and balances mitochondrial content to optimum levels.

However, the CS activity measured in Betashot participants was from a mixture of WBC subtypes. Differences in bioenergetic profiles and mtDNA copy number are observed between these WBC subtypes (Chacko et al., 2013; Knez et al., 2016; Kramer et al., 2014), and although one paper reported no differences in CS expression between monocytes and lymphocytes (Kramer et al., 2014), further evidence of comparisons of CS activity between subtypes is lacking. Thus, the suggestion that Betashot may alter mitochondrial content in WBCs must be considered cautiously, as it remains to be demonstrated if the data reflects changes in CS activity or in WBC subtype populations. A WBC differential count of participant samples may provide further information into the effects of Betashot, as absolute count and relative proportions of each subtype would be provided. If correlated with seizure control data, alongside WBC CS activities, this information may also provide further insight into the potential seizure control effects of Betashot.

Whilst the use of peripheral blood cells to observe the potential neuronal effects of Betashot may seem counterintuitive at first, WBCs offer potential insight into the association of inflammation with seizure pathology. Inflammation has been speculated to play an integral role in epilepsy (Kleen & Holmes, 2008; Vezzani et al., 2011). Infection and fevers are a known cause of epilepsy (see Chapter 1), leading to inflammatory responses that trigger seizures (Bartfai et al., 2007; Riazi, Galic, & Pittman, 2010), whilst evidence of proinflammatory markers has been found in brain tissue of epilepsy patients (Crespel et al., 2002; Ravizza et al., 2008). Moreover, experimental models of seizures have also been shown to induce inflammatory responses within the brain (De Simoni et al., 2000; Foresti et al., 2009; Heida & Pittman, 2005; Minami, Kuraishi, & Satoh, 1991). Changes in glial function, innate immune cells of the brain, are also thought to contribute to epilepsy (Devinsky et al.,

2013; Tian et al., 2005). In addition to the neuroinflammation observed in the brain, systemic changes in inflammation are mirrored by inflammatory responses within the brain, similar to those generated in the periphery, a process thought to occur via cytokine signalling (Galic, Riazi, & Pittman, 2012; Riazi et al., 2010). Peripheral inflammation has been found to increase seizure susceptibility by eliciting neuroinflammation and oxidative stress (Ho et al., 2015), whilst concomitant brain and peripheral inflammation has been observed in a genetic mouse model of epilepsy (Okuneva et al., 2016). Leukocyte recruitment to the brain has also been postulated to contribute to neuroinflammation and seizure pathogenesis. In an experimental model of epilepsy, leukocytes were shown to adhere to the vasculature of the brain, resulting in seizures that were significantly suppressed when adherence was blocked (Fabene et al., 2009). Interestingly, elevated levels of leukoctyes were also found in the cortical tissue of epilepsy patients, suggesting the same phenomenon may occur in humans (Fabene et al., 2009).

Whilst it remains unclear if inflammation precedes seizures or vice versa in the pathogenesis of epilepsy, it is nonetheless apparent that seizures and inflammation are closely associated. Consequently, the inflammatory response system may provide an alternative target for antiepileptic therapies. In experimental models, the KD and high-fat MCT feeding have been shown to reduce inflammation (Dupuis et al., 2015; Geng et al., 2016; Nandivada et al., 2016; Ruskin, Kawamura, & Masino, 2009), potentially contributing to the anti-seizure effects observed in the classical and MCT KDs. With brain and peripheral inflammation seemingly associated in the generation of seizures, it may be hypothesised that changes in seizure modulation and neuroinflammation following treatment may be reflected peripherally. Thus, whilst the current WBC data provides only a limited snapshot of what may potentially occur in participants, the use

of WBC activity presents a window into the potential effects of Betashot on these systems. However, further evidence, as described above, is necessary to effectively relate this data with participant outcomes and provide a clearer picture of what may be occurring within the brain.

Interestingly, a growing body of evidence suggests that the C10 target PPARγ may also play a significant role in inflammation. Although primarily involved in adipogenesis (Farmer, 2005), PPARγ is highly expressed in the immune system, within spleen cells and in macrophages (Braissant et al., 1996; Ricote et al., 1998), as well as in glial cells and granule cells of the hippocampal dentate gyrus (Bernardo, Levi, & Minghetti, 2000; Braissant et al., 1996; Moreno, Farioli-vecchioli, & Cerù, 2004). Furthermore, PPARγ agonists have been shown to exert a range of anti-inflammatory effects, including inhibition of inflammatory macrophage activation (Ricote et al., 1998), attenuation of inflammatory cytokine expression (Cunard et al., 2002; Luo et al., 2006) and reduced glial cell activation (Heneka et al., 2005; Park et al., 2007; Sundararajan et al., 2005) in several inflammation models. Furthermore, in seizure models, PPARγ-mediated seizure control has been demonstrated with the synthetic PPARγ agonist pioglitazone, where reduced inflammation was postulated to play a role (Abdallah, 2010). It is also worth noting, however, that although pioglitazone is considered primarily a PPARγ agonist, it has also been found to repress endothelial and hepatic inflammatory responses in a PPARα-dependent manner (Orasanu et al., 2008). Whilst mainly involved in modulating fatty acid oxidation, PPARα activation has been shown to be implicated in mitigating neuronal inflammation (Chistyakov et al., 2015; Esmaeili et al., 2016; Gray et al., 2011). How pioglitazone-mediated agonism PPARα affects inflammation specifically in seizure models remains to be seen, but there remains a possibility that the reported PPARγ effects may be enhanced by PPARα activity. The

contribution of PPARγ in attenuating seizure-related inflammation is further supported by evidence that a KD rich in polyunsaturated fatty acids (PUFAs) decreases neuronal inflammation in an animal seizure model, as PUFAs are dietary ligands of PPARγ (Grygiel-Górniak, 2014; Jeong et al., 2011). Thus, exploiting the anti-inflammatory effects of PPARγ may contribute to the amelioration of seizures. With C10 defined as a PPARγ ligand (Malapaka et al., 2012), this raises the potential for the MCFA to exert similar anti-inflammatory effects through agonism of PPARγ. Therefore, the observed changes in Betashot participant WBC CS activity (or WBC populations) may originate from alterations in inflammatory response and/or seizures. However, further work is clearly needed to examine the potential PPARγ-mediated anti-inflammatory effects of C10. Moreover, how this may occur through a dietary intervention such as Betashot requires further investigation.

7.2 CONCLUSION

Examining the biochemical effects of C8 and C10 in neuronal cells and in drug-resistant epilepsy patients, this thesis presents a number of findings that may be potentially beneficial within the context of the MCT KD.

Within the neuronal cell line tested here, C10, but not C8, appears to exert a potential regulatory effect on mitochondrial content, refining mitochondrial enrichment to optimum levels, whilst also potentially enhancing mitochondrial function. The mechanisms through which this may occur have yet to be understood, although it is thus hypothesised that the interplay between mitochondrial biogenesis and mitophagy may be involved.

Furthermore, carnitine-dependence of neuronal C10 β-oxidation results in sluggish metabolism of the MCFA, which is further reduced in the presence of C8. Partially carnitine-dependent, C8 may be preferentially oxidised, permitting C10 to accumulate to the critical concentrations necessary for interaction with mitochondrial and anti-seizure targets.

In line with these findings, raised plasma levels of C8 and C10 were observed in drug-resistant epilepsy patients consuming the C10-enriched MCT product Betashot. The distinct lack of ketosis, and negligible changes in blood lipids and carnitine/acylcarnitines, in patients further supports this. Correlating this data to seizure control may provide further information into the effects of C10 in patients. Interestingly, in drug-resistant epilepsy patients, there is evidence to suggest that mitochondrial content in white blood cells are significantly raised. Treatment with the C10-enriched Betashot was found to reduce mitochondrial levels to control values. How this may occur requires further investigation, but the data may reflect the C10-induced regulatory effect observed on mitochondrial levels in neurons. Considerations for the role of the inflammatory system are needed, however, as PPARγ is thought to attenuate inflammatory responses.

Overall, the data suggest that a shift towards greater C10 enrichment in the MCT KD may improve on currently available therapies, through increased accumulation of C10 and potential beneficial effects on mitochondria.

7.3 FURTHER WORK

To further confirm and expand on the findings presented within this thesis, a range of additional investigations may be considered.

Firstly, the experiments described in this thesis were carried out in undifferentiated SH-SY5Y cells. Differentiating the cell line results in more neuronal-like cells (Agholme et al., 2010), and therefore may provide an improved *in vitro* neuronal model for these experiments. Other *in vitro* models to consider include using astrocytes, particularly in co-culture with SH-SY5Y, as well as microglia and primary murine neurons to generate a more comprehensive insight into the various effects of C10. Specific applications of these models in relation to the work discussed throughout this thesis are also highlighted below.

Elucidating the mechanisms behind the effects of C10 on mitochondrial content may be informative. As previously discussed, gene expression profiling and pharmacological inhibitors may provide further insight into the potential interplay between mitochondrial biogenesis and mitophagy. Co-localisation studies using imaging techniques, or alternatively, western blotting of key markers may also be utilised. How these regulatory effects of C10 relate to the activity of the electron transport chain may also be examined. Furthermore, *in vivo* models could also be utilised to examine how C10 affects mitochondria in the brain.

A key effect of C10 described in several studies is its ability to enhance antioxidant levels. The relationship between ROS production, antioxidant

levels and the observed increase in mitochondrial membrane potential in this thesis requires further understanding. Similar flow cytometry methods utilising ROS-sensitive fluorochromes may be employed, as well as measurement of antioxidant activities. The effects of C10 on mitochondrial membrane potential, as well as on energy charge, in stress conditions are also of interest. Electron transport chain inhibitors, such as rotenone, could be used. Insight into these effects in both neuronal and glial models, as described above, could be useful.

In addition to examining β-oxidation in neuronal cells, C8 and C10 β-oxidation in astrocytes or *in vivo* may be informative, utilising the same methods applied in this thesis. Co-culture of SH-SY5Y cells and astrocytes may also provide insight into how these MCFAs are metabolised within this system, as the two cell types are thought to cooperate metabolically (Schönfeld & Reiser, 2013). Other oxidative routes of C8 and C10 may also be considered, such as potential peroxisomal β-oxidation or microsomal ω-oxidation. Stable isotope labelling could also be utilised to examine the metabolic fate of C8 and C10 in patients, as understanding this may provide information required for accurate dosing with Betashot or other C10-based products.

Regarding the Betashot feasibility study, further analysis of participant data, collating all available data at the end of the study, is needed. Seizure control data require examination and correlation with the biochemical data analysed thus far. Investigating the potential chain elongation of C8/C10 in participant plasma using GC-MS may also be informative. Furthermore, more work needs to be done to examine the effects of Betashot on WBC CS activity, increasing

the n numbers currently available and investigating the potential role of WBC populations in the observed effects. Experimentally, the role of C10 in inflammation could be further characterised, *in vitro* or *in vivo*, using bacterial endotoxin lipopolysaccharide (LPS), which has been shown to increase epileptogenesis *in vivo* via inflammation (Auvin et al., 2010). The effects of C10 on cellular models of neuroinflammation could also be examined via primary microglia and/or astrocyte cells or cell lines. PPARγ antagonists could also be used to determine the mechanisms of any potential C10-mediated effects. Finally, the KD/MCT KD are hypothesised to exert disease-modifying effects (Gasior, Rogawski, & Hartman, 2006). Examining the long-term effects of Betashot consumption on metabolic/gene expression in participants may be beneficial.

BIBLIOGRAPHY

Abdallah, D. M. (2010). Anticonvulsant potential of the peroxisome proliferator-activated receptor gamma agonist pioglitazone in pentylenetetrazole-induced acute seizures and kindling in mice. *Brain Research*, *1351*, 246–253.

Agholme, L., Lindström, T., Kågedal, K., Marcusson, J., & Hallbeck, M. (2010). An in vitro model for neuroscience: differentiation of SH-SY5Y cells into cells with morphological and biochemical characteristics of mature neurons. *Journal of Alzheimer's Disease*, *20*, 1069–82.

Albers, W. R., Siegel, G. J., & Xie, Z.-J. (2012). Membrane Transport. In *Basic Neurochemistry* (Eighth, pp. 40–62). New York, NY: Academic Press.

Ames III, A. (2000). CNS energy metabolism as related to function. *Brain Research Reviews*, *34*, 42–68.

Araujo, B., Torres, L., Stein, M., Romero Cabral, F., Herai, R., Okamoto, O., & Cavalheiro, E. (2014). Decreased expression of proteins involved in energy metabolism in the hippocampal granular layer of rats submitted to the pilocarpine epilepsy model. *Neuroscience Letters*, *561*, 46–51.

Astrup, J., Møller Sørensen, P., & Rahbek Sørensen, H. (1981). Oxygen and Glucose Consumption Related to Na+-K+ Transport in Canine Brain. *Stroke*, *12*(6), 726–731.

Atkinson, D. E. (1968). The Energy Charge of the Adenylate Pool as a Regulatory Parameter. Interaction with Feedback Modifiers. *Biochemistry*, *7*(11), 4030–4034.

Attwell, D., & Laughlin, S. B. (2001). An Energy Budget for Signaling in the Grey Matter of the Brain. *Journal of Cerebral Blood Flow & Metabolism*, *21*(10), 1133–1145.

Audesirk, G. J. (2010). 13.24 - In Vitro Systems in Neurotoxicological Studies. In C. A. McQueen (Ed.), *Comprehensive Toxicology* (2nd ed., pp. 415–432). Oxford: Elsevier.

Auestad, N., Korsak, R. A., Morrow, J. W., & Edmond, J. (1991). Fatty Acid Oxidation and Ketogenesis by Astrocytes in Primary Culture. *Journal of Neurochemistry*, *56*(4), 1376–1386.

Auvin, S., Shin, D., Mazarati, A., & Sankar, R. (2010). Inflammation induced by LPS enhances epileptogenesis in immature rat and may be partially reversed by IL1RA. *Epilepsia*, *51*(Suppl 3), 34–38.

Barbi de Moura, M., Santana dos Santos, L., & Van Houten, B. (2010). Mitchondrial Dysfunction in Neurodegenerative Diseases and Cancer. *Environmental and Molecular Mutagenesis*, *51*, 391–405.

Bartfai, T., Sanchez-Alavez, M., Andell-Jonsson, S., Schultzberg, M., Vezzani, A., Danielsson, E., & Conti, B. (2007). Interleukin-1 system in CNS stress: Seizures, fever, and neurotrauma. *Annals of the New York Academy of Sciences*, *1113*, 173–177.

Beal, M. F., Hyman, B. T., & Koroshetz, W. (1993). Do defects in mitochondrial energy metabolism underlie the pathology of neurodegenerative diseases? *Trends in Neurosciences*, *16*(4), 125–131.

Benz, R., & McLaughlin, S. (1983). The molecular mechanism of action of the proton ionophore FCCP (carbonylcyanide p-trifluoromethoxyphenylhydrazone). *Biophysical Journal*, *41*(3), 381–398.

Berg, J. M., Tymoczko, J. L., & Stryer, L. (2012). *Biochemistry* (Seventh). New York, NY: W.H. Freeman.

Berger, J., & Moller, D. E. (2002). The mechanisms of action of PPARs. *Annual Review of Medicine*, *53*, 409–35.

Bernardo, A., Levi, G., & Minghetti, L. (2000). Role of the peroxisome proliferator-activated receptor-gamma (PPAR-gamma) and its natural ligand 15-deoxy-Delta12, 14-prostaglandin J2 in the regulation of microglial functions. *The*

European Journal of Neuroscience, *12*, 2215–23.

Berry-Kravis, E., Booth, G., Sanchez, A. C., & Woodbury-Kolb, J. (2001). Carnitine levels and the ketogenic diet. *Epilepsia*, *42*(11), 1445–1451.

Bhatt, D. P., Chen, X., Geiger, J. D., & Rosenberger, T. A. (2012). A sensitive HPLC-based method to quantify adenine nucleotides in primary astrocyte cell cultures. *Journal of Chromatography B: Analytical Technologies in the Biomedical and Life Sciences*, *889–890*(701), 110–115.

Biedler, J. L., Roffler-Tarlov, S., Schachner, M., & Freedman, L. S. (1978). Multiple neurotransmitter synthesis by human neuroblastoma cell lines and clones. *Cancer Research*, *38*(11 Pt 1), 3751–3757. Retrieved from http://www.ncbi.nlm.nih.gov/pubmed/29704

Bink, K., Walch, A., Feuchtinger, A., Eisenmann, H., Hutzler, P., Höfler, H., & Werner, M. (2001). TO-PRO-3 is an optimal fluorescent dye for nuclear counterstaining in dual-colour FISH on paraffin sections. *Histochemistry and Cell Biology*, *115*(4), 293–9.

Binnie, C. D. (2000). Vagus nerve stimulation for epilepsy: A review. *Seizure*, *9*(3), 161–169.

Boone, C., & Adamec, J. (2016). Top-Down Proteomics. In P. Ciborowski & J. Silberring (Eds.), *Proteomic Profiling and Analytical Chemistry: The Crossroads: Second Edition* (Second, pp. 175–191). Amsterdam: Elsevier.

Bough, K. J., Wetherington, J., Hassel, B., Pare, J. F., Gawryluk, J. W., Greene, J. G., … Dingledine, R. J. (2006). Mitochondrial biogenesis in the anticonvulsant mechanism of the ketogenic diet. *Annals of Neurology*, *60*(2), 223–35.

Bradford, M. M. (1976). A rapid and sensitive method for the quantitation of microgram quantities of protein utilizing the principle of protein-dye binding. *Analytical Biochemistry*, *72*(1–2), 248–254.

Braissant, O., Foufelle, F., Scotto, C., Dauça, M., & Wahli, W. (1996). Differential Expression of Peroxisome Proliferator-Activated Receptors (PPARs): Tissue Distribution of PPAR-α, -β, and -γ in the Adult Rat. *Endocrinology*, *137*(1), 354–366.

Brodie, M. J., & Kwan, P. (2005). Epilepsy in elderly people. *BMJ*, *331*(7528), 1317–1322.

Bromfield, E., Cavazos, J., & Sirven, J. (Eds.). (2006). Basic Mechanisms Underlying Seizures and Epilepsy. In *An Introduction to Epilepsy*. West Hartford, CT: American Epilepsy Society.

Calderón, N., Betancourt, L., Hernández, L., & Rada, P. (2017). A ketogenic diet modifies glutamate, gamma-aminobutyric acid and agmatine levels in the hippocampus of rats: A microdialysis study. *Neuroscience Letters*, *642*, 158–162.

Canene-Adams, K. (2013). Reverse-phase HPLC Analysis and Purification of Small Molecules. In J. Lorsch (Ed.), *Methods in Enzymology* (Volume 533, pp. 291–301). Academic Press.

Cantó, C., & Auwerx, J. (2009). PGC-1alpha, SIRT1 and AMPK, an energy sensing network that controls energy expenditure. *Current Opinion in Lipidology*, *20*, 98–105.

Carlsson, M., Wessman, Y., Almgren, P., & Groop, L. (2000). High levels of nonesterified fatty acids are associated with increased familial risk of cardiovascular disease. *Arteriosclerosis, Thrombosis, and Vascular Biology*, *20*(6), 1588–1594.

Cassidy-Stone, A., Chipuk, J. E., Ingerman, E., Song, C., Yoo, C., Kuwana, T., … Nunnari, J. (2008). Chemical Inhibition of the Mitochondrial Division Dynamin Reveals Its Role in Bax/Bak-Dependent Mitochondrial Outer Membrane Permeabilization. *Developmental Cell*, *14*(2), 193–204.

Cervenka, M. C., Henry, B. J., Felton, E. A., Patton, K., & Kossoff, E. H. (2016). Establishing an Adult Epilepsy Diet Center: Experience, efficacy and challenges. *Epilepsy and Behavior*, *58*, 61–68.

Chacko, B. K., Kramer, P. A., Ravi, S., Johnson, M. S., Hardy, R. W., Ballinger, S. W., & Darley-Usmar, V. M. (2013). Methods for defining distinct bioenergetic profiles in platelets, lymphocytes, monocytes, and neutrophils, and the oxidative burst from human blood. *Laboratory Investigation*, *93*(6), 690–700.

Chalmers, R., Stanley, C. A., English, N., & Wigglesworth, J. S. (1997). Mitochondrial carnitine-acylcarnitine translocase deficiency presenting as sudden neonatal death. *The Journal of Pediatrics*, *131*(2), 220–225.

Chang, P., Augustin, K., Boddum, K., Williams, S., Sun, M., Terschak, J. A., … Williams, R. S. B. (2016). Seizure control by decanoic acid through direct AMPA receptor inhibition. *Brain*, *139*(Pt 2), 431–433.

Chang, P., Terbach, N., Plant, N., Chen, P. E., Walker, M. C., & Williams, R. S. B. (2012). Seizure control by ketogenic diet-associated medium chain fatty acids. *Neuropharmacology*, *69*, 1–10.

Chang, S.-J., & Yu, B.-C. (2010). Mitochondrial matters of the brain: mitochondrial dysfunction and oxidative status in epilepsy. *Journal of Bioenergetics and Biomembranes*, *42*(6), 457–459.

Chistyakov, D. V, Aleshin, S. E., Astakhova, A. A., Sergeeva, M. G., & Reiser, G. (2015). Regulation of peroxisome proliferator-activated receptors (PPAR) α and -γ of rat brain astrocytes in the course of activation by toll-like receptor agonists. *Journal of Neurochemistry*, *134*(1), 113–124.

Clapcote, S. J., Duffy, S., Xie, G., Kirshenbaum, G., Bechard, A. R., Rodacker Schack, V., … Roder, J. C. (2009). Mutation I810N in the α3 isoform of Na+, K+-ATPase causes impairments in the sodium pump and hyperexcitability in the CNS. *Proceedings*

of the National Academy of Sciences of the United States of America, *106*(33), 14085–14090.

Cock, H. R., Tong, X., Hargreaves, I. P., Heales, S. J. R., Clark, J. B., Patsalos, P. N., … Walker, M. C. (2002). Mitochondrial dysfunction associated with neuronal death following status epilepticus in rat. *Epilepsy Research*, *48*(3), 157–168.

Compton, S. J., & Jones, C. G. (1985). Mechanism of dye response and interference in the Bradford protein assay. *Analytical Biochemistry*, *151*(2), 369–374.

Coppola, G., Veggiotti, P., Cusmai, R., Bertoli, S., Cardinali, S., Dionisi-Vici, C., … Pascotto, A. (2002). The ketogenic diet in children, adolescents and young adults with refractory epilepsy: An Italian multicentric experience. *Epilepsy Research*, *48*(3), 221–227.

Crespel, A., Coubes, P., Rousset, M., Brana, C., Rougier, A., Rondouin, G., … Lerner-Natoli, M. (2002). Inflammatory reactions in human medial temporal lobe epilepsy with hippocampal sclerosis. *Brain Research*, *952*, 159–169.

Cunard, R., Ricote, M., DiCampli, D., Archer, D. C., Kahn, D. A., Glass, C. K., & Kelly, C. J. (2002). Regulation of Cytokine Expression by Ligands of Peroxisome Proliferator Activated Receptors. *The Journal of Immunology*, *168*, 2795–2802.

Dahlin, M., Elfving, A., Ungerstedt, U., & Amark, P. (2005). The ketogenic diet influences the levels of excitatory and inhibitory amino acids in the CSF in children with refractory epilepsy. *Epilepsy Research*, *64*, 115–125.

Dai, Y., Wolfgang, M. J., Cha, S. H., & Lane, M. D. (2007). Localization and effect of ectopic expression of CPT1c in CNS feeding centers. *Biochemical and Biophysical Research Communications*, *359*(3), 469–474.

Dattilo, A. M., & Kris-Etherton, P. M. (1992). Effects of weight reduction on blood lipids and lipoproteins: a meta-analysis. *American Journal of Clinical Nutrition*, *56*(2), 320–328.

De Simoni, M. G., Perego, C., Ravizza, T., Moneta, D., Conti, M., Marchesi, F., … Vezzani, A. (2000). Inflammatory cytokines and related genes are induced in the rat hippocampus by limbic status epilepticus. *The European Journal of Neuroscience*, *12*(7), 2623–2633.

De Vogel-Van Den Bosch, J., Hoeks, J., Timmers, S., Houten, S. M., Van Dijk, P. J., Boon, W., … Schrauwen, P. (2011). The effects of long-or medium-chain fat diets on glucose tolerance and myocellular content of lipid intermediates in rats. *Obesity*, *19*(4), 792–799.

Dean, H. G., Bonser, J. C., & Gent, J. P. (1989). HPLC analysis of brain and plasma for octanoic and decanoic acids. *Clinical Chemistry*, *35*(9), 1945–1948.

Dell, C. A., Likhodii, S. S., Musa, K., Ryan, M. A., Burnham, W. M., & Cunnane, S. C. (2001). Lipid and fatty acid profiles in rats consuming different high-fat ketogenic diets. *Lipids*, *36*, 373–8.

Devinsky, O., Vezzani, A., Najjar, S., De Lanerolle, N. C., & Rogawski, M. A. (2013). Glia and epilepsy: excitability and inflammation. *Trends in Neurosciences*, *36*(3), 174–184.

DeVivo, D. C., Leckie, M. P., Ferrendelli, J. S., & McDougal, D. B. (1978). Chronic Ketosis and Cerebral Metabolism. *Annals of Neurology*, *3*(4), 331–337.

Dienel, G. A., & Hertz, L. (2001). Glucose and Lactate Metabolism During Brain Activation. *Journal of Neuroscience Research*, *66*, 824–838.

Divakaruni, A. S., & Brand, M. D. (2011). The Regulation and Physiology of Mitochondrial Proton Leak. *Physiology*, *26*(3), 192–205.

Drexler, H. G., & Uphoff, C. C. (2002). Mycoplasma contamination of cell cultures: Incidence, sources, effects, detection, elimination, prevention. *Cytotechnology*, *39*(2), 75–90.

Du, M., Li, J., Wang, R., & Wu, Y. (2016). The influence of potassium concentration on

epileptic seizures in a coupled neuronal model in the hippocampus. *Cognitive Neurodynamics*, *10*, 405–414.

Duchen, M. R. (2004). Mitochondria in health and disease: Perspectives on a new mitochondrial biology. *Molecular Aspects of Medicine*, *25*(4), 365–451.

Dupuis, N., Curatolo, N., Benoist, J. F., & Auvin, S. (2015). Ketogenic diet exhibits anti-inflammatory properties. *Epilepsia*, *56*(7), e95–e98.

Eaton, S. (2002). Control of mitochondrial β-oxidation flux. *Progress in Lipid Research*, *41*(3), 197–239.

Ebert, D., Haller, R. G., & Walton, M. E. (2003). Energy contribution of octanoate to intact rat brain metabolism measured by 13C nuclear magnetic resonance spectroscopy. *The Journal of Neuroscience*, *23*(13), 5928–5935.

Ebrahimi-Fakhari, D., Saffari, A., Wahlster, L., Di Nardo, A., Turner, D., Lewis, T. L., … Sahin, M. (2016). Impaired Mitochondrial Dynamics and Mitophagy in Neuronal Models of Tuberous Sclerosis Complex. *Cell Reports*, *17*, 1053–1070.

Erakovic, V., Zupan, G., Varljen, J., & Simonic, A. (2003). Pentylenetetrazol-induced seizures and kindling: changes in free fatty acids, superoxide dismutase, and glutathione peroxidase activity. *Neurochemistry International*, *42*(2), 173–178.

Erecińska, M., Nelson, D., Daikhin, Y., & Yudkoff, M. (1996). Regulation of GABA Level in Rat Brain Synaptosomes: Fluxes Through Enzymes of the GABA Shunt and Effects of Glutamate, Calcium, and Ketone Bodies. *Journal of Neurochemistry*, *67*, 2325–2334.

Esmaeili, M. A., Yadav, S., Gupta, R. K., Waggoner, G. R., Deloach, A., Calingasan, N. Y., … Kiaei, M. (2016). Preferential PPAR-α activation reduces neuroinflammation and blocks neurodegeneration in vivo. *Human Molecular Genetics*, *25*(2), 317–327.

Fabene, P. F., Mora, G. N., Martinello, M., Rossi, B., Ottoboni, L., Bach, S., … Constantin,

G. (2009). A role for leukocyte-endothelial adhesion mechanisms in epilepsy. *Nature Medicine*, *14*(12), 1377–1383.

Farmer, S. R. (2005). Regulation of PPARgamma activity during adipogenesis. *International Journal of Obesity*, *29 Suppl 1*, S13-6.

Fernandes, M., Naffah-Mazzacorati, M. G., & Cavalheiro, E. A. (1996). Na+K+ ATPase Activity in the Rat Hippocampus: A Study in the Pilocarpine Model of Epilepsy. *Neurochemistry International*, *28*(5/6), 497–500.

Fisher, R. S., Van Emde Boas, W., Blume, W., Elger, C., Genton, P., Lee, P., & Engel, J. (2005). Epileptic seizures and epilepsy: Definitions proposed by the International League Against Epilepsy (ILAE) and the International Bureau for Epilepsy (IBE). *Epilepsia*, *46*(4), 470–472.

Folbergrová, J., & Kunz, W. S. (2012). Mitochondrial dysfunction in epilepsy. *Mitochondrion*, *12*, 35–40.

Foresti, M. L., Arisi, G. M., Katki, K., Montañez, A., Sanchez, R. M., & Shapiro, L. A. (2009). Chemokine CCL2 and its receptor CCR2 are increased in the hippocampus following pilocarpine-induced status epilepticus. *Journal of Neuroinflammation*, *6*(40).

Fox, T. D. (2012). Mitochondrial protein synthesis, import, and assembly. *Genetics*, *192*(4), 1203–1234.

Frantseva, M. ., Perez Velazquez, J. ., Tsoraklidis, G., Mendonca, a. ., Adamchik, Y., Mills, L. ., … Burnham, M. . (2000). Oxidative stress is involved in seizure-induced neurodegeneration in the kindling model of epilepsy. *Neuroscience*, *97*(3), 431–435.

Fraser, D. D., Whiting, S., Andrew, R. D., Macdonald, E. A., Musa-Veloso, K., & Cunnane, S. C. (2003). Elevated polyunsaturated fatty acids in blood serum obtained from children on the ketogenic diet. *Neurology*, *60*, 1026–1029.

Freeman, J. M., Vining, E. P. G., Pillas, D., Pyzik, P., Casey, J., & Kelly, L. (1998). The efficacy of the ketogenic diet-1998: a prospective evaluation of intervention in 150 children. *Pediatrics*, *102*(6), 1358–63.

French, J. a. (2007). Refractory epilepsy: Clinical overview. *Epilepsia*, *48*(SUPPL. 1), 3–7.

Furtado Gouveia, T. L., Vieira de Sousa, P. V, Saores de Almeida, S., Bocca Nejm, M., Vieira de Brito, J. M., Monterazzo Cysneiros, R., … da Graça Naffah-Mazzacorati, M. (2015). High serum levels of proinflammatory markers during epileptogenesis. Can omega-3 fatty acid administration reduce this process? *Epilepsy & Behavior*, *51*, 300–305.

Galic, M. A., Riazi, K., & Pittman, Q. J. (2012). Cytokines and brain excitability. *Frontiers in Neuroendocrinology*, *33*(1), 116–125.

Gan, X., Huang, S., Wu, L., Wang, Y., Hu, G., Li, G., … Yan, S. S. (2014). Inhibition of ERK-DLP1 signaling and mitochondrial division alleviates mitochondrial dysfunction in Alzheimer's disease cybrid cell. *Biochimica et Biophysica Acta (BBA) - Molecular Basis of Disease*, *1842*(2), 220–231.

Gasior, M., French, A., Joy, M. T., Tang, R. S., Hartman, A. L., & Rogawski, M. A. (2007). The Anticonvulsant Activity of Acetone, the Major Ketone Body in the Ketogenic Diet, Is Not Dependent on Its Metabolites Acetol, 1,2-Propanediol, Methylglyoxal, or Pyruvic Acid. *Epilepsia*, *48*(4), 793–800.

Gasior, M., Rogawski, M. A., & Hartman, A. L. (2006). Neuroprotective and disease-modifying effects of the ketogenic diet. *Behavioural Pharmacology*, *17*(5–6), 431–439.

Gegg, M. E., Cooper, J. M., Chau, K. Y., Rojo, M., Schapira, A. H. V., & Taanman, J. W. (2010). Mitofusin 1 and mitofusin 2 are ubiquitinated in a PINK1/parkin-dependent manner upon induction of mitophagy. *Human Molecular Genetics*,

19(24), 4861–4870.

Geng, S., Zhu, W., Xie, C., Li, X., Wu, J., Liang, Z., … Zhong, C. (2016). Medium-chain triglyceride ameliorates insulin resistance and inflammation in high fat diet-induced obese mice. *European Journal of Nutrition*, *55*(3), 931–940.

Georgakopoulos, N. D., Wells, G., & Campanella, M. (2017). The pharmacological regulation of cellular mitophagy. *Nature Chemical Biology*, *13*(2), 136–146.

Geyelin, H. (1921). Fasting as a method for treating epilepsy. *Med Rec*, *99*, 1037–1039.

Gilbert, D. L., Pyzik, P. L., & Freeman, J. M. (2000). The Ketogenic Diet: Seizure Control Correlates Better With Serum β-Hydroxybutyrate Than With Urine Ketones. *Journal of Child Neurology*, *15*(12), 787–790.

Gray, E., Ginty, M., Kemp, K., Scolding, N., & Wilkins, A. (2011). Peroxisome proliferator-activated receptor-α agonists protect cortical neurons from inflammatory mediators and improve peroxisomal function. *European Journal of Neuroscience*, *33*(8), 1421–32.

Grisar, T., Guillaume, D., & Delgado-Escueta, A. V. (1992). Contribution of Na+, K+-ATPase to focal epilepsy?: a brief review. *Epilepsy Research*, *12*, 141–149.

Grygiel-Górniak, B. (2014). Peroxisome proliferator-activated receptors and their ligands: nutritional and clinical implications--a review. *Nutrition Journal*, *13*(17).

Haglund, M. M., & Schwartzkroin, P. A. (1990). Role of Na-K Pump Potassium Regulation and IPSPs in Seizures and Spreading Depression in Immature Rabbit Hippocampal Slices. *Journal of Neurophysiology*, *63*(2), 225–239.

Haidukewych, D., Forsythe, W. I., & Sills, M. (1982). Monitoring octanoic and decanoic acids in plasma from children with intractable epilepsy treated with medium-chain triglyceride diet. *Clinical Chemistry*, *28*(4 Pt 1), 642–5. Retrieved from http://www.ncbi.nlm.nih.gov/pubmed/7074833

Hall, C. N., Klein-Flugge, M. C., Howarth, C., & Attwell, D. (2012). Oxidative

Phosphorylation, Not Glycolysis, Powers Presynaptic and Postsynaptic Mechanisms Underlying Brain Information Processing. *Journal of Neuroscience*, *32*(26), 8940–8951.

Hardie, D. G., & Hawley, S. A. (2001). AMP-activated protein kinase: The energy charge hypothesis revisited. *BioEssays*, *23*(12), 1112–1119.

Heida, J. G., & Pittman, Q. J. (2005). Causal links between brain cytokines and experimental febrile convulsions in the rat. *Epilepsia*, *46*(12), 1906–1913.

Heneka, M. T., Sastre, M., Dumitrescu-Ozimek, L., Hanke, A., Dewachter, I., Kuiperi, C., … Landreth, G. E. (2005). Acute treatment with the PPARγ agonist pioglitazone and ibuprofen reduces glial inflammation and Aβ1-42 levels in APPV717I transgenic mice. *Brain*, *128*, 1442–1453.

Hill, J., Peters, J., Swift, L., Yang, D., Sharp, T., Abumrad, N., & Greene, H. (1990). Changes in blood lipids during six days of overfeeding with medium or long chain triglycerides. *Journal of Lipid Research*, *31*, 407–416.

Ho, Y., Lin, Y., Wu, C. J., Chao, Y., Chang, A. Y. W., & Chan, J. Y. H. (2015). Peripheral inflammation increases seizure susceptibility via the induction of neuroinflammation and oxidative stress in the hippocampus. *Journal of Biomedical Science*, *22*(46).

Holm, T. H., & Lykke-Hartmann, K. (2016). Insights into the Pathology of the α3 Na+/K+-ATPase Ion Pump in Neurological Disorders; Lessons from Animal Models. *Frontiers in Physiology*, *7*(209).

Hughes, S. D. (2014). *The Contribution of Decanoic Acid to the Neuroprotective Mechanism of the Ketogenic Diet*. University College London.

Hughes, S. D., Kanabus, M., Anderson, G., Hargreaves, I. P., Rutherford, T., O'Donnell, M., … Heales, S. J. R. (2014). The ketogenic diet component decanoic acid increases mitochondrial citrate synthase and complex I activity in neuronal cells.

Journal of Neurochemistry, *129*(3), 426–433.

Huttenlocher, P. R. (1976). Ketonemia and Seizures: Metabolic and Anticonvulsant Effects of Two Ketogenic Diets in Childhood Epilepsy. *Pediatric Research*, *10*(5), 536–540.

Huttenlocher, P. R., Wilbourn, A., & Signore, J. (1971). Medium-chain triglycerides as a therapy for intractable childhood epilepsy. *Neurology*, *21*(11), 1097–103.

Ikeda, Y., Shirakabe, A., Maejima, Y., Zhai, P., Sciarretta, S., Toli, J., … Sadoshima, J. (2015). Endogenous Drp1 mediates mitochondrial autophagy and protects the heart against energy stress. *Circulation Research*, *116*(2), 264–278.

Ivankovic, D., Chau, K. Y., Schapira, A. H. V., & Gegg, M. E. (2016). Mitochondrial and lysosomal biogenesis are activated following PINK1/parkin-mediated mitophagy. *Journal of Neurochemistry*, *136*(2), 388–402.

Jacobs, R. A., Díaz, V., Meinild, A.-K., Gassmann, M., & Lundby, C. (2013). The C57Bl/6 mouse serves as a suitable model of human skeletal muscle mitochondrial function. *Experimental Physiology*, *98*(4), 908–921.

Jarrett, S. G., Milder, J. B., Liang, L. P., & Patel, M. (2008). The ketogenic diet increases mitochondrial glutathione levels. *Journal of Neurochemistry*, *106*(3), 1044–1051.

Jastroch, M., Divakaruni, A. S., Mookerjee, S., Treberg, J. R., & Brand, M. D. (2010). Mitochondrial proton and electron leaks. *Essays in Biochemistry*, *47*, 53–67.

Jeong, E. A., Jeon, B. T., Shin, H. J., Kim, N., Lee, D. H., Kim, H. J., … Roh, G. S. (2011). Ketogenic diet-induced peroxisome proliferator-activated receptor-γ activation decreases neuroinflammation in the mouse hippocampus after kainic acid-induced seizures. *Experimental Neurology*, *232*(2), 195–202.

Jin, S. M., & Youle, R. J. (2012). PINK1- and Parkin-mediated mitophagy at a glance. *Journal of Cell Science*, *125*(4), 795–799.

Kageyama, Y., Hoshijima, M., Seo, K., Bedja, D., Polina, S.-S., Andrabi, S. A., … Sesaki,

H. (2014). Parkin-independent mitophagy requires Drp1 and maintains the integrity of mammalian heart and brain. *The EMBO Journal*, *33*(23), 2798–2813.

Kalapos, M. P. (2003). On the mammalian acetone metabolism: from chemistry to clinical implications. *Biochimica et Biophysica Acta (BBA) - General Subjects*, *1621*(2), 122–139.

Kanabus, M. M., Fassone, E., Hughes, S. D., Bilooei, S. F., Rutherford, T., Donnell, M. O., … Rahman, S. (2016). The pleiotropic effects of decanoic acid treatment on mitochondrial function in fibroblasts from patients with complex I deficient Leigh syndrome. *Journal of Inherited Metabolic Disease*, 1–12.

Kanabus, M. M., Heales, S. J., & Rahman, S. (2014). Development of pharmacological strategies for mitochondrial disorders. *British Journal of Pharmacology*, *171*(8), 1798–817.

Kang, H. C., Chung, D. E., Kim, D. W., & Kim, H. D. (2004). Early- and late-onset complications of the ketogenic diet for intractable epilepsy. *Epilepsia*, *45*(9), 1116–23.

Kann, O., Huchzermeyer, C., Kovács, R., Wirtz, S., & Schuelke, M. (2011). Gamma oscillations in the hippocampus require high complex I gene expression and strong functional performance of mitochondria. *Brain*, *134*, 345–358.

Kann, O., Kovács, R., Njunting, M., Behrens, C. J., Otáhal, J., Lehmann, T. N., … Heinemann, U. (2005). Metabolic dysfunction during neuronal activation in the ex vivo hippocampus from chronic epileptic rats and humans. *Brain*, *128*(10), 2396–2407.

Keene, D. L. (2006). A systematic review of the use of the ketogenic diet in childhood epilepsy. *Pediatric Neurology*, *35*(1), 1–5.

Kellogg, M. D. (2017). Measurement of Biological Materials. In S. Robertson & G. H. Williams (Eds.), *Clinical and Translational Science* (Second). Academic Press.

Kerner, J., & Hoppel, C. (2000). Fatty acid import into mitochondria. *Biochimica et Biophysica Acta - Molecular and Cell Biology of Lipids*, *1486*(1), 1–17.

Khabbush, A., Orford, M., Tsai, Y.-C., Rutherford, T., O'Donnell, M., Eaton, S., & Heales, S. J. R. (2017). Neuronal decanoic acid oxidation is markedly lower than that of octanoic acid: A mechanistic insight into the medium-chain triglyceride ketogenic diet. *Epilepsia*, *58*, 1423–1429.

Khurana, D. S., Salganicoff, L., Melvin, J., Hobdell, E., Valencia, I., Hardison, H., … Legido, A. (2008). Epilepsy and respiratory chain defects in children with mitochondrial encephalopathies. *Neuropaediatrics*, *39*(1), 8–13.

Kim, D. Y., & Rho, J. M. (2008). The ketogenic diet and epilepsy. *Current Opinion in Clinical Nutrition and Metabolic Care*, *11*, 113–20.

Kim, H., Lee, J. Y., Park, K. J., Kim, W.-H., Roh, G. S., Korhonen, L., … Koh, Y. (2016). A mitochondrial division inhibitor, Mdivi-1, inhibits mitochondrial fragmentation and attenuates kainic acid-induced hippocampal cell death. *BMC Neuroscience*, *17*(1), 33.

King, L. J., Lowry, O. H., Passonneau, J. V, & Venson, V. (1967). Effects of Convulsants on Energy Reserves in the Cerebral Cortex. *Journal of Neurochemistry*, *14*, 599–611.

Kleen, J. K., & Holmes, G. L. (2008). Brain inflammation initiates seizures. *Nature Medicine*, *14*(12), 1309–1310.

Klein, P., Tyrlikova, I., & Mathews, G. C. (2014). Dietary treatment in adults with refractory epilepsy: A review. *Neurology*, *83*(21), 1978–1985.

Klingenberg, M. (2008). The ADP and ATP transport in mitochondria and its carrier. *Biochimica et Biophysica Acta (BBA) - Biomembranes*, *1778*(10), 1978–2021.

Knez, J., Winckelmans, E., Plusquin, M., Thijs, L., Cauwenberghs, N., Gu, Y., … Kuznetsova, T. (2016). Correlates of Peripheral Blood Mitochondrial DNA

Content in a General Population. *American Journal of Epidemiology*, *183*(2), 138–146.

Kochetkov, N. K., Shibaev, V. N., & Kost, A. A. (1971). New reaction of adenine and cytosine derivatives, potentially useful for nucleic acids modification. *Tetrahedron Letters*, *12*(22), 1993–1996.

Kossoff, E. H. (2012). Efficacy of ketogenic dietary therapy: what is the evidence? In E. Neal (Ed.), *Dietary Treatment of Epilepsy: Practical Implementation of Ketogenic Therapy* (pp. 24–33). Chichester: Wiley-Blackwell.

Kossoff, E. H., Zupec-Kania, B. A., Amark, P. E., Ballaban-Gil, K. R., Christina Bergqvist, A. G., Blackford, R., … Yim, G. (2009). Optimal clinical management of children receiving the ketogenic diet: Recommendations of the International Ketogenic Diet Study Group. *Epilepsia*, *50*(2), 304–317.

Kostyak, J. C., Kris-Etherton, P., Bagshaw, D., Delany, J. P., & Farrell, P. A. (2007). Relative fat oxidation is higher in children than adults. *Nutrition Journal*, *6*(19).

Kovac, S., Domijan, A.-M., Walker, M. C., & Abramov, A. Y. (2012). Prolonged seizure activity impairs mitochondrial bioenergetics and induces cell death. *Journal of Cell Science*, *125*(7), 1796–1806.

Kovacs, R., Kardos, J., Heinemann, U., & Kann, O. (2005). Mitochondrial Calcium Ion and Membrane Potential Transients Follow the Pattern of Epileptiform Discharges in Hippocampal Slice Cultures. *Journal of Neuroscience*, *25*(17), 4260–4269.

Kovalevich, J., & Langford, D. (2013). Considerations for the Use of SH-SY5Y Neuroblastoma Cells in Neurobiology. In S. Amini & M. K. White (Eds.), *Neuronal Cell Culture: Methods and Protocols, Methods in Molecular Biology* (Vol. 1078, pp. 9–21). New York: Springer Science.

Koves, T. R., Ussher, J. R., Noland, R. C., Slentz, D., Mosedale, M., Ilkayeva, O., …

Muoio, D. M. (2008). Mitochondrial Overload and Incomplete Fatty Acid Oxidation Contribute to Skeletal Muscle Insulin Resistance. *Cell Metabolism*, *7*, 45–56.

Kramer, P. A., Ravi, S., Chacko, B., Johnson, M. S., & Darley-Usmar, V. M. (2014). A review of the mitochondrial and glycolytic metabolism in human platelets and leukocytes: Implications for their use as bioenergetic biomarkers. *Redox Biology*, *2*(1), 206–210.

Kroemer, G., Galluzzi, L., & Brenner, C. (2007). Mitochondrial Membrane Permeabilization in Cell Death. *Physiology Reveiw*, *87*, 99–163.

Kudin, A. P., Kudina, T. A., Seyfried, J., Vielhaber, S., Beck, H., Elger, C. E., & Kunz, W. S. (2002). Seizure-dependent modulation of mitochondrial oxidative phosphorylation in rat hippocampus. *European Journal of Neuroscience*, *15*, 1105–1114. Retrieved from http://0.182.215.30

Kudin, A. P., Zsurka, G., Elger, C. E., & Kunz, W. S. (2009). Mitochondrial involvement in temporal lobe epilepsy. *Experimental Neurology*, *218*(2), 326–332.

Kulkarni, A. D., Patel, H. M., Surana, S. J., Belgamwar, V. S., & Pardeshi, C. V. (2016). Brain–blood ratio: implications in brain drug delivery. *Expert Opinion on Drug Delivery*, *13*(1), 85–92.

Kunz, W. S., Kudin, A. P., Vielhaber, S., Blümcke, I., Zuschratter, W., Schramm, J., … Elger, C. E. (2000). Mitochondrial complex I deficiency in the epileptic focus of patients with temporal lobe epilepsy. *Annals of Neurology*, *48*(5), 766–773.

Kwan, P., Arzimanoglou, A., Berg, A. T., Brodie, M. J., Hauser, W. A., Mathern, G., … French, J. (2010). Definition of drug resistant epilepsy: Consensus proposal by the ad hoc Task Force of the ILAE Commission on Therapeutic Strategies. *Epilepsia*, *51*(6), 1069–1077.

Kwan, P., & Brodie, M. J. (2000). Early Identification of Refractory Epilepsy. *New*

England Journal of Medicine, *342*, 314–319.

Lambrechts, D. A. J. E., de Kinderen, R. J. A., Vles, H. S. H., de Louw, A. J., Aldenkamp, A. P., & Majoie, M. J. M. (2015). The MCT-ketogenic diet as a treatment option in refractory childhood epilepsy: A prospective study with 2-year follow-up. *Epilepsy and Behavior*, *51*, 261–266.

Lambrechts, D. A. J. E., Wielders, L. H. P., Aldenkamp, A. P., Kessels, F. G. H., de Kinderen, R. J. A., & Majoie, M. J. M. (2012). The ketogenic diet as a treatment option in adults with chronic refractory epilepsy: efficacy and tolerability in clinical practice. *Epilepsy & Behavior*, *23*, 310–314.

Larsen, S., Nielsen, J., Hansen, C. N., Nielsen, L. B., Wibrand, F., Stride, N., … Hey-Mogensen, M. (2012). Biomarkers of mitochondrial content in skeletal muscle of healthy young human subjects. *Journal of Physiology*, *590*(14), 3349–3360.

Lee, J., & Wolfgang, M. J. (2012). Metabolomic profiling reveals a role for CPT1c in neuronal oxidative metabolism. *BMC Biochemistry*, *13*(1), 23.

Lee, O., & O'Brien, P. J. (2010). Modifications of Mitochondrial Function by Toxicants. *Comprehensive Toxicology*, 411–445.

Lee, Y. M., Kang, H. C., Lee, J. S., Kim, S. H., Kim, E. Y., Lee, S. K., … Kim, H. D. (2008). Mitochondrial respiratory chain defects: Underlying etiology in various epileptic conditions. *Epilepsia*, *49*(4), 685–690.

Lenaz, G. (2001). The Mitochondrial Production of Reactive Oxygen Species: Mechanisms and Implications in Human Pathology. *IUBMB Life (International Union of Biochemistry and Molecular Biology: Life)*, *52*, 159–164.

Liang, L.-P., & Patel, M. (2004). Mitochondrial oxidative stress and increased seizure susceptibility in Sod2(-/+) mice. *Free Radical Biology & Medicine*, *36*(5), 542–54.

Liang, L.-P., & Patel, M. (2006). Seizure-induced changes in mitochondrial redox status. *Free Radical Biology & Medicine*, *40*(2), 316–22.

Liang, L.-P., Waldbaum, S., Rowley, S., Huang, T.-T., Day, B., & Patel, M. (2012). Mitochondrial oxidative stress and epilepsy in SOD2 deficient mice: attenuation by a lipophilic metalloporphyrin. *Neurobiology of Disease*, *45*(3), 1068–1076.

Lightowlers, R. N., Taylor, R. W., & Turnbull, D. M. (2015). Mutations causing mitochondrial disease: What is new and what challenges remain? *Science*, *349*(6255), 1494–1499.

Likhodii, S. S., Musa, K., Mendonca, A., Dell, C., McIntyre Burnham, W., & Cunnane, S. C. (2000). Dietary fat, ketosis, and seizure resistance in rats on the ketogenic diet. *Epilepsia*, *41*(11), 1400–1410.

Likhodii, S. S., Nylen, K., & McIntyre Burnham, W. (2008). Acetone as an Anticonvulsant. *Epilepsia*, *49*(Suppl. 8), 83–86.

Liotta, A., Rösner, J., Huchzermeyer, C., Wojtowicz, A., Kann, O., Schmitz, D., … Kovács, R. (2012). Energy demand of synaptic transmission at the hippocampal Schaffer-collateral synapse. *Journal of Cerebral Blood Flow & Metabolism*, *32*, 2076–2083.

Liu, Y. C., & Wang, H.-S. (2012). Medium-chain triglyceride ketogenic diet, an effective treatment for drug-resistant epilepsy and a comparison with other ketogenic diets. *Biomedical Journal*, *36*(1), 9–15.

Lund, T. M., Risa, Ø., Sonnewald, U., Schousboe, A., & Waagepetersen, H. S. (2009). Availability of neurotransmitter glutamate is diminished when β-hydroxybutyrate replaces glucose in cultured neurons. *Journal of Neurochemistry*, *110*, 80–91.

Lundgaard, I., Li, B., Xie, L., Kang, H., Sanggaard, S., Haswell, J. D. R., … Nedergaard, M. (2015). Direct neuronal glucose uptake Heralds activity-dependent increases in cerebral metabolism. *Nature Communications*, *6*, 6807.

Luo, C., Li, Y., Wang, H., Feng, Z., Li, Y., Long, J., & Liu, J. (2013). Mitochondrial accumulation under oxidative stress is due to defects in autophagy. *Journal of*

Cellular Biochemistry, *114*, 212–219.

Luo, Y., Yin, W., Signore, A. P., Zhang, F., Hong, Z., Wang, S., … Chen, J. (2006). Neuroprotection against focal ischemic brain injury by the peroxisome proliferator-activated receptor-γ agonist rosiglitazone. *Journal of Neurochemistry*, *97*(2), 435–448.

Ly, J. D., Grubb, D. R., & Lawen, a. (2003). The mitochondrial membrane potential in apoptosis; an update. *Apoptosis*, *8*(2), 115–128.

Malapaka, R. R. V, Khoo, S., Zhang, J., Choi, J. H., Zhou, X. E., Xu, Y., … Xu, H. E. (2012). Identification and mechanism of 10-carbon fatty acid as modulating ligand of peroxisome proliferator-activated receptors. *The Journal of Biological Chemistry*, *287*(1), 183–95.

Malinska, D., Kulawiak, B., Kudin, A. P., Kovacs, R., Huchzermeyer, C., Kann, O., … Kunz, W. S. (2010). Complex III-dependent superoxide production of brain mitochondria contributes to seizure-related ROS formation. *Biochimica et Biophysica Acta (BBA) - Bioenergetics*, *1797*(6–7), 1163–1170.

Marchi, S., Giorgi, C., Suski, J. M., Agnoletto, C., Bononi, A., Bonora, M., … Pinton, P. (2012). Mitochondria-Ros Crosstalk in the Control of Cell Death and Aging. *Journal of Signal Transduction*, *2012*, 1–17.

Marco, R., Pestaña, A., Sebastian, J., & Sols, A. (1974). Oxaloacetate metabolic crossroads in liver. Enzyme compartmentation and regulation of gluconeogenesis. *Molecular and Cellular Biochemistry*, *3*(1), 53–70.

Mariani, E., Polidori, M., Cherubini, A., & Mecocci, P. (2005). Oxidative stress in brain aging, neurodegenerative and vascular diseases: An overview. *Journal of Chromatography B*, *827*(1), 65–75.

Marten, B., Pfeuffer, M., & Schrezenmeir, J. (2006). Medium-chain triglycerides. *International Dairy Journal*, *16*(11), 1374–1382.

McDonald, T. S., Tan, K. N., Hodson, M. P., & Borges, K. (2014). Alterations of hippocampal glucose metabolism by even versus uneven medium chain triglycerides. *Journal of Cerebral Blood Flow and Metabolism*, *34*(1), 153–60.

McGarry, J., & Brown, N. (1997). The mitochondrial carnitine palmitoyltransferase system. From concept to molecular analysis. *European Journal of Biochemistry / FEBS*, *244*(1), 1–14.

McKeigue, P. M., Laws, A., Chen, Y. D., Marmot, M. G., & Reaven, G. M. (1993). Relation of plasma triglyceride and apoB levels to insulin-mediated suppression of nonesterified fatty acids. Possible explanation for sex differences in lipoprotein pattern. *Arteriosclerosis and Thrombosis*, *13*, 1187–1192.

McMaster, M. C. (2008). *GC/MS: A Practical User's Guide* (Second). Hoboken, NJ: John Wiley & Sons, Inc.

McNally, M. A., & Hartman, A. L. (2012). Ketone bodies in epilepsy. *Journal of Neurochemistry*, *121*(1), 28–35.

McPherson, P. A. C., & McEneny, J. (2012). The biochemistry of ketogenesis and its role in weight management, neurological disease and oxidative stress. *Journal of Physiology and Biochemistry*, *68*(1), 141–151.

Megiddo, I., Colson, A., Chisholm, D., Dua, T., Nandi, A., & Laxminarayan, R. (2016). Health and economic benefits of public financing of epilepsy treatment in India: An agent-based simulation model. *Epilepsia*, *57*(3), 464–474.

Mergenthaler, P., Lindauer, U., Dienel, G., & Meisel, A. (2013). Sugar for the brain: the role of glucose in physiological and pathological brain function. *Trends in Neuroscience*, *36*(10), 587–597.

Meyers, D. E., Basha, H. I., & Koenig, M. K. (2013). Mitochondrial cardiomyopathy: pathophysiology, diagnosis, and management. *Texas Heart Institute Journal*, *40*(4), 385–94.

Minami, M., Kuraishi, Y., & Satoh, M. (1991). Effects of kainic acid on messenger RNA levels of IL-1 beta, IL-6, TNF alpha and LIF in the rat brain. *Biochemical and Biophysical Research Communications*, *176*(2), 593–598.

Mohanraj, R., & Brodie, M. J. (2013). Early predictors of outcome in newly diagnosed epilepsy. *Seizure*, *22*(5), 333–344.

Mookerjee, S., Divakaruni, A. S., Jastroch, M., & Brand, M. D. (2010). Mitochondrial uncoupling and lifespan. *Mechanisms of Ageing and Development*, *131*(7–8), 463–472.

Moreno, S., Farioli-vecchioli, S., & Cerù, M. P. (2004). Immunolocalization of peroxisome proliferator-activated receptors and retinoid X receptors in the adult rat CNS. *Neuroscience*, *123*(1), 131–145.

Morris, A. (2005). Cerebral ketone body metabolism. *Journal of Inherited Metabolic Disease*, *28*, 109–121.

Morris, G. L., & Mueller, W. (1999). Long-term treatment with vagus nerve stimulation in patients with refractory epilepsy. The Vagus Nerve Stimulation Study Group E01-E05. *Neurology*, *53*(8), 1731–5.

Mosek, A., Natour, H., Neufeld, M. Y., Shiff, Y., & Vaisman, N. (2009). Ketogenic diet treatment in adults with refractory epilepsy: A prospective pilot study. *Seizure*, *18*, 30–33.

Muccio, Z., & Jackson, G. (2009). Isotope Ratio Mass Spectrometry. *The Analyst*, *134*(2), 213–22.

Nakazawa, M., Kodama, S., & Matsuo, T. (1983). Effects of ketogenic diet on electroconvulsive threshold and brain contents of adenosine nucleotides. *Brain and Development*, *5*, 375–380.

Nandivada, P., Fell, G. L., Pan, A. H., Nose, V., Ling, P. R., Bistrian, B. R., & Puder, M. (2016). Eucaloric Ketogenic Diet Reduces Hypoglycemia and Inflammation in

Mice with Endotoxemia. *Lipids*, *51*(6), 1–12.

Narendra, D., Tanaka, A., Suen, D. F., & Youle, R. J. (2008). Parkin is recruited selectively to impaired mitochondria and promotes their autophagy. *Journal of Cell Biology*, *183*(5), 795–803.

Narendra, D., Walker, J. E., & Youle, R. (2012). Mitochondrial quality control mediated by PINK1 and Parkin: Links to parkinsonism. *Cold Spring Harbor Perspectives in Biology*, *4*(11).

Neal, E. G. (2012a). Carnitine. In E. Neal (Ed.), *Dietary Treatment of Epilepsy: Practical Implementation of Ketogenic Therapy* (pp. 166–171). Chichester: John Wiley & Sons, Inc.

Neal, E. G. (2012b). Introduction to the ketogenic diet and other dietary treatments. In E. Neal (Ed.), *Dietary Treatment of Epilepsy: Practical Implementation of Ketogenic Therapy* (pp. 2–10). Chichester: Wiley-Blackwell.

Neal, E. G., Chaffe, H., Schwartz, R. H., Lawson, M. S., Edwards, N., Fitzsimmons, G., … Cross, J. H. (2009). A randomized trial of classical and medium-chain triglyceride ketogenic diets in the treatment of childhood epilepsy. *Epilepsia*, *50*(5), 1109–17.

Okuneva, O., Li, Z., Körber, I., Tegelberg, S., Joensuu, T., Tian, L., & Lehesjoki, A.-E. (2016). Brain inflammation is accompanied by peripheral inflammation in Cstb–/– mice, a model for progressive myoclonus epilepsy. *Journal of Neuroinflammation*, *13*(298).

Olendorf, W. (1971). Blood Brain Barrier Permeability to Lactate. *European Neurology*, *6*(1–6), 49–55.

Olendorf, W. (1973). Carrier-mediated blood-brain barrier transport of short-chain monocarboxylic organic acids. *American Journal of Physiology*, *224*(6), 1450–1453.

Onyango, I. G., Lu, J., Rodova, M., Lezi, E., Crafter, A. B., & Swerdlow, R. H. (2010). Regulation of neuron mitochondrial biogenesis and relevance to brain health. *Biochimica et Biophysica Acta*, *1802*(1), 228–34.

Orasanu, G., Ziouzenkova, O., Devchand, P. R., Nehra, V., Hamdy, O., Horton, E. S., & Plutzky, J. (2008). The Peroxisome Proliferator-Activated Receptor-γ Agonist Pioglitazone Represses Inflammation in a Peroxisome Proliferator-Activated Receptor-α-Dependent Manner In Vitro and In Vivo in Mice. *Journal of the American College of Cardiology*, *52*(10), 869–881.

Orata, F. (2012). Derivatization Reactions and Reagents for Gas Chromatography Analysis. In M. A. Mohd (Ed.), *Advanced Gas Chromatography - Progress in Agricultural, Biomedical and Industrial Applications*. InTech.

Palikaras, K., Lionaki, E., & Tavernarakis, N. (2015a). Balancing mitochondrial biogenesis and mitophagy to maintain energy metabolism homeostasis. *Cell Death and Differentiation*, *22*(9), 1399–1401.

Palikaras, K., Lionaki, E., & Tavernarakis, N. (2015b). Coordination of mitophagy and mitochondrial biogenesis during ageing in C. elegans. *Nature*, *521*(7553), 525–528.

Palikaras, K., & Tavernarakis, N. (2014). Mitochondrial homeostasis: The interplay between mitophagy and mitochondrial biogenesis. *Experimental Gerontology*, *56*, 182–188.

Papamandjaris, A., MacDougall, D., & Jones, P. (1998). Medium chain fatty acid metabolism and energy expenditure: obesity treatment implications. *Life Sciences*, *62*(14), 1203–1215.

Papamandjaris, A., White, M., Raeini-Sarjaz, M., & Jones, P. (2000). Endogenous fat oxidation during medium chain versus long chain triglyceride feeding in healthy women. *International Journal of Obesity*, *24*(9), 1158–66. Retrieved from

http://www.ncbi.nlm.nih.gov/pubmed/11033985

Parini, R., Invernizzi, F., Menni, F., Garavaglia, B., Melotti, D., Rimoldi, M., ... Taroni, F. (1999). Medium-chain triglyceride loading test in carnitine-acylcarnitine translocase deficiency: Insights on treatment. *Journal of Inherited Metabolic Disease*, *22*, 733–739.

Park, J. H., Ko, J., Hwang, J., & Koh, H. C. (2015). Dynamin-related protein 1 mediates mitochondria-dependent apoptosis in chlorpyrifos-treated SH-SY5Y cells. *NeuroToxicology*, *51*, 145–157.

Park, S. W., Yi, J. H., Miranpuri, G., Satriomo, I., Bowen, K., Resnick, D. K., & Vemuganti, R. (2007). Thiazolidnedione class of peroxisome proliferator-activated receptor γ agonists prevents neuronal damage, motor dysfunction, myelin loss, neuropathic pain, and inflammation after spinal cord injury in adults rats. *The Journal of Pharmacology and Experimental Therapeutics*, *320*(3), 1002–1012.

Patel, M. (2004). Mitochondrial dysfunction and oxidative stress: cause and consequence of epileptic seizures. *Free Radical Biology & Medicine*, *37*(12), 1951–62.

Pathak, D., Shields, L. Y., Mendelsohn, B. A., Haddad, D., Lin, W., Gerencser, A. A., ... Nakamura, K. (2015). The role of mitochondrially derived ATP in synaptic vesicle recycling. *Journal of Biological Chemistry*, *290*(37), 22325–22336.

Perry, S. W., Norman, J. P., Barbieri, J., Brown, E. B., & Gelbard, H. A. (2011). Mitochondrial membrane potential probes and the proton gradient: a practical usage guide. *Biotechniques*, *50*(2), 98–115.

Popa-Wagner, A., Mitran, S., Sivanesan, S., Chang, E., & Buga, A.-M. (2013). ROS and Brain Diseases : The Good, the Bad, and the Ugly. *Oxidative Medicine and Cellular Longevity*, (Article ID 963520).

Porter, R. K., Hulbert, A. J., & Brand, M. D. (1996). Allometry of mitochondrial proton leak: influence of membrane surface area and fatty acid composition. *American Journal of Physiology - Regulatory, Integrative and Comparative Physiology*, *271*(6), R1550–R1560.

Portilla, D., Dai, G., Peters, J. M., Gonzalez, F. J., Crew, M. D., & Proia, A. D. (2000). Etomoxir-induced PPARalpha-modulated enzymes protect during acute renal failure. *Am J Physiol Renal Physiol*, *278*(4), F667-75. Retrieved from http://ajprenal.physiology.org/cgi/content/full/278/4/F667%5Cnhttp://www.ncbi.nlm.nih.gov/entrez/query.fcgi?cmd=Retrieve&db=PubMed&dopt=Citation&list_uids=10751229

Pratt, C. W., & Cornley, K. (2014). *Essential Biochemistry* (Third). New York, NY: John Wiley & Sons, Inc.

Price, N. T., van der Leij, F. R., Jackson, V. N., Corstorphine, C. G., Thomson, R., Sorensen, A., & Zammit, V. A. (2002). A Novel Brain-Expressed Protein Related to Carnitine Palmitoyltransferase I. *Genomics*, *80*(4), 433–442.

Purves, D., Augustine, G., Fitzpatrick, D., Hall, W., LaMantia, A.-S., McNamara, J., & Williams, S. (Eds.). (2004). *Neuroscience* (Third). Sunderland, MA: SinauerAssociates.

Rahman, S. (2012). Mitochondrial disease and epilepsy. *Developmental Medicine and Child Neurology*, *54*(5), 397–406.

Rangaraju, V., Calloway, N., & Ryan, T. A. (2014). Activity-driven local ATP synthesis is required for synaptic function. *Cell*, *156*(4), 825–835.

Ratheiser, K., Schneeweiß, B., Waldhäusl, W., Fasching, P., Korn, A., Nowotny, P., … Wolf, H. P. O. (1991). Inhibition by etomoxir of carnitine palmitoyltransferase I reduces hepatic glucose production and plasma lipids in non-insulin-dependent diabetes mellitus. *Metabolism*, *40*(11), 1185–1190.

Ravizza, T., Gagliardi, B., Noé, F., Boer, K., Aronica, E., & Vezzani, A. (2008). Innate and adaptive immunity during epileptogenesis and spontaneous seizures: Evidence from experimental models and human temporal lobe epilepsy. *Neurobiology of Disease*, *29*, 142–160.

Reichard, G. A., Haff, A. C., Skutches, C. L., Paul, P., Holroyde, C. P., & Owen, O. E. (1979). Plasma acetone metabolism in the fasting human. *Journal of Clinical Investigation*, *63*, 619–626.

Reichmann, H., Maltese, W., & DeVivo, D. (1988). Enzymes of Fatty Acid Beta-Oxidation in Developing Brain. *Journal of Neurochemistry*, *51*, 339–44. Retrieved from http://www.ncbi.nlm.nih.gov/pubmed/2899130

Rho, J. M., Anderson, G. D., Donevan, S. D., & White, H. S. (2002). Acetoacetate, Acetone, and Dibenzylamine (a Contaminant in L-(+)-β-Hydroxybutyrate) Exhibit Direct Anticonvulsant Actions in Vivo. *Epilepsia*, *43*(4), 358–361.

Rho, J. M., & Sankar, R. (2008). The ketogenic diet in a pill: is this possible? *Epilepsia*, *49 Suppl 8*, 127–33.

Riazi, K., Galic, M. A., & Pittman, Q. J. (2010). Contributions of peripheral inflammation to seizure susceptibility: Cytokines and brain excitability. *Epilepsy Research*, *89*(1), 34–42.

Rich, P. R., & Maréchal, A. (2010). The mitochondrial respiratory chain. *Essays In Biochemistry*, *47*, 1–23.

Ricote, M., Li, A. C., Willson, T. M., Kelly, C. J., & Glass, C. K. (1998). The peroxisome proliferator-activated receptor-gamma is a negative regulator of macrophage activation. *Nature*, *391*(6662), 79–82.

Rogawski, M. A. (2016). A fatty acid in the MCT ketogenic diet for epilepsy treatment blocks AMPA receptors. *Brain*, *139*, 304–316.

Rosdah, A. A., K Holien, J., Delbridge, L. M. D., Dusting, G. J., & Lim, S. Y. (2016).

Mitochondrial fission - a drug target for cytoprotection or cytodestruction? *Pharmacology Research & Perspectives*, *4*(3), e00235.

Ross, D. L., Swaiman, K. F., Torres, F., & Hansen, J. (1985). Early biochemical and EEG correlates of the ketogenic diet in children with atypical absence epilepsy. *Pediatric Neurology*, *1*, 104–108.

Ross, R. A., Spengler, B. A., & Biedler, J. L. (1983). Coordinate morphological and biochemical interconversion of human neuroblastoma cells. *Journal of the National Cancer Institute*, *71*(4), 741–747. Retrieved from http://www.ncbi.nlm.nih.gov/pubmed/6137586

Rowley, S., Liang, L. P., Fulton, R., Shimizu, T., Day, B., & Patel, M. (2015). Mitochondrial respiration deficits driven by reactive oxygen species in experimental temporal lobe epilepsy. *Neurobiology of Disease*, *75*, 151–158.

Ruskin, D. N., Kawamura, M., & Masino, S. A. (2009). Reduced pain and inflammation in juvenile and adult rats fed a ketogenic diet. *PLoS ONE*, *4*(12), e8349.

Sabbagh, S. El, Lebre, A.-S., Bahi-Buisson, N., Delonlay, P., Soufflet, C., Boddaert, N., … Desguerre, I. (2010). Epileptic phenotypes in children with respiratory chain disorders. *Epilepsia*, *51*(7), 1225–1235.

Saez-Atienzar, S., Bonet-Ponce, L., Blesa, J. R., Romero, F. J., Murphy, M. P., Jordan, J., & Galindo, M. F. (2014). The LRRK2 inhibitor GSK2578215A induces protective autophagy in SH-SY5Y cells: involvement of Drp-1-mediated mitochondrial fission and mitochondrial-derived ROS signaling. *Cell Death and Disease*, *5*(8), e1368.

Samala, R., Willis, S., & Borges, K. (2008). Anticonvulsant profile of a balanced ketogenic diet in acute mouse seizure models. *Epilepsy Research*, *81*, 119–127.

Sanders, A. P., Kramer, R. S., Woodhall, B., & Currie, W. D. (1970). Brain Adenosine Triphosphate: Decreased Concentration Precedes Convulsions. *Science*,

169(3941), 206–208.

Santo-Domingo, J., & Demaurex, N. (2012). The renaissance of mitochondrial pH. *The Journal of General Physiology*, *139*(6), 415–423.

Scharfman, H. E. (2007). The Neurobiology of Epilepsy. *Current Neurology and Neuroscience Reports*, *7*(4), 348–354.

Scharfman, H. E. (2015). Metabolic Control of Epilepsy. *Neuroscience*, *347*(6228), 1312–1313.

Schneider, L., Giordano, S., Zelickson, B. R., Johnson, M., Benavides, G., Ouyang, X., … Darley-usmar, V. M. (2011). Differentiation of SH-SY5Y cells to a neuronal phenotype changes cellular bioenergetics and the response to oxidative stress. *Free Radical Biology and Medicine*, *51*(11), 2007–2017.

Schoeler, N. E., Bell, G., Yuen, A., Kapelner, A. D., Heales, S. J. R., Cross, J. H., & Sisodiya, S. (2017). An examination of biochemical parameters and their association with response to ketogenic dietary therapies. *Epilepsia*, *58*(5), 893–900.

Schoeler, N. E., Wood, S., Aldridge, V., Sander, J. W., Cross, J. H., & Sisodiya, S. M. (2014). Ketogenic dietary therapies for adults with epilepsy: Feasibility and classification of response. *Epilepsy and Behavior*, *37*, 77–81.

Schönfeld, P., & Reiser, G. (2013). Why does brain metabolism not favor burning of fatty acids to provide energy ? - Reflections on disadvantages of the use of free fatty acids as fuel for brain. *Journal of Cerebral Blood Flow & Metabolism*, *33*, 1493–1499.

Schooneman, M. G., Vaz, F. M., Houten, S. M., & Soeters, M. R. (2013). Acylcarnitines: Reflecting or inflicting insulin resistance? *Diabetes*, *62*(1), 1–8.

Schwartz, R. H., Boyes, S., & Aynsley-Green, A. (1989a). Metabolic effects of three ketogenic diets in the treatment of severe epilepsy. *Developmental Medicine and Child Neurology*, *31*, 152–160.

Schwartz, R. H., Eaton, J., Bower, B. D., & Aynsley-Green, A. (1989b). Ketogenic Diets in the Treatment of Epilepsy: Short-Term Clinical Effects. *Developmental Medicine and Child Neurology*, *31*, 145–151.

Scientific Advisory Committee on Nutrition (SACN). (2011). *Dietary Reference Values for Energy*. *Dietary Reference Values for Energy*. UK: Crown.

Selby, P. L., & Sherratt, H. S. A. (1989). Substituted 2-oxiranecarboxylic acids: a new group of candidate hypoglycemic drugs. *Trends in Pharmacological Sciences*, *10*, 495–500.

Sengupta, A., & Ghosh, M. (2012). Comparison of native and capric acid-enriched mustard oil effects on oxidative stress and antioxidant protection in rats. *British Journal of Nutrition*, *107*(06), 845–849.

Sengupta, A., Ghosh, M., & Bhattacharyya, D. K. (2014). Antioxidative Effect of Rice Bran Oil and Medium Chain Fatty Acid Rich Rice Bran Oil in Arsenite Induced Oxidative Stress in Rats. *Journal of Oleo Science*, *63*(11), 1117–1124.

Seo, J. H., Lee, Y. M., Lee, J. S., Kim, S. H., & Kim, H. D. (2010). A case of Ohtahara syndrome with mitochondrial respiratory chain complex I deficiency. *Brain and Development*, *32*(3), 253–257.

Seymour, K., Bluml, S., Sutherling, J., Sutherling, W., & Ross, B. (1999). Identification of cerebral acetone by 1H-MRS in patients with epilepsy controlled by ketogenic diet. *MAGMA*, *8*(1), 33–42.

Shabalina, I. G., Backlund, E. C., Bar-Tana, J., Cannon, B., & Nedergaard, J. (2008). Within brown-fat cells, UCP1-mediated fatty acid-induced uncoupling is independent of fatty acid metabolism. *Biochimica et Biophysica Acta - Bioenergetics*, *1777*(7–8), 642–650.

Shepherd, D., & Garland, P. B. (1969). The kinetic properties of citrate synthase from rat liver mitochondria. *The Biochemical Journal*, *114*, 597–610. Retrieved from

http://www.pubmedcentral.nih.gov/articlerender.fcgi?artid=1184933&tool=pmcentrez&rendertype=abstract

Sills, M., Forsythe, W., & Haidukewych, D. (1986). Role of octanoic and decanoic acids in the control of seizures. *Archives of Disease in Childhood*, *61*, 1173–1177.

Sipos, I., Tretter, L., & Adam-Vizi, V. (2003). Quantitative relationship between inhibition of respiratory complexes and formation of reactive oxygen species in isolated nerve terminals. *Journal of Neurochemistry*, *84*(1), 28. Retrieved from isi:000183156200094%5CnISI:000179790800013

Sirven, J., Whedon, B., Caplan, D., Liporace, J., Glosser, D., O'Dwyer, J., & Sperling, M. R. (1999). The ketogenic diet for intractable epilepsy in adults: preliminary results. *Epilepsia*, *40*(12), 1721–1726.

Socała, K., Nieoczym, D., Pieróg, M., & Wlaź, P. (2015). Role of the adenosine system and glucose restriction in the acute anticonvulsant effect of caprylic acid in the 6Hz psychomotor seizure test in mice. *Progress in Neuro-Psychopharmacology and Biological Psychiatry*, *57*, 44–51.

Solesio, M. E., Saez-atienzar, S., Jordán, J., & Galindo, M. F. (2012). Characterization of mitophagy in the 6-hydoxydopamine Parkinson's disease model. *Toxicological Sciences*, *129*(2), 411–420.

Somjen, G. G. (2002). Ion Regulation in the Brain : Implications for Pathophysiology. *Neuroscientist*, *8*, 254–267.

Spector, R. (1988). Fatty acid transport through the blood-brain barrier. *Journal of Neurochemistry*, *50*(2), 639–643.

Spurway, T. D., Pogson, C. I., Sherratt, H. S. A., & Agius, L. (1997). Etomoxir, sodium 2-[6-(4-chlorophenoxy)hexyl]oxirane-2-carboxylate, inhibits triacylglycerol depletion in hepatocytes and lipolysis in adipocytes. *FEBS Letters*, *404*, 111–114.

Sullivan, P. G., Rippy, N. A., Dorenbos, K., Concepcion, R. C., Agarwal, A. K., & Rho, J.

M. (2004). The Ketogenic Diet Increases Mitochondrial Uncoupling Protein Levels and Activity. *Annals of Neurology*, *55*(4), 576–580.

Sundararajan, S., Gamboa, J. L., Victor, N. A., Wanderi, E. W., Lust, W. D., & Landreth, G. E. (2005). Peroxisome proliferator-activated receptor-gamma ligands reduce inflammation and infarction size in transient focal ischemia. *Neuroscience*, *130*, 685–696.

Swartz, M. (2010). HPLC detectors: A brief review. *Journal of Liquid Chromatography and Related Technologies*, *33*(9–12), 1130–1150.

Tan, K. N., Carrasco-Pozo, C., McDonald, T. S., Puchowicz, M., & Borges, K. (2017). Tridecanoin is anticonvulsant, antioxidant, and improves mitochondrial function. *Journal of Cerebral Blood Flow & Metabolism*, *37*(6), 2035–2048.

Tasdemir, E., Galluzzi, L., Maiuri, M. C., Criollo, A., Vitale, I., Hangen, E., … Kroemer, G. (2008). Methods for Assessing Autophagy and Autophaghic Cell Death. In V. Deretic (Ed.), *Methods in Molecular Biology, vol 445: Autophagosome and Phagosome* (pp. 29–76). Totowa, NJ: Humana Press.

Taylor, R. W., & Turnbull, D. M. (2005). Mitochondrial DNA mutations in human disease. *Nature Reviews Genetics*, *6*(5), 389–402.

Téllez-Zenteno, J. F., Dhar, R., & Wiebe, S. (2005). Long-term seizure outcomes following epilepsy surgery: A systematic review and meta-analysis. *Brain*, *128*(5), 1188–1198.

Thavendiranathan, P., Mendonca, A., Dell, C., Likhodii, S. S., Musa, K., Iracleous, C., … Burnham, W. M. (2000). The MCT ketogenic diet: effects on animal seizure models. *Experimental Neurology*, *161*(2), 696–703.

Thevenet, J., De Marchi, U., Domingo, J. S., Christinat, N., Bultot, L., Lefebvre, G., … Wiederkehr, A. (2016). Medium-chain fatty acids inhibit mitochondrial metabolism in astrocytes promoting astrocyte-neuron lactate and ketone body

shuttle systems. *The FASEB Journal*, *30*(5), 1913–1926.

Thio, L. L., Wong, M., & Yamada, K. A. (2000). Ketone bodies do not directly alter excitatory or inhibitory hippocampal synaptic transmission. *Neurology*, *54*, 325–331.

Tian, G. F., Azmi, H., Takano, T., Xu, Q., Peng, W., Lin, J., … Nedergaard, M. (2005). An astrocytic basis of epilepsy. *Nature Medicine*, *11*(9), 973–981.

Turrens, J. F. (2003). Mitochondrial formation of reactive oxygen species. *The Journal of Physiology*, *552*(Pt 2), 335–44.

Twig, G., Elorza, A., Molina, A. J. A., Mohamed, H., Wikstrom, J. D., Walzer, G., … Shirihai, O. S. (2008). Fission and selective fusion govern mitochondrial segregation and elimination by autophagy. *The EMBO Journal*, *27*(2), 433–446.

Uittenbogaard, M., & Chiaramello, A. (2014). Mitochondrial biogenesis: a therapeutic target for neurodevelopmental disorders and neurodegenerative diseases. *Current Pharmaceutical Design*, *20*(35), 5574–93.

Vaillend, C., Mason, S. E., Cuttle, M. F., & Alger, B. E. (2002). Mechanisms of Neuronal Hyperexcitability Caused by Partial Inhibition of Na+-K+-ATPases in the Rat CA1 Hippocampal Region. *Journal of Neurophysiology*, *88*, 2963–2978.

van Delft, R., Lambrechts, D. A. J. E., Verschuure, P., Hulsman, J., & Majoie, M. (2010). Blood beta-hydroxybutyrate correlates better with seizure reduction due to ketogenic diet than do ketones in the urine. *Seizure*, *19*, 36–39.

Vezzani, A., French, J., Bartfai, T., & Baram, T. Z. (2011). The role of inflammation in epilepsy. *Nature Reviews Neurology*, *7*(1), 31–40.

Voet, D., Voet, J. G., & Pratt, C. W. (2013). *Fundamentals of Biochemistry* (Fourth). Hoboken, NJ: John Wiley & Sons, Inc.

Waagepetersen, H. S., Sonnewald, U., Larsson, O. M., & Schousboe, A. (1999). Synthesis of Vesicular GABA From Glutamine Involves TCA Cycle Metabolism in

Neocortical Neurons. *Journal of Neuroscience Research*, *57*, 342–349.

Waldbaum, S., & Patel, M. (2010). Mitochondria, oxidative stress, and temporal lobe epilepsy. *Epilepsy Research*, *88*, 23–45.

Wallace, D. C., Lott, M. T., Shoffner, J. M., & Ballinger, S. (1994). Mitochondrial DNA Mutations in Epilepsy and Neurological Disease. *Epilepsia*, *35*(Suppl. 1), S43–S50.

Wallace, H., Shorvon, S., & Tallis, R. (1998). Age-specific incidence and prevalence rates of treated epilepsy in an unselected population of 2,052,922 and age-specific fertility rates of women with epilepsy. *Lancet*, *352*(9145), 1970–1973.

Wang, Z. J., Bergqvist, C., Hunter, J. V, Jin, D., Wang, D.-J., Wehrli, S., & Zimmerman, R. A. (2003). In Vivo Measurement of Brain Metabolites Using Two-Dimensional Double-Quantum MR Spectroscopy — Exploration of GABA Levels in a Ketogenic Diet. *Magnetic Resonance in Medicine*, *49*, 615–619.

Wibisono, C., Rowe, N., Beavis, E., Kepreotes, H., Mackie, F. E., Lawson, J. a., & Cardamone, M. (2015). Ten-Year Single-Center Experience of the Ketogenic Diet: Factors Influencing Efficacy, Tolerability, and Compliance. *The Journal of Pediatrics*, *166*(4), 1030–6.

Wilder, R. (1921). The effect on ketonemia on the course of epilepsy. *Mayo Clinic Bulletin*, *2*, 307.

Wilkins, B. (2015). *The retention and storage of pathological records and specimens (5th edition)*. *The Royal College of Pathologists*. London.

Will, Y., Hynes, J., Ogurtsov, V. I., & Papkovsky, D. B. (2006). Analysis of mitochondrial function using phosphorescent oxygen-sensitive probes. *Nature Protocols*, *1*(6), 2563–2572.

Winkler, E., & Klingenberg, M. (1994). Effect of fatty acids on H+ transport activity of the reconstituted uncoupling protein. *Journal of Biological Chemistry*, *269*(4), 2508–2515.

Wlaź, P., Socała, K., Nieoczym, D., Łuszczki, J. J., Arnowska, I., Arnowski, T., … Gasior, M. I. (2012). Anticonvulsant profile of caprylic acid, a main constituent of the medium-chain triglyceride (MCT) ketogenic diet, in mice. *Neuropharmacology*, *62*(4), 1882–1889.

Wlaź, P., Socała, K., Nieoczym, D., Żarnowski, T., Żarnowska, I., Czuczwar, S. J., & Gasior, M. (2015). Acute anticonvulsant effects of capric acid in seizure tests in mice. *Progress in Neuro-Psychopharmacology and Biological Psychiatry*, *57*, 110–116.

Wojtczak, L., & Schönfeld, P. (1993). Effect of fatty acids on energy coupling processes in mitochondria. *Biochimica et Biophysica Acta (BBA) - Bioenergetics*, *1183*, 41–57.

Wolfgang, M. J., Cha, S. H., Millington, D. S., Cline, G., Shulman, G. I., Suwa, A., … Lane, M. D. (2008). Brain-specific carnitine palmitoyl-transferase-1c: Role in CNS fatty acid metabolism, food intake, and body weight. *Journal of Neurochemistry*, *105*(4), 1550–1559.

Wolfgang, M. J., Kurama, T., Dai, Y., Suwa, A., Asaumi, M., Matsumoto, S.-I., … Lane, M. D. (2006). The brain-specific carnitine palmitoyltransferase-1c regulates energy homeostasis. *Proceedings of the National Academy of Sciences of the United States of America*, *103*(19), 7282–7.

World Health Organization. (2005). *Atlas: Epilepsy Care in the World*. Geneva: WHO.

Wu, M., Liu, X., Chi, X., Zhang, L., Xiong, W., Chiang, S. M. V., … Li, J. (2017). Mitophagy in Refractory Temporal Lobe Epilepsy Patients with Hippocampal Sclerosis. *Cellular and Molecular Neurobiology*, Epub.

Xie, H., Hu, L., & Li, G. (2010). SH-SY5Y human neuroblastoma cell line: in vitro cell model of dopaminergic neurons in Parkinson's disease. *Chinese Medical Journal*, *123*(8), 1086–1092.

Yang, S.-Y., He, X.-Y., & Schulz, H. (1987). Fatty acid oxidation in rat brain is limited by the low activity of 3-ketoacyl-coenzyme A thiolase. *Journal of Biological Chemistry*, *262*(27), 13027–13032.

You, Y. Q., Ling, P. R., Qu, Z., & Bistrian, B. R. (1998). Effect of Continuous Enteral Medium-Chain Fatty Acid Infusion on Lipid Metabolism in Rats. *Lipids*, *33*(3), 261–266.

Youle, R. J., & Narendra, D. P. (2011). Mechanisms of mitophagy. *Nature Reviews Molecular Cell Biology*, *12*(1), 9–14.

Yudkoff, M., Daikhin, Y., Nissim, I., Lazarow, A., & Nissim, I. (2001). Brain Amino Acid Metabolism and Ketosis. *Journal of Neuroscience Research*, *66*, 272–281.

Zhu, J., Wang, K. Z. Q., & Chu, C. T. (2013). After the banquet: Mitochondrial biogenesis, mitophagy and cell survival. *Autophagy*, *9*(11), 1663–1676.

Zoratti, R., Godsland, I. F., Chaturvedi, N., Crook, D., Stevenson, J. C., & McKeigue, P. M. (2000). Relation of plasma lipids to insulin resistance, nonesterified fatty acid levels, and body fat in men from three ethnic groups: relevance to variation in risk of diabetes and coronary disease. *Metabolism*, *49*(2), 245–252.

Zorova, L. D., Popkov, V. A., Plotnikov, E. Y., Silachev, D. N., Pevzner, I. B., Jankauskas, S. S., … Zorov, D. B. (2017). Mitochondrial membrane potential. *Analytical Biochemistry*, *[In Press]*, 1–10.

Zsurka, G., & Kunz, W. S. (2015). Mitochondrial dysfunction and seizures: the neuronal energy crisis. *The Lancet Neurology*, *14*, 956–966.

PATENT

A patent application for the use of a C10- and C8-based composition (C10 to C8 ratio of 70:30 to 90:10 wt/wt) in a range of therapies was filed with the European Patent Office on 10th April 2017.

In particular, the invention relates to the use of the composition in the treatment of epilepsy, or epileptic seizures, and disorders involving the AMPA receptor, such as amyotrophic lateral sclerosis (ALS), Alzheimer's disease, cancer and ischaemia,

Patent Application Number: EP17165690.3

ABSTRACTS AND AWARDS

ABSTRACTS:

5th Global Symposium on Ketogenic Diet Therapies 2016

Poster: Differential Oxidation of Octanoic and Decanoic Acid in Neuronal Cells: Potential Mechanistic Insights into the MCT-based Ketogenic diet.

Aziza Khabbush, Michael Orford, Yi-Chen Tsai, Simon Eaton, Simon Heales

British Inherited Metabolic Disease Group: BIMDG 2016

Poster: Decanoic acid treatment improves mitochondrial profile of fibroblasts from patients with complex I deficient Leigh syndrome: a step towards personalised medicine?

Marta Kanabus, Aziza Khabbush, Elisa Fassone, Sean David Hughes, Sara Farahi Bilooei, Tricia Rutherford, Maura O' Donnell, Simon Heales, Shamima Rahman

Early Careers Mitoscientist Meeting 2017

Presentation: Decanoic acid is poorly oxidised by neuronal cells – A mechanistic insight into how the medium-chain ketogenic diet may improve mitochondrial function

Aziza Khabbush

AWARDS:

- **ICH PhD Poster Competition 2015** – Special Commendation
- **ICH PhD Poster Competition 2016** – First Prize in Genetics and Genomic Medicine
- **UCL Doctoral School Research Poster Competition 2017** – First Prize in Population Health Sciences

- **Early Careers Mitoscientist Meeting 2017 Biochemical Society Prize** - Best Presentation, awarded by the Biochemical Society
- **GOSH Open House Festival 2017** – Poster Competition Winner

OTHER EVENTS:

Presentation at **Young Epilepsy Retreat 2015**

Poster at **MedCity/NIHR Biomedical Research Centre Showcase London 2017**

PUBLICATIONS

The findings presented in Chapter 4 were published in:

Khabbush, A., Orford, M., Tsai, Y., Rutherford, T., O'Donnell, M., Eaton, S. and Heales, S. J. (2017). Neuronal decanoic acid oxidation is markedly lower than that of octanoic acid: A mechanistic insight into the medium-chain triglyceride ketogenic diet. *Epilepsia, 58*, 1423-1429.

A review of MCT KD in a range of disorders was published in:

Augustin, K., Khabbush, A., Williams, S., Eaton, S., Orford, M., Cross, J. H., Heales, S.J.R., Walker, M.C. and Williams, R. S. B. (2018). Mechanisms of action for the medium-chain triglyceride ketogenic diet in neurological and metabolic disorders. *The Lancet Neurology, 17*(1), 84–93.